LETICIA FERNANDA DE OLIVEIRA

INVESTIGATING THE GENETIC ARCHITECTURE OF HEAT STRESS RESPONSE AND RELATED TRAITS IN PIG POPULATIONS

Thesis submitted to the Animal Science Graduate Program of the Universidade Federal de Viçosa in partial fulfillment of the requirements for the degree of *Doctor Scientiae*.

Advisor: Renata Veroneze

Co-advisor: Luiz Fernando Brito

VIÇOSA – MINAS GERAIS

2024

Ficha catalográfica elaborada pela Biblioteca Central da Universidade Federal de Viçosa - Campus Viçosa

T
O48i
2024

Oliveira, Letícia Fernanda de, 1995-
Investigando a arquitetura genética da resposta ao estresse térmico e características relacionadas em populações de suínos / Letícia Fernanda de Oliveira. – Viçosa, MG, 2024.
415 f.: il. (algumas color.).

Orientador: Renata Veroneze.
Tese (doutorado) - Universidade Federal de Viçosa, Departamento de Zootecnia, 2024.
Referências bibliográficas: f. 30-36, f. 277-286.
DOI: https://doi.org/10.47328/ufvbbt.2024.140
Modo de acesso: World Wide Web.

1. Suínos. 2. Genômica. 3. Genética animal. 4. Efeitos da temperatura. I. Veroneze, Renata, 1984-. II. Universidade Federal de Viçosa. Departamento de Zootecnia. Doutorado em Zootecnia. III. Título.

CDD 22. ed. 636

Bibliotecário(a) responsável: Kellen dos Santos Silva Barbosa CRB-6/ES 548

LETICIA FERNANDA DE OLIVEIRA

INVESTIGATING THE GENETIC ARCHITECTURE OF HEAT STRESS RESPONSE AND RELATED TRAITS IN PIG POPULATIONS

Thesis submitted to the Animal Science Graduate Program of the Universidade Federal de Viçosa in partial fulfillment of the requirements for the degree of *Doctor Scientiae*.

APPROVED: March 4, 2024

Assent:

Documento assinado digitalmente
gov.br
LETICIA FERNANDA DE OLIVEIRA
Data: 03/05/2024 08:39:02-0300
Verifique em https://validar.iti.gov.br

_____

Letícia Fernanda de Oliveira

Author

Documento assinado digitalmente
gov.br
RENATA VERONEZE
Data: 03/05/2024 08:49:11-0300
Verifique em https://validar.iti.gov.br

_____

Renata Veroneze

Advisor

I dedicate this work to my parents, siblings, and nephew.

ACKNOWLEDGMENTS

First, I would like to say that I am so thankful for my family always inspiring me and motivating me to keep studying. They are my support in every step I take in my journey and the people I can always talk to when I need to find peace and love. I am also very thankful to my uncle, Tio João Roberto, and his family who were so receptive and became my family in the United States and helped me in many moments.

I am deeply thankful to having Renata Veroneze as my advisor during my master and now PhD degree. She is a very thoughtful person, which is not only thinking about her students' professional success but also their well-being. I am deeply grateful for the guidance and support of both my advisor, Renata Veroneze, and my co-advisor, Luiz Brito. They have not only been amazing teachers but also supportive friends for me and their other students. I am also thankful for the reception I had from Luiz Brito and his lab at Purdue University, who helped during most part of this work.

I am also very grateful for all friends I have made during this journey. Having friends who were there in many moments I needed to help me with work or to just relax and have fun. I am especially thankful for my friends that were also my roommates in Republica CowNerd that were always so supportive and all fun moments we had in that apartment. I am also thankful to Marion, who I could live with for a few months and could learn so much from her. I am also grateful to the friends I made at Animal Science Department in Viçosa and in Brito's lab, they always helped me in my work when I asked, and we also shared many moments of joy and fun.

I would like to express my gratitude to the Universidade Federal de Viçosa and the Graduate Program in Animal Science for providing me the opportunity to pursue this course. This study was financed in part by the Coordenação de Aperfeiçoamento de Pessoal de Nível Superior – Brasil (CAPES) – Finance Code 001 and the Conselho

Nacional de Desenvolvimento Científico e Tecnológico (CNPq, Brazil), which granted the scholarship. Additionally, I would like to thank Luiz Brito, and Purdue University for their support during the period of my sandwich Ph.D. program.

ABSTRACT

OLIVEIRA, Letícia Fernanda de, D.Sc., Universidade Federal de Viçosa, March, 2024. **Investigating the genetic architecture of heat stress response and related traits in pig populations.** Advisor: Renata Veroneze. Co-advisor: Luiz Fernando Brito.

Global warming presents a significant challenge to livestock production, impacting animal welfare and performance. The resulting increase in temperatures promotes heat stress (HS) as a major concern in animal production, highlighting the need to breed for more resilient animals. Enhancing heat tolerance could improve animals' ability to cope with HS conditions. To make genetic progress in HS resilience, it is crucial to understand the genetic architecture of traits related to resilience and the genetic mechanisms underlying the heat stress response. This study aimed to investigate the genetic architecture of HS response indicators and related traits in pigs, with three main objectives. First, to assess the impact of non-additive genetic effects on variance components estimation in two independent datasets: crossbred and purebred populations, and in genomic prediction in a purebred population. Second, to identify genomic regions, candidate genes, and potential pleiotropic variants significantly associated with indicators of HS response in lactating sows using imputed whole-genome sequence (WGS) data. Third, to detect copy number variations (CNVs) and CNV regions (CNVRs) in pigs and explore their associations with physiological and anatomical indicators of HS response measured in crossbred (Large White x Landrace) lactating sows. The inclusion of non-additive genetic effects in the models did not improve the accuracy of genomic breeding values for performance traits in purebred pigs. However, there was a significant re-ranking of selection candidates depending on the model fitted. Low non-additive genetic variance estimates were observed for most heat tolerance indicators in crossbred pigs, except for the panting score and hair density. Physiological and anatomical indicators of HS response in lactating sows were found to have additive genetic variation but they are

highly polygenic. Candidate genes associated with heat shock protein activities, immune response, and cellular oxidative stress were identified, indicating their importance in HS response. Various CNVs and CNVRs were identified in the genome of the crossbred pig population evaluated. Fifteen CNVRs were significantly associated with physiological and anatomical indicators of HS response in lactating sows. Several genes involved in immune and stress responses overlapped with the CNVRs, suggesting that these CNVRs might contribute to climatic resilience in pigs during the lactation stage.

Keywords: climatic resilience; genomic prediction; non-additive genetic effects; pleiotropy; genome-wide association study; copy number variation.

RESUMO

OLIVEIRA, Letícia Fernanda de, D.Sc., Universidade Federal de Viçosa, março de 2024. **Investigando a arquitetura genética da resposta ao estresse térmico por calor e características relacionadas em suínos**. Orientadora: Renata Veroneze. Coorientador: Luiz Fernando Brito.

O aquecimento global apresenta um desafio significativo para a produção animal, impactando o bem-estar e o desempenho animal. O aumento resultante nas temperaturas promove o estresse térmico (HS) na produção animal, destacando a necessidade de criar animais mais resilientes. A melhoria da tolerância ao calor poderia ampliar a capacidade dos animais de lidar com condições de HS. Para promover o melhoramento da resiliência ao HS, é crucial entender a arquitetura genética de características relacionados à resiliência e os mecanismos genéticos subjacentes à resposta ao HS. Este estudo teve como objetivo investigar a arquitetura genética de indicadores de resposta ao HS e características relacionados em suínos, apresentando três objetivos principais. Primeiro, avaliar o impacto dos efeitos genéticos não aditivos na estimativa de componentes de variância em dois bancos de dados independentes: populações cruzadas e puras, e na predição genômica em uma população pura. Segundo, identificar regiões genômicas, genes candidatos e variantes pleiotrópicas potencialmente associadas a indicadores de resposta ao HS em porcas lactantes usando dados imputados de sequência completa do genoma (WGS). Terceiro, detectar variações no número de cópias (CNVs) e regiões de CNV (CNVRs) em suínos e explorar suas associações com indicadores fisiológicos e anatômicos de resposta ao HS mensurados em porcas lactantes cruzadas (Large White x Landrace). A inclusão de efeitos genéticos não aditivos nos modelos não melhorou a acurácia dos valores genômicos para características de desempenho em suínos puros. No entanto, houve um reordenamento significativo de candidatos à seleção dependendo do modelo ajustado. Baixas estimativas de variância genética não-aditiva foram observadas

para a maioria dos indicadores de resposta ao HS em suínos cruzados, exceto para escore de ofegação e densidade de pelos. Indicadores fisiológicos e anatômicos de resposta ao HS em porcas lactantes apresentaram variância genética aditiva, mas altamente poligênicos. Genes candidatos associados a atividades de proteínas de choque térmico, resposta imune e estresse oxidativo celular foram identificados, indicando sua importância na resposta ao HS. Várias CNVs e CNVRs foram identificados no genoma de suínos da população estudada. 15 CNVRs foram significativamente associados a indicadores fisiológicos e anatômicos de resposta ao HS em porcas lactantes. Vários genes envolvidos em respostas imunes e de estresse foram observados nas CNVRs, sugerindo que essas CNVRs podem contribuir para a resiliência climática em porcas durante o estágio de lactação.

Palavras-chave: resiliência climática; predição genômica; efeitos genéticos não aditivos; pleiotropia; estudo de associação genômica ampla; variação no número de cópias.

SUMMARY

CHAPTER 1: Genetic architecture for traits related to resilience in pigs

Introduction

Fitness can be defined as the ability of an individual or a genotype to survive in an environment and contribute to the gene pool of the following generation, leaving descendants after a given long period [1]. The concept of fitness is directly related to the ability of the individual or a class of genotypes to adapt to an environment. Individuals who do not have appropriate adaptability may become extinct if they cannot respond to environmental changes [1], such as global warming. The ability of a group of animals to respond to environmental changes and reproduce successfully, leaving offspring, is crucial for the population survival over multiple generations under natural or artificial selection.

It is important to highlight that the short and medium-term responses to environmental changes are acclimation and acclimatization, respectively, and these concepts differ from adaptation [2]. Acclimation refers to phenotypic and physiological responses in the short-term to a specific environmental stressor, while acclimatization is achieved when animals undergo to gene expression reprogramming, along with changes in metabolic pathways due to prolonged exposure to the stress factor [3, 4]. Despite that, adaptation is the long-term response that is achieved through physical or physiological modifications over time and involves both the occurrence of genotypic adaptations across generations and phenotypic changes when adverse environments persist over several generations [5, 6]. Typically, animals undergo acclimatization to environmental changes, resulting in induced phenotypic alterations rather than genetic changes, although these changes act to improve animals' fitness to the environment [5].

The ability of animals to respond to environmental changes has become an important concern in the livestock industry turning resilient and robust animals desirable in the production system. Resilience can be defined as the ability of the animal to be minimally affected by a disturbance or to rapidly return to the state before exposure to the disturbance [7]. On the other hand, Knap [8] defines robust pigs as animals that combine high production potential with resilience to external stressors, being able to express their high production potential in a wide variety of environmental conditions. According to Colditz and Hine [9], resilience tends to be expressed in response to environmental changes lasting for a matter of days while robustness is a consequence of longer lasting environmental conditions. Thus, resilience can be associated with acclimation and acclimatization, while robustness can be associated with adapted animals. Selecting for resilient animals that can reprogram their gene expression due to prolonged exposure to the stress factor can improve robustness in long-term.

To select animals more resilient and robust, that will present better performance under stressors conditions such as diseases and heat stress, it is crucial to understand the genetic architecture of fitness and resilience related traits as well as the genes and biological processes that might be acting on these traits. In this way, this review aimed to address the challenges associated with selecting for fitness and adaptation-related traits and explore the underlying genetic architecture in pigs.

Breeding for resilience-related traits

The importance of selecting for fitness has been discussed for a long time [8, 10]. However, it has been more focused on reproductive traits [8], particularly for maternal lines aiming to increase litter size and birth weight and decrease preweaning mortality, having as the final objective to obtain a higher number of finished pigs per sow. Although

selecting for reproductive traits is still important because their high economic impact in the swine industry, there are many fitness and resilience-related traits that lead to robustness and have not (or have recently) been included in breeding programs. Due to the differences in production systems with a vast variety of environmental conditions and the new challenges imposed by climate changes, the necessity of selecting for robust and disease resilient animals has become a relevant discussion [7–9, 11].

In recent years, which have been recorded as the warmest since the registration began [12], the climate changes have gained even more prominence. Raising animals in high temperatures can lead to heat stress conditions, resulting in reduced animal performance and economic losses. Heat stress becomes an even more significant issue in swine production because pigs lack functional sweat glands, making it difficult for them to dissipate heat. Besides that, heat stress also presents negative effects on immune responses [13] making the animals more susceptible to diseases. The globalization and increased transportation of animals and products have also increased the risk of pathogen transmission, leading to the emergence of endemic diseases and outbreaks in many animal production systems. Therefore, selection for disease resilience has also become a relevant goal in many breeding programs [11].

Breeding animals for resilience to heat stress and disease is a way to improve animal welfare [9]. Additionally, it increases the profit in the pig industry due to reducing health and labor costs [7]. Furthermore, it can also reduce the decrease in production during disturbances such as heat stress and disease outbreaks. However, selecting for resilience can be challenging, since pigs under selection are placed in nucleus herds with highly controlled environments. In such environments, they may not experience the same natural stressors and challenges as animals in commercial production. The primary challenge in selecting for resilience lies in obtaining phenotypic data to be used to predict

the breeding values. Although progeny testing can be utilized to measure performance under disease or heat stress challenges, these approaches tend to be costly and pose difficulties in designing and recording phenotypes on a large scale [11].

Another challenge to be addressed is defining the phenotypes to be collected and included in the genetic evaluations since it is difficult to measure resilience directly. Thus, it is crucial to identify traits that can serve as indicators of resilience and understand the underlying mechanisms involved in responding to challenges as heat stress and disease. These traits should enable the identification of animals that exhibit reduced sensitivity or rapid recovery from the disturbances. Several studies have evaluated animals' response to disease challenges or heat stress analyzing parameters such as hormonal levels and immune responses [14–18].

The levels of hormones, such as cortisol and thyroid hormones, after a disturbance present additive genetic variance and they can be associated with resilience [17, 19], since those hormones are involved in stress response. Moreover, immunity traits present substantial genetic variation, however, most of the immunity traits are not highly correlated, implying that most of these traits should be included in a selection index to provide adequate genetic gain for immune response [16]. It is desirable that phenotypes to measure resilience should be biologically relevant and easy to measure, presenting low cost and being non-invasive [2]. In this way, the inclusion of blood parameters may not be suitable to be used in breeding programs. Therefore, alternative phenotypic measurements that align with these criteria should be explored to effectively assess resilience in breeding programs.

Phenotypes, such as behavior and body temperature, that are easier to measure can be used to evaluate animals’ response to heat stress and disease challenges. Body temperature, such as rectal temperatures can indicate the ability of the animal to dissipate

heat and keep euthermia under heat stress [2, 14] and/or fever as a response to a disease challenge. Another phenotype that can be measured, particularly to evaluate resilience to heat stress, is the respiration rate which is the main way to dissipate heat via evaporation in pigs [2, 6]. Additionally, the use of new technologies to collect phenotypes can be explored, such as images to evaluate changes in animal behavior due to a stressor and infrared thermography for measuring body surface temperature [15]. The use of cameras to obtain images and infrared thermography is a non-invasive method for rapidly obtaining phenotypic data that are efficient, reliable, and have no impact on animal welfare [15].

Colditz and Hine [9] suggest measuring production/performance traits when the animals are exposed to the stressor and calculate the deviation between observed production and estimated production should be a good indicator of resilience. However, as presented by Berghof et al. [7], this proposed measure does not cover the whole concept of resilience, since some animals can present a severe drop in production but might have a rapid recover. Then, Berghof et al. [7] proposed the use of variation of deviations, autocorrelation of deviations, and skewness of deviations of the individuals' performance that allows to capture the severity and duration of environmental perturbation. According to Berghof et al. [7], resilient animals are expected to present a small variance, and both autocorrelation and skewness around zero.

Does resilience-related traits have genetic variability?

A trait to be included in a breeding program should present economic relevance and genetic variability. In this way, it is important to know the variance components and heritability of the traits to estimate the expected genetic gains. Cheng et al. [20] reported that resilience to a polymicrobial natural disease challenge present genetic variability and

125 can be improved by selection. They observed that subjective health score, treatment, and
126 mortality rates presented low heritability estimates, while performance traits under
127 disease challenge had moderate to high heritability estimates. Cheng et al. [20] derived
128 resilience indicator traits from day-to-day variation in feed intake, which had low to
129 moderate heritability estimates, suggesting that these resilience indicator traits can be
130 used for the selection of more resilient animals.

131 Resilience is modulated by immunity [21], then more resilient animals also
132 present better immune responses when exposed to challenges. Immune responses to
133 diseases have been reported as having moderate to high heritability estimates. Flori et al.
134 [16] observed that almost of 54 immune traits measured in a pig population three weeks
135 after vaccination against *Mycoplasma hyopneumoniae* presented moderate to high
136 heritability estimates. These immune traits comprised traits related to immune response
137 (e.g., phagocytosis, lymphocyte proliferation) or traits related to total leukocyte and
138 leukocyte subpopulation counts. Bai et al. [18] observed that most of the complete blood
139 count traits measured at 2-weeks before, and at 2- and 6- weeks after a natural disease
140 challenge have moderate heritability, ranging from 0.11 ± 0.03 to 0.27 ± 0.04. Bai et al.
141 [18] also evaluated the treatment rate for each animal, which was the number of treatment
142 events in the natural challenge, standardized by the number of days spent in the natural
143 challenge, observing heritability estimate of 0.04 ± 0.01.

144 Besides acknowledging the genetic parameters for the traits, it is also important
145 to understand that how/when the phenotype is recorded might also influence the
146 estimates. In a study evaluating rectal and cutaneous temperatures measured twice a day
147 (at 0700 h and 1200 h) in a tropical humid climate, Gourdine et al. [22] used a random
148 regression model to estimate heritability as a function of days in lactation. They found
149 that heritability estimates were generally lower in the early days of lactation, with the

largest heritabilities and genetic variances estimated in mid-lactation. Based on these findings, Gourdine et al. [22] suggest that measurements taken during the middle of lactation and at 1200 h are best for discriminating heat-tolerant animals.

It is also relevant to highlight that the same traits may exhibit distinct levels of genetic variability in the presence of a stressor factor compared to when the factor is absent. For example, Scanlan et al. [23] verified greater heritability and additive genetic variance estimates for reproductive performance during porcine reproductive and respiratory syndrome (PRRS) and porcine epidemic diarrhea outbreaks. On the other hand, Tiezzi et al. [24] verified that heritability estimates were higher under comfortable conditions compared to HS conditions (greater than 0.05 vs. 0.02 for total number of piglets born; 0.10 vs. 0.05 for number of piglets born alive; greater than 0.20 vs. 0.10 for average piglet birth weight). They also observed a decrease in heritability estimates with increasing relative humidity, which is one of the environmental factors that hinders heat dissipation.

Freitas et al. [25], considering a population of Large White pigs, found different patterns of heritability estimates when using genomic reaction norm models. It was observed an increase in heritability (h^2) estimates as the values of environmental variables, such as mean temperature, average relative humidity, and temperature-humidity index increased for total number of piglets born (h^2 ranging from 0.09 to 0.12), number of piglets born alive (h^2 ranging from 0.08 to 0.12), and number of stillborn piglets (h^2 ranging from 0.04 to 0.09). However, for the number of piglets weaned (h^2 ranging from 0.07 to 0.31), and weaning weight (h^2 ranging from 0.05 to 0.26), higher heritability estimates were observed at extreme values of environmental variables, while lower estimates were found closer to the mean.

When analyzing hot carcass weight in animals under heat stress and thermoneutral conditions as two distinct traits in a bivariate animal model, Dodd et al. [26] obtained a higher heritability for the trait under HS ($h^2 = 0.25$) compared to conditions without HS ($h^2 = 0.20$). They also found a genetic correlation of 0.63 between the two traits. Based on the changes in heritability and genetic correlation, hot carcass weight under HS and thermoneutral conditions were determined to be distinct traits, indicating the need of separate selection [26].

The heritability estimates are in general low to moderate and vary across the stages of life and how the traits are measured. Genetic parameters for traits related to resilience reported in literature are presented in Table 1. Heritability estimates for traits such as rectal temperature vary across the stages of life and how the traits are measured. The use of new technologies, such as computation vision, can provide more precise phenotypes that can also help to provide more accurate breeding values estimates. The inclusion of resilience related traits in breeding programs combined with genomic prediction can increase the genetic gains for resilience in pigs.

Table 1. Heritability estimates (h^2) for resilience-related traits in pigs.

Physiologic stage	N[a]	Trait	h^2	Reference
Newborn pigs	415	RT[1]	0.10 - 0.55	Varona et al. [27]
	395	RT[2]	0.02 - 0.58	
Lactating sows	842	RT[3]	0.35 ± 0.09	Gourdine et al. [22]
	245	CT[4]	0.34 ± 0.12	
	403	RR[5]	0.39 ± 0.13	
Prepubertal gilts	214	ΔRT[6]	0.49	Kim et al. [28]
		ΔRR[7]	0.39	
Postpubertal gilts	91	ΔRT[6]	0.83	
Growing pigs at 19 weeks of age	630	RT[8]	0.04 ± 0.05 to 0.13 ± 0.07	Gourdine et al. [29]
	663	RT[9]	0.12 ± 0.07 to 0.17 ± 0.07	

Growing pigs at 23 weeks of age	627	RT[8]	0.07 ± 0.06 to 0.34 ± 0.12	
	663	RT[9]	0.08 ± 0.06 to 0.10 ± 0.05	
Nursery pig at 6 weeks of age	298	$Cortisol_{ACTH}$[10]	0.68 ± 0.12	Larzul et al. [19]
	298	$Cortisol_{basal}$[11]	0.36 ± 0.09	
Nursery pig at 6 weeks of age	1792	T3[12]	0.16 ± 0.05	Goor et al. [17]
Fetuses at 96 or 105 days	1187	T3[13]	0.10 ± 0.06	
	1187	T4[14]	0.10 ± 0.06	

[a]Number of animals used on the study.

[1]Rectal temperature at birth; [2] Rectal temperature 30 minutes after birth; [3]Rectal temperature; [4]Cutaneous temperature; [5]Respiration rate; [6]Change in prepubertal rectal temperature from thermoneutral conditions to heat stress environment; [7]Change in prepubertal respiration rate from thermoneutral conditions to heat stress environment; [8]Rectal temperature in temperate environment; [9]Rectal temperature in tropical environment; [10]Cortisol concentration 1 hour after adrenocorticotropic hormone injection; [11]Basal cortisol level; [12]Triiodothyronine (T3) level measured in serum at 11 days post inoculation with Porcine Reproductive and Respiratory Syndrome (PRRS); [13]Triiodothyronine (T3) level measured in serum at 12 or 21 days post maternal inoculation with PRRS; [14]Thyroxine (T4) level measured in serum at 12 or 21 days post maternal inoculation with PRRS.

Genetic correlations between resilience traits

For a trait to be included in a breeding program, it must exhibit genetic variability. However, it is equally important to comprehend the genetic relationship between the selected traits. Based on the genetic correlations between resilience-related traits, it is possible to define which traits should be included in the breeding program. It is also crucial to know the genetic correlations between resilience-related traits and production traits to promote desirable genetic gains for all traits. This knowledge allows a comprehensive assessment of how the trait interacts with and impacts other desired traits within the breeding program.

For thermoregulatory traits, Gourdine et al. [22] observed high and positive correlations between rectal temperature and cutaneous temperature, and moderate and positive correlations between respiration rate and both rectal and cutaneous temperatures. For immune response traits, Bai et al. [18] observed that complete count blood traits showed moderate to high correlations with treatment rates, indicating that a well-

206 functioning immune system plays an important role in the resilience of the animals. A
207 more recent study reported that it is plausible to perform a multi-trait selection for
208 immunocompetence in pigs since there are high genetic correlations between innate and
209 adaptive traits and the molecular markers for T helper, memory T-helper, and γδ T cells
210 [30]. Furthermore, the selection for resilience under one disease can improve the
211 resilience for other diseases that affect pig production, as reported by Scanlan et al. [23],
212 who observed high genetic correlations between porcine reproductive and respiratory
213 syndrome (PRRS) and porcine epidemic diarrhea (PED) statuses.

214 Putz et al. [31] derived some traits to evaluate the variability of feed intake and
215 the time spent at the feeder: root mean square error (RMSE) within animal from the
216 regression of feed intake ($RMSE_{FI}$) and feeding duration ($RMSE_{DUR}$), quantile regression
217 for feed intake (QR_{FI}) and for feeding duration (QR_{DUR}). The resilience traits derived by
218 Putz et al. [31] presented positive and moderate genetic correlations between them,
219 however, these traits presented positive moderate to high genetic correlations with
220 mortality and treatment rate. Putz et al. [31] also verified negative and high genetic
221 correlations between both QR_{FI} and QR_{DUR} with production traits. The results observed
222 by Putz et al. [31] suggest that the traits proposed by them can be used in a breeding
223 program to obtain more resilient animals.

224 A comprehensive understanding of the genetic relationship between resilience and
225 production traits is important when selecting animals that are both resilient and
226 productive. This knowledge facilitates the identification of individuals with optimal
227 genetic potential, leading to improved genetic gains and a more economically efficient
228 production system. Cheng et al. [32] reported strong negative genetic correlations of
229 growth rate in a challenge nursery with treatment and mortality rates in the MHC region.
230 They also found a strong positive genetic correlation between growth rate in the challenge

nursery and growth rate in the finisher. Van Goor et al. [17] also reported that thyroid hormone levels following PRRSV infection had positive genetic correlations with growth rate. In a natural disease challenge, Van Goor et al. [17] observed that resilience indicator traits derived from day-to-day variation in feed intake had strong genetic correlations with treatment and mortality rates, while treatment and mortality rates and subjective health scores were genetically highly correlated with each other.

Acknowledging how the resilience traits are genetically correlated with each other and their genetic correlations with other traits of economic interest, such as growth rate and mortality, helps to define the traits to be included in a breeding program. The genetic correlation estimates are also required when calculating selection indexes, which are essential tools for selecting animals with enhanced resilience and productivity. By employing selection indexes, a balanced approach can be achieved, effectively considering both resilience and production factors in the breeding process, since the traits present a weight according to their economic values and/or desirable genetic gain to be achieved.

Genome-wide association studies for resilience-related traits

The identification of genomic regions that explain different proportions of genetic variance for resilience-related traits through genome-wide association studies (GWAS), allows the identification of candidate genes within these regions and provides insights into the biological mechanisms involved in resilience.

Using a single-step approach to estimate marker effects, Tiezzi et al. [24] identified many significant genomic windows distributed across all autosomes associated with heat tolerance based on reproductive traits. However, each of the identified windows explained no more than 0.5% of the additive genetic variance, indicating that heat

256 tolerance is a widely polygenic trait. The genomic regions identified by Tiezzi et al. [24]
257 have previously been reported to be associated with traits such as body temperature,
258 hemoglobin content, stress coping behavior, cortisol levels, heart size, and various
259 pathways associated with fatty acid biosynthesis. The analyses performed by Tiezzi et al.
260 [24] confirm that the heat stress-indicative traits analyzed are involved in important
261 biological mechanisms for the response to heat stress.

262 Conducting GWAS for hot carcass weight under HS or thermoneutral conditions,
263 Dodd et al. [26] identified the genes *CEP44*, which may be linked to the ability to
264 maintain cell division under HS conditions; *FBXO8*, a gene involved in the ubiquitination
265 system that is associated with various cellular processes (cell cycle and division,
266 apoptosis, antigen processing, among others) and *HPGD*, a gene involved in
267 prostaglandin metabolism, which is implicated in inflammatory processes, a common
268 response to bodily stress or infection. Isolated peaks were also identified on chromosome
269 1, which were associated with growth factors and body mass deposition, and on
270 chromosome 14, associated with disease susceptibility, subcutaneous fat thickness, and
271 nutrient utilization.

272 Kim et al. [28], using a limited number of observations, did not identify significant
273 markers associated with respiration rate, rectal temperature, and skin temperature.
274 However, despite the limitations, Kim et al. [28] did identify some genes known to be
275 involved in physiological adaptation to general stresses. Nonetheless, further studies with
276 larger sample sizes need to be conducted to identify genes and metabolic pathways
277 involved in pig thermoregulation.

278 Other studies have investigated the disease resilience and immune response during
279 disease challenges. Investigating disease resilience in pigs through complete blood count
280 traits, Bai et al. [33] identified five genomic regions associated with white blood cells and

nine genomic regions associated with red blood cells and platelet traits. Bai et al. [33] reported that the genes nearby the identified genomic regions have a potential role in immune response pathways that influence disease resilience. In a large-scale natural polymicrobial disease challenge, Cheng et al. [32] found that the major histocompatibility complex (MHC) and other immune-related genes are linked to disease resilience features. Cheng et al. [32] also observed that the associated genomic regions contained genes that were differentially expressed following bacteria or virus infection and immune stimulation are involved in functional pathways related to inflammatory immune response, and these regions were also enriched with QTL related to disease susceptibility and immune capacity.

There is still a need for more studies evaluating the genetic architecture, genes, and biological pathways of resilience. So far, it is possible to understand that resilience traits are very polygenic and are associated with a variety of biological mechanisms and pathways including stress coping behavior, cortisol levels, and immune response pathways.

Non-additive genetic effects in resilience traits

Non-additive genetic effects refer to the influence of genetic factors that cannot be explained by adding up the effects of individual genes, i.e., additive effects, and the main non-additive genetic effects are dominance and epistasis. Dominance is the effect due to the interactions between alleles at the same locus, while epistasis is the interactions of alleles from two or more loci [34]. For the interactions between two loci, there are three types of epistasis: additive-by-additive, additive-by-dominance, and dominance-by-dominance. Wade et al. [35] summarized that additive-by-additive epistasis is the interactions between homozygotes at both loci, additive-by-dominance epistasis is the

306 interactions between homozygotes at locus A and heterozygotes at locus B and vice-versa,
307 and dominance-by-dominance epistasis is the interactions between heterozygotes at both
308 loci.

309 Non-additive genetic effects are reported to play an important role in heterosis,
310 which refers to the superior mean of crossbred offspring compared to the average
311 performance of its purebred parents [36–38]. Crossbreeding schemes are widely explored
312 in pig production, therefore it is important to evaluate the impact of non-additive genetic
313 effects on the traits of interest. Non-additive genetic effects have been reported to have
314 more influence on adaptation and fitness traits than on performance and morphological
315 traits [39–42]. Culbertson et al. [43] observed significant dominance variance for number
316 of piglets born alive and litter weight, while Vitezica et al. [44] reported substantial
317 dominance and epistasis variance for litter size, and Lopes et al. [45] identified significant
318 quantitative trait loci (QTL) with additive and dominance effects for teat number.

319 Non-additive genetic effects also play a significant role in some fertility and
320 reproduction traits in Holstein cattle, with epistasis being more relevant than dominance
321 effects [46, 47]. It was also observed that non-additive genetic effects significantly
322 influence survival and fitness-related traits in Atlantic salmon [48, 49]. In summary, non-
323 additive genetic effects influence fitness and adaptation traits in many species, and it is
324 expected that traits related to resilience are also substantially influenced by non-additive
325 genetic effects, especially in crossbred pigs that are used in commercial herds. Thus, other
326 studies with a focus on non-additive effects for resilience traits must be carried out to
327 improve our understanding of these traits.

328

CNVs: variation structures

Copy number variation (CNV) is a genomic phenomenon where individuals within a population have different numbers of copies of a given gene or genomic region. CNV is defined as a segment of DNA 1 kilobase (kb) or larger, manifested with a variable copy number, involving either gain (duplication) or loss (deletion) of copies in a particular DNA segment [50]. CNV serves as a source of genetic variation influencing phenotypes that may modify gene expression within and near the rearranged region, contributing to phenotypic diversity and evolution [51].

The CNVs might represent an adaptive mutation stimulated by specific environmental factors, rather than occurring randomly [52, 53]. The CNVs have been shown to impact gene dosage, gene structure, and the regulation of recessive alleles, thereby influencing phenotypic traits related to adaptation, disease resistance, and environmental stress tolerance [53, 54]. Furthermore, Wang et al. [54] highlighted that CNVs have been found to affect essential biological processes, metabolic functions, and cellular components. For example, CNVs have been associated with genes related to heat shock proteins (HSPs), which play a crucial role in environmental stress tolerance and adaptation in climates with heat stress. Paudel et al. [55] reported that CNVs contribute to adaptation by enriching genes related to sensory perception, neurological processes, and response to stimulus, as well as variations in antimicrobial-related and detoxification genes, indicating their potential role in adaptation to the wild pigs and behavioral changes during pig domestication.

The CNVs can lead to the evolution of new genes and gene functions, impacting phenotypes and potentially conferring resilience to specific environmental challenges [55]. Moreover, Paudel et al. [55] observed that larger populations tend to have more CNV regions, reflecting the demographic history and suggesting that CNVs are reflective

of adaptation to different environments. As highlighted by Cayuela et al. [53], CNVs play a crucial role in influencing fitness-related traits and local environmental conditions, such as temperature, in marine fish populations. Lauer et al. [56] observed that CNVs can confer a fitness benefit and increase the amount of DNA in the genome that can accumulate mutations, potentially increasing the rate of adaptive evolution, and driving rapid adaptive evolution in microbial populations.

In summary, the adaptive potential of CNVs contributes to rapid evolutionary changes in various scenarios, making them a crucial aspect of genetic variation. The identification and comprehension of CNVs offer valuable insights into the genetic background of resilience and adaptation to specific environmental conditions. This understanding can be applied to the selection of animals more resilient by providing insights into the genetic mechanisms that underlie adaptation, potentially informing breeding strategies aiming at enhancing resilience in specific environments.

Final considerations

Fitness and adaptation play crucial roles in survival and effective reproduction in challenging environments. The response to immediate environmental changes is reflected in acclimation traits, while acclimatization involves more lasting genetic and physiological modifications in response to prolonged stress. The need to select more resilient and robust pigs has become even more relevant due to climate change and the increasing in thermal and disease stresses. Selecting for resilience becomes challenging due to the difficulty of obtaining accurate and large-scale phenotypic data in highly controlled environments. Then, it is important to identify traits indicative of resilience, such as behavior, body temperature, and immune response. These traits can serve as valuable indicators of resilience and should therefore be carefully chosen for inclusion in

379 selection programs. Studies on the heritability of resilience-related traits indicate that
380 many of these traits are moderately to highly heritable, suggesting that the inclusion of
381 these traits in breeding programs, combined with genomic prediction, can lead to
382 significant genetic gains. Additionally, genetic correlations between these traits offer
383 insights into the indirect genetic gain achievable in one trait through selection for another.
384 The genetic correlations also help determine which resilience-related traits should be
385 included in a selection index within a breeding program.

386 The GWAS revealed that many of these traits are polygenic, influenced by
387 multiple loci. These studies identified genes and biological pathways associated with
388 response to heat stress, disease resistance, and other resilience traits. However, more
389 research is needed for a comprehensive understanding of the genetic architecture of these
390 traits. Additionally, non-additive effects, such as dominance and epistasis, might play an
391 important role in traits associated with adaptation and fitness, highlighting the complexity
392 of the genetic basis of these traits, especially in crossbred pigs that explore heterosis.
393 Finally, CNVs can influence gene expression and modulate phenotypes associated with
394 resilience. Understanding this structural variation in the genome can be fundamental for
395 more effective selection strategies. A deep understanding of these genetic aspects can
396 contribute to more efficient genetic improvement programs, aiming for more adaptable,
397 disease-resistant, and productive pigs in challenging environments.

398

399 **References**

400 1. Barker JSF. Defining fitness in natural and domesticated populations. In: Adaptation
401 and fitness in animal populations: evolutionary and breeding perspectives on
402 genetic resource management. Springer; 2009. p. 3–14.
403 2. Gourdine JL, Rauw WM, Gilbert H, Poullet N. The Genetics of Thermoregulation in
404 Pigs: A Review. Frontiers in Veterinary Science. 2021;8.

405 3. Collier RJ, Gebremedhin KG. Thermal biology of domestic animals. Annu Rev Anim
406 Biosci. 2015;3:513–32.
407 4. Archana P, Aleena J, Pragna P, Vidya M, Abdul Niyas P, Bagath M, et al. Role of heat
408 shock proteins in livestock adaptation to heat stress. Journal of Dairy, Veterinary
409 & Animal Research. 2017;Volume 5 Issue 1.
410 5. Collier RJ, Baumgard LH, Zimbelman RB, Xiao Y. Heat stress: Physiology of
411 acclimation and adaptation. Animal Frontiers. 2019;9:12–9.
412 6. Johnson JS. Heat stress: Impact on livestock well-being and productivity and mitigation
413 strategies to alleviate the negative effects. Animal Production Science.
414 2018;58:1404–13.
415 7. Berghof TVL, Poppe M, Mulder HA. Opportunities to improve resilience in animal
416 breeding programs. Front Genet. 2019;10 JAN:410180.
417 8. Knap PW. Breeding robust pigs. Aust J Exp Agric. 2005;45:763–73.
418 9. Colditz IG, Hine BC. Resilience in farm animals: biology, management, breeding and
419 implications for animal welfare. Anim Prod Sci. 2016;56:1961–83.
420 10. Tholen E, Bunter KL, Hermesch S, Graser HU. The genetic foundation of fitness and
421 reproduction traits in Australian pig populations. 2. Relationships between
422 weaning to conception interval, farrowing interval, stayability, and other common
423 reproduction and production traits. Aust J Agric Res. 1996;47:1275–90.
424 11. Bai X, Plastow GS. Breeding for disease resilience: opportunities to manage
425 polymicrobial challenge and improve commercial performance in the pig
426 industry. CABI Agriculture and Bioscience 2022 3:1. 2022;3:1–17.
427 12. NOAA National Centers for Environmental Information. Monthly Global Climate
428 Report for Annual 2022. 2023.

13. Chauhan SS, Rashamol VP, Bagath M, Sejian V, Dunshea FR. Impacts of heat stress on immune responses and oxidative stress in farm animals and nutritional strategies for amelioration. International Journal of Biometeorology 2021 65:7. 2021;65:1231–44.

14. Renaudeau D, Collin A, Yahav S, De Basilio V, Gourdine JL, Collier RJ. Adaptation to hot climate and strategies to alleviate heat stress in livestock production. In: Animal. 2012. p. 707–28.

15. Sejian V, Bhatta R, Gaughan JB, Dunshea FR, Lacetera N. Review: Adaptation of animals to heat stress. Animal. 2018;12:S431–44.

16. Flori L, Gao Y, Laloë D, Lemonnier G, Leplat JJ, Teillaud A, et al. Immunity Traits in Pigs: Substantial Genetic Variation and Limited Covariation. PLoS One. 2011;6:e22717.

17. Van Goor A, Pasternak A, Walugembe M, Chehab N, Hamonic G, Dekkers JCM, et al. Genome wide association study of thyroid hormone levels following challenge with porcine reproductive and respiratory syndrome virus. Front Genet. 2023;14:1110463.

18. Bai X, Putz AM, Wang Z, Fortin F, Harding JCS, Dyck MK, et al. Exploring Phenotypes for Disease Resilience in Pigs Using Complete Blood Count Data From a Natural Disease Challenge Model. Front Genet. 2020;11:507546.

19. Larzul C, Terenina E, Foury A, Billon Y, Louveau I, Merlot E, et al. The cortisol response to ACTH in pigs, heritability and influence of corticosteroid-binding globulin. animal. 2015;9:1929–34.

20. Cheng J, Putz AM, Harding JCS, Dyck MK, Fortin F, Plastow GS, et al. Genetic analysis of disease resilience in wean-to-finish pigs from a natural disease challenge model. J Anim Sci. 2020;98:1–14.

454 21. Dantzer R, Cohen S, Russo SJ, Dinan TG. Resilience and immunity. Brain Behav
455 Immun. 2018;74:28–42.
456 22. Gourdine JL, Mandonnet N, Giorgi M, Renaudeau D. Genetic parameters for
457 thermoregulation and production traits in lactating sows reared in tropical climate.
458 Animal. 2017;11:365–74.
459 23. Scanlan CL, Putz AM, Gray KA, Serão NVL. Genetic analysis of reproductive
460 performance in sows during porcine reproductive and respiratory syndrome
461 (PRRS) and porcine epidemic diarrhea (PED) outbreaks. J Anim Sci Biotechnol.
462 2019;10:1–12.
463 24. Tiezzi F, Brito LF, Howard J, Huang YJ, Gray K, Schwab C, et al. Genomics of Heat
464 Tolerance in Reproductive Performance Investigated in Four Independent
465 Maternal Lines of Pigs. Front Genet. 2020;11.
466 25. Freitas PHF, Johnson JS, Chen S, Oliveira HR, Tiezzi F, Lázaro SF, et al. Definition
467 of Environmental Variables and Critical Periods to Evaluate Heat Tolerance in
468 Large White Pigs Based on Single-Step Genomic Reaction Norms. Front Genet.
469 2021;12.
470 26. Dodd GR, Gray K, Huang Y, Fragomeni B. Single-Step GBLUP and GWAS Analyses
471 Suggests Implementation of Unweighted Two Trait Approach for Heat Stress in
472 Swine. Animals. 2022;12.
473 27. Varona L, Casellas J, Piedrafita J, Sá Nchez † A, Garcia-Casado P, Arqué M, et al.
474 Bayes factor analysis for the genetic background of physiological and vitality
475 variables of F 2 Iberian × Meishan newborn piglets 1. 2005.
476 28. Kim K-S, Seibert JT, Edea Z, Graves KL, Kim E-S, Keating AF, et al.
477 Characterization of the acute heat stress response in gilts: III. Genome-wide
478 association studies of thermotolerance traits in pigs RUNNING HEAD: Genetic

479 control of heat stress response in gilts. 2018.
480 https://doi.org/10.1093/jas/sky131/4970896.
481 29. Gourdine JL, Riquet J, Rosé R, Poullet N, Giorgi M, Billon Y, et al. Genotype by
482 environment interactions for performance and thermoregulation responses in
483 growing pigs,. J Anim Sci. 2019;97:3699–713.
484 30. Ballester M, Jové-Juncà T, Pascual A, López-Serrano S, Crespo-Piazuelo D,
485 Hernández-Banqué C, et al. Genetic architecture of innate and adaptive immune
486 cells in pigs. Front Immunol. 2023;14:1058346.
487 31. Putz AM, Harding JCS, Dyck MK, Fortin F, Plastow GS, Dekkers JCM. Novel
488 resilience phenotypes using feed intake data from a natural disease challenge
489 model in wean-to-finish pigs. Front Genet. 2019;10 JAN:388793.
490 32. Cheng J, Fernando R, Cheng H, Kachman SD, Lim KS, Harding JCS, et al. Genome-
491 wide association study of disease resilience traits from a natural polymicrobial
492 disease challenge model in pigs identifies the importance of the major
493 histocompatibility complex region. G3 Genes|Genomes|Genetics. 2022;12.
494 33. Bai X, Yang T, Putz AM, Wang Z, Li C, Fortin F, et al. Investigating the genetic
495 architecture of disease resilience in pigs by genome-wide association studies of
496 complete blood count traits collected from a natural disease challenge model.
497 BMC Genomics 2021 22:1. 2021;22:1–15.
498 34. Falconer DS, Mackay TFC. Introduction to Quantitative Genetics. 4th edition.
499 Harlow, Essex, UK: Longmans Green; 1996.
500 35. Wade MJ, Winther RG, Agrawal AF, Goodnight CJ. Alternative definitions of
501 epistasis: dependence and interaction. Trends Ecol Evol. 2001;16:498–504.
502 36. William RL, Pollak E. Theory of Heterosis. J Dairy Sci. 1985;68:2411–7.

503 37. Bunning H, Wall E, Chagunda MGG, Banos G, Simm G. Heterosis in cattle
504 crossbreeding schemes in tropical regions: meta-analysis of effects of breed
505 combination, trait type, and climate on level of heterosis. J Anim Sci. 2019;97:29–
506 34.
507 38. Su G, Christensen OF, Ostersen T, Henryon M, Lund MS. Estimating Additive and
508 Non-Additive Genetic Variances and Predicting Genetic Merits Using Genome-
509 Wide Dense Single Nucleotide Polymorphism Markers. PLoS One. 2012;7.
510 39. Roff DA, Emerson K. EPISTASIS AND DOMINANCE: EVIDENCE FOR
511 DIFFERENTIAL EFFECTS IN LIFE-HISTORY VERSUS
512 MORPHOLOGICAL TRAITS. Evolution (N Y). 2006;60:1981–90.
513 40. Mackay TFC. Epistasis and quantitative traits: Using model organisms to study gene-
514 gene interactions. Nature Reviews Genetics. 2014;15:22–33.
515 41. Mackay TFC, Moore JH. Why epistasis is important for tackling complex human
516 disease genetics. Genome Medicine. 2014;6.
517 42. Merilä J, Sheldon BC. Genetic architecture of fitness and nonfitness traits: empirical
518 patterns and development of ideas. Heredity 1999 83:2. 1999;83:103–9.
519 43. Culbertson MS, Mabry JW, Misztal I, Gengler N, Bertrand JK, Varona L. Estimation
520 of dominance variance in purebred Yorkshire swine. J Anim Sci. 1998;76:448–
521 51.
522 44. Vitezica ZG, Reverter A, Herring W, Legarra A. Dominance and epistatic genetic
523 variances for litter size in pigs using genomic models. Genetics Selection
524 Evolution. 2018;50.
525 45. Lopes MS, Bastiaansen JWM, Harlizius B, Knol EF, Bovenhuis H. A genome-wide
526 association study reveals dominance effects on number of teats in pigs. PLoS One.
527 2014;9.

528 46. Alves K, Brito LF, Baes CF, Sargolzaei M, Robinson JAB, Schenkel FS. Estimation
529 of additive and non-additive genetic effects for fertility and reproduction traits in
530 North American Holstein cattle using genomic information. Journal of Animal
531 Breeding and Genetics. 2020;137:316–30.
532 47. Jiang J, Shen B, O'Connell JR, VanRaden PM, Cole JB, Ma L. Dissection of additive,
533 dominance, and imprinting effects for production and reproduction traits in
534 Holstein cattle. BMC Genomics. 2017;18:1–13.
535 48. Houde ALS, Black CA, Wilson CC, Pitcher TE, Neff BD. Genetic and maternal
536 effects on juvenile survival and fitness-related traits in three populations of
537 Atlantic salmon. Canadian Journal of Fisheries and Aquatic Sciences.
538 2015;72:751–8.
539 49. Houde AL, Wilson CC, Neff BD. Genetic architecture of survival and fitness-related
540 traits in two populations of Atlantic salmon. Heredity 2013 111:6. 2013;111:513–
541 9.
542 50. Feuk L, Carson AR, Scherer SW. Structural variation in the human genome. Nature
543 Reviews Genetics 2006 7:2. 2006;7:85–97.
544 51. Henrichsen CN, Chaignat E, Reymond A. Copy number variants, diseases and gene
545 expression. Hum Mol Genet. 2009;18:R1–8.
546 52. Hull RM, Cruz C, Jack C V., Houseley J. Environmental change drives accelerated
547 adaptation through stimulated copy number variation. PLoS Biol. 2017;15.
548 53. Cayuela H, Dorant Y, Mérot C, Laporte M, Normandeau E, Gagnon-Harvey S, et al.
549 Thermal adaptation rather than demographic history drives genetic structure
550 inferred by copy number variants in a marine fish. Mol Ecol. 2021;30:1624–41.

551 54. Wang MD, Dzama K, Rees DJG, Muchadeyi FC. Tropically adapted cattle of Africa:
552 Perspectives on potential role of copy number variations. Animal Genetics.
553 2016;47:154–64.
554 55. Paudel Y, Madsen O, Megens HJ, Frantz LAF, Bosse M, Bastiaansen JWM, et al.
555 Evolutionary dynamics of copy number variation in pig genomes in the context
556 of adaptation and domestication. BMC Genomics. 2013;14.
557 56. Lauer S, Avecilla G, Spealman P, Sethia G, Brandt N, Levy SF, et al. Single-cell copy
558 number variant detection reveals the dynamics and diversity of adaptation. PLoS
559 Biol. 2018;16.

CHAPTER 2: Investigating the impact of non-additive genetic effects in the estimation of variance components and genomic predictions for heat tolerance and performance traits in crossbred and purebred pig populations

Abstract

Background: Non-additive genetic effects are often ignored in livestock genetic evaluations. However, fitting them in the models could improve the accuracy of genomic breeding values. Furthermore, non-additive genetic effects contribute to heterosis, which could be optimized through mating designs. Traits related to fitness and adaptation, such as heat tolerance, tend to be more influenced by non-additive genetic effects. In this context, the primary objectives of this study were to estimate variance components and assess the predictive performance of genomic prediction of breeding values based on alternative models and two independent datasets, including performance records from a purebred pig population and heat tolerance indicators recorded in crossbred lactating sows.

Results: Including non-additive genetic effects when modelling performance traits in purebred pigs had no effect on the residual variance estimates for most of the traits, but lower additive genetic variances were observed, especially when additive-by-additive epistasis was included in the models. Furthermore, including non-additive genetic effects did not improve the prediction accuracy of genomic breeding values, but there was animal re-ranking across the models. For the heat tolerance indicators recorded in a crossbred population, most traits had small non-additive genetic variance with large standard error estimates. Nevertheless, panting score and hair density presented substantial additive-by-additive epistatic variance. Panting score had an epistatic variance estimate of 0.1379, which accounted for 82.22% of the total genetic variance. For hair density, the epistatic

This paper was published at BMC Genomic Data: https://doi.org/10.1186/s12863-023-01174-x

variance estimates ranged from 0.1745 to 0.1845, which represent 64.95% to 69.59% of the total genetic variance.

Conclusions: Including non-additive genetic effects in the models did not improve the accuracy of genomic breeding values for performance traits in purebred pigs, but there was substantial re-ranking of selection candidates depending on the model fitted. Except for panting score and hair density, low non-additive genetic variance estimates were observed for heat tolerance indicators in crossbred pigs.

Keywords: climatic resilience, dominance, epistasis, Landrace, Large White, maternal-line pigs.

Background

Phenotypes are the result of the individual genotypic value, environmental deviation, and interactions between genotype and the environment. The genotypic values can be divided in additive (breeding values) and non-additive genetic effects due to interactions between alleles at the same locus (dominance) and two or more loci (epistasis) [1]. Non-additive genetic effects are often ignored in livestock genetic evaluations due to the greater importance of additive effects for breeding value estimation, and the fact that breeding animals pass alleles and not genotypes to their offspring [2–5]. Furthermore, non-additive genetic effects can be confounded with non-genetic effects, such as maternal and permanent environmental effects, and the analyses incorporating non-additive genetic effects are often more complex and computationally demanding [4–6].

Although breeders are mainly interested in the estimates of breeding values, fitting non-additive genetic effects in the genomic prediction models can increase the accuracy

of the breeding values [7–9]. Furthermore, fitting non-additive genetic effects in the models can yield more accurate predictions of future performance and better mating plans to maximize offspring performance by exploring the combination of additive and non-additive genetic effects [2]. The increasing availability of large-scale genomic datasets has enabled the study of the non-additive actions of genes in numerous complex traits, including the evaluation of non-additive genetic effects in genomic prediction of breeding values (e.g., [2, 9, 10]), genome-wide association studies (e.g.,[11–13]), and the development of new methods for the estimation and applications of non-additive genetic effects in breeding programs [6, 9, 14–16]. It is also important to note that accounting for inbreeding in variance component estimation and genomic prediction ensures unbiased variance components, minimizes bias issues in the estimates, accounts for directional dominance, and prevents inflation of dominance variance estimates [17–19].

Non-additive genetic effects are expected to have a greater impact in crossbred performance as compared to purebred populations, mainly due to heterosis [20–22]. As pig production is based on crossbreeding schemes, it is important to evaluate the magnitude of non-additive effects for different traits measured on purebred and crossbred populations, as well as evaluate the impact of these effects on the predictive ability of genomic breeding values. In general, adaptation and fitness traits tend to be more influenced by non-additive genetic effects (e.g., [17, 22–24]). In this context, heat tolerance indicators are key fitness traits to be included in swine breeding programs for improving pig health, welfare, and production [25, 26]. Breeding for improved heat tolerance is becoming more important due to the increase in global temperatures that directly impact swine health, performance, and welfare [27, 28]. Although estimates of additive genetic variance and heritability have been reported for heat stress traits in pigs

This paper was published at BMC Genomic Data: https://doi.org/10.1186/s12863-023-01174-x

(e.g., [29–31]), the impact of non-additive effects on direct indicators of heat tolerance in crossbred pigs is still unknown.

Non-additive genetic effects can be of different magnitude in purebred and crossbred populations [20–22], as well for across traits with different genetic architecture. Therefore, there is a need to evaluate the impact of non-additive genetic effects into genomic prediction models for a diverse set of traits, including production, fitness, and adaptation, within both purebred and crossbred populations. In this context, the primary objectives of this study were to estimate additive and non-additive genetic variance components for different trait groups (i.e., production, fitness, and adaptation traits) in independent purebred and crossbred populations. In addition, the impact of non-additive effects in the accuracy of genomic prediction of purebred animals was evaluated.

Results

The results obtained are presented separately for each of the two datasets evaluated.

Dataset 1: Purebred pig population

Variance components and heritability estimates

Variance components and heritabilities were estimated for five traits representing phenotypes routinely collected from birth to breeding in a single nucleus pig line population [32]. Table 1 presents the estimates of variance components and Table 2 shows the estimates of heritability and non-additive genetic variance ratios for all five traits in the purebred pig population. All the fitted models converged for all traits, with the exception of the model including all non-additive genetic effects evaluated and inbreeding depression (MAIDE3) that did not converge for one of the traits (T3). When inbreeding was included as a covariate in the models, a small decrease in the additive

100 genetic variance was observed (Table 1). For most of the traits, lower residual and
101 additive genetic variance estimates were observed when incorporating non-additive
102 genetic effects in the analyses.

103 Low dominance variance components were estimated, ranging from 0 to 0.0576
104 for T1, T2, T3, and T4, and ranging from 138.0280 to 171.8660 for T5. Notably, the
105 dominance variance ratios across all traits were found to be small, accompanied by
106 relatively large standard errors. T5 had the highest dominance variance ratio, which
107 ranged from 0.0397 to 0.0437, while for the other traits it ranged from 0 to 0.0206.
108 However, the estimates of additive-by-additive epistatic variance were notably higher
109 than the dominance variance estimates. These ratios were approximately 0.12 for T1, 0.24
110 for T2, 0.28 to 0.43 for T3, 0.09 for T4, and 0.13 to 0.15 for T5, indicating a more
111 substantial contribution of additive-by-additive epistasis to the variance components for
112 these traits.

113 In general, there was a greater decrease in the additive genetic variance when
114 additive-by-additive epistasis was included in the models (MAE, MAIE, MADE1,
115 MAIDE1, MADE2, MAIDE2, MADE3, MAIDE3). However, for T1 the additive genetic
116 variance estimates also presented larger standard errors (Table 1), indicating that the
117 inclusion of epistasis in the model decreased precision of the additive genetic variance
118 estimates for T1. As a consequence of the decrease in the additive genetic variance, a
119 reduction in the heritability estimates (h_a^2) were observed when additive-by-additive
120 epistasis was fitted in the models (Table 2). Nevertheless, the variance components for
121 additive-by-dominance and dominance-by-dominance epistasis were small and their
122 variance ratios (h_{ad}^2 and h_{dd}^2) were close to zero for almost all traits, except T3.

123 **Table 1.** Variance component estimates based on models including or not inbreeding and non-additive genetic effects.

Trait	Model[1]	$\widehat{\sigma_a^2}$	$\widehat{\sigma_d^2}$	$\widehat{\sigma_{aa}^2}$	$\widehat{\sigma_{ad}^2}$	$\widehat{\sigma_{dd}^2}$	$\widehat{\sigma_e^2}$
T1	MA	0.0477 ± 0.0214	-	-	-	-	1.4103 ± 0.0418
	MAI	0.0463 ± 0.0214	-	-	-	-	1.4117 ± 0.0418
	MAE	0.0190 ± 0.0229	-	0.1864 ± 0.0942	-	-	1.2540 ± 0.0871
	MAIE	0.0169 ± 0.0229	-	0.1880 ± 0.0945	-	-	1.2545 ± 0.0871
	MAD	0.0477 ± 0.0214	8.92×10^{-8} ± 0.0000	-	-	-	1.4103 ± 0.0418
	MAID	0.0463 ± 0.0214	8.93×10^{-8} ± 0.0000	-	-	-	1.4117 ± 0.0418
	MADE1	0.0190 ± 0.0229	8.42×10^{-8} ± 0.0000	0.1864 ± 0.0956	-	-	1.2542 ± 0.0890
	MAIDE1	0.0169 ± 0.0229	9.89×10^{-8} ± 0.0000	0.1880 ± 0.0959	-	-	1.2547 ± 0.0890
	MADE2	0.0190 ± 0.0229	9.10×10^{-8} ± 0.0000	0.1864 ± 0.0942	9.96×10^{-7} ± 0.0000	-	1.2542 ± 0.0870
	MAIDE2	0.0169 ± 0.0229	9.11×10^{-8} ± 0.0000	0.1880 ± 0.0945	1.03×10^{-6} ± 0.0000	-	1.2547 ± 0.0870
	MADE3	0.0190 ± 0.0232	8.54×10^{-8} ± 0.0000	0.1864 ± 0.1030	4.67×10^{-7} ± 0.0000	1.16×10^{-6} ± 0.0000	1.2542 ± 0.2248
	MAIDE3	0.0169 ± 0.0232	8.45×10^{-8} ± 0.0000	0.1880 ± 0.1033	4.33×10^{-7} ± 0.0000	1.22×10^{-6} ± 0.0000	1.2547 ± 0.2249
T2	MA	0.2945 ± 0.0339	-	-	-	-	0.7975 ± 0.0277
	MAI	0.2946 ± 0.0340	-	-	-	-	0.7978 ± 0.0277

This paper was published at BMC Genomic Data: https://doi.org/10.1186/s12863-023-01174-x

T3	MAE	0.2276 ± 0.0355	-	0.2643 ± 0.0766	-	-	0.5943 ± 0.0617
	MAIE	0.2263 ± 0.0356	-	0.2665 ± 0.0768	-	-	0.5934 ± 0.0618
	MAD	0.2927 ± 0.0339	0.0221 ± 0.0240	-	-	-	0.7766 ± 0.0350
	MAID	0.2926 ± 0.0340	0.0224 ± 0.0238	-	-	-	0.7767 ± 0.0350
	MADE1	0.2266 ± 0.0354	0.0201 ± 0.0237	0.2625 ± 0.0768	-	-	0.5768 ± 0.0639
	MAIDE1	0.2250 ± 0.0355	0.0209 ± 0.0238	0.2651 ± 0.0768	-	-	0.5750 ± 0.0640
	MADE2	0.2267 ± 0.0354	0.0201 ± 0.0237	0.2625 ± 0.0768	$9.23x10^{-7}$ ± 0.0000	-	0.5768 ± 0.0639
	MAIDE2	0.2250 ± 0.0355	0.0209 ± 0.0238	0.2651 ± 0.0768	$9.20x10^{-7}$ ± 0.0000	-	0.5750 ± 0.0640
	MADE3	0.2267 ± 0.0354	0.0201 ± 0.0237	0.2625 ± 0.0768	$9.23x10^{-7}$ ± 0.0000	$1.20x10^{-6}$ ± 0.0000	0.5768 ± 0.0639
	MAIDE3	0.2250 ± 0.0355	0.0209 ± 0.0238	0.2651 ± 0.0768	$9.20x10^{-7}$ ± 0.0000	$1.20x10^{-6}$ ± 0.0000	0.5750 ± 0.0640
	MA	0.1881 ± 0.0257	-	-	-	-	0.7151 ± 0.0227
	MAI	0.1869 ± 0.0256	-	-	-	-	0.7158 ± 0.0227
	MAE	0.1049 ± 0.0239	-	0.3895 ± 0.0625	-	-	0.4094 ± 0.0494
	MAIE	0.1033 ± 0.0238	-	0.3901 ± 0.0625	-	-	0.4097 ± 0.0494
	MAD	0.1857 ± 0.0257	0.0186 ± 0.0207	-	-	-	0.6982 ± 0.0291
	MAID	0.1845 ± 0.0256	0.0194 ± 0.0209	-	-	-	0.6982 ± 0.0292

This paper was published at BMC Genomic Data: https://doi.org/10.1186/s12863-023-01174-x

	MADE1	0.1048 ± 0.0239	$1.10x10^{-7}$ ± 0.0000	0.3891 ± 0.0632	-	-	0.4090 ± 0.0506
	MAIDE1	0.1032 ± 0.0238	$1.43x10^{-7}$ ± 0.0000	0.3897 ± 0.0632	-	-	0.4093 ± 0.0506
	MADE2	0.1133 ± 0.0243	$2.61x10^{-7}$ ± 0.0000	0.2550 ± 0.0704	0.4553 ± 0.1227	-	0.0802 ± 0.0991
	MAIDE2	0.1118 ± 0.0243	$3.08x10^{-7}$ ± 0.0000	0.2561 ± 0.0705	0.4536 ± 0.1229	-	0.0818 ± 0.0986
	MADE3	0.1139 ± 0.0242	$1.89x10^{-7}$ ± 0.0000	0.2656 ± 0.0695	0.0841 ± 0.2002	0.4381 ± 0.1849	$1.19x10^{-4}$ ± 0.0000
	MAIDE3*	-	-	-	-	-	-
T4	MA	1.7199 ± 0.1708	-	-	-	-	3.4330 ± 0.1147
	MAI	1.7206 ± 0.1710	-	-	-	-	3.4340 ± 0.1148
	MAE	1.5743 ± 0.1846	-	0.4672 ± 0.2938	-	-	3.0851 ± 0.2441
	MAIE	1.5738 ± 0.1845	-	0.4727 ± 0.2936	-	-	3.0819 ± 0.2444
	MAD	1.7172 ± 0.1710	0.0576 ± 0.0847	-	-	-	3.3777 ± 0.1378
	MAID	1.7178 ± 0.1711	0.0585 ± 0.0848	-	-	-	3.3779 ± 0.1379
	MADE1	1.5794 ± 0.1849	0.0351 ± 0.0835	0.4445 ± 0.2983	-	-	3.0682 ± 0.2476
	MAIDE1	1.5790 ± 0.1851	0.0355 ± 0.0826	0.4494 ± 0.2976	-	-	3.0649 ± 0.2480
	MADE2	1.5794 ± 8.5400	0.0351 ± 0.4200	0.4445 ± 0.2983	$3.10x10^{-7}$ ± 0.0000	-	3.0681 ± 0.2476
	MAIDE2	1.5790 ± 0.1851	0.0355 ± 0.0826	0.4494 ± 0.2976	$3.10x10^{-7}$ ± 0.0000	-	3.0649 ± 0.2480

This paper was published at BMC Genomic Data: https://doi.org/10.1186/s12863-023-01174-x

	MADE3	1.5794 ± 0.1849	0.0351 ± 0.0835	0.4445 ± 0.2983	$4.91x10^{-7}$ ± 0.0000	$6.38x10^{-6}$ ± 0.0000	3.0681 ± 0.2476
	MAIDE3	1.5790 ± 0.1851	0.0355 ± 0.0826	0.4494 ± 0.2976	$4.90x10^{-7}$ ± 0.0000	$6.37x10^{-6}$ ± 0.0000	3.0649 ± 0.2480
T5	MA	1,310.6200 ± 122.0317	-	-	-	-	2,190.1200 ± 74.7226
	MAI	1,313.0200 ± 122.1414	-	-	-	-	2,186.8400 ± 74.6617
	MAE	1,146.0400 ± 129.7894	-	539.2420 ± 202.7226	-	-	1,786.3800 ± 163.5879
	MAIE	1,149.1100 ± 129.8429	-	535.6400 ± 202.8939			1,786.0400 ± 163.7067
	MAD	1,303.6700 ± 121.8383	171.8660 ± 65.5977	-	-	-	2,022.8200 ± 90.7908
	MAID	1,305.2600 ± 121.8730	158.4950 ± 65.4938	-	-	-	2,033.7900 ± 90.9973
	MADE1	1,168.3800 ± 130.5453	151.9660 ± 64.9427	451.3190 ± 205.1450	-	-	1,703.5000 ± 167.0098
	MAIDE1	1,167.8900 ± 130.4905	138.0280 ± 64.4991	457.6490 ± 205.2238	-	-	1,710.3400 ± 167.0254
	MADE2	1,168.3800 ± 130.5453	151.9660 ± 64.9427	451.3180 ± 205.1445	0.0012 ± 0.0000	-	1,703.4900 ± 167.0088
	MAIDE2	1,167.8900 ± 130.4905	138.0280 ± 64.4991	457.6490 ± 205.2238	0.0012 ± 0.0000	-	1,710.3400 ± 167.0254
	MAIDE3	1,167.8800 ± 130.9283	138.0280 ± 65.7276	457.6430 ± 231.1328	0.0012 ± 0.0000	0.0036 ± 0.0000	1,710.3200 ± 337.3412

$\widehat{\sigma_a^2}$: additive genetic variance estimate

$\widehat{\sigma_d^2}$: dominance variance estimate

$\widehat{\sigma_{aa}^2}$: additive-by-additive epistatic variance estimate

This paper was published at BMC Genomic Data: https://doi.org/10.1186/s12863-023-01174-x

$\widehat{\sigma_{ad}^2}$: additive-by-dominance epistatic variance estimate

$\widehat{\sigma_{dd}^2}$: dominance-by-dominance epistatic variance estimate

$\widehat{\sigma_e^2}$: residual variance estimate

[1]MA: $\mathbf{y} = \mathbf{X\beta} + \mathbf{Za} + \boldsymbol{\varepsilon}$; MAI: $\mathbf{y} = \mathbf{X\beta} + \mathbf{fb} + \mathbf{Za} + \boldsymbol{\varepsilon}$; MAE: $\mathbf{y} = \mathbf{X\beta} + \mathbf{Za} + \mathbf{Z}\boldsymbol{e_{aa}} + \boldsymbol{\varepsilon}$; MAIE: $\mathbf{y} = \mathbf{X\beta} + \mathbf{fb} + \mathbf{Za} + \mathbf{Z}\boldsymbol{e_{aa}} + \boldsymbol{\varepsilon}$; MAD: $\mathbf{y} = \mathbf{X\beta} + \mathbf{Za} + \mathbf{Zd} + \boldsymbol{\varepsilon}$; MAID: $\mathbf{y} = \mathbf{X\beta} + \mathbf{fb} + \mathbf{Za} + \mathbf{Zd} + \boldsymbol{\varepsilon}$; MADE1: $\mathbf{y} = \mathbf{X\beta} + \mathbf{Za} + \mathbf{Zd} + \mathbf{Z}\boldsymbol{e_{aa}} + \boldsymbol{\varepsilon}$; MAIDE1: $\mathbf{y} = \mathbf{X\beta} + \mathbf{fb} + \mathbf{Za} + \mathbf{Zd} + \mathbf{Z}\boldsymbol{e_{aa}} + \boldsymbol{\varepsilon}$; MADE2: $\mathbf{y} = \mathbf{X\beta} + \mathbf{Za} + \mathbf{Zd} + \mathbf{Z}\boldsymbol{e_{aa}} + \mathbf{Z}\boldsymbol{e_{ad}} + \boldsymbol{\varepsilon}$; MAIDE2: $\mathbf{y} = \mathbf{X\beta} + \mathbf{fb} + \mathbf{Za} + \mathbf{Zd} + \mathbf{Z}\boldsymbol{e_{aa}} + \mathbf{Z}\boldsymbol{e_{ad}} + \boldsymbol{\varepsilon}$; MADE3: $\mathbf{y} = \mathbf{X\beta} + \mathbf{Za} + \mathbf{Zd} + \mathbf{Z}\boldsymbol{e_{aa}} + \mathbf{Z}\boldsymbol{e_{ad}} + \mathbf{Z}\boldsymbol{e_{dd}} + \boldsymbol{\varepsilon}$; MAIDE3: $\mathbf{y} = \mathbf{X\beta} + \mathbf{fb} + \mathbf{Za} + \mathbf{Zd} + \mathbf{Z}\boldsymbol{e_{aa}} + \mathbf{Z}\boldsymbol{e_{ad}} + \mathbf{Z}\boldsymbol{e_{dd}} + \boldsymbol{\varepsilon}$

*Model MAIDE3 did not converge for T3.

124

125

This paper was published at BMC Genomic Data: https://doi.org/10.1186/s12863-023-01174-x

126 **Table 2.** Heritability estimates based on models including or not inbreeding and non-additive genetic effects.

Trait	Model[1]	h_a^2	h_d^2	h_{aa}^2	h_{ad}^2	h_{dd}^2
T1	MA	0.0327 ± 0.0146	-	-	-	-
	MAI	0.0318 ± 0.0146	-	-	-	-
	MAE	0.0130 ± 0.0157	-	0.1277 ± 0.0642	-	-
	MAIE	0.0116 ± 0.0157	-	0.1288 ± 0.0642	-	-
	MAD	0.0327 ± 0.0147	$6.12x10^{-08}$ ± 0.0232	-	-	-
	MAID	0.0318 ± 0.0147	$6.12x10^{-08}$ ± 0.0232	-	-	-
	MADE1	0.0130 ± 0.0157	$5.77x10^{-08}$ ± 0.0000	0.1277 ± 0.0642	-	-
	MAIDE1	0.0116 ± 0.0157	$6.77x10^{-08}$ ± 0.0241	0.1288 ± 0.0652	-	-
	MADE2	0.0130 ± 0.0160	$6.23x10^{-08}$ ± 0.0247	0.1277 ± 0.0743	$6.82x10^{-07}$ ± 0.1535	-
	MAIDE2	0.0116 ± 0.0160	$6.23x10^{-08}$ ± 0.0247	0.1288 ± 0.0743	$6.82x10^{-07}$ ± 0.1536	-
	MADE3	0.0130 ± 0.0160	$5.85x10^{-08}$ ± 0.0249	0.1277 ± 0.0743	$3.20x10^{-07}$ ± 0.2644	$7.96x10^{-07}$ ± 0.2910
	MAIDE3	0.0116 ± 0.0160	$5.79x10^{-08}$ ± 0.0248	0.1288 ± 0.0743	$2.97x10^{-07}$ ± 0.2646	$8.35x10^{-07}$ ± 0.2913
T2	MA	0.2697 ± 0.0263	-	-	-	-

This paper was published at BMC Genomic Data: https://doi.org/10.1186/s12863-023-01174-x

	MAI	0.2696 ± 0.0264	-	-	-	-
	MAE	0.2095 ± 0.0300	-	0.2433 ± 0.0698	-	-
	MAIE	0.2083 ± 0.0301	-	0.2453 ± 0.0700	-	-
	MAD	0.2680 ± 0.0265	0.0205 ± 0.0219	-	-	-
	MAID	0.2680 ± 0.0265	0.0205 ± 0.0219	-	-	-
	MADE1	0.2087 ± 0.0299	0.0185 ± 0.0217	0.2417 ± 0.0700	-	-
	MAIDE1	0.2071 ± 0.0301	0.0193 ± 0.0219	0.2441 ± 0.0701	-	-
	MADE2	0.2086 ± 0.0301	0.0185 ± 0.0222	0.2417 ± 0.0775	8.50×10^{-07} ± 0.1390	-
	MAIDE2	0.2071 ± 0.0302	0.0193 ± 0.0223	0.2441 ± 0.0776	8.47×10^{-07} ± 0.1391	-
	MADE3	0.2086 ± 0.0301	0.0185 ± 0.0224	0.2417 ± 0.0775	8.50×10^{-07} ± 0.2355	1.10×10^{-06} ± 0.2698
	MAIDE3	0.2071 ± 0.0302	0.0193 ± 0.0225	0.2441 ± 0.0776	8.47×10^{-07} ± 0.2357	1.10×10^{-06} ± 0.2703
T3	MA	0.2083 ± 0.0253	-	-	-	-
	MAI	0.2071 ± 0.0253	-	-	-	-
	MAE	0.1161 ± 0.0255	-	0.4309 ± 0.0663	-	-
	MAIE	0.1144 ± 0.0254	-	0.4319 ± 0.0663	-	-

This paper was published at BMC Genomic Data: https://doi.org/10.1186/s12863-023-01174-x

	MAD	0.2058 ± 0.0254	0.0206 ± 0.0230	-	-	-
	MAID	0.2045 ± 0.0253	0.0215 ± 0.0231	-	-	-
	MADE1	0.1161 ± 0.0255	$1.22x10^{-07}$ ± 0.0210	0.4309 ± 0.0669	-	-
	MAIDE1	0.1144 ± 0.0254	$1.59x10^{-07}$ ± 0.0211	0.4319 ± 0.0669	-	-
	MADE2	0.1254 ± 0.0258	$2.89x10^{-08}$ ± 0.0222	0.2821 ± 0.0769	0.5037 ± 0.1373	-
	MAIDE2	0.1238 ± 0.0257	$3.41x10^{-08}$ ± 0.0222	0.2835 ± 0.0769	0.5022 ± 0.1375	-
	MADE3	0.1263 ± 0.0257	$2.10x10^{-10}$ ± 0.0216	0.2946 ± 0.0759	0.0932 ± 0.2235	0.4859 ± 0.2068
	MAIDE3*	-	-	-	-	-
	MA	0.3338 ± 0.0263	-	-	-	-
	MAI	0.3338 ± 0.0263	-	-	-	-
	MAE	0.3071 ± 0.0304	-	0.0911 ± 0.0574	-	-
T4	MAIE	0.3069 ± 0.0304	-	0.0922 ± 0.0575	-	-
	MAD	0.3333 ± 0.0263	0.0112 ± 0.0164	-	-	-
	MAID	0.3333 ± 0.0263	0.0114 ± 0.0164	-	-	-
	MADE1	0.3080 ± 0.0304	0.0068 ± 0.0161	0.0867 ± 0.0581	-	-

This paper was published at BMC Genomic Data: https://doi.org/10.1186/s12863-023-01174-x

	MAIDE1	0.3079 ± 0.0304	0.0069 ± 0.0162	0.0876 ± 0.0582	-	-
	MADE2	0.3080 ± 0.0306	0.0068 ± 0.0165	0.0867 ± 0.0656	$6.06x10^{-08}$ ± 0.1172	-
	MAIDE2	0.3079 ± 0.0306	0.0069 ± 0.0165	0.0876 ± 0.0657	$6.05x10^{-08}$ ± 0.1173	-
	MADE3	0.3080 ± 0.0306	0.0068 ± 0.0166	0.0867 ± 0.0656	$9.57x10^{-07}$ ± 0.1856	$1.24x10^{-06}$ ± 0.2251
	MAIDE3	0.3079 ± 0.0306	0.0069 ± 0.0166	0.0876 ± 0.0657	$9.56x10^{-07}$ ± 0.1860	$1.24x10^{-06}$ ± 0.2256
T5	MA	0.3744 ± 0.0264	-	-	-	-
	MAI	0.3752 ± 0.0264	-	-	-	-
	MAE	0.3301 ± 0.0309	-	0.1553 ± 0.0584	-	-
	MAIE	0.3311 ± 0.0310	-	0.1543 ± 0.0585	-	-
	MAD	0.3727 ± 0.0265	0.0491 ± 0.0187	-	-	-
	MAID	0.3732 ± 0.0265	0.0453 ± 0.0187	-	-	-
	MADE1	0.3362 ± 0.0309	0.0437 ± 0.0186	0.1299 ± 0.0590	-	-
	MAIDE1	0.3362 ± 0.0309	0.0397 ± 0.0186	0.1317 ± 0.0591	-	-
	MADE2	0.3362 ± 0.0310	0.0437 ± 0.0190	0.1299 ± 0.0666	$3.36x10^{-07}$ ± 0.1166	-
	MAIDE2	0.3362 ± 0.0311	0.0397 ± 0.0189	0.1317 ± 0.0667	$3.55x10^{-07}$ ± 0.1166	-

This paper was published at BMC Genomic Data: https://doi.org/10.1186/s12863-023-01174-x

MADE3	0.3362 ± 0.0311	0.0437 ± 0.0190	0.1299 ± 0.0666	$3.33\text{x}10^{-07}$ ± 0.1860	$1.02\text{x}10^{-06}$ ± 0.2256
MAIDE3	0.3362 ± 0.0311	0.0397 ± 0.0190	0.1317 ± 0.0667	$3.58\text{x}10^{-07}$ ± 0.1862	$1.02\text{x}10^{-06}$ ± 0.2151

h_a^2: additive heritability or narrow-sense heritability

h_d^2: dominance variance ratio

h_{aa}^2: epistatic additive-by-additive variance ratio

h_{ad}^2: epistatic additive-by-dominance variance ratio

h_{dd}^2: epistatic dominance-by-dominance variance ratio

[1]MA: $\mathbf{y} = \mathbf{X\beta} + \mathbf{Za} + \boldsymbol{\varepsilon}$; MAI: $\mathbf{y} = \mathbf{X\beta} + \mathbf{fb} + \mathbf{Za} + \boldsymbol{\varepsilon}$; MAE: $\mathbf{y} = \mathbf{X\beta} + \mathbf{Za} + \mathbf{Z}\boldsymbol{e_{aa}} + \boldsymbol{\varepsilon}$; MAIE: $\mathbf{y} = \mathbf{X\beta} + \mathbf{fb} + \mathbf{Za} + \mathbf{Z}\boldsymbol{e_{aa}} + \boldsymbol{\varepsilon}$; MAD: $\mathbf{y} = \mathbf{X\beta} + \mathbf{Za} + \mathbf{Zd} + \boldsymbol{\varepsilon}$; MAID: $\mathbf{y} = \mathbf{X\beta} + \mathbf{fb} + \mathbf{Za} + \mathbf{Zd} + \boldsymbol{\varepsilon}$; MADE1: $\mathbf{y} = \mathbf{X\beta} + \mathbf{Za} + \mathbf{Zd} + \mathbf{Z}\boldsymbol{e_{aa}} + \boldsymbol{\varepsilon}$; MAIDE1: $\mathbf{y} = \mathbf{X\beta} + \mathbf{fb} + \mathbf{Za} + \mathbf{Zd} + \mathbf{Z}\boldsymbol{e_{aa}} + \boldsymbol{\varepsilon}$; MADE2: $\mathbf{y} = \mathbf{X\beta} + \mathbf{Za} + \mathbf{Zd} + \mathbf{Z}\boldsymbol{e_{aa}} + \mathbf{Z}\boldsymbol{e_{ad}} + \boldsymbol{\varepsilon}$; MAIDE2: $\mathbf{y} = \mathbf{X\beta} + \mathbf{fb} + \mathbf{Za} + \mathbf{Zd} + \mathbf{Z}\boldsymbol{e_{aa}} + \mathbf{Z}\boldsymbol{e_{ad}} + \boldsymbol{\varepsilon}$; MADE3: $\mathbf{y} = \mathbf{X\beta} + \mathbf{Za} + \mathbf{Zd} + \mathbf{Z}\boldsymbol{e_{aa}} + \mathbf{Z}\boldsymbol{e_{ad}} + \mathbf{Z}\boldsymbol{e_{dd}} + \boldsymbol{\varepsilon}$; MAIDE3: $\mathbf{y} = \mathbf{X\beta} + \mathbf{fb} + \mathbf{Za} + \mathbf{Zd} + \mathbf{Z}\boldsymbol{e_{aa}} + \mathbf{Z}\boldsymbol{e_{ad}} + \mathbf{Z}\boldsymbol{e_{dd}} + \boldsymbol{\varepsilon}$

*Model MAIDE3 did not converge for T3.

127

This paper was published at BMC Genomic Data: https://doi.org/10.1186/s12863-023-01174-x

Predictive ability of genomic breeding values

Figure 1 presents the average bias, dispersion, and accuracy values obtained for the genomic breeding values for all five traits. As expected, greater accuracies were obtained for traits with higher h_a^2. Fitting inbreeding and/or dominance in the models did not impact the accuracy of breeding values compared to those obtained based on the MA model (Figure 1).Models including epistasis (MAE, MAIE, MADE1, MAIDE1, MADE2, MAIDE2, MADE3, and MAIDE3) presented on average a relative decrease in accuracy of 31.58%, 13.97%, 3.50%, 0.82%, and 1.34% for T1, T2, T3, T4, and T5, respectively, when compared to MA (Figure 1). The observed bias was close to zero and the dispersion estimates were close to one for all traits and models (Figure 1), indicating that the inclusion of non-additive genetic effects in the model did not influence the dispersion of breeding values.

In this section, all models incorporating non-additive genetic effects were compared to the additive animal model. To assess the impact of including non-additive genetic effects in the model on animals' selection, we calculated the change in an animals' ranking in comparison to the additive model (MA) based on Spearman's rank correlation, as shown in Table 3. The percentage of commonly selected individuals when selecting the top 1%, 5%, 10%, and 20% based on different genomic prediction models were compared to the selected individuals based on MA. Table 4 shows the percentage of coincidence of the top 1%, 5%, 10%, and 20% best animals between the MA and the models including non-additive genetic effects. The models including epistasis effect presented the lowest percentage of coincidence of the top animals in comparison to the MA model. This percentage varied from 68.57% for trait T3 to 97.59% for T4. Although there was little change in the Spearman correlations across models (Table 3), the percentage of coincidence between the best animals according to MA were higher for

153 models including inbreeding and/or dominance (MAI, MAD, and MAID). However, the
154 percentage of coincidence decreased for models including epistasis (MAE, MAIE,
155 MADE1, MAIDE1, MADE2, MAIDE2, MADE3, and MAIDE3), as shown in Table 4.

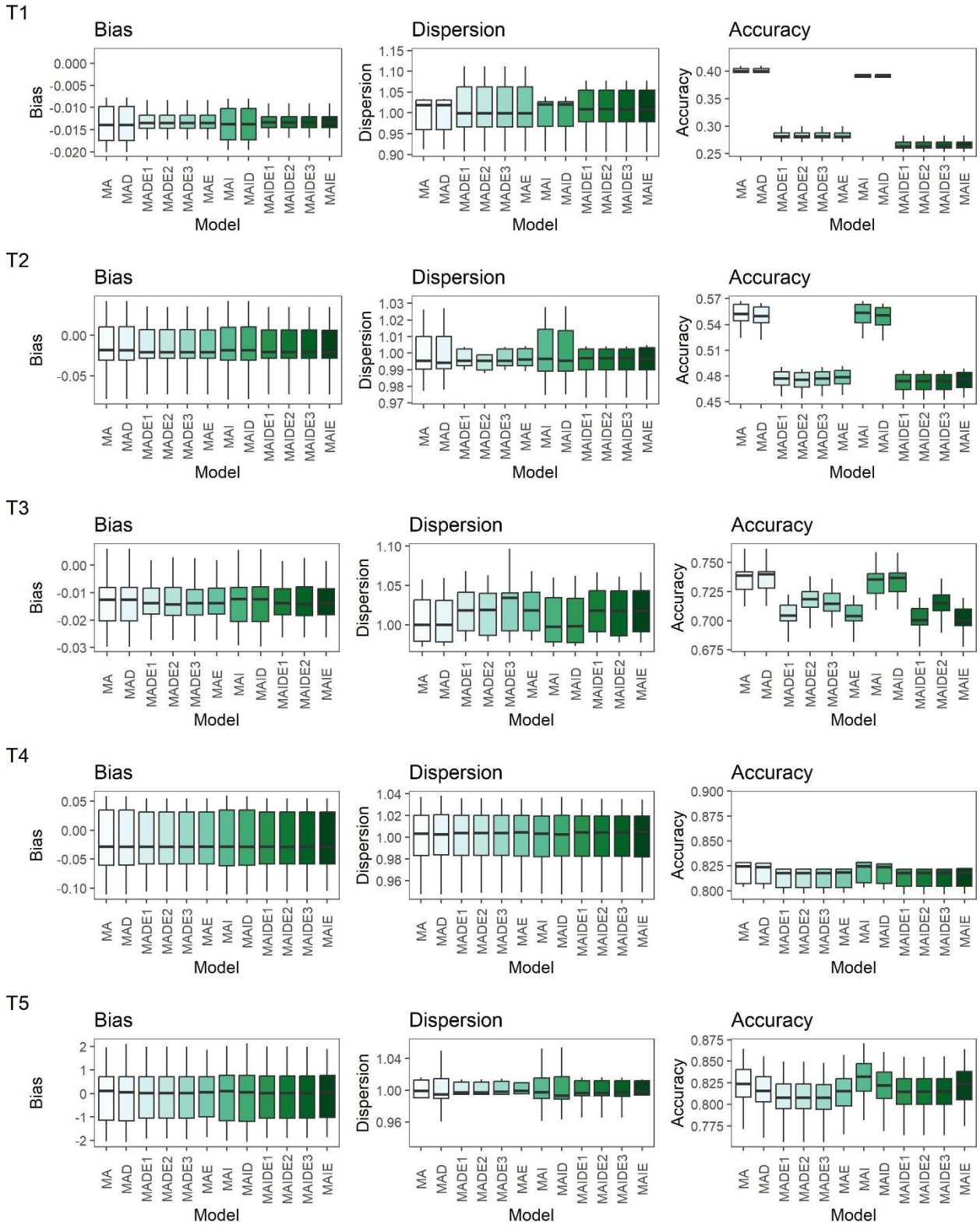

156

This paper was published at BMC Genomic Data: https://doi.org/10.1186/s12863-023-01174-x

157 **Figure 1.** Bias, dispersion, and accuracy estimates of genomic breeding values obtained
158 using the Linear Regression method.

159

160 **Table 3.** Spearman's rank correlation between the additive genetic model (MA) and other
161 models considering non-additive genetic effects.

Model[1]	T1	T2	T3	T4	T5
MAI	0.9990	1.000	0.9996	1.0000	0.9993
MAE	0.9844	0.9952	0.9645	0.9989	0.9968
MAIE	0.9856	0.9952	0.9630	0.9989	0.996
MAD	1.0000	0.9999	0.9998	0.9999	0.9985
MAID	0.9990	0.9999	0.9995	0.9999	0.9985
MADE1	0.9844	0.9951	0.9644	0.9989	0.9966
MAIDE1	0.9856	0.9950	0.9630	0.9989	0.9964
MADE2	0.9844	0.9951	0.9692	0.9989	0.9966
MAIDE2	0.9856	0.9950	0.9678	0.9989	0.9964
MADE3	0.9844	0.9951	0.9716	0.9989	0.9966
MAIDE3*	0.9856	0.9950	-	0.9989	0.9964

[1]MA: $\mathbf{y} = \mathbf{X\beta} + \mathbf{Za} + \boldsymbol{\varepsilon}$; MAI: $\mathbf{y} = \mathbf{X\beta} + \mathbf{fb} + \mathbf{Za} + \boldsymbol{\varepsilon}$; MAE: $\mathbf{y} = \mathbf{X\beta} + \mathbf{Za} + \mathbf{Z}\boldsymbol{e}_{aa} + \boldsymbol{\varepsilon}$; MAIE: $\mathbf{y} = \mathbf{X\beta} + \mathbf{fb} + \mathbf{Za} + \mathbf{Z}\boldsymbol{e}_{aa} + \boldsymbol{\varepsilon}$; MAD: $\mathbf{y} = \mathbf{X\beta} + \mathbf{Za} + \mathbf{Zd} + \boldsymbol{\varepsilon}$; MAID: $\mathbf{y} = \mathbf{X\beta} + \mathbf{fb} + \mathbf{Za} + \mathbf{Zd} + \boldsymbol{\varepsilon}$; MADE1: $\mathbf{y} = \mathbf{X\beta} + \mathbf{Za} + \mathbf{Zd} + \mathbf{Z}\boldsymbol{e}_{aa} + \boldsymbol{\varepsilon}$; MAIDE1: $\mathbf{y} = \mathbf{X\beta} + \mathbf{fb} + \mathbf{Za} + \mathbf{Zd} + \mathbf{Z}\boldsymbol{e}_{aa} + \boldsymbol{\varepsilon}$; MADE2: $\mathbf{y} = \mathbf{X\beta} + \mathbf{Za} + \mathbf{Zd} + \mathbf{Z}\boldsymbol{e}_{aa} + \mathbf{Z}\boldsymbol{e}_{ad} + \boldsymbol{\varepsilon}$; MAIDE2: $\mathbf{y} = \mathbf{X\beta} + \mathbf{fb} + \mathbf{Za} + \mathbf{Zd} + \mathbf{Z}\boldsymbol{e}_{aa} + \mathbf{Z}\boldsymbol{e}_{ad} + \boldsymbol{\varepsilon}$; MADE3: $\mathbf{y} = \mathbf{X\beta} + \mathbf{Za} + \mathbf{Zd} + \mathbf{Z}\boldsymbol{e}_{aa} + \mathbf{Z}\boldsymbol{e}_{ad} + \mathbf{Z}\boldsymbol{e}_{dd} + \boldsymbol{\varepsilon}$; MAIDE3: $\mathbf{y} = \mathbf{X\beta} + \mathbf{fb} + \mathbf{Za} + \mathbf{Zd} + \mathbf{Z}\boldsymbol{e}_{aa} + \mathbf{Z}\boldsymbol{e}_{ad} + \mathbf{Z}\boldsymbol{e}_{dd} + \boldsymbol{\varepsilon}$

*The model MAIDE3 did not converge for T3

This paper was published at BMC Genomic Data: https://doi.org/10.1186/s12863-023-01174-x

162 **Table 4.** Percentage of commonly selected animals between the additive model and
163 models including non-additive genetic effects.

Trait	Model[1]	1%	5%	10%	20%
T1	MAI	97.14%	96.02%	96.88%	97.73%
	MAE	82.86%	86.93%	88.10%	89.09%
	MAIE	82.86%	86.36%	87.54%	89.38%
	MAD	100.00%	100.00%	100.00%	100.00%
	MAID	97.14%	96.02%	96.88%	97.73%
	MADE1	82.86%	86.36%	88.10%	89.09%
	MAIDE1	82.86%	86.36%	87.25%	89.38%
	MADE2	82.86%	86.36%	88.10%	89.09%
	MAIDE2	82.86%	86.36%	87.25%	89.38%
	MADE3	82.86%	86.36%	88.10%	89.09%
	MAIDE3	82.86%	86.36%	87.25%	89.38%
T2	MAI	100.00%	100.00%	100.00%	100.00%
	MAE	77.14%	92.05%	91.78%	94.05%
	MAIE	77.14%	91.48%	91.78%	94.33%
	MAD	97.14%	98.86%	98.58%	99.15%
	MAID	97.14%	98.30%	98.30%	99.15%
	MADE1	80.00%	92.05%	91.50%	94.05%
	MAIDE1	77.14%	92.05%	91.50%	94.05%
	MADE2	80.00%	92.05%	91.50%	94.05%
	MAIDE2	77.14%	92.05%	91.50%	94.05%
	MADE3	80.00%	92.05%	91.50%	94.05%

This paper was published at BMC Genomic Data: https://doi.org/10.1186/s12863-023-01174-x

	MAIDE3	77.14%	92.05%	91.50%	94.05%
T3	MAI	94.29%	97.73%	98.30%	98.30%
	MAE	71.43%	76.14%	79.32%	84.56%
	MAIE	71.43%	77.27%	78.47%	84.70%
	MAD	94.29%	99.43%	98.87%	99.15%
	MAID	94.29%	97.73%	97.73%	98.16%
	MADE1	71.43%	76.14%	79.32%	84.56%
	MAIDE1	71.43%	77.27%	78.47%	84.70%
	MADE2	71.43%	76.70%	81.59%	86.54%
	MAIDE2	71.43%	78.41%	80.45%	86.40%
	MADE3	68.57%	77.84%	81.87%	87.11%
	MAIDE3*	-	-	-	-
T4	MAI	100.00%	100.00%	99.72%	99.72%
	MAE	94.29%	97.73%	96.60%	97.45%
	MAIE	94.29%	97.73%	96.60%	97.59%
	MAD	100.00%	98.86%	99.43%	99.43%
	MAID	100.00%	98.86%	99.15%	99.58%
	MADE1	97.14%	97.73%	96.60%	97.45%
	MAIDE1	97.14%	97.73%	96.60%	97.59%
	MADE2	97.14%	97.73%	96.60%	97.45%
	MAIDE2	97.14%	97.73%	96.60%	97.59%
	MADE3	97.14%	97.73%	96.60%	97.45%
	MAIDE3	97.14%	97.73%	96.60%	97.59%
T5	MAI	100.00%	96.02%	96.32%	98.16%

MAE	88.57%	95.45%	95.18%	96.03%
MAIE	88.57%	94.32%	94.05%	95.61%
MAD	94.29%	96.59%	96.88%	97.45%
MAID	94.29%	96.59%	96.32%	97.45%
MADE1	91.43%	94.32%	95.75%	96.03%
MAIDE1	88.57%	95.45%	94.62%	95.61%
MADE2	91.43%	94.32%	95.75%	96.03%
MAIDE2	88.57%	95.45%	94.62%	95.61%
MADE3	91.43%	94.32%	95.75%	96.03%
MAIDE3	88.57%	95.45%	94.62%	95.61%

[1]MA: $\mathbf{y} = \mathbf{X\beta} + \mathbf{Za} + \boldsymbol{\varepsilon}$; MAI: $\mathbf{y} = \mathbf{X\beta} + \mathbf{fb} + \mathbf{Za} + \boldsymbol{\varepsilon}$; MAE: $\mathbf{y} = \mathbf{X\beta} + \mathbf{Za} + \mathbf{Z}\boldsymbol{e}_{aa} + \boldsymbol{\varepsilon}$; MAIE: $\mathbf{y} = \mathbf{X\beta} + \mathbf{fb} + \mathbf{Za} + \mathbf{Z}\boldsymbol{e}_{aa} + \boldsymbol{\varepsilon}$; MAD: $\mathbf{y} = \mathbf{X\beta} + \mathbf{Za} + \mathbf{Zd} + \boldsymbol{\varepsilon}$; MAID: $\mathbf{y} = \mathbf{X\beta} + \mathbf{fb} + \mathbf{Za} + \mathbf{Zd} + \boldsymbol{\varepsilon}$; MADE1: $\mathbf{y} = \mathbf{X\beta} + \mathbf{Za} + \mathbf{Zd} + \mathbf{Z}\boldsymbol{e}_{aa} + \boldsymbol{\varepsilon}$; MAIDE1: $\mathbf{y} = \mathbf{X\beta} + \mathbf{fb} + \mathbf{Za} + \mathbf{Zd} + \mathbf{Z}\boldsymbol{e}_{aa} + \boldsymbol{\varepsilon}$; MADE2: $\mathbf{y} = \mathbf{X\beta} + \mathbf{Za} + \mathbf{Zd} + \mathbf{Z}\boldsymbol{e}_{aa} + \mathbf{Z}\boldsymbol{e}_{ad} + \boldsymbol{\varepsilon}$; MAIDE2: $\mathbf{y} = \mathbf{X\beta} + \mathbf{fb} + \mathbf{Za} + \mathbf{Zd} + \mathbf{Z}\boldsymbol{e}_{aa} + \mathbf{Z}\boldsymbol{e}_{ad} + \boldsymbol{\varepsilon}$; MADE3: $\mathbf{y} = \mathbf{X\beta} + \mathbf{Za} + \mathbf{Zd} + \mathbf{Z}\boldsymbol{e}_{aa} + \mathbf{Z}\boldsymbol{e}_{ad} + \mathbf{Z}\boldsymbol{e}_{dd} + \boldsymbol{\varepsilon}$; MAIDE3: $\mathbf{y} = \mathbf{X\beta} + \mathbf{fb} + \mathbf{Za} + \mathbf{Zd} + \mathbf{Z}\boldsymbol{e}_{aa} + \mathbf{Z}\boldsymbol{e}_{ad} + \mathbf{Z}\boldsymbol{e}_{dd} + \boldsymbol{\varepsilon}$

*Model MAIDE3 did not converge for T3.

164

165 The values of Akaike Information Criterion (AIC) (Table S1) suggested that the inclusion
166 of epistasis in the prediction models for T2, T3, and T5 improved the predictive
167 performance of the models. Although, the Likelihood Ratio Test (LRT; Table S2) for the
168 models fitted for the purebred pig population showed that the inclusion of epistasis was
169 significant for the traits T2, T3 and T5, and incorporating dominance effect was also
170 significant for T5.

This paper was published at BMC Genomic Data: https://doi.org/10.1186/s12863-023-01174-x

Dataset 2: Crossbred pig population

Variance components and heritability estimates

We also estimated variance components and heritabilities for heat tolerance indicators in a crossbred (Large White x Landrace) population. Table 5 presents variance component estimates and Table 6 presents the estimates of heritability and non-additive genetic variance ratios for traits related to heat stress response in lactating sows for models including or not non-additive genetic effects. All heat stress related traits have substantial additive genetic variability (Table 5) with heritability estimates ranging from 0.0231 to 0.2639 (Table 6). However, all traits had small non-additive genetic variance with large standard error estimates, except panting score (PS) and hair density (HD) (Table 5). PS presented a h^2_{aa} estimate of 0.1342, which corresponds to 82.22% of the total genetic variance for both models including epistasis (MAIEpe and MAIDEpe). HD presented h^2_{aa} estimates of 0.4232 and 0.4493 for MAIE and MAIDE models, respectively. The proportion of the total genetic variance explained by additive-by-additive epistasis for HD ranged from 64.95% to 69.59% for the MAIE and MAIDE models, respectively (Table 6).

As observed for the purebred population (Dataset 1), the inclusion of non-additive genetic effects in the model did not affect the residual variance estimates for most of the traits, except for HD (Table 5). However, for HD and PS there was also a decrease in the additive genetic variance estimates (Table 5) when epistasis was included in the model. When both dominance and epistasis were included in the repeatability model (for all heat stress-related traits, except HD), there was a decrease in the permanent environmental variance estimate for most of the traits.

This paper was published at BMC Genomic Data: https://doi.org/10.1186/s12863-023-01174-x

194 **Table 5.** Variance components for traits related to heat tolerance based on models fitting non-additive genetic effects.

Trait[1]	Model[2]	$\widehat{\sigma_a^2}$	$\widehat{\sigma_d^2}$	$\widehat{\sigma_{aa}^2}$	$\widehat{\sigma_{pe}^2}$	$\widehat{\sigma_e^2}$
T_{Vall}	MAIpe	0.0626 ± 0.0107	-	-	0.1274 ± 0.0081	0.3047 ± 0.0005
	MAIDpe	0.0618 ± 0.0111	0.0050 ± 0.0140	-	0.1237 ± 0.0128	0.3047 ± 0.0005
	MAIDEpe	0.0616 ± 0.0121	0.0047 ± 0.0144	0.0031 ± 0.0340	0.1213 ± 0.0294	0.3047 ± 0.0005
	MAIEpe	0.0618 ± 0.0120		0.0050 ± 0.0336	0.1231 ± 0.0290	0.3047 ± 0.0005
T_{V4days}	MAIpe	0.0653 ± 0.0113	-	-	0.1266 ± 0.0086	0.1378 ± 0.0014
	MAIDpe	0.0642 ± 0.0116	0.0068 ± 0.0145	-	0.1216 ± 0.0132	0.1378 ± 0.0014
	MAIDEpe	0.0642 ± 0.0116	0.0068 ± 0.0145	$3.48x10^{-9}$ ± 0.00000	0.1216 ± 0.0132	0.1378 ± 0.0014
	MAIEpe	0.0653 ± 0.0113	-	$3.48x10^{-9}$ ± 0.00000	0.1266 ± 0.0086	0.1378 ± 0.0014
T_{ES}	MAIpe	0.0316 ± 0.0069	-	-	0.0507 ± 0.0059	0.7287 ± 0.0074
	MAIDpe	0.0316 ± 0.0069	$1.84x10^{-8}$ ± 0.00000	-	0.0507 ± 0.0059	0.7287 ± 0.0074
	MAIDEpe	0.0316 ± 0.0069	$1.84x10^{-8}$ ± 0.00000	$1.84x10^{-8}$ ± 0.00000	0.0507 ± 0.00589	0.7287 ± 0.0074
	MAIEpe	0.0316 ± 0.0069	-	$1.84x10^{-8}$ ± 0.00000	0.0507 ± 0.00589	0.7287 ± 0.0074
T_{SS}	MAIpe	0.0445 ± 0.0100	-	-	0.1176 ± 0.0090	0.6119 ± 0.0062

This paper was published at BMC Genomic Data: https://doi.org/10.1186/s12863-023-01174-x

	MAIDpe	0.0437 ± 0.0104	0.0045 ± 0.0165	-	0.1145 ± 0.0145	0.6119 ± 0.0062
	MAIDEpe	0.0437 ± 0.0104	0.0045 ± 0.0165	$1.54x10^{-7}$ ± 0.00000	0.1145 ± 0.0145	0.6119 ± 0.0062
	MAIEpe	0.0445 ± 0.0100	-	$1.54x10^{-7}$ ± 0.00000	0.1176 ± 0.0090	0.6119 ± 0.0062
T_{RS}	MAIpe	0.0276 ± 0.0063	-	-	0.0739 ± 0.0056	0.3577 ± 0.0036
	MAIDpe	0.0276 ± 0.0063	$9.05x10^{-9}$ ± 0.00000	-	0.0739 ± 0.0056	0.3577 ± 0.0036
	MAIDEpe	0.0276 ± 0.0063	$9.05x10^{-9}$ ± 0.00000	$9.05x10^{-9}$ ± 0.00000	0.0739 ± 0.0056	0.3577 ± 0.0036
	MAIEpe	0.0276 ± 0.0063	-	$9.05x10^{-9}$ ± 0.00000	0.0739 ± 0.0056	0.3577 ± 0.0036
T_{TS}	MAIpe	0.0283 ± 0.0067	-	-	0.0730 ± 0.0060	0.4525 ± 0.0046
	MAIDpe	0.0278 ± 0.0070	0.0021 ± 0.0096	-	0.0716 ± 0.0089	0.4525 ± 0.0046
	MAIDEpe	0.0278 ± 0.0070	0.0021 ± 0.0096	$1.14x10^{-8}$ ± 0.00000	0.0716 ± 0.00889	0.4525 ± 0.0046
	MAIEpe	0.0283 ± 0.0067	-	$1.14x10^{-8}$ ± 0.00000	0.0730 ± 0.0060	0.4525 ± 0.0046
RR	MAIpe	34.7580 ± 7.0790	-	-	70.3639 ± 5.9429	442.7150 ± 4.4814
	MAIDpe	34.7580 ± 7.0790	$1.11x10^{-5}$ ± 0.00000	-	70.3639 ± 5.9429	442.7150 ± 4.4814
	MAIDEpe	34.7580 ± 7.0790	$1.11x10^{-5}$ ± 0.00000	$1.11x10^{-5}$ ± 0.00000	70.3639 ± 5.9429	442.7150 ± 4.4814
	MAIEpe	34.7580 ± 7.0790	-	$1.11x10^{-5}$ ± 0.00000	70.3639 ± 5.9429	442.7150 ± 4.4814

This paper was published at BMC Genomic Data: https://doi.org/10.1186/s12863-023-01174-x

PS	MAIpe	0.0551 ± 0.0185	-	-	0.1297 ± 0.0195	0.8463 ± 0.0191
	MAIDpe	0.0542 ± 0.0194	0.0044 ± 0.0291	-	0.1267 ± 0.0282	0.8463 ± 0.0191
	MAIDEpe	0.0298 ± 0.0204	$2.14x10^{-8}$ ± 0.00000	0.1379 ± 0.0711	0.0137 ± 0.0623	0.8463 ± 0.0191
	MAIEpe	0.0298 ± 0.0204	-	0.1379 ± 0.0711	0.0137 ± 0.0623	0.8463 ± 0.0191
HD	MAI	0.1088 ± 0.0247	-	-	-	0.3052 ± 0.0206
	MAID	0.1040 ± 0.0256	0.0289 ± 0.0366	-	-	0.2854 ± 0.0324
	MAIDE1	0.0795 ± 0.0278	0.0147 ± 0.0367	0.1745 ± 0.1015	-	0.1437 ± 0.0876
	MAIE	0.0806 ± 0.0275	-	0.1845 ± 0.0997	-	0.1455 ± 0.0876

$\widehat{\sigma_a^2}$: additive genetic variance estimate

$\widehat{\sigma_d^2}$: dominance variance estimate

$\widehat{\sigma_{aa}^2}$: additive-by-additive epistatic variance estimate

$\widehat{\sigma_{pe}^2}$: permanent environmental variance estimate

$\widehat{\sigma_e^2}$: residual variance estimate

This paper was published at BMC Genomic Data: https://doi.org/10.1186/s12863-023-01174-x

[1]T_{Vall}: all measures (every 10 minutes) of vaginal temperatures during four days (°C); T_{V4days}: four-time measures of vaginal temperatures during four days (°C); T_{ES}: ear skin temperature; T_{SS}: shoulder skin temperature; T_{RS}: rump skin temperature; T_{TS}: tail skin temperature; RR: respiration rate; PS: panting score; HD: hair density.

[2]MAIpe: $\mathbf{y} = \mathbf{X\beta} + \mathbf{fb} + \mathbf{Za} + \mathbf{Zpe} + \boldsymbol{\varepsilon}$; MAIEpe: $\mathbf{y} = \mathbf{X\beta} + \mathbf{fb} + \mathbf{Za} + \mathbf{Zpe} + \mathbf{Z}\boldsymbol{e_{aa}} + \boldsymbol{\varepsilon}$; MAIDpe: $\mathbf{y} = \mathbf{X\beta} + \mathbf{fb} + \mathbf{Za} + \mathbf{Zpe} + \mathbf{Zd} + \boldsymbol{\varepsilon}$; MAIDEpe: $\mathbf{y} = \mathbf{X\beta} + \mathbf{fb} + \mathbf{Za} + \mathbf{Zd} + \mathbf{Z}\boldsymbol{e_{aa}} + \mathbf{Zpe} + \boldsymbol{\varepsilon}$; MAI: $\mathbf{y} = \mathbf{X\beta} + \mathbf{fb} + \mathbf{Za} + \boldsymbol{\varepsilon}$; MAIE: $\mathbf{y} = \mathbf{X\beta} + \mathbf{fb} + \mathbf{Za} + \mathbf{Z}\boldsymbol{e_{aa}} + \boldsymbol{\varepsilon}$; MAID: $\mathbf{y} = \mathbf{X\beta} + \mathbf{fb} + \mathbf{Za} + \mathbf{Zd} + \boldsymbol{\varepsilon}$; MAIDE1: $\mathbf{y} = \mathbf{X\beta} + \mathbf{fb} + \mathbf{Za} + \mathbf{Zd} + \mathbf{Z}\boldsymbol{e_{aa}} + \boldsymbol{\varepsilon}$

195

196 **Table 6.** Heritability estimates and variance ratios considering models fitting non-additive genetic effects for heat tolerance indicators.

Trait	Model	h_a^2	h_d^2	h_{aa}^2	$\widehat{\sigma_d^2}/\widehat{\sigma_g^2}$	$\widehat{\sigma_{aa}^2}/\widehat{\sigma_g^2}$
T_{Vall}	MAIpe	0.1266 ± 0.0203	-	-	-	-
	MAIDpe	0.1248 ± 0.0211	0.0102 ± 0.0285	-	0.0753 ± 0.1990	-
	MAIDEpe	0.1239 ± 0.0232	0.0096 ± 0.0290	0.0062 ± 0.0670	0.0686 ± 0.2038	0.0442 ± 0.4633
	MAIEpe	0.1249 ± 0.0229	-	0.0102 ± 0.0660	-	0.0754 ± 0.4577
T_{V4days}	MAIpe	0.1982 ± 0.0310	-	-	-	-

This paper was published at BMC Genomic Data: https://doi.org/10.1186/s12863-023-01174-x

	MAIDpe	0.1944 ± 0.0323	0.0206 ± 0.0441	-	0.0959 ± 0.1898	-
	MAIDEpe	0.1944 ± 0.0323	0.0206 ± 0.0441	0.0000 ± 0.0000	0.0959 ± 0.1898	0.0000 ± 0.0000
	MAIEpe	0.1982 ± 0.0310	-	0.0000 ± 0.0000	-	0.0000 ± 0.0000
T_{ES}	MAIpe	0.039 ± 0.0083	-	-	-	-
	MAIDpe	0.039 ± 0.0083	0.0000 ± 0.0000		0.0000 ± 0.0000	-
	MAIDEpe	0.039 ± 0.0083	0.0000 ± 0.0000	0.0000 ± 0.0000	0.0000 ± 0.0000	0.0000 ± 0.0000
	MAIEpe	0.039 ± 0.0083	-	0.0000 ± 0.0000	-	0.0000 ± 0.0000
T_{SS}	MAIpe	0.0575 ± 0.0126	-	-	-	-
	MAIDpe	0.0564 ± 0.0132	0.0058 ± 0.0211	-	0.0925 ± 0.3148	-
	MAIDEpe	0.0564 ± 0.0132	0.0058 ± 0.0211	0.0000 ± 0.0000	0.0925 ± 0.3148	0.0000 ± 0.0000
	MAIEpe	0.0575 ± 0.0126	-	0.0000 ± 0.0000	-	0.0000 ± 0.0000
T_{RS}	MAIpe	0.0601 ± 0.0134	-	-	-	-
	MAIDpe	0.0601 ± 0.0134	0.0000 ± 0.0000	-	0.0000 ± 0.0000	
	MAIDEpe	0.0601 ± 0.0134	0.0000 ± 0.0000	0.0000 ± 0.0000	0.0000 ± 0.0000	0.0000 ± 0.0000

This paper was published at BMC Genomic Data: https://doi.org/10.1186/s12863-023-01174-x

	MAIEpe	0.0601 ± 0.0134	-	0.0000 ± 0.0000		0.0000 ± 0.0000
T_{TS}	MAIpe	0.051 ± 0.0119	-	-	-	-
	MAIDpe	0.0501 ± 0.0124	0.0038 ± 0.0174	-	0.0708 ± 0.3052	-
	MAIDEpe	0.0501 ± 0.0124	0.0038 ± 0.0174	0.0000 ± 0.0000	0.0708 ± 0.3052	0.0000 ± 0.0000
	MAIEpe	0.0501 ± 0.0119	-	0.0000 ± 0.0000	-	0.0000 ± 0.0000
RR	MAIpe	0.0634 ± 0.0126	-	-	-	-
	MAIDpe	0.0634 ± 0.0126	0.0000 ± 0.0000	-	0.0000 ± 0.0000	-
	MAIDEpe	0.0634 ± 0.0126	0.0000 ± 0.0000	0.0000 ± 0.0000	0.0000 ± 0.0000	0.0000 ± 0.0000
	MAIEpe	0.0634 ± 0.0126	-	0.0000 ± 0.0000		0.0000 ± 0.0000
PS	MAIpe	0.0535 ± 0.0176	-	-		-
	MAIDpe	0.0526 ± 0.0185	0.0042 ± 0.0286	-	0.0744 ± 0.4744	-
	MAIDEpe	0.0290 ± 0.0198	0.0000 ± 0.0000	0.1342 ± 0.0689	0.0000 ± 0.0000	0.8222 ± 0.1527
	MAIEpe	0.0290 ± 0.0198	-	0.1342 ± 0.0689	-	0.8222 ± 0.1527
HD	MAI	0.2629 ± 0.0535	-	-	-	-

This paper was published at BMC Genomic Data: https://doi.org/10.1186/s12863-023-01174-x

MAID	0.2494 ± 0.0567	0.0662 ± 0.0869	-	0.2097 ± 0.2335	-
MAIDE1	0.1928 ± 0.0641	0.0356 ± 0.0875	0.4232 ± 0.2468	0.0546 ± 0.1338	0.6495 ± 0.2020
MAIE	0.1964 ± 0.0632	-	0.4493 ± 0.2419	-	0.6959 ± 0.1617

h_a^2: additive heritability or narrow-sense heritability

h_d^2: dominance variance ratio

h_{aa}^2: epistatic additive-by-additive variance ratio

$\widehat{\sigma_d^2}/\widehat{\sigma_g^2}$: ratio of the total genetic variance explained by dominance

$\widehat{\sigma_{aa}^2}/\widehat{\sigma_g^2}$: ratio of the total genetic variance explained by additive-by-additive epistasis

[1]T_{Vall}: all measures (every 10 minutes) of vaginal temperatures during four days (°C); T_{V4days}: four-time measures of vaginal temperatures during four days (°C); T_{ES}: ear skin temperature; T_{SS}: shoulder skin temperature; T_{RS}: rump skin temperature; T_{TS}: tail skin temperature; RR: respiration rate; PS: panting score; HD: hair density.

[2] MAIpe: $\mathbf{y} = \mathbf{X\beta} + \mathbf{fb} + \mathbf{Za} + \mathbf{Zpe} + \boldsymbol{\varepsilon}$; MAIEpe: $\mathbf{y} = \mathbf{X\beta} + \mathbf{fb} + \mathbf{Za} + \mathbf{Zpe} + \mathbf{Z}\boldsymbol{e_{aa}} + \boldsymbol{\varepsilon}$; MAIDpe: $\mathbf{y} = \mathbf{X\beta} + \mathbf{fb} + \mathbf{Za} + \mathbf{Zpe} + \mathbf{Zd} + \boldsymbol{\varepsilon}$; MAIDEpe: $\mathbf{y} = \mathbf{X\beta} + \mathbf{fb} + \mathbf{Za} + \mathbf{Zd} + \mathbf{Z}\boldsymbol{e_{aa}} + \mathbf{Zpe} + \boldsymbol{\varepsilon}$; MAI: $\mathbf{y} = \mathbf{X\beta} + \mathbf{fb} + \mathbf{Za} + \boldsymbol{\varepsilon}$; MAIE: $\mathbf{y} = \mathbf{X\beta} + \mathbf{fb} + \mathbf{Za} + \mathbf{Z}\boldsymbol{e_{aa}} + \boldsymbol{\varepsilon}$; MAID: $\mathbf{y} = \mathbf{X\beta} + \mathbf{fb} + \mathbf{Za} + \mathbf{Zd} + \boldsymbol{\varepsilon}$; MAIDE1: $\mathbf{y} = \mathbf{X\beta} + \mathbf{fb} + \mathbf{Za} + \mathbf{Zd} + \mathbf{Z}\boldsymbol{e_{aa}} + \boldsymbol{\varepsilon}$

197

This paper was published at BMC Genomic Data: https://doi.org/10.1186/s12863-023-01174-x

198 ***Model comparison for the crossbred pig dataset***

199 For the crossbred population, the models also presented similar values of Akaike
200 Information Criterion (AIC) (Table S3). LRT (Table S4) for the models fitted for the
201 crossbred pig population showed that fitting epistasis in the models had a significant
202 effect only for PS. The models for the other traits did not have better goodness of fit when
203 dominance and/or epistasis were fitted.

204

205 **Discussion**

206 We aimed to estimate variance components and evaluate the predictive ability of
207 genomic models including non-additive genetic effects for different traits in purebred and
208 crossbred populations. In general, we observed small estimates for dominance variance
209 and the inclusion of additive-by-additive epistasis in the model reduced the estimates of
210 additive genetic variance. The inclusion of non-additive genetic effects in models for
211 genomic prediction resulted in changes in animals' ranking and in the groups of animals
212 to be selected. Since two different independent populations were used in this study, the
213 Discussion section was structured into two subsections to discuss the findings for each
214 population separately.

215

216 **Dataset 1: Purebred pig population**

217 One way to account for inbreeding depression in genomic prediction is by fitting
218 the inbreeding coefficient as a covariate in the model. The benefit of doing so is that
219 unbiased variance components may be obtained because the variance component
220 estimates may be inflated when inbreeding or heterozygosity are not fitted within the
221 models[17–19]. According to Bolormaa et al. [4] and Xiang et al. [19], inbreeding or
222 heterozygosity are fitted within the models to account for directional dominance (i.e., a

higher percentage of positive than negative dominance effects), otherwise, the variance components for the dominance effects will be biased. Vitezica et al. [17] also reported that in the absence of inbreeding within the models, the estimates for dominance variance were inflated for litter size in a purebred pig line. In the present study, there was a slight decrease in the additive genetic variance when the models adjusted for inbreeding depression, suggesting that not fitting inbreeding in the model might generate overestimated additive genetic variances.

The heritability estimates obtained from the models including only the additive and dominance genetic effects (MAD) corroborate with the estimates reported in previous studies using the same public dataset [32]. The studies reported dominance variance aiming to propose different methods for obtaining additive and dominance genetic variance components [33–35]. The dominance variance ratio estimates for T3 reported by Da et al. [33] and Liu et al. [35] were greater than estimated in this study (0.07 vs 0.02), and the dominance variance ratio estimated for T5 was smaller than that one reported by Nishio and Satoh [34] (0.045 vs 0.063). Da et al. [36] proposed multifactorial methods with SNP and haplotypes to calculate the genomic relationship matrix and fitted the epistasis effects up to third-order in the genomic prediction models. When comparing the estimates from the most complete models, in general, Da et al. [36] reported similar heritability (0.02 vs 0.01, 0.22 vs 0.21, 0.13 vs 0.12, 0.33 vs 0.31, 0.36 vs 0.34 for T1, T2, T3, T4, and T5, respectively) and lower additive-by-additive epistatic variance ratio estimates (0.04 vs 0.13, 0.18 vs 0.24, 0.28 vs 0.29, 0.02 vs 0.09, 0.05 vs 0.13 for T1, T2, T3, T4, and T5, respectively). The differences between estimates reported by each study using the same dataset might be due to different methods and/or parametrization considered to obtain the genomic relationship matrices in each study.

This paper was published at BMC Genomic Data: https://doi.org/10.1186/s12863-023-01174-x

The method to obtain the relationship matrices applied in this study, proposed by Vitezica et al. [6], is a flexible approach that can also be applied for populations that are not in Hardy-Weinberg equilibrium. However, it assumes linkage equilibrium between the genetic markers to ensure orthogonality between variance components. The non-orthogonality is clearly observed when there are significant changes in the variance estimates and when new variance components are introduced into the model [6]. In this study, the non-orthogonality between the variance components was noticeable when epistasis, especially additive-by-additive, was added to the model. This source of non-orthogonality might be due to linkage disequilibrium (LD) between the markers since this first dataset is from a nucleus purebred pig line, which is under intense selection pressure for various traits. Vitezica et al. [6] also reported high additive-by-additive variance and a sum of non-additive variances greater than the additive variance for a simulated high LD scenario due to strong selection. The additive, dominance, and epistasis effects are assumed independent of each other under the linkage equilibrium assumption [37, 38].However, the presence of LD might affect the magnitude of dominance and epistasis variance due to the correlation between markers by introducing dependency between the genetic additive and non-additive values, which could lead to overestimation of the non-additive genetic variance components. As a result, the partition between additive and non-additive components is more difficult when LD between markers is present [39]. It is worth noting that many complex traits are predominantly additive [40], and the additive genetic variance often comprises most of the total genetic variance for most traits [41]. Accurate estimation of additive genetic variance components can be achieved without assuming linkage equilibrium. Therefore, incorporating non-additive genetic effects into genomic prediction may not offer significant advantages for selection purposes. However, to evaluate the genetic architecture of complex traits, there is still a need to develop

272 methods for accurately estimating non-additive genetic variance components without
273 assuming linkage equilibrium, especially considering that many livestock populations are
274 subjected to intensive selective breeding (a major cause of LD).

275 As summarized by Wade et al. [42], for two bi-allelic loci, epistasis can be
276 considered in different ways: (i) additive-by-additive, interactions between homozygotes
277 at both loci; (ii) additive-by-dominance, interactions between homozygotes at locus A
278 and heterozygotes at locus B and vice-versa; (iii) dominance-by-dominance, interactions
279 between heterozygotes at both loci. The first dataset used in this study belongs to a
280 purebred population, which could be one of the reasons why the variance components for
281 additive-by-dominance and dominance-by-dominance epistasis are close to zero.
282 Purebred populations tend to exhibit reduced heterozygosity, which can make it more
283 challenging to accurately estimate additive-by-dominance and dominance-by-dominance
284 epistatic effects [43]. The results indicate that although there may be those types of
285 interactions between loci in the purebred population evaluated, they might be mostly
286 captured by the additive genetic variance [41].

287 All models presented dispersion close to one, indicating that there is no inflation
288 or deflation for the genomic estimated breeding values (GEBVs) [44]. The GEBVs also
289 presented bias close to zero in all models, which is desirable, since biased estimates
290 compromise the estimates of genetic trends and genetic gains in breeding programs [44].
291 However, the accuracy differed across traits and traits with higher (additive) heritability
292 yielded greater accuracies, which agrees with the literature [45–47]. Different accuracies
293 were estimated for each model, and there was a decrease in the accuracy when epistasis
294 effects were incorporated in the models, which can be associated with the decrease in the
295 additive genetic variance components for those models, since this variance component
296 are used to compute the accuracy [44].

297 Although models including epistatic effects were significantly better (based on
298 LRT parameter) for some traits (T2, T3, and T5), including epistasis had lower GEBV
299 accuracies for traits with lower heritability (T1, T2, and T3). It is noticeable that models
300 including epistatic effects had greater standard errors for the additive genetic variance
301 and heritability estimates for T1, which is the trait with the lowest heritability. This
302 suggests that the available data might not be sufficient to effectively distinguish between
303 additive genetic and epistasis effects. Therefore, larger datasets may be required to obtain
304 more accurate estimates of non-additive genetic effects [22], particularly for traits with
305 low heritability.

306 Another factor influencing this inferior accuracy for models including epistasis
307 may be due to the non-orthogonality between the components, especially between
308 additive genetic effects and additive-by-additive epistasis. At the same time, when only
309 additive genetic effects were fitted in the models, part of the additive-by-additive epistasis
310 was captured by the additive genetic component, as previously reported in other studies
311 [3, 48]. Even though models including additive-by-additive epistasis was significantly
312 better (based on LRT parameter) and this effect accounted for a relevant proportion of
313 phenotypic variance for some traits in the purebred population, including epistasis in the
314 model may capture part of the additive genetic variance [3]. The ranking of selection
315 candidates also changed for models as a consequence of the change in variance partition
316 due to the inclusion of non-additive genetic effects in the models.

317 In general, models including epistasis presented the largest changes in ranking of
318 the animals in comparison to the additive model. According to Piccoli et al. [49], the
319 degree of reranking is directly associated with the accuracies of estimates and, at the same
320 time, it is difficult to compare the reranking considering real datasets since the true
321 breeding values are unknown. However, it is noticeable that epistasis plays an important

role in genomic prediction and might change the selected animals when considered in a genetic evaluation program, which would impact genetic progress for the traits evaluated. There are studies investigating the impact of incorporating epistasis into genomic predictions aiming to develop methods that effectively integrate this effect into genomic prediction models (e.g., [50, 51]). Previous studies have shown that including all possible marker interactions in the prediction model does not improve the prediction ability [52, 53]. However, there is an improvement in prediction ability when only some interactions between markers are included in the model, being selected only those interactions with greater effects [52, 53].

Dataset 2: crossbred pig population

Since all heat stress-related traits had substantial additive genetic variability, including them in a selection program is feasible and can lead to genetic progress. Although, it should be noted that phenotypes measured in crossbred animals are expected to be more influenced by non-additive genetic effects than in purebred populations [21, 22]. Small non-additive genetic variances were observed for most of the traits evaluated in the crossbred dataset. Additionally, the estimates for dominance and epistasis variances had large standard errors which illustrates the difficulty of obtaining good estimates [17] and suggesting that the dataset was not large enough [19].

Besides HD and PS having considerable epistasis estimates, models including epistatic effects were significant better (based on LRT parameter) only for PS and no significant dominance variance was observed for any trait related to heat stress in the crossbred population. However, HD and PS are categorical traits and, threshold models [54–56] should be more suitable for genetically evaluating them. As highlighted by Alves

et al. [3], there might be some limitations in estimating non-additive genetic effects for categorical traits.

Estimating non-additive genetic variances is also difficult, since they are often, or at least partially, confounded with other effects, such as common environmental or maternal effects [4]. In this study, it is noticeable that, for traits related to heat stress, there was a confoundment between permanent environmental and non-additive genetic effects. This was observed through a reduction in the variance of permanent environmental effects when non-additive genetic effects were included in the model. This observation, particularly regarding PS, is similar to the results reported by Vitezica et al. [17]. The authors also reported that including non-additive genetic effects in the model did not have a large impact on residual variances and the non-additive genetic effects were captured by the permanent environmental effects [17].

The findings from this study suggest that the gene actions for heat stress-related traits in this population are mainly additive, or at least most of the non-additive genetic effects are captured by the additive genetic component. Although the dataset used in this study came only from crossbred animals, the pure breeds used for crossbreeding are both considered maternal breeds (Large White and Landrace) and genetically related [57–59]. Thus, in crossings between lines or breeds with high genetic distance it would be expected higher heterosis and greater non-additive genetic variance estimates [21] in comparison to the present study.

Implications and future studies

Quantitative traits are controlled by many genes with additive and potentially non-additive gene actions, and their phenotypic expression are the result of many developmental and biochemical pathways comprised of loci networks that interact at the

371 genetic and molecular levels, generating the epistasis effects [60]. Thus, the magnitude
372 of the epistasis effects depends on how many pathways are involved in the expression of
373 certain phenotypes and how these pathways are connected and interact between them. In
374 the other hand, the magnitude of dominance effects depends on the deviations of
375 genotypic values from breeding values for each locus. If the proportion of positive
376 dominance effects is greater than the proportion of negative dominance effects, it is
377 referred to as directional dominance [1, 9]. Heterosis and inbreeding depression are
378 directly dependent on non-additive genetic effects [9, 17]. Although it is expected that
379 non-additive genetic variation would be larger in crossbred populations [5, 9, 22, 61],
380 most of the traits measured in the crossbred population did not present substantial non-
381 additive genetic variance ratios. Additionally, fitting non-additive genetic effects in the
382 models did not improve the prediction ability of breeding values for the purebred
383 population. However, including non-additive genetic effects, especially additive-by-
384 additive epistasis, changed the animal's ranking and can therefore affect selection
385 decisions.

386 Many studies have suggested that non-additive genetic effects are greater in traits
387 related to fitness and adaptation than in morphological traits [62–65]. Considering the
388 importance of selecting more climatically resilient animals, it is necessary to elucidate
389 the genetic background of traits related to heat stress, especially for crossbred pigs. In our
390 study, although models including non-additive genetic effects were not significant (based
391 on LRT parameter) for most of the traits related to heat stress response, these effects might
392 play an important role in gene action for those traits. Thus, it would be important to
393 perform studies considering a larger dataset including records from purebred and
394 crossbred populations and evaluate different crossings as well.

395

This paper was published at BMC Genomic Data: https://doi.org/10.1186/s12863-023-01174-x

Conclusions

Including dominance effects in genomic prediction models did not improve the predictive ability of the models and most traits had none to low dominance variance. In the purebred population, low dominance variance ratios were observed, potentially due to reduced heterozygosity. Although models including additive-by-additive epistasis effects in genomic prediction exhibited significantly better fit for some traits, it led to lower accuracy when genomically predicting breeding values for traits with low heritability. For the evaluated populations and models, the inclusion of non-additive genetic effects did not improve genomic prediction accuracy. The non-orthogonality between variance components, especially between additive and additive-by-additive epistasis, suggests the presence of linkage disequilibrium challenges in the partition of additive and non-additive genetic effects. Therefore, there is still a need for developing methods able to accurately estimate non-additive variance components without assuming linkage equilibrium.

Traits related to heat stress in the crossbred population had substantial additive genetic variability, indicating their suitability for inclusion in selection programs. The difficulty in estimating non-additive genetic effects and the confounding with other effects, such as permanent environmental effects, is a challenge to obtain accurate estimates. Models incorporating non-additive genetic effects in genomic prediction for heat stress-related traits did not perform better than the additive model for most of the traits evaluated. Future studies should use larger datasets when they become available, including both purebred and crossbred animals, to better understand the contribution of non-additive genetic effects, particularly for traits related to adaptation, welfare, and resilience.

This paper was published at BMC Genomic Data: https://doi.org/10.1186/s12863-023-01174-x

Methods

Dataset 1: purebred pig population

Purebred dataset description

We used a public dataset [32] including pedigree, genotypic, and phenotypic information from a single nucleus pig line from Pig Improvement Company (PIC, Hendersonville, TN, USA). This dataset consisted of 3,534 individuals with genotypes for 52,843 SNPs and phenotypes for five performance traits that represent a small number of phenotypes that are routinely collected from birth in the genetic nucleus and with heritability estimates ranging from 0.07 to 0.62. The phenotype was either pre-corrected for environmental factors and rescaled by correcting for the overall mean (traits 3, 4, and 5) or was a rescaled, weighted mean of corrected progeny phenotypes (traits 1 and 2). The data also includes a pedigree file with parents and grandparents of the genotyped animals [32]. The descriptive statistics of the traits are presented in Table 7.

Table 7. Descriptive statistics of a public dataset from a purebred pig population[32]

Trait	Number of observations	Mean	SD[1]
T1	2,804	-0.0452	1.2077
T2	2,715	0.0049	1.1230
T3	3,141	0.7058	0.9607
T4	3,152	-1.0726	2.3276
T5	3,184	37.9888	60.4468

[1]SD: standard deviation

The quality control of genotype data consisted of removing SNPs with call rate lower than 0.90, minor allele frequency (MAF) less than 0.01, and extreme deviation from Hardy-Weinberg equilibrium (p-value < 10^{-5}). After quality control, 40,828 SNPs and 3,534 individuals remained for further analyses. No animals were removed during the quality control due their genotypes were imputed [32], then all animals presented higher call rate (> 0.90).

Variance components estimation

Different models including or not inbreeding and non-additive genetic effect of dominance and epistasis were fitted to estimate variance components:

MA: $\mathbf{y} = \mathbf{X\beta} + \mathbf{Za} + \boldsymbol{\varepsilon}$;

MAI: $\mathbf{y} = \mathbf{X\beta} + \mathbf{fb} + \mathbf{Za} + \boldsymbol{\varepsilon}$;

MAE: $\mathbf{y} = \mathbf{X\beta} + \mathbf{Za} + \mathbf{Ze_{aa}} + \boldsymbol{\varepsilon}$;

MAIE: $\mathbf{y} = \mathbf{X\beta} + \mathbf{fb} + \mathbf{Za} + \mathbf{Ze_{aa}} + \boldsymbol{\varepsilon}$;

MAD: $\mathbf{y} = \mathbf{X\beta} + \mathbf{Za} + \mathbf{Zd} + \boldsymbol{\varepsilon}$;

MAID: $\mathbf{y} = \mathbf{X\beta} + \mathbf{fb} + \mathbf{Za} + \mathbf{Zd} + \boldsymbol{\varepsilon}$;

MADE1: $\mathbf{y} = \mathbf{X\beta} + \mathbf{Za} + \mathbf{Zd} + \mathbf{Ze_{aa}} + \boldsymbol{\varepsilon}$;

MAIDE1: $\mathbf{y} = \mathbf{X\beta} + \mathbf{fb} + \mathbf{Za} + \mathbf{Zd} + \mathbf{Ze_{aa}} + \boldsymbol{\varepsilon}$;

MADE2: $\mathbf{y} = \mathbf{X\beta} + \mathbf{Za} + \mathbf{Zd} + \mathbf{Ze_{aa}} + \mathbf{Ze_{ad}} + \boldsymbol{\varepsilon}$;

MAIDE2: $\mathbf{y} = \mathbf{X\beta} + \mathbf{fb} + \mathbf{Za} + \mathbf{Zd} + \mathbf{Ze_{aa}} + \mathbf{Ze_{ad}} + \boldsymbol{\varepsilon}$;

MADE3: $\mathbf{y} = \mathbf{X\beta} + \mathbf{Za} + \mathbf{Zd} + \mathbf{Ze_{aa}} + \mathbf{Ze_{ad}} + \mathbf{Ze_{dd}} + \boldsymbol{\varepsilon}$;

MAIDE3: $\mathbf{y} = \mathbf{X\beta} + \mathbf{fb} + \mathbf{Za} + \mathbf{Zd} + \mathbf{Ze_{aa}} + \mathbf{Ze_{ad}} + \mathbf{Ze_{dd}} + \boldsymbol{\varepsilon}$;

where $\boldsymbol{y}$ is the vector of observations; $\boldsymbol{\beta}$ is the vector of fixed effects; $\mathbf{f}$ is the vector of inbreeding coefficient based on pedigree; $\mathbf{b}$ is the inbreeding depression; $\mathbf{a}$ is the vector of additive genetic effects with $\mathbf{a} \sim N(0, \mathbf{G_A}\sigma_a^2)$, where σ_a^2 is the additive genetic

variance and $\mathbf{G_A}$ is the genomic additive relationship matrix; $\mathbf{d}$ is the vector of dominance effects with $\mathbf{d} \sim N(0, \mathbf{G_D}\sigma_d^2)$ where σ_d^2 is the dominance variance and $\mathbf{G_D}$ the genomic dominance relationship matrix; $\mathbf{e_{aa}}$ is the vector of additive-by-additive epistatic effects, $\mathbf{e_{aa}} \sim N(0, \mathbf{G_{AA}}\sigma_{aa}^2)$, where σ_{aa}^2 is the additive-by-additive epistatic variance and $\mathbf{G_{AA}}$ the genomic additive-by-additive epistatic relationship matrix; $\mathbf{e_{ad}}$ is the vector of additive-by-dominance epistatic effects, $\mathbf{e_{ad}} \sim N(0, \mathbf{G_{AD}}\sigma_{ad}^2)$, where σ_{ad}^2 is the additive-by-dominance epistatic variance and $\mathbf{G_{AD}}$ the genomic additive-by-dominance epistatic relationship matrix; $\mathbf{e_{dd}}$ is the vector of dominance-by-dominance epistatic effects, $\mathbf{e_{dd}} \sim N(0, \mathbf{G_{DD}}\sigma_{dd}^2)$, where σ_{dd}^2 is the dominance-by-dominance epistatic variance and $\mathbf{G_{DD}}$ the genomic dominance-by-dominance relationship matrix; $\boldsymbol{\varepsilon}$ is the vector of residuals, $\boldsymbol{\varepsilon} \sim N(0, \mathbf{I}\sigma_\varepsilon^2)$, where σ_ε^2 is the residual variance and $\mathbf{I}$ an identity matrix; $\mathbf{X}$ and $\mathbf{Z}$ are incidence matrices of fixed and genetic effects, respectively.

The genomic additive relationship matrix ($\mathbf{G_A}$) was computed according to the method proposed by VanRaden [66]: $\mathbf{G_A} = \frac{\mathbf{MM'}}{2\sum p_i q_i}$, where the $\mathbf{M}$ matrix contains elements equal to $(2 - 2p_i)$, $(1 - 2p_i)$, $(-2p_i)$ for A_1A_1, A_1A_2, and A_2A_2 genotypes, respectively, being p_i the frequency of the allele A_1 in the SNP i and q_i is equal to $1 - p_i$. The genomic dominance relationship matrix ($\mathbf{G_D}$) was computed according to the method proposed by Vitezica et al. [5]: $\mathbf{G_D} = \frac{\mathbf{WW'}}{4\sum p_i^2 q_i^2}$, where the $\mathbf{W}$ matrix contains elements equal to $(-2q_i^2)$, $(2p_iq_i)$, $(-2p_i^2)$ for A_1A_1, A_1A_2, and A_2A_2 genotypes, respectively. The genomic epistatic relationship matrices were computed according to the methods proposed by Vitezica et al. [6]: $\mathbf{G_{AA}} = \frac{G_A \odot G_A}{tr(G_A \odot G_A)/n}$, $\mathbf{G_{AD}} = \frac{G_A \odot G_D}{tr(G_A \odot G_D)/n}$, and $\mathbf{G_{DD}} = \frac{G_D \odot G_D}{tr(G_D \odot G_D)/n}$ being $\odot$ the Hadamard product, tr the matrix trace, and n the number of animals.

The analyses were performed using the ASREML software [67]. To understand how the phenotypic variance was split when different non-additive genetic effects were

included in the models, variance components were estimated for each model. Estimates of additive heritability or narrow-sense heritability (h_a^2), dominance variance ratio (h_d^2), epistatic additive-by-additive variance ratio (h_{aa}^2), epistatic additive-by-dominance variance ratio (h_{ad}^2), and epistatic dominance-by-dominance variance ratio (h_{dd}^2) were computed as the ratio of estimates of additive genetic variance ($\widehat{\sigma_a^2}$), dominance variance ($\widehat{\sigma_d^2}$), additive-by-additive epistatic variance ($\widehat{\sigma_{aa}^2}$), additive-by-dominance epistatic variance ($\widehat{\sigma_{ad}^2}$), and dominance-by-dominance epistatic variance ($\widehat{\sigma_{dd}^2}$) to the total phenotypic variance ($\widehat{\sigma_p^2}$).

Predictive ability

Bias, dispersion, and accuracy estimates were obtained using the Linear Regression (LR) method [44]. LR method is based on the comparison of breeding values estimated from partial datasets with a dataset containing all information (whole dataset). The whole dataset was composed of all animals and their observations, while ten partial datasets were generated by setting 10% of records missing to perform a 10-fold cross-validation. The prediction bias was computed as:

$$\mu_{wp} = \overline{\widehat{\boldsymbol{u}}_p} - \overline{\widehat{\boldsymbol{u}}_w},$$

where μ_{wp} is the bias, $\overline{\widehat{\boldsymbol{u}}_p}$ is the GEBV mean predicted with partial information ($GEBV_p$) and $\overline{\widehat{\boldsymbol{u}}_w}$ is the GEBV mean predicted with whole information ($GEBV_w$). The GEBV dispersion is the slope of the regression ($b_{w,p}$) of $GEBV_w$ ($\widehat{\boldsymbol{u}}_w$) on $GEBV_p$ ($\widehat{\boldsymbol{u}}_p$), and was obtained as:

$$b_{w,p} = \frac{cov(\widehat{\boldsymbol{u}}_p, \widehat{\boldsymbol{u}}_w)}{var(\widehat{\boldsymbol{u}}_p)}$$

The accuracy was obtained as:

$$acc_p = \sqrt{\frac{cov(\hat{\boldsymbol{u}}_p, \hat{\boldsymbol{u}}_w)}{(1-\bar{F})\widehat{\sigma_a^2}}}$$

where acc_p is the accuracy, $\bar{F}$ is the mean inbreeding coefficient based on pedigree from the animals with partial information, and $\widehat{\sigma_a^2}$ is the estimated additive genetic variance using the whole population.

Model comparison

The AIC [68] LRT parameters were used to compare the models. LRT was computed separately for the models that included or not the inbreeding coefficient as a covariate. This was done to specifically assess the impact of incorporating random non-additive genetic effects on the model, while isolating the influence of the inbreeding coefficient. The LRT statistic was calculated as:

$$\text{LRT} = -2(\text{LogL}_{\text{reduced model}} - \text{LogL}_{\text{complete model}}),$$

in which $\text{LogL}_{\text{reduced model}}$ and $\text{LogL}_{\text{complete model}}$ are the likelihood logarithms for the reduced (i.e., from additive model; MA or MAI) and complete models (i.e., from the models including non-additive genetic effects), respectively. The level of significance used was 0.05.

We also evaluated the impact of the model used on the ranking of the animals and the proportion of commonly selected individuals based on the GEBVs from different models. The Spearman's rank correlation was calculated to evaluate the re-ranking between the GEBVs from the MA model, which is the most used approach for GEBV calculation, and the other evaluated models. Assuming different selection intensities, the top 1%, 5%, 10%, and 20% of the animals were ranked according to their GEBVs based on the MA model and compared with the animals selected based on the models including non-additive effects.

534

535 **Dataset 2: crossbred pig population**

536 ***Crossbred dataset description***

537 To evaluate the contribution of non-additive genetic effects on traits related to heat
538 stress in lactating sows, we used a dataset previously described by Johnson et al. [69]. In
539 summary, a total of 1,645 multiparous lactating sows (Large White × Landrace) were
540 housed in either a naturally ventilated or mechanically ventilated farrowing barn.
541 Thermoregulatory and anatomical traits were measured in 1,381 sows. The traits included
542 in this study were skin surface temperature from ear (T_{ES}), shoulder (T_{SS}), rump (T_{RS}),
543 and tail (T_{TS}); vaginal temperature considering the whole data measured every 10 minutes
544 (T_{Vall}), and the average of the six records per hour corresponding to 08:00, 12:00, 16:00,
545 and 20:00 hours during four days (T_{V4days}); respiration rate (RR), panting score (PS; score
546 scale from 0 to 3), and hair density (HD, score scale from 0 to 2) (the data collection is
547 described in details by Johnson et al. [69]). All animals were genotyped using the
548 PorcineSNP50K (50,703 SNPs) Bead Chip (Illumina, San Diego, CA, USA). Quality
549 control of genotype data consisted of removing SNPs with a call rate lower than 0.90 and
550 minor allele frequency (MAF) less than 0.01. It was also removed animals with call rate
551 lower than 0.90. After quality control, 49,536 SNPs for 1,625 animals remained for
552 further analyses. The descriptive statistics for the continuous traits are shown in Table 8.

553

554 **Table 8.** Descriptive statistics for continuous heat stress indicators in Landrace x Large White crossbred pig population.

Trait[1]	Number of animals	Number of observations	Mean	Minimum	Maximum	Standard deviation
T_{Vall}	1,381	932,708	39.74	37.08	42.35	0.76
T_{V4days}	1,381	21,415	39.70	37.10	42.70	0.77
T_{ES}	1,381	21,411	36.70	32.50	40.70	1.07
T_{SS}	1,381	21,414	36.50	32.30	39.80	1.08
T_{RS}	1,381	21,414	37.20	33.60	39.90	0.92
TT_S	1,381	21,413	36.90	33.20	40.00	0.95
RR	1,381	21,360	73.00	12.00	172.00	28.28

[1]T_{Vall}: all measures (every 10 minutes) of vaginal temperatures (°C); T_{V4days}: average of the six records per hour corresponding to 08:00, 12:00, 16:00, and 20:00 hours during four days (°C); T_{ES}: ear skin temperature (°C); T_{SS}: shoulder skin temperature (°C); T_{RS}: rump skin temperature (°C); T_{TS}: tail skin temperature (°C); RR: respiration rate (breaths per minute). Data collection protocols have been described in Johnson et al. [69].

555

This paper was published at BMC Genomic Data: https://doi.org/10.1186/s12863-023-01174-x

Estimation of variance components for traits related to heat stress

As performed for Dataset 1, we also fitted different models including or not non-additive genetic effect of dominance and epistasis to estimate variance components. However, we did not include additive-by-dominance and dominance-by-dominance epistasis effects to avoid overparametrized models, since this second dataset is small.

For the trait HD, the models MAI, MAID, MAIDE1, and MAIE previously mentioned were used. For skin temperatures, vaginal temperatures, PS, and RR repeatability models were fitted:

MAIpe: $\mathbf{y} = \mathbf{X\beta} + \mathbf{fb} + \mathbf{Za} + \mathbf{Zpe} + \boldsymbol{\varepsilon}$;

MAIDpe: $\mathbf{y} = \mathbf{X\beta} + \mathbf{fb} + \mathbf{Za} + \mathbf{Zd} + \mathbf{Zpe} + \boldsymbol{\varepsilon}$;

MAIDEpe: $\mathbf{y} = \mathbf{X\beta} + \mathbf{fb} + \mathbf{Za} + \mathbf{Zd} + \mathbf{Z}\boldsymbol{e_{aa}} + \mathbf{Zpe} + \boldsymbol{\varepsilon}$;

MAIEpe: $\mathbf{y} = \mathbf{X\beta} + \mathbf{fb} + \mathbf{Za} + \mathbf{Z}\boldsymbol{e_{aa}} + \mathbf{Zpe} + \boldsymbol{\varepsilon}$;

where $\mathbf{f}$ is the vector of genomic inbreeding coefficient; $\mathbf{b}$ is the inbreeding depression; $\boldsymbol{pe} \sim N(0, \boldsymbol{I}\sigma^2_{pe})$ where σ^2_{pe} is the permanent environmental variance and $\boldsymbol{I}$ an identity matrix; all other effects and matrices in the models have been previously described. The fixed effects for each trait were included as previously defined by Freitas et al. [70]. For T_{Vall}, the fixed effects were the concatenation of week and day of measurement; parity; concatenation of barn type and room; and in-barn environmental temperature as a linear covariate. For T_{V4days}, the fixed effects were concatenation of week, day, and time of measurement; parity; days in lactation; concatenation of barn type and room; and in-barn environmental temperature as a linear covariate. The fixed effects fitted for skin surface temperature (T_{ES}, T_{SS}, T_{RS}, and T_{TS}) and RR were trait recorder; concatenation of week, day, and time of measurement; parity; days in lactation; concatenation of barn type and room; and in-barn environmental temperature as a linear covariate. For PS, the fixed effects were trait recorder; concatenation of week and day of measurement; parity; days

581 in lactation; concatenation of barn type and room; and in-barn environmental temperature
582 as a linear covariate. The fixed effects fitted for HD were trait recorder and parity.
583 The variance components for dataset 2 were estimated following the same
584 methods described for dataset 1. The analyses were also performed using ASREML
585 software [71]. The estimates of additive heritability (h_a^2), dominance variance ratio (h_d^2),
586 and epistatic additive-by-additive variance ratio (h_{aa}^2) were computed, as described for
587 dataset 1. The ratio of the total genetic variance ($\widehat{\sigma_g^2} = \widehat{\sigma_a^2} + \widehat{\sigma_d^2} + \widehat{\sigma_{aa}^2}$) explained by
588 dominance ($\widehat{\sigma_d^2}/\widehat{\sigma_g^2}$) and epistasis additive-by-additive ($\widehat{\sigma_{aa}^2}/\widehat{\sigma_g^2}$) were also estimated.
589
590 ***Model comparison***
591 The AIC [68] and LRT parameters were also used to compare the models'
592 adjustment. LRT was computed comparing the models including non-additive genetic
593 effects with the additive animal model (MAIpe). The statistic was calculated as previously
594 described and the level of significance used was 0.05.
595
596 **References**
597 1. Falconer DS, Mackay TFC. Introduction to Quantitative Genetics. 4th edition. Harlow,
598 Essex, UK: Longmans Green; 1996.
599 2. Aliloo H, Pryce JE, González-Recio O, Cocks BG, Hayes BJ. Accounting for
600 dominance to improve genomic evaluations of dairy cows for fertility and milk
601 production traits. Genetics Selection Evolution. 2016;48.
602 3. Alves K, Brito LF, Baes CF, Sargolzaei M, Robinson JAB, Schenkel FS. Estimation
603 of additive and non-additive genetic effects for fertility and reproduction traits in
604 North American Holstein cattle using genomic information. Journal of Animal
605 Breeding and Genetics. 2020;137:316–30.

This paper was published at BMC Genomic Data: https://doi.org/10.1186/s12863-023-01174-x

606 4. Bolormaa S, Pryce JE, Zhang Y, Reverter A, Barendse W, Hayes BJ, et al. Non-
607 additive genetic variation in growth, carcass and fertility traits of beef cattle.
608 Genetics Selection Evolution. 2015;47.
609 5. Vitezica ZG, Varona L, Legarra A. On the additive and dominant variance and
610 covariance of individuals within the genomic selection scope. Genetics.
611 2013;195:1223–30.
612 6. Vitezica ZG, Legarra A, Toro MA, Varona L. Orthogonal estimates of variances for
613 additive, dominance, and epistatic effects in populations. Genetics.
614 2017;206:1297–307.
615 7. Nazarian A, Gezan SA. GenoMatrix: A Software Package for Pedigree-Based and
616 Genomic Prediction Analyses on Complex Traits. Journal of Heredity.
617 2016;107:372–9.
618 8. Sun C, VanRaden PM, Cole JB, O'Connell JR. Improvement of prediction ability for
619 genomic selection of dairy cattle by including dominance effects. PLoS One.
620 2014;9.
621 9. Varona L, Legarra A, Herring W, Vitezica ZG. Genomic selection models for
622 directional dominance: An example for litter size in pigs. Genetics Selection
623 Evolution. 2018;50.
624 10. Wientjes YCJ, Bijma P, Calus MPL, Zwaan BJ, Vitezica ZG, van den Heuvel J. The
625 long-term effects of genomic selection: 1. Response to selection, additive genetic
626 variance, and genetic architecture. Genetics Selection Evolution. 2022;54.
627 11. Jiang J, Shen B, O'Connell JR, VanRaden PM, Cole JB, Ma L. Dissection of additive,
628 dominance, and imprinting effects for production and reproduction traits in
629 Holstein cattle. BMC Genomics. 2017;18.

This paper was published at BMC Genomic Data: https://doi.org/10.1186/s12863-023-01174-x

12. Nagai R, Kinukawa M, Watanabe T, Ogino A, Kurogi K, Adachi K, et al. Genome-wide detection of non-additive quantitative trait loci for semen production traits in beef and dairy bulls. Animal. 2022;16.

13. Zhu Z, Bakshi A, Vinkhuyzen AAE, Hemani G, Lee SH, Nolte IM, et al. Dominance genetic variation contributes little to the missing heritability for human complex traits. Am J Hum Genet. 2015;96:377–85.

14. Jiang Y, Schmidt RH, Reif JC. Haplotype-based genome-wide prediction models exploit local epistatic interactions among markers. G3: Genes, Genomes, Genetics. 2018;8:1687–99.

15. Legarra A, Garcia-Baccino CA, Wientjes YCJ, Vitezica ZG. The correlation of substitution effects across populations and generations in the presence of nonadditive functional gene action. Genetics. 2021;219.

16. Xiang T, Christensen OF, Vitezica ZG, Legarra A. Genomic model with correlation between additive and dominance effects. Genetics. 2018;209:711–23.

17. Vitezica ZG, Reverter A, Herring W, Legarra A. Dominance and epistatic genetic variances for litter size in pigs using genomic models. Genetics Selection Evolution. 2018;50.

18. Aliloo H, Pryce JE, González-Recio O, Cocks BG, Goddard ME, Hayes BJ. Including nonadditive genetic effects in mating programs to maximize dairy farm profitability. J Dairy Sci. 2017;100:1203–22.

19. Xiang T, Christensen OF, Vitezica ZG, Legarra A. Genomic evaluation by including dominance effects and inbreeding depression for purebred and crossbred performance with an application in pigs. Genetics Selection Evolution. 2016;48:1–14.

20. William RL, Pollak E. Theory of Heterosis. J Dairy Sci. 1985;68:2411–7.

This paper was published at BMC Genomic Data: https://doi.org/10.1186/s12863-023-01174-x

655 21. Bunning H, Wall E, Chagunda MGG, Banos G, Simm G. Heterosis in cattle
656 crossbreeding schemes in tropical regions: meta-analysis of effects of breed
657 combination, trait type, and climate on level of heterosis. J Anim Sci. 2019;97:29–
658 34.
659 22. Su G, Christensen OF, Ostersen T, Henryon M, Lund MS. Estimating Additive and
660 Non-Additive Genetic Variances and Predicting Genetic Merits Using Genome-
661 Wide Dense Single Nucleotide Polymorphism Markers. PLoS One. 2012;7.
662 23. Culbertson MS, Mabry JW, Misztal I, Gengler N, Bertrand JK, Varona L. Estimation
663 of dominance variance in purebred Yorkshire swine. J Anim Sci. 1998;76:448–
664 51.
665 24. Norris D, Varona L, Ngambi JW, Visser DP, Mbajiorgu CA, Voordewind SF.
666 Estimation of the additive and dominance variances in SA Duroc pigs. Livest Sci.
667 2010;131:144–7.
668 25. Brito LF, Oliveira HR, McConn BR, Schinckel AP, Arrazola A, Marchant-Forde JN,
669 et al. Large-Scale Phenotyping of Livestock Welfare in Commercial Production
670 Systems: A New Frontier in Animal Breeding. Front Genet. 2020;11:793.
671 26. Freitas PHF, Johnson JS, Chen S, Oliveira HR, Tiezzi F, Lázaro SF, et al. Definition
672 of Environmental Variables and Critical Periods to Evaluate Heat Tolerance in
673 Large White Pigs Based on Single-Step Genomic Reaction Norms. Front Genet.
674 2021;12.
675 27. Johnson JS. Heat stress: Impact on livestock well-being and productivity and
676 mitigation strategies to alleviate the negative effects. Animal Production Science.
677 2018;58:1404–13.
678 28. Cui Y, Wang C, Hao Y, Gu X, Wang H. Chronic heat stress induces acute phase
679 responses and serum metabolome changes in finishing pigs. Animals. 2019;9.

This paper was published at BMC Genomic Data: https://doi.org/10.1186/s12863-023-01174-x

680 29. Gourdine JL, Riquet J, Rosé R, Poullet N, Giorgi M, Billon Y, et al. Genotype by
681 environment interactions for performance and thermoregulation responses in
682 growing pigs,. J Anim Sci. 2019;97:3699–713.
683 30. Varona L, Casellas J, Piedrafita J, Sánchez A, Garcia-Casado P, Arqué M, et al. Bayes
684 factor analysis for the genetic background of physiological and vitality variables
685 of F2 Iberian × Meishan newborn piglets. J Anim Sci. 2005;83:334–9.
686 31. Kim KS, Seibert JT, Edea Z, Graves KL, Kim ES, Keating AF, et al. Characterization
687 of the acute heat stress response in gilts: III. Genome-wide association studies of
688 thermotolerance traits in pigs. J Anim Sci. 2018;96:2074–85.
689 32. Cleveland MA, Hickey JM, Forni S. A common dataset for genomic analysis of
690 livestock populations. G3: Genes, Genomes, Genetics. 2012;2:429–35.
691 33. Da Y, Wang C, Wang S, Hu G. Mixed model methods for genomic prediction and
692 variance component estimation of additive and dominance effects using SNP
693 markers. PLoS One. 2014;9.
694 34. Nishio M, Satoh M. Including dominance effects in the genomic BLUP method for
695 genomic evaluation. PLoS One. 2014;9.
696 35. Liu T, Luo C, Ma J, Wang Y, Shu D, Qu H, et al. Including dominance effects in the
697 prediction model through locus-specific weights on heterozygous genotypes can
698 greatly improve genomic predictive abilities. Heredity (Edinb). 2022;128:154–8.
699 36. Da Y, Liang Z, Prakapenka D. Multifactorial methods integrating haplotype and
700 epistasis effects for genomic estimation and prediction of quantitative traits. Front
701 Genet. 2022;13.
702 37. KEMPTHORNE O. The correlation between relatives in a random mating population.
703 Proc R Soc Lond B Biol Sci. 1954;143:102–13.

704 38. Cockerham CC. An Extension of the Concept of Partitioning Hereditary Variance for
705 Analysis of Covariances among Relatives When Epistasis Is Present. Genetics.
706 1954;39:859.
707 39. Hill WG, Mäki-Tanila A. Expected influence of linkage disequilibrium on genetic
708 variance caused by dominance and epistasis on quantitative traits. Journal of
709 Animal Breeding and Genetics. 2015;132:176–86.
710 40. Hivert V, Sidorenko J, Rohart F, Goddard ME, Yang J, Wray NR, et al. Estimation
711 of non-additive genetic variance in human complex traits from a large sample of
712 unrelated individuals. Am J Hum Genet. 2021;108:786–98.
713 41. Hill WG, Goddard ME, Visscher PM. Data and Theory Point to Mainly Additive
714 Genetic Variance for Complex Traits. PLoS Genet. 2008;4:e1000008.
715 42. Wade MJ, Winther RG, Agrawal AF, Goodnight CJ. Alternative definitions of
716 epistasis: dependence and interaction. Trends Ecol Evol. 2001;16:498–504.
717 43. Iversen MW, Nordbø Ø, Gjerlaug-Enger E, Grindflek E, Lopes MS, Meuwissen T.
718 Effects of heterozygosity on performance of purebred and crossbred pigs.
719 Genetics Selection Evolution. 2019;51:1–13.
720 44. Legarra A, Reverter A. Semi-parametric estimates of population accuracy and bias of
721 predictions of breeding values and future phenotypes using the LR method.
722 Genetics Selection Evolution. 2018;50.
723 45. Zhang A, Wang H, Beyene Y, Semagn K, Liu Y, Cao S, et al. Effect of trait
724 heritability, training population size and marker density on genomic prediction
725 accuracy estimation in 22 bi-parental tropical maize populations. Front Plant Sci.
726 2017;8:1916.
727 46. Meuwissen TH. Accuracy of breeding values of “unrelated” individuals predicted by
728 dense SNP genotyping. 2009. https://doi.org/10.1186/1297-9686-41-35.

729 47. Combs E, Bernardo R. Accuracy of Genomewide Selection for Different Traits with
730 Constant Population Size, Heritability, and Number of Markers. Plant Genome.
731 2013;6:plantgenome2012.11.0030.
732 48. Muñoz PR, Resende MFR, Gezan SA, Resende MDV, de los Campos G, Kirst M, et
733 al. Unraveling additive from nonadditive effects using genomic relationship
734 matrices. Genetics. 2014;198:1759–68.
735 49. Piccoli ML, Brito LF, Braccini J, Oliveira HR, Cardoso FF, Roso VM, et al.
736 Comparison of genomic prediction methods for evaluation of adaptation and
737 productive efficiency traits in Braford and Hereford cattle. Livest Sci. 2020;231.
738 50. Martini JWR, Wimmer V, Erbe M, Simianer H. Epistasis and covariance: How gene
739 interaction translates into genomic relationship. Theor Appl Genet.
740 2016;129:963–76.
741 51. Martini JWR, Gao N, Cardoso DF, Wimmer V, Erbe M, Cantet RJC, et al. Genomic
742 prediction with epistasis models: On the marker-coding-dependent performance
743 of the extended GBLUP and properties of the categorical epistasis model (CE).
744 BMC Bioinformatics. 2017;18:1–16.
745 52. Vojgani E, Pook T, Martini JWR, Hölker AC, Mayer M, Schön CC, et al. Accounting
746 for epistasis improves genomic prediction of phenotypes with univariate and
747 bivariate models across environments. Theoretical and Applied Genetics.
748 2021;134:2913–30.
749 53. Ober U, Huang W, Magwire M, Schlather M, Simianer H, Mackay TFC. Accounting
750 for Genetic Architecture Improves Sequence Based Genomic Prediction for a
751 Drosophila Fitness Trait. PLoS One. 2015;10:e0126880.
752 54. Harville DA, Mee RW. A Mixed-Model Procedure for Analyzing Ordered
753 Categorical Data. Biometrics. 1984;40:393.

This paper was published at BMC Genomic Data: https://doi.org/10.1186/s12863-023-01174-x

754 55. Gilmour AR, Anderson RD, Rae AL. The analysis of binomial data by a generalized
755 linear mixed model. Biometrika. 1985;72:593–9.
756 56. Gianola D, Foulley JL. Sire evaluation for ordered categorical data with a threshold
757 model. Génétique, sélection, évolution 1983 15:2. 1983;15:1–23.
758 57. Wang L, Sørensen P, Janss L, Ostersen T, Edwards D. Genome-wide and local pattern
759 of linkage disequilibrium and persistence of phase for 3 Danish pig breeds. BMC
760 Genet. 2013;14:1–11.
761 58. Grossi DA, Jafarikia M, Brito LF, Buzanskas ME, Sargolzaei M, Schenkel FS.
762 Genetic diversity, extent of linkage disequilibrium and persistence of gametic
763 phase in Canadian pigs. BMC Genet. 2017;18:1–13.
764 59. Boré R, Brito LF, Jafarikia M, Bouquet A, Maignel L, Sullivan B, et al. Genomic data
765 reveals large similarities among Canadian and French maternal pig lines. Can J
766 Anim Sci. 2018;98:809–17.
767 60. Mackay TFC. The genetic architecture of quantitative traits. Annu Rev Genet.
768 2001;35:303–39.
769 61. Varona L, Legarra A, Toro MA, Vitezica ZG. Non-additive effects in genomic
770 selection. Frontiers in Genetics. 2018;9 MAR.
771 62. Roff DA, Emerson K. EPISTASIS AND DOMINANCE: EVIDENCE FOR
772 DIFFERENTIAL EFFECTS IN LIFE-HISTORY VERSUS
773 MORPHOLOGICAL TRAITS. Evolution (N Y). 2006;60:1981–90.
774 63. Mackay TFC. Epistasis and quantitative traits: Using model organisms to study gene-
775 gene interactions. Nature Reviews Genetics. 2014;15:22–33.
776 64. Mackay TFC, Moore JH. Why epistasis is important for tackling complex human
777 disease genetics. Genome Medicine. 2014;6.

This paper was published at BMC Genomic Data: https://doi.org/10.1186/s12863-023-01174-x

778 65. Merilä J, Sheldon BC. Genetic architecture of fitness and nonfitness traits: empirical
779 patterns and development of ideas. Heredity 1999 83:2. 1999;83:103–9.
780 66. VanRaden PM. Efficient Methods to Compute Genomic Predictions. J Dairy Sci.
781 2008;91:4414–23.
782 67. Gilmour AR, Gogel BJ, Cullis BR, Welham Sj, Thompson R. ASReml user guide
783 release 4.1 structural specification. Hemel hempstead: VSN international ltd.
784 2015.
785 68. Akaike H. A New Look at the Statistical Model Identification. IEEE Trans Automat
786 Contr. 1974;19:716–23.
787 69. Johnson JS, Wen H, Freitas PHF, Maskal JM, Hartman SO, Byrd MK, et al.
788 Evaluating phenotypes associated with heat tolerance and identifying moderate
789 and severe heat stress thresholds in lactating sows housed in mechanically or
790 naturally ventilated barns during the summer under commercial conditions. J
791 Anim Sci. 2023. https://doi.org/10.1093/JAS/SKAD129.
792 70. Freitas PHF, Johnson JS, Wen H, Maskal JM, Tiezzi F, Maltecca C, et al. Genetic
793 parameters for automatically-measured vaginal temperature, respiration
794 efficiency, and other thermotolerance indicators measured on lactating sows under
795 heat stress conditions. Genetics Selection Evolution. 2023;55:1–14.
796 71. Gilmour AR, Gogel BJ, Welham SJ. ASReml User Guide Functional Specification.
797 2015.
798

799 **Supplementary Information**

800 **Table S1.** Akaike information criterion (AIC) of model comparison for the purebred pig
801 population

Trait	Model	AIC	Parameters
T1	MA	3,863.83	2
	MAI	3,863.11	2
	MAE	3,862.02	3
	MAIE	3,861.25	3
	MAD	3,865.83	3
	MAID	3,865.11	3
	MADE1	3,864.02	4
	MAIDE1	3,863.25	4
	MADE2	3,866.02	5
	MAIDE2	3,865.25	5
	MADE3	3,868.02	6
	MAIDE3	3,867.25	6
T2	MA	2,712.44	2
	MAI	2,712.71	2
	MAE	2,701.22	3
	MAIE	2,701.36	3
	MAD	2,713.47	3
	MAID	2,713.72	3
	MADE1	2,702.37	4
	MAIDE1	2,702.45	4

This paper was published at BMC Genomic Data: https://doi.org/10.1186/s12863-023-01174-x

	MADE2	2,704.37	5
	MAIDE2	2,704.45	5
	MADE3	2,706.37	6
	MAIDE3	2,706.45	6
T3	MA	2,621.71	2
	MAI	2,621.59	2
	MAE	2,580.50	3
	MAIE	2,580.11	3
	MAD	2,623.15	3
	MAID	2,622.99	3
	MADE1	2,582.50	4
	MAIDE1	2,582.11	4
	MADE2	2,570.46	5
	MAIDE2	2,570.23	5
	MADE3	2,568.15	6
	MAIDE3	-	-
T4	MA	7,888.88	2
	MAI	7,888.00	2
	MAE	7,888.03	3
	MAIE	7,887.10	3
	MAD	7,890.30	3
	MAID	7,889.40	3
	MADE1	7,889.81	4
	MAIDE1	7,888.88	4

This paper was published at BMC Genomic Data: https://doi.org/10.1186/s12863-023-01174-x

	MADE2	7,891.81	5
	MAIDE2	7,890.88	5
	MADE3	7,893.81	6
	MAIDE3	7,892.88	6
T5	MA	28,635.05	2
	MAI	28,624.10	2
	MAE	28,629.19	3
	MAIE	28,618.39	3
	MAD	28,625.71	3
	MAID	28,616.85	3
	MADE1	28,622.47	4
	MAIDE1	28,613.47	4
	MADE2	28,624.47	5
	MAIDE2	28,615.47	5
	MADE3	28,626.47	6
	MAIDE3	28,617.47	6

[1]MA: $\mathbf{y} = \mathbf{X\beta} + \mathbf{Za} + \boldsymbol{\varepsilon}$; MAI: $\mathbf{y} = \mathbf{X\beta} + \mathbf{fb} + \mathbf{Za} + \boldsymbol{\varepsilon}$; MAE: $\mathbf{y} = \mathbf{X\beta} + \mathbf{Za} + \mathbf{Ze}_{aa} + \boldsymbol{\varepsilon}$; MAIE: $\mathbf{y} = \mathbf{X\beta} + \mathbf{fb} + \mathbf{Za} + \mathbf{Ze}_{aa} + \boldsymbol{\varepsilon}$; MAD: $\mathbf{y} = \mathbf{X\beta} + \mathbf{Za} + \mathbf{Zd} + \boldsymbol{\varepsilon}$; MAID: $\mathbf{y} = \mathbf{X\beta} + \mathbf{fb} + \mathbf{Za} + \mathbf{Zd} + \boldsymbol{\varepsilon}$; MADE1: $\mathbf{y} = \mathbf{X\beta} + \mathbf{Za} + \mathbf{Zd} + \mathbf{Ze}_{aa} + \boldsymbol{\varepsilon}$; MAIDE1: $\mathbf{y} = \mathbf{X\beta} + \mathbf{fb} + \mathbf{Za} + \mathbf{Zd} + \mathbf{Ze}_{aa} + \boldsymbol{\varepsilon}$; MADE2: $\mathbf{y} = \mathbf{X\beta} + \mathbf{Za} + \mathbf{Zd} + \mathbf{Ze}_{aa} + \mathbf{Ze}_{ad} + \boldsymbol{\varepsilon}$; MAIDE2: $\mathbf{y} = \mathbf{X\beta} + \mathbf{fb} + \mathbf{Za} + \mathbf{Zd} + \mathbf{Ze}_{aa} + \mathbf{Ze}_{ad} + \boldsymbol{\varepsilon}$; MADE3: $\mathbf{y} = \mathbf{X\beta} + \mathbf{Za} + \mathbf{Zd} + \mathbf{Ze}_{aa} + \mathbf{Ze}_{ad} + \mathbf{Ze}_{dd} + \boldsymbol{\varepsilon}$; MAIDE3: $\mathbf{y} = \mathbf{X\beta} + \mathbf{fb} + \mathbf{Za} + \mathbf{Zd} + \mathbf{Ze}_{aa} + \mathbf{Ze}_{ad} + \mathbf{Ze}_{dd} + \boldsymbol{\varepsilon}$*Model MAIDE3 did not converge for T3.

802

803 **Table S2.** Likelihood ratio test (LRT) of model comparison for the purebred pigs dataset.

Trait	Model[1]	DF[2]	LRT	p-value	Model	DF	LRT	p-value
T1	MAE	1	3.80	0.0513	MAIE	1	3.88	0.0489
	MAD	1	0.00	1.0000	MAID	1	0.00	1.0000
	MADE1	2	3.80	0.1496	MAIDE1	2	3.88	0.1437
	MADE2	3	3.80	0.2839	MAIDE2	3	3.88	0.2747
	MADE3	4	3.80	0.4337	MAIDE3	4	3.88	0.4225
T2	MAE	1	13.22	0.0003	MAIE	1	13.36	0.0003
	MAD	1	0.98	0.3222	MAID	1	1.00	0.3173
	MADE1	2	14.08	0.0009	MAIDE1	2	14.26	0.0008
	MADE2	3	14.08	0.0028	MAIDE2	3	14.26	0.0026
	MADE3	4	14.08	0.007	MAIDE3	4	14.26	0.0065
T3	MAE	1	43.22	<0.0001	MAIE	1	43.48	<0.0001
	MAD	1	0.58	0.4463	MAID	1	0.62	0.4310
	MADE1	2	43.22	<0.0001	MAIDE1	2	43.48	<0.0001
	MADE2	3	57.26	<0.0001	MAIDE2	3	57.36	<0.0001
	MADE3	4	61.56	<0.0001	MAIDE3*	4	-	-
T4	MAE	1	2.86	0.0908	MAIE	1	2.90	0.0886
	MAD	1	0.58	0.4463	MAID	1	0.60	0.4386
	MADE1	2	3.06	0.2165	MAIDE1	2	3.12	0.2101
	MADE2	3	3.06	0.3825	MAIDE2	3	3.12	0.3735
	MADE3	4	3.06	0.5478	MAIDE3	4	3.12	0.5379
T5	MAE	1	7.88	0.0050	MAIE	1	7.72	0.0055
	MAD	1	11.34	0.0008	MAID	1	9.24	0.0024
	MADE1	2	16.6	0.0002	MAIDE1	2	14.64	0.0007
	MADE2	3	16.6	0.0009	MAIDE2	3	14.64	0.0022

MADE3	4	16.6	0.0023	MAIDE3	4	14.64	0.0055

[1]MA: $\mathbf{y = X\beta + Za + \varepsilon}$; MAI: $\mathbf{y = X\beta + fb + Za + \varepsilon;}$ MAE: $\mathbf{y = X\beta + Za + Ze_{aa} + \varepsilon;}$ MAIE: $\mathbf{y = X\beta + fb + Za + Ze_{aa} + \varepsilon;}$ MAD: $\mathbf{y = X\beta + Za + Zd + \varepsilon;}$ MAID: $\mathbf{y = X\beta + fb + Za + Zd + \varepsilon;}$ MADE1: $\mathbf{y = X\beta + Za + Zd + Ze_{aa} + \varepsilon;}$ MAIDE1: $\mathbf{y = X\beta + fb + Za + Zd + Ze_{aa} + \varepsilon;}$ MADE2: $\mathbf{y = X\beta + Za + Zd + Ze_{aa} + Ze_{ad} + \varepsilon;}$ MAIDE2: $\mathbf{y = X\beta + fb + Za + Zd + Ze_{aa} + Ze_{ad} + \varepsilon;}$ MADE3: $\mathbf{y = X\beta + Za + Zd + Ze_{aa} + Ze_{ad} + Ze_{dd} + \varepsilon;}$ MAIDE3: $\mathbf{y = X\beta + fb + Za + Zd + Ze_{aa} + Ze_{ad} + Ze_{dd} + \varepsilon}$

[2]DF: degrees of freedom

*The model MAIDE3 did not converge for T3

804

805 **Table S3.** Akaike information criterion (AIC) of model comparison for the crossbred pig
806 population

Trait[1]	Model[2]	AIC	Parameters
TV_{all}	MAIpe	-162156	3
	MAIDpe	-162155	4
	MAIDEpe	-162153	5
	MAIEpe	-162155	4
TV_{4days}	MAIpe	-15530.2	3
	MAIDpe	-15528.5	4
	MAIDEpe	-15526.5	5
	MAIEpe	-15528.2	4
T_{ES}	MAIpe	16355.28	3
	MAIDpe	16357.28	4

	MAIDEpe	16359.28	5
	MAIEpe	16357.28	4
T_{SS}	MAIpe	13521.56	3
	MAIDpe	13523.46	4
	MAIDEpe	13525.46	5
	MAIEpe	13523.56	4
T_{RS}	MAIpe	2449.65	3
	MAIDpe	2451.65	4
	MAIDEpe	2453.65	5
	MAIEpe	2451.65	4
T_{TS}	MAIpe	7073.62	3
	MAIDpe	7075.52	4
	MAIDEpe	7077.52	5
	MAIEpe	7075.62	3
RR	MAIpe	149523.2	3
	MAIDpe	149525.2	4
	MAIDEpe	149527.2	5
	MAIEpe	149525.2	4
PS	MAIpe	5593.27	3
	MAIDpe	5595.22	4
	MAIDEpe	5588.49	5
	MAIEpe	5586.49	4
HD	MAI	104.39	2
	MAID	105.67	3

This paper was published at BMC Genomic Data: https://doi.org/10.1186/s12863-023-01174-x

MAIDE	104.7	4
MAIE	102.93	3

[1]TV_{all}: all measures (every 10 minutes) of vaginal temperatures during four days (°C); TV_{4days}: four-time measures of vaginal temperatures during four days (°C); T_{ES}: ear skin temperature; T_{SS}: shoulder skin temperature; T_{RS}: rump skin temperature; T_{TS}: tail skin temperature; RR: respiration rate; PS: panting score; HD: hair density.
[2]MAIpe: $\mathbf{y} = \mathbf{X\beta} + \mathbf{fb} + \mathbf{Za} + \mathbf{Zpe} + \boldsymbol{\varepsilon}$; MAIEpe: $\mathbf{y} = \mathbf{X\beta} + \mathbf{fb} + \mathbf{Za} + \mathbf{Zpe} + \mathbf{Z}\boldsymbol{e}_{aa} + \boldsymbol{\varepsilon}$; MAIDpe: $\mathbf{y} = \mathbf{X\beta} + \mathbf{fb} + \mathbf{Za} + \mathbf{Zpe} + \mathbf{Zd} + \boldsymbol{\varepsilon}$; MAIDEpe: $\mathbf{y} = \mathbf{X\beta} + \mathbf{fb} + \mathbf{Za} + \mathbf{Zd} + \mathbf{Z}\boldsymbol{e}_{aa} + \mathbf{Zpe} + \boldsymbol{\varepsilon}$; MAI: $\mathbf{y} = \mathbf{X\beta} + \mathbf{fb} + \mathbf{Za} + \boldsymbol{\varepsilon}$; MAIE: $\mathbf{y} = \mathbf{X\beta} + \mathbf{fb} + \mathbf{Za} + \mathbf{Z}\boldsymbol{e}_{aa} + \boldsymbol{\varepsilon}$; MAID: $\mathbf{y} = \mathbf{X\beta} + \mathbf{fb} + \mathbf{Za} + \mathbf{Zd} + \boldsymbol{\varepsilon}$; MAIDE1: $\mathbf{y} = \mathbf{X\beta} + \mathbf{fb} + \mathbf{Za} + \mathbf{Zd} + \mathbf{Z}\boldsymbol{e}_{aa} + \boldsymbol{\varepsilon}$

807

808 **Table S4.** Likelihood ratio test (LRT) of model comparison for the crossbred pig dataset.

Trait[1]	Model[2]	DF[3]	LRT	p-value
TV_{all}	MAIDpe	1	0.4	0.5271
	MAIDEpe	2	0.8	0.6703
	MAIEpe	1	0.6	0.4386
TV_{4days}	MAIDpe	1	0.34	0.5598
	MAIDEpe	2	0.34	0.8437
	MAIEpe	1	0	1.0000
T_{ES}	MAIDpe	1	0	1.0000
	MAIDEpe	2	0	1.0000
	MAIEpe	1	0	1.0000
T_{SS}	MAIDpe	1	0.1	0.7518
	MAIDEpe	2	0.1	0.9512
	MAIEpe	1	0	1.0000

This paper was published at BMC Genomic Data: https://doi.org/10.1186/s12863-023-01174-x

T_{RS}	MAIDpe	1	0	1.0000
	MAIDEpe	2	0	1.0000
	MAIEpe	1	0	1.0000
T_{TS}	MAIDpe	1	0.1	0.7518
	MAIDEpe	2	0.1	0.9512
	MAIEpe	1	0	1.0000
RR	MAIDpe	1	0	1.0000
	MAIDEpe	2	0	1.0000
	MAIEpe	1	0	1.0000
PS	MAIDpe	1	0.04	0.8415
	MAIDEpe	2	8.76	0.0125
	MAIEpe	1	8.76	0.0031
HD	MAID	1	0.7194	0.3963
	MAIDE	2	3.6876	0.1582
	MAIE	1	3.4596	0.0629

[1]TV_{all}: all measures (every 10 minutes) of vaginal temperatures during four days (°C); TV_{4days}: four-time measures of vaginal temperatures during four days (°C); T_{ES}: ear skin temperature; T_{SS}: shoulder skin temperature; T_{RS}: rump skin temperature; T_{TS}: tail skin temperature; RR: respiration rate; PS: panting score; HD: hair density.
[2]MAIpe: $\mathbf{y} = \mathbf{X\beta} + \mathbf{fb} + \mathbf{Za} + \mathbf{Zpe} + \boldsymbol{\varepsilon}$; MAIEpe: $\mathbf{y} = \mathbf{X\beta} + \mathbf{fb} + \mathbf{Za} + \mathbf{Zpe} + \mathbf{Ze_{aa}} + \boldsymbol{\varepsilon}$; MAIDpe: $\mathbf{y} = \mathbf{X\beta} + \mathbf{fb} + \mathbf{Za} + \mathbf{Zpe} + \mathbf{Zd} + \boldsymbol{\varepsilon}$; MAIDEpe: $\mathbf{y} = \mathbf{X\beta} + \mathbf{fb} + \mathbf{Za} + \mathbf{Zd} + \mathbf{Ze_{aa}} + \mathbf{Zpe} + \boldsymbol{\varepsilon}$; MAI: $\mathbf{y} = \mathbf{X\beta} + \mathbf{fb} + \mathbf{Za} + \boldsymbol{\varepsilon}$; MAIE: $\mathbf{y} = \mathbf{X\beta} + \mathbf{fb} + \mathbf{Za} + \mathbf{Ze_{aa}} + \boldsymbol{\varepsilon}$; MAID: $\mathbf{y} = \mathbf{X\beta} + \mathbf{fb} + \mathbf{Za} + \mathbf{Zd} + \boldsymbol{\varepsilon}$; MAIDE1: $\mathbf{y} = \mathbf{X\beta} + \mathbf{fb} + \mathbf{Za} + \mathbf{Zd} + \mathbf{Ze_{aa}} + \boldsymbol{\varepsilon}$

[3]DF: degrees of freedom

809

This paper was published at BMC Genomic Data: https://doi.org/10.1186/s12863-023-01174-x

CHAPTER 3: Genomic regions, candidate genes, and pleiotropic variants associated with physiological and anatomical indicators of heat stress response in lactating sows

Abstract

Background: Heat stress (HS) poses significant threats to the sustainability of livestock production. Genetically improving heat tolerance could enhance animal welfare and minimize production losses during HS events. Measuring phenotypic indicators of HS response and understanding their genetic background are crucial steps to optimize breeding schemes for improved climatic resilience. The identification of genomic regions and candidate genes influencing the traits of interest, including variants with pleiotropic effects, enables the refinement of genotyping panels used to perform genomic prediction of breeding values and contributes to unraveling the biological mechanisms influencing heat stress response. Therefore, the main objectives of this study were to identify genomic regions, candidate genes, and potential pleiotropic variants significantly associated with indicators of HS response in lactating sows using imputed whole-genome sequence (WGS) data. Phenotypic records for 18 traits and genomic information from 1,645 lactating sows were available for the study. The genotypes from the PorcineSNP50K panel containing 50,703 single nucleotide polymorphisms (SNPs) were imputed to WGS and after quality control, 1,622 animals and 7,065,922 SNPs were included in the analyses.

Results: A total of 1,388 unique SNPs located on sixteen chromosomes were found to be associated with 11 traits. Twenty gene ontology terms and 11 biological pathways were shown to be associated with variability in ear skin temperature, shoulder skin temperature, rump skin temperature, tail skin temperature, respiration rate, panting score, vaginal

temperature automatically measured every 10 minutes, vaginal temperature measured at 0800 h, hair density score, body condition score, and ear area. Seven, five, six, two, seven, 15, and 14 genes with potential pleiotropic effects were identified for indicators of skin temperature, vaginal temperature, animal temperature, respiration rate, thermoregulatory traits, anatomical traits, and all traits, respectively.

Conclusions: Physiological and anatomical indicators of HS response in lactating sows are heritable but highly polygenic. The candidate genes found are associated with important gene ontology terms and biological pathways related to heat shock protein activities, immune response, and cellular oxidative stress. Many of the candidate genes with pleiotropic effects are involved in catalytic activities to reduce cell damage from oxidative stress and cellular mechanisms related to immune response.

Keywords: climatic resilience, pleiotropy, Landrace, Large White, maternal-line pigs, GWAS

Background

Global warming has become a major concern for the long-term sustainability of livestock production. The ten warmest years on record since 1880 have all occurred after 2010, and the nine years from 2014 to 2022 are the nine warmest years on record [1]. These higher temperatures have a direct impact on animal production systems due to increased incidence of heat stress (HS) [2]. The absence of functional sweat glands in pigs limits their ability to use evaporative heat loss through sweating, reducing their thermoregulation ability in hot environments [2, 3]. Furthermore, intensive genetic selection for greater productive and reproductive performance has been associated with an increased metabolic heat production, making the animals more sensitive to high

environmental temperatures [4]. In this context, breeding for greater heat tolerance could improve the animals' ability to cope with HS conditions.

Breeding pigs for improved resilience to HS is possible as there is genetic variability in their response to HS [5–8]. One alternative for genetically identifying animals that perform better under HS conditions is through the use of reaction norm approach that model the genetic merit of an individual over an environmental gradient [9]. In general, reaction norm models are based on variability in performance traits across a continuous environmental gradient. Estimated breeding values for heat tolerance (slope of the reaction norms) based on this approach tend to be unfavorably correlated with the level of production (e.g., [7]). Therefore, identifying physiological, behavioral, and anatomical indicators of HS response that could be incorporated in selection indexes to breed for improved climatic resilience is promising in modern pig breeding programs [10]. Breeding for indicators of HS response could capture additional biological mechanisms involved in HS response and enable improvements in climatic resilience without compromising productivity [11]. Johnson et al. [10] described several traits as HS response indicators, such as skin and automatically-recorded vaginal temperatures, and respiration rate, and Freitas et al. [11] showed that these traits are heritable, i.e., they can be improved through genetic selection. Understanding the genetic background of these novel traits is a key step before including them in a breeding scheme. This includes the detection of quantitative trait loci (QTL) and the identification of candidate genes and biological pathways controlling the phenotypic expression of these HS indicator traits.

Genome-wide association studies (GWAS) enable the identification of genomic markers statistically associated with the traits of interest. GWAS is based on the principle of identifying genomic markers in linkage disequilibrium (LD) with the QTL affecting the trait of interest [12]. Various studies have reported genomic regions associated with

heat tolerance based on reaction norm models for reproductive traits [6] and productive traits such as hot carcass weight [8, 13]. Kim et al. [14] did not identify significant markers associated with respiration rate, rectal temperature, and skin temperature in crossbred gilts, however, they did report some genes known to be involved in physiological adaptation to general stressors. However, there is still a lack of studies aiming to identify candidate genes associated with physiological indicators of HS, such as vaginal temperature, skin temperature, and respiration rate in pigs using many phenotypic records and genomic markers.

Heat stress indicator traits may share metabolic pathways. A single locus can be involved in the expression of more than one trait, which is a phenomenon known as pleiotropy [15]. Pleiotropy occurs when a single causal variant or multiple variants within the same gene (or region) are associated with different phenotypes. Furthermore, pleiotropy also occurs when one phenotype causes a second phenotype, and a genetic variant is directly associated with the initial phenotype [16]. Pleiotropy is one of the causes of genetic correlation between traits. In this context, Freitas et al. [11] reported positive and moderate to high genetic correlations among physiological indicators of HS response such as skin temperature, vaginal temperature, panting score, and respiration rate. Identifying genes with pleiotropic effects and the genetic correlation between traits allows breeders to understand the biological results of the correlated response in multiple-trait selection. In this context, the primary objectives of this study were to identify genomic regions associated with physiological and anatomical indicators of HS response in lactating sows using imputed whole-genome sequence (WGS) data and identify pleiotropic variants. In addition, candidate genes, gene ontology (GO) terms, and metabolic pathways were identified in the significant genomic regions associated with the HS responses of lactating sows.

Results

Overview

We performed GWAS for 18 indicators of HS response and anatomical traits in crossbred lactating sows (Large White x Landrace) and found candidate genes and pleiotropic variants affecting these traits. The thermoregulatory indicator traits evaluated were ear skin temperature (T_{ES}), shoulder skin temperature (T_{SS}), rump skin temperature (T_{RS}), tail skin temperature (T_{TS}), respiration rate (RR), panting score (PS), vaginal temperature automatically measured every 10 min (T_{Vall}), the average of the six records per hour corresponding to 0800, 1200, 1600, and 2000 h during four days (T_{V4days}), and single records corresponding to 0800, 1200, 1600, and 2000 h measured at the first day of collection (T_{V8h}, T_{V12h}, T_{V16h}, T_{V20h}, respectively). The anatomical traits evaluated were hair density (HD), body size (BS), body condition score (BCS) using a sow caliper (BCS_{cal}), visual BCS (BCS_{vis}), ear length (EL), and ear area (EA). The variance components and genetic parameters for the traits evaluated in this study have been previously reported by Freitas et al. [11]. A description of all the studied traits and their corresponding heritability estimates, as previously reported by Freitas et al. [11], is presented in Table 1. The significant SNPs were identified based on their respective p-values, with adjustment for multiple testing using the Bonferroni correction at a significance level of $\alpha = 0.05$ for genome-wide significance. To take into account the dependence among tests due to linkage disequilibrium, α was divided by the number of independent chromosome segments (Me).

Table 1. Description of the evaluated traits and heritability estimates reported by Freitas et al. [11]

Trait Name	Trait abbreviation	[a]Description	[b]h^2
Ear skin temperature	T_{ES}	Ear skin surface temperature collected at 0800, 1200, 1600, and 2000 h daily during a period of four consecutive days.	0.04 ± 0.01
Shoulder skin temperature	T_{SS}	Shoulder skin surface temperature collected at 0800, 1200, 1600, and 2000 h daily during a period of four consecutive days.	0.06 ± 0.01
Rump skin temperature	T_{RS}	Rump skin surface temperature collected at 0800, 1200, 1600, and 2000 h daily during a period of four consecutive days.	0.06 ± 0.01
Tail skin temperature	T_{TS}	Tail skin surface temperature collected at 0800, 1200, 1600, and 2000 h daily during a period of four consecutive days.	0.05 ± 0.01
Respiration Rate	RR	Respiration rate was measured by counting flank movements for 15 s and multiplying by 4 to calculate breaths per minute (bpm) at 0800, 1200, 1600, and 2000 h daily during four consecutive days.	0.06 ± 0.01
Panting score	PS	A subjective panting score assessed at 15:30 h during four consecutive days and scored from 0 to 3 (0: if it was with closed mouth and normal breathing; 1: closed mouth and rapid breathing; 2: open mouth and rapid breathing; 3: open mouth and rapid breathing with obvious salivation).	0.05 ± 0.01

Vaginal temperature - All records	T_{Vall}	Vaginal temperature automatically recorded in 10 min intervals over four days using calibrated thermochron temperature recorders.	0.15 ± 0.02
Vaginal temperature - 4 days	T_{V4days}	The average vaginal temperature of the six records per hour corresponding to 0800, 1200, 1600, and 2000 h during four consecutive days.	0.22 ± 0.03
Vaginal temperature at 8:00 h	T_{V8h}	The average vaginal temperature of the six records per hour corresponding to 0800 h on the first day of collection.	0.25 ± 0.05
Vaginal temperature at 12:00 h	T_{V12h}	The average vaginal temperature of the six records per hour corresponding to 1200 h on the first day of collection.	0.29 ± 0.05
Vaginal temperature at 16:00 h	T_{V16h}	The average vaginal temperature of the six records per hour corresponding to 1600 h on the first day of collection.	0.22 ± 0.03
Vaginal temperature at 20:00 h	T_{V20h}	The average vaginal temperature of the six records per hour corresponding to 2000 h on the first day of collection.	0.22 ± 0.03
Hair density	HD	A subjective visual score ranging from 0 to 2, being the score 0 = hairless or limited hair cover, 1 = normal or moderate hair cover, and 2 = sow with greater than normal hair cover.	0.57 ± 0.09
Body size	BS	A visual score of the animal's body size into three categories: small, medium, or large.	0.53 ± 0.06

Body condition score - caliper	BCS_{cal}	Body condition score measured using a sow caliper tool.	0.60 ± 0.07
Body condition score - visual	BCS_{vis}	A visual body condition score based on five categories: 1 = emaciated, 2 = thin, 3 = ideal, 4 = fat, and 5 = overly fat.	0.53 ± 0.07
Ear area	EA	The ear area was calculated using a photo taken with a digital camera, where a 10.2 × 15.2 cm grid card containing 1 cm × 1 cm squares was placed next to the sows' ear.	0.57 ± 0.12
Ear length	EL	The ear length was calculated using a photo taken with a digital camera, where a 10.2 × 15.2 cm grid card containing 1 cm × 1 cm squares was placed next to the sows' ear.	0.53 ± 0.12

[a]Data collection protocols have been described by Johnson et al. [10] and Freitas et al. [11]

[b]These heritability estimates were previously reported by Freitas et al. [11]

125

126 **Genome-wide association and post-GWAS indicators of heat stress response**
127 **in lactating sows**

128 The medium-density genotypes were imputed to WGS using the Swine
129 Imputation (SWIM) Server [17] and the imputed genotypes were used to perform GWAS
130 for all traits included in the study. A total of 1,388 SNPs across 16 chromosomes were
131 associated with T_{ES}, T_{SS}, T_{RS}, T_{TS}, RR, PS, T_{Vall}, T_{V8h}, HD, BCS_{cal}, and EA (Table S1).

132 T_{SS} and T_{RS} are influenced by many significant genomic regions located on many
133 chromosomes (Figure 1.b-c), indicating that these traits are highly polygenic. For T_{ES},
134 significant peaks located on chromosomes 5, 7, 12, and 16 were identified (Figure 1.a),
135 while for T_{TS}, we observed significant peaks located on chromosomes 4, 6, and 15 (Figure
136 1.d). Two significant genomic regions located on chromosomes 7 and 8 were identified
137 for RR (Figure 1.e) and one significant region on chromosome 9 was found to be
138 associated with PS (Figure 1.f).

139 The Manhattan plots for vaginal temperature traits are shown in Figure 2. One
140 significant marker was observed on chromosome 1 (Figure 2.a) for $T_{Vall,}$ and one
141 significant peak (228 SNPs) on chromosome 2 for T_{V8h} (Figure 2.c). No significant SNPs
142 were observed for T_{V4days}, T_{V12h}, T_{V16h}, and T_{V20h} after Bonferroni correction for multiple
143 tests (Figure 2). Figure 3 shows the results of GWAS for anatomical traits. Two
144 significant SNPs located on chromosomes 2 and 7 and a significant peak (13 SNPs) on
145 chromosome 15 were identified for HD (Figure 3.a). Four significant SNPs located on
146 chromosome 13 were found to be associated with BCS_{cal} (Figure 3.c), while three
147 significant SNPs on chromosome 7 were identified to be associated with EA (Figure 3.e).
148 No significant SNPs were observed for BS, BCS_{vis}, and EL after multiple testing
149 correction (Figure 3). The Q-Q plots for the GWAS analyses for all evaluated traits are
150 presented in Figures S1-S3 (Additional File 1). The lambda values (genomic inflation
151 factor) ranged from 1.00 to 1.32.
152

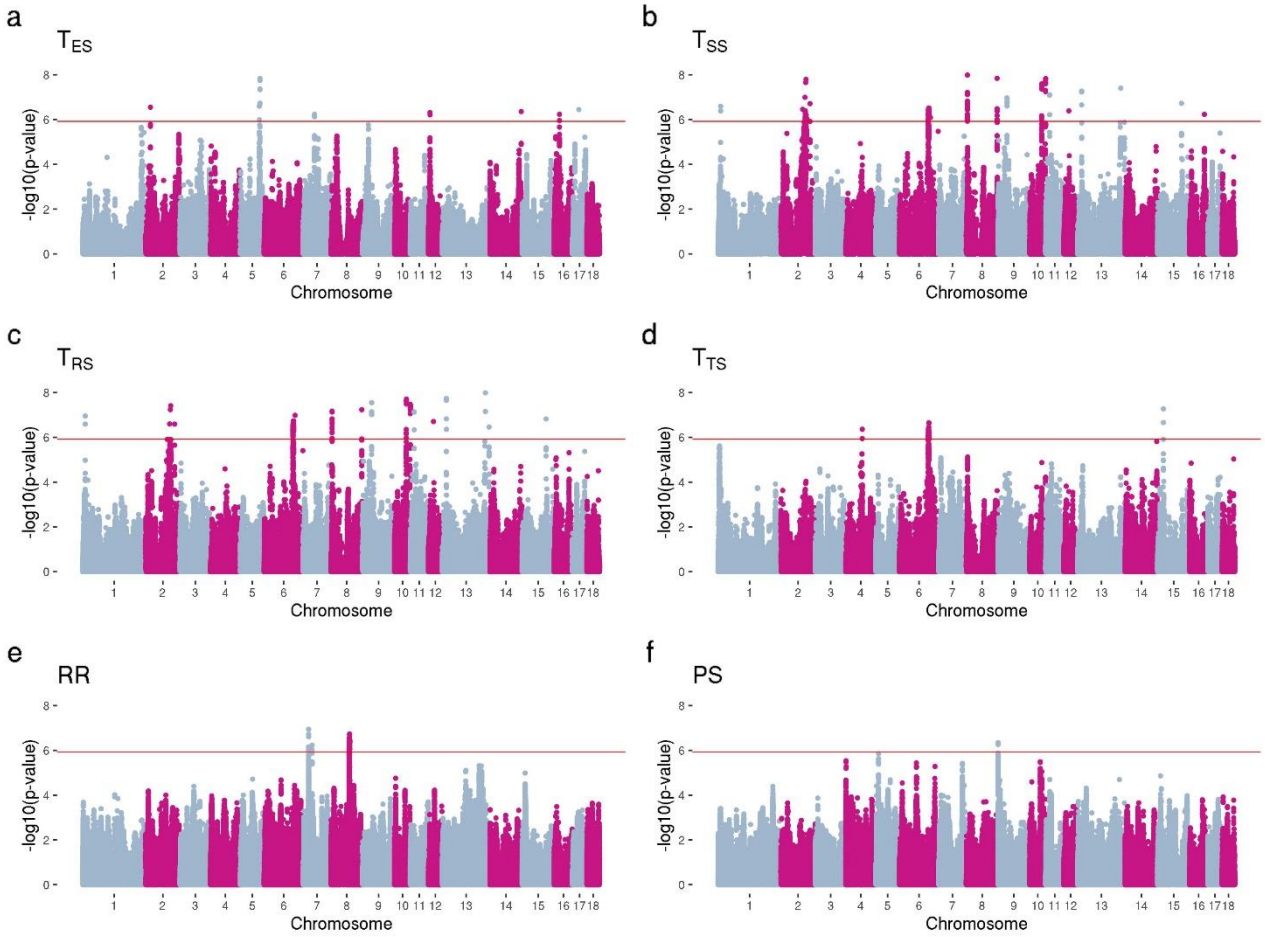

153

154 **Figure 1.** Manhattan plots for skin temperatures, respiration rate and panting score using

155 whole genome sequence data.

156 -log10(p-values) for ear skin temperature (T_{ES}; **a**), shoulder skin temperature (T_{SS}; **b**),

157 rump skin temperature (T_{RS}; **c**), tail skin temperature (T_{TS}; **d**), respiration rate (RR; **e**),

158 and panting score (PS; **f**). Genome-wide significance level is shown in a red line.

159

160 Genomic windows of 100 kb on each side of significant genomic markers were

161 used to identify candidate genes associated with each trait, as shown in Table S2. A total

162 of 26, 151, 102, 35, 63, eight, two, 93, four, four, and 11 genes were identified to be

163 associated with T_{ES}, T_{SS}, T_{RS}, T_{TS}, RR, PS, T_{Vall}, T_{V8h}, HD, BCS_{cal}, and EA, respectively.

164 The functional enrichment analyses enabled the identification of 20 GO terms (five

165 biological processes, four cellular components, and 11 molecular functions), and 11

166 metabolic pathways (Table 2). The complete list of all GO and metabolic pathways
167 identified, including those considered to be statistically significant and suggestive, are
168 shown in Table S3.

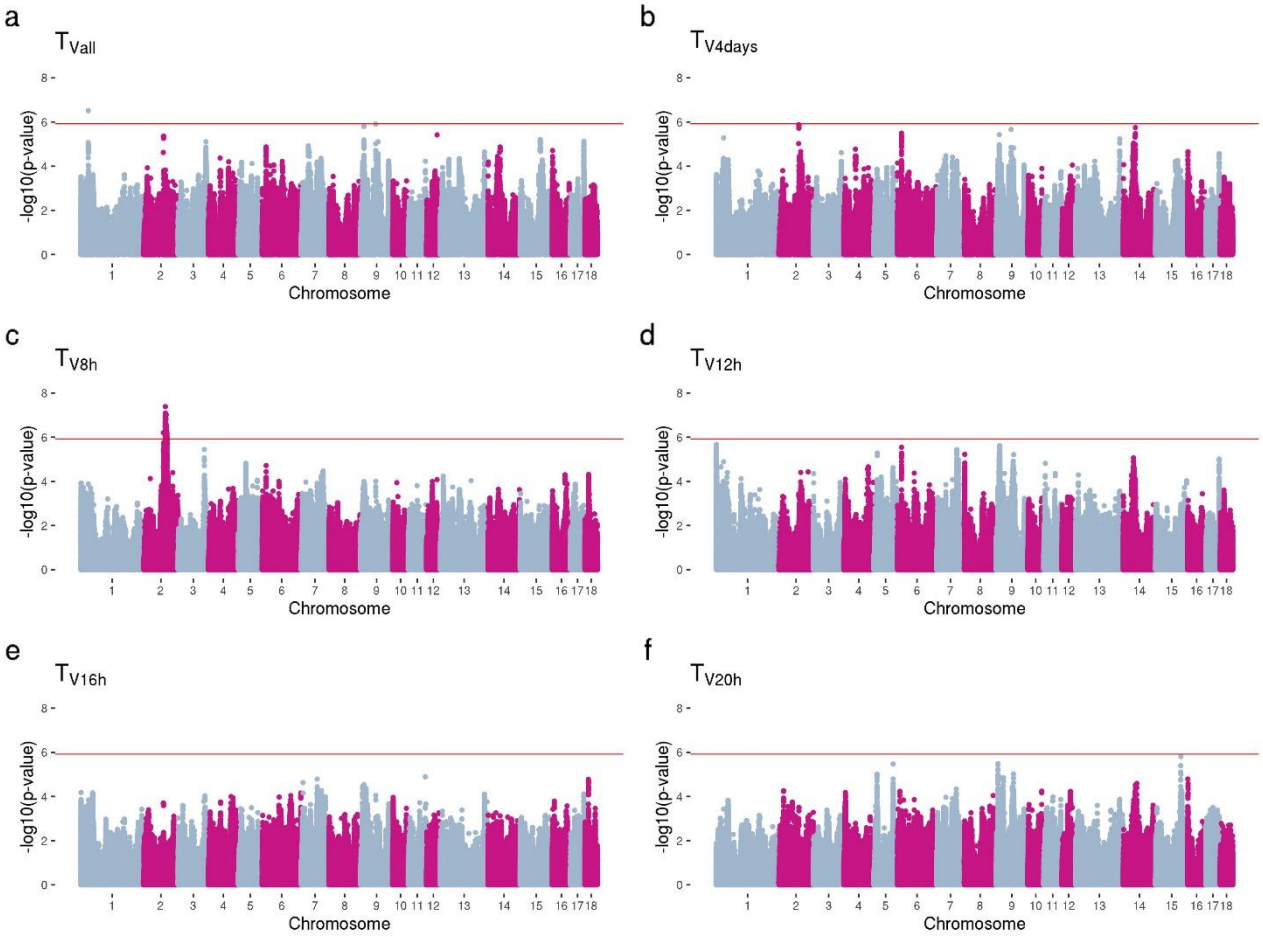

169

170 **Figure 2.** Manhattan plots of GWAS for vaginal temperatures using whole genome
171 sequence data.
172 -log10(p-values) for all measures (every 10 minutes) of vaginal temperatures for four
173 days (TV_{all}; **a**), four-time measures of vaginal temperatures for four days (T_{V4days}; **b**),
174 vaginal temperature measured on the first day at 8:00 (T_{V8h}; **c**), at 12:00 (T_{V12h}; **d**), at
175 16:00 (T_{V16h}; **e**), and at 20:00 (T_{V20h}; **f**). Genome-wide significance level is shown in a
176 red line.

177

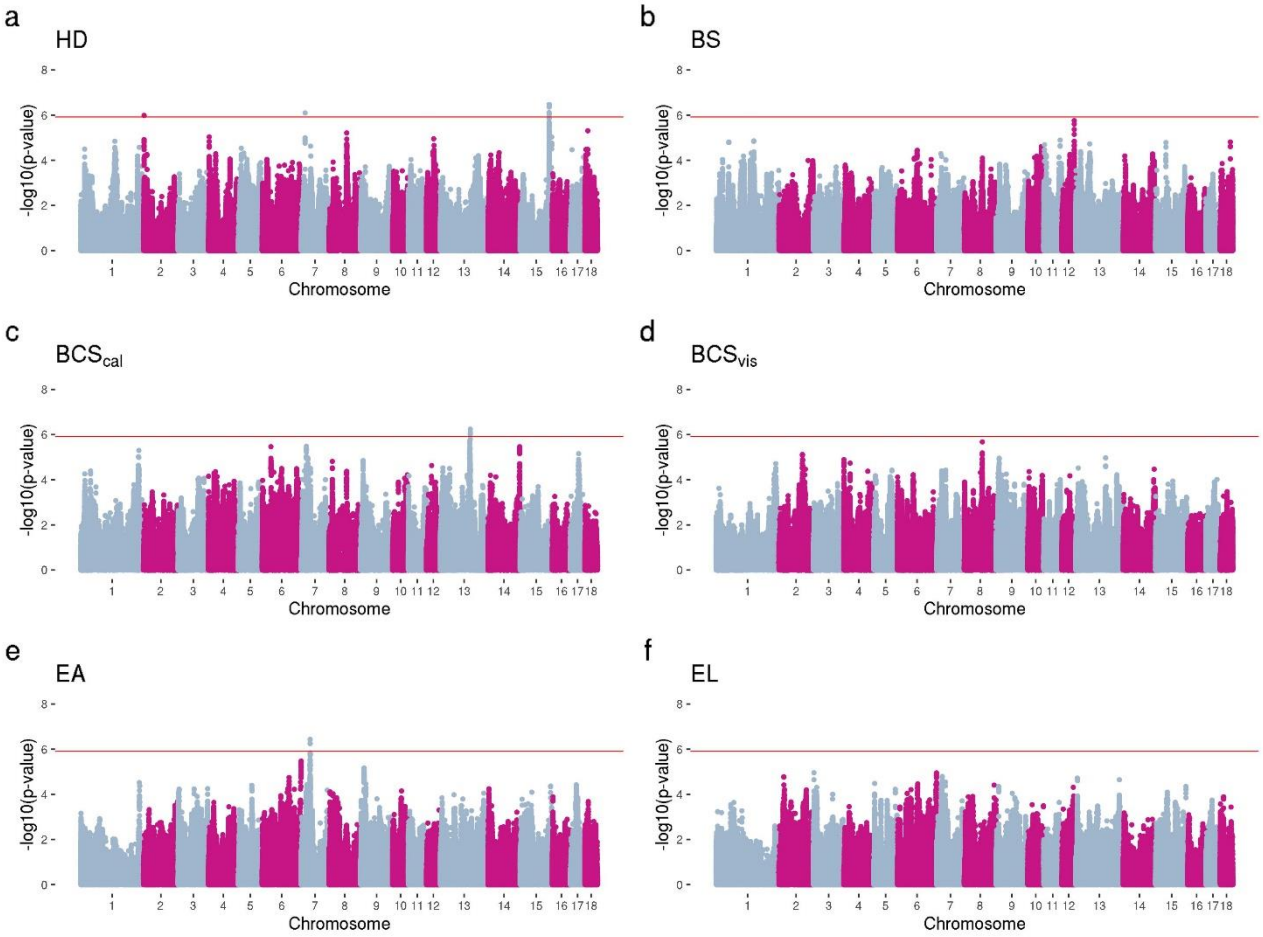

Figure 3. Manhattan plots of GWAS for anatomical traits using whole genome sequence data.

-log10(p-values) for hair density (HD; **a**), body size (BS; **b**), body condition score using a sow caliper (BCS_{cal}; **c**) and visual (BCS_{vis}; **d**), ear area (EA; **e**), and ear length (EL; **f**). Genome-wide significance level is shown in a red line.

184 **Table 2.** Significant gene ontology terms and pathways for heat stress related traits

Trait	Category	Term	p-value	Genes
EA	Pathway	ssc04659 Th17 cell differentiation	0.0477	*HSP90AB1, NFKBIE*
RR	Biological process	GO:0042026 protein refolding	0.0322	*ENSSSCG00000029160, HSPA1L*
RR	Biological process	GO:0034620 cellular response to unfolded protein	0.0390	*ENSSSCG00000029160, HSPA1L*
RR	Biological process	GO:0007130 synaptonemal complex assembly	0.0412	*BAG6, EHMT2*
RR	Biological process	GO:0006402 mRNA catabolic process	0.0412	*LSM2, DXO*
RR	Molecular function	GO:0051787 misfolded protein binding	0.0010	*BAG6, ENSSSCG00000029160, HSPA1L*
RR	Molecular function	GO:0016597 amino acid binding	0.0171	*AARS2, DDAH2*
RR	Molecular function	GO:0002161 aminoacyl-tRNA editing activity	0.0214	*AARS2, VARS1*
RR	Molecular function	GO:0005496 steroid binding	0.0298	*CYP21A2, NR3C2*
RR	Pathway	ssc04610 Complement and coagulation cascades	0.0130	*CFB, C4A, C2*
RR	Pathway	ssc05150 Staphylococcus aureus infection	0.0169	*CFB, C4A, C2*
RR	Pathway	ssc03040 Spliceosome	0.0295	*LSM2, HSPA1L, CDC5L*
T_{ES}	Molecular function	GO:0005229 intracellular calcium activated chloride channel activity	0.0182	*ANO4, TTYH2*
T_{ES}	Molecular function	GO:0003777 microtubule motor activity	0.0444	*KIF19, DNAI2*

T_{ES}	Molecular function	GO:0005254 chloride channel activity	0.0454	*ANO4, TTYH2*
T_{RS}, T_{SS}	Cellular component	GO:0098797 plasma membrane protein complex	0.0308	*EVC2, EVC*
T_{RS}, T_{SS}	Cellular component	GO:0005634 nucleus	0.0387	*NR1D1, THRA, ADNP2, NIF3L1, PIP4K2A, MRPS18C, ORC2, EBF1, NUDT12, CLK1, CDC6, SAMD13, PARD6G, EVC2, RNASEH2B, HSBP1L1, ABRAXAS1, HELQ, FUBP1*
T_{RS}, T_{SS}	Molecular function	GO:0070181 small ribosomal subunit rRNA binding	0.0271	*MRPS18C, ABRAXAS1*
T_{RS}, T_{SS}	Molecular function	GO:0003688 DNA replication origin binding	0.0437	*ORC2, CDC6*
T_{RS}	Pathway	ssc01100 Metabolic pathways	0.0486	*STT3B, COQ2, UOX, ALG9, NUDT12, ENSSSCG00000016093, GPAT3, ENSSSCG00000003754, ENSSSCG00000024765, PIP4K2A, HPSE*
T_{TS}	Biological process	GO:0007098 centrosome cycle	0.0275	*SSX2IP, PARD6G*

185

186 **Pleiotropic effects**

187 As traits are correlated and pleiotropic effects are expected, a multiple-trait
188 analysis, as proposed by Bolormaa et al. [18] was also performed. First, the traits were
189 decorrelated using Cholesky transformation [19, 20] and grouped into seven categories:
190 skin surface temperature traits (T_{ES}, T_{SS}, T_{RS}, and T_{TS}), vaginal temperatures (T_{Vall},
191 T_{V4days}, T_{V8h}, T_{V12h}, T_{V16h}, and T_{V20h}), indicators of animal temperature (i.e., all skin
192 surface and vaginal temperature traits), respiration rate traits (RR and PS),
193 thermoregulatory indicators (i.e., all skin surface temperatures, vaginal temperatures, and
194 respiration traits), anatomical traits (BCS_{cal}, BCS_{vis}, HD, BS, EA, and EL), and a
195 combination of all traits.

196 We identified one significant SNP with potential pleotropic effect for the skin
197 temperature group of traits, six significant variants for the vaginal temperatures group of
198 traits, six significant markers for the group of traits related to animal temperature, one
199 significant marker for respiration rate traits, four significant markers for the
200 thermoregulatory traits, and 21 significant markers for anatomical traits (Figure 4). The
201 significant marker observed for the skin temperatures group was also observed for the
202 group containing all traits. The same significant region on chromosome 7 was observed
203 for vaginal temperature and animal temperature groups, which was also observed for the
204 thermoregulatory traits group.

205 Seven, five, six, two, seven, 15, and 14 genes were identified for the trait groups
206 of vaginal temperature, animal temperatures, respiration traits, thermoregulatory traits,
207 anatomical traits, and all traits, respectively (Table 3). Five common genes (*ENPP5*,
208 *ENPP4*, *RCAN2*, *U6*, and *CLIC5*) were annotated for the vaginal temperatures, animal
209 body temperatures, and thermoregulatory traits groups. Only one significant ($p = 0.0269$)
210 GO term of biological process (GO:0007605 - Sensory perception of sound) for the

211 animal temperatures group, involving the annotated genes *ADGRV1* and *CLIC5* was
212 identified.

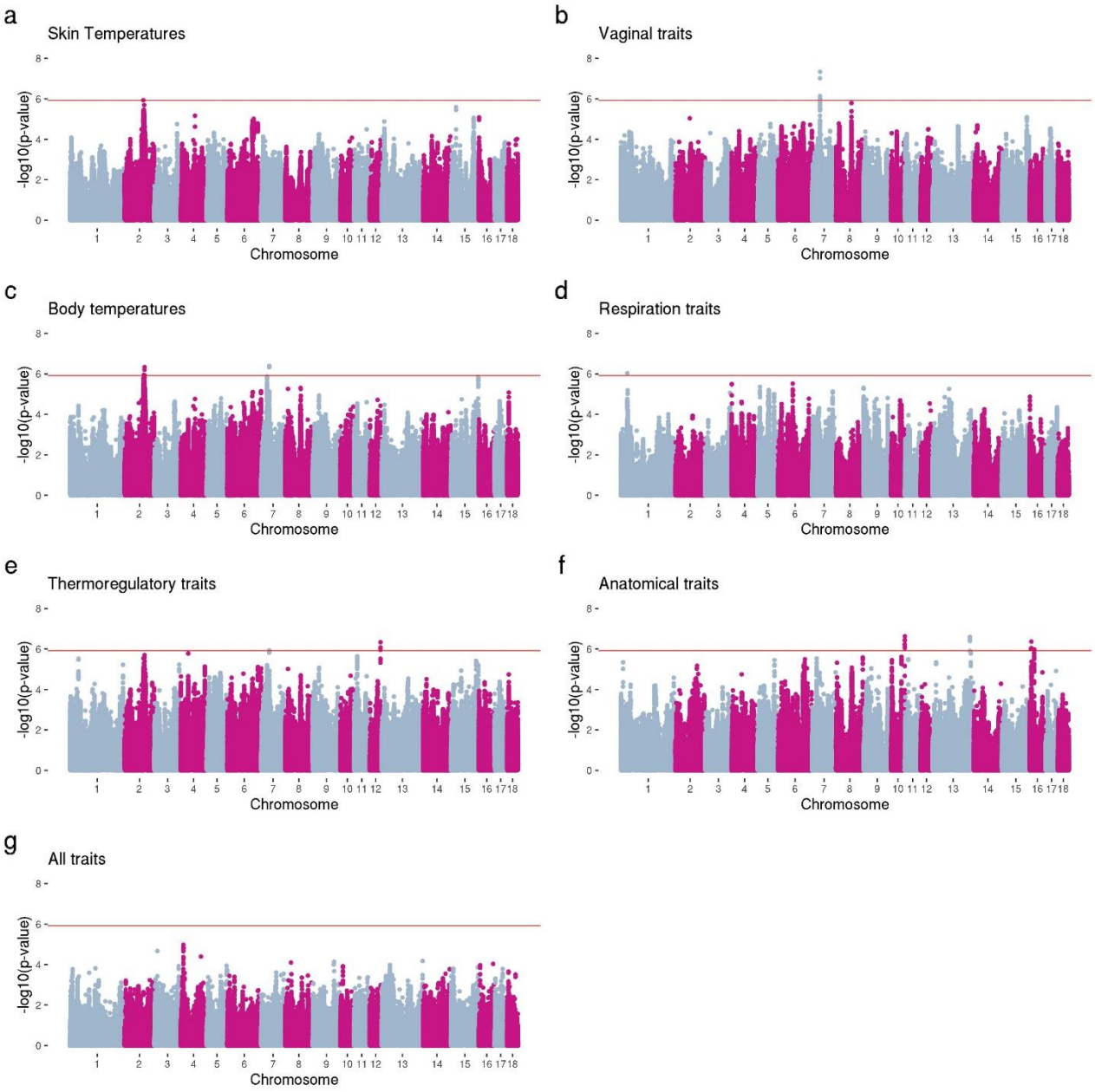

213

214 **Figure 4.** Manhattan plots for multiple-trait analysis for different categories of traits.
215 (**a**) The category skin temperatures included the traits ear skin temperature (T_{ES}), shoulder
216 skin temperature (T_{SS}), rump skin temperature (T_{RS}), tail skin temperature (T_{TS}). (**b**) The
217 category vaginal temperatures included all measures (every 10 minutes) of vaginal
218 temperatures for four days (TV_{all}), four-time measures of vaginal temperatures for four

days (T_{V4days}), vaginal temperature measured on the first day at 8:00 (T_{V8h}), at 12:00 (T_{V12h}), at 16:00 (T_{V16h}), and at 20:00 (T_{V20h}). (**c**) The category animal temperature included the traits T_{ES}, T_{SS}, T_{RS}, T_{TS}, T_{Vall}, T_{V4days}, T_{V8h}, T_{V12h}, T_{V16h}, and T_{20h}. (**d**) The category respiration traits included respiration rate (RR) and panting score (PS). (**e**) The category thermoregulatory traits included the traits T_{ES}, T_{SS}, T_{RS}, T_{TS}, T_{Vall}, T_{V4days}, T_{V8h}, T_{V12h}, T_{V16h}, T_{20h}, RR, and PS. (**f**) The category anatomical traits included the traits hair density (HD), body size (BS), body condition score using a sow caliper (BCS_{cal}) and visual (BCS_{vis}), ear area (EA), and ear length (EL). (**g**) The category all traits included the traits (T_{ES}, T_{SS}, T_{RS}, T_{TS}, T_{Vall}, T_{V4days}, T_{V8h}, T_{V12h}, T_{V16h}, T_{20h}, RR, PS, HD, BS, BCS_{cal}, BCS_{vis}, EA, and EL). Genome-wide significance level is shown in a red line.

Discussion

Genome-wide association for heat stress indicators

The traits evaluated in this study included physiological and anatomical indicators of heat stress response in lactating sows. The physiological indicators are response to mechanisms used by the animal to dissipate heat, such as increasing body temperature and respiration rate [21, 22]. The anatomical indicators are anatomical characteristics that affect the ability of the animal to dissipate heat, such as the animal's surface area, hair density, and body mass [23]. The heritability estimates for the traits evaluated in this study were previously reported by Freitas et al. [11]. Skin temperatures (i.e., T_{ES}, T_{SS}, T_{RS}, and T_{TS}), RR, and PS exhibited low heritability estimates, ranging from 0.04 to 0.06; vaginal temperatures (i.e., T_{Vall}, T_{V4days}, T_{V8h} T_{V12h}, T_{V16h}, and T_{V20h}) were moderately heritable, with estimates ranging from 0.15 to 0.29 [11]; and, anatomical traits (i.e., BCS_{cal}, BCS_{vis}, HD, BS, EA, and EL) showed moderate to high heritability estimates, ranging from 0.25 to 0.40 [11].

244 **Table 3.** Candidate genes with pleiotropic effects for physiological and anatomical indicators of heat stress response

Category[1]	Chr[2]	Position (bp)	Genes	Biotype
Skin temperatures	2	95,549,933	*TMEM161B*	protein coding
	2	95,549,933	*ENSSSCG00000054377*	lncRNA
	2	95,549,933	*ENSSSCG00000044415*	lncRNA
	2	95,549,933	*ENSSSCG00000061590*	lncRNA
	2	95,549,933	*ENSSSCG00000053188*	lncRNA
	2	95,549,933	*ENSSSCG00000051977*	lncRNA
	2	95,549,933	*U6*	snRNA
Vaginal temperatures	7	40,890,048	*ENPP4*	protein coding
	7	40,890,048	*ENPP5*	protein coding
	7	40,890,048	*RCAN2*	protein coding
	7	40,722,404 – 40,890,048	*CLIC5*	protein coding
	7	40,722,404 – 40,890,048	*U6*	snRNA
Animal temperatures	2	98,311,250	*ADGRV1*	protein coding
	2	98,311,250	*ENSSSCG00000058343*	lncRNA
	2	98,311,250	*ENSSSCG00000060683*	lncRNA
	2	98,311,250	*ENSSSCG00000057324*	lncRNA
	2	98,311,250	*ENSSSCG00000060037*	lncRNA
	2	98,311,250	*U6*	snRNA
	2	101,726,071 – 101,807,832	*MCTP1*	protein coding
	2	101,807,832	*ENSSSCG00000045627*	protein coding
	2	102,512,272	*ENSSSCG00000039731*	protein coding
	2	102,512,272	*ELL2*	protein coding
	2	102,512,272	*ENSSSCG00000048636*	lncRNA

	7	40,890,048	*ENPP4*	protein coding
	7	40,890,048	*ENPP5*	protein coding
	7	40,890,048	*RCAN2*	protein coding
	7	40,722,404 - 40,890,048	*CLIC5*	protein coding
	7	40,722,404 - 40,890,048	*U6*	snRNA
Respiration traits	1	32,189,900	*AKAP7*	protein coding
	1	32,189,900	*ENSSSCG00000062940*	lncRNA
Thermoregulatory traits	7	40,890,048	*ENPP4*	protein coding
	7	40,890,048	*ENPP5*	protein coding
	7	40,890,048	*RCAN2*	protein coding
	7	40,890,048	*CLIC5*	protein coding
	7	40,890,048	*U6*	snRNA
	12	54,342,040 – 54,347,768	*NTN1*	protein coding
	12	54,342,040 – 54,347,769	*STX8*	protein coding
Anatomical traits	10	68,752,585	*ENSSSCG00000011162*	protein coding
	10	68,752,585 – 69,231,514	*DIP2C*	protein coding
	10	69,069,560 – 69,352,432	*ZMYND11*	protein coding
	10	68,752,585	*ENSSSCG00000052560*	Processed pseudogene
	10	68,752,585	*ENSSSCG00000042778*	lncRNA
	10	68,752,585	*ENSSSCG00000056287*	lncRNA
	16	22,842,569	*GDNF*	protein coding
	16	22,823,916 – 22,842,569	*WDR70*	protein coding
	16	6,726,539	*ENSSSCG00000016796*	protein coding
	16	8,253,548	*CDH18*	protein coding
	16	8,687,034	*ENSSSCG00000050005*	protein coding
	16	6,726,539	*ENSSSCG00000051524*	lncRNA
	16	8,687,034	*ENSSSCG00000060866*	lncRNA

	16	8,687,034	*ENSSSCG00000061416*	lncRNA
	16	8,687,034	*ENSSSCG00000057598*	lncRNA
All traits	2	95,953,423	*ENSSSCG00000060814*	lncRNA
	2	95,953,423	*ENSSSCG00000063280*	lncRNA
	2	95,953,423	*ENSSSCG00000055379*	lncRNA
	2	95,953,423	*ENSSSCG00000060171*	lncRNA
	2	95,953,423	*ENSSSCG00000059644*	lncRNA
	2	95,953,423	*ENSSSCG00000056869*	lncRNA
	2	95,953,423	*ENSSSCG00000056397*	lncRNA
	2	95,953,423	*ENSSSCG00000053066*	lncRNA
	4	121,737,114	*ENSSSCG00000059304*	lncRNA
	4	121,737,114	*ENSSSCG00000057332*	lncRNA
	4	121,737,114	*ENSSSCG00000061167*	lncRNA
	7	85,032,675	*MCTP2*	protein coding
	7	85,032,675	*ENSSSCG00000035989*	protein coding
	7	85,032,675	*ENSSSCG00000054967*	lncRNA

[1]The category skin temperatures included the traits ear skin temperature (T_{ES}), shoulder skin temperature (T_{SS}), rump skin temperature (T_{RS}), tail skin temperature (T_{TS}). The category vaginal temperatures included all measures (every 10 minutes) of vaginal temperatures for four days (TV_{all}), four-time measures of vaginal temperatures for four days (T_{V4days}), vaginal temperature measured on the first day at 8:00 (T_{V8h}), at 12:00 (T_{V12h}), at 16:00 (T_{V16h}), and at 20:00 (T_{V20h}). The category animal temperature included the traits T_{ES}, T_{SS}, T_{RS}, T_{TS}, T_{Vall}, T_{V4days}, T_{V8h}, T_{V12h}, T_{V16h}, and T_{20h}. The category respiration traits included respiration rate (RR) and panting score (PS). The category thermoregulatory traits included the traits T_{ES}, T_{SS}, T_{RS}, T_{TS}, T_{Vall}, T_{V4days}, T_{V8h}, T_{V12h}, T_{V16h}, T_{20h}, RR, and PS. The category anatomical traits included the traits hair

density (HD), body size (BS), body condition score using a sow caliper (BCS_{cal}) and visual (BCS_{vis}), ear area (EA), and ear length (EL). The category all traits included the traits (T_{ES}, T_{SS}, T_{RS}, T_{TS}, T_{Vall}, T_{V4days}, T_{V8h}, T_{V12h}, T_{V16h}, T_{20h}, RR, PS, HD, BS, BCS_{cal}, BCS_{vis}, EA, and EL).

[2]Chr: Chromosome.

245

246 The statistical power of GWAS is impacted by various factors, including trait
247 heritability [24, 25]. A higher heritability increases statistical power, as heritability is a
248 key determinant of effect size [24]. Consequently, as heritability increases, the effect size
249 of each causal variant can also increase, thereby increasing the probability of identifying
250 causal variants [24, 25]. Additionally, the performance of GWAS can be improved by
251 using higher density genotyping. Several studies have shown that performing GWAS
252 using whole-genome sequence (WGS) data can improve QTL detection [26–28] because
253 it contains most causal mutations in the genome and can enable the identification of
254 variants that are highly linked and closer to the causal mutations as compared to
255 genotyping platforms with less SNPs. However, sequencing a large number of animals is
256 still expensive. A more cost-effective approach is the use of genotype imputation from
257 low-density to WGS data [28, 29].

258 In this study, the genomic inflation factor across the 18 evaluated traits ranged
259 from 1.00 to 1.32, which suggested that the results might be slightly inflated for some
260 traits. Although the inflation factor may indicate small population structure effects, Yang
261 et al. [30] showed that significant inflation of test statistics is expected under polygenic
262 inheritance even when there is no population stratification. Additionally, the genomic
263 inflation factor reflects the trait heritability and the number of causal variants [30]. The
264 range of observed values are within those observed in the literature for other complex
265 traits. Multiple markers located on sixteen chromosomes, each with relatively small effect
266 sizes (Table S1), were associated with the physiological and anatomical indicators of HS
267 response in lactating sows, suggesting that these traits are highly polygenic. For some of
268 the evaluated traits, no significant markers were identified, which could be due to the
269 study sample size or the polygenic nature of the study traits. Polygenic traits are
270 influenced by numerous loci with small effects on trait expression, reducing the

likelihood of identifying significant markers in association studies [31]. Furthermore, identifying markers associated with such traits requires larger sample sizes and more phenotypic records to enhance the power of the association analyses [31]. The amount of data used in this study might not be sufficient to identify associated markers with some of these traits (e.g., T_{V4days}, T_{V12h}).

Some genomic regions were commonly found to be significant for the skin surface temperature traits, which was already expected since these traits are highly genetically correlated (from 0.78 to 0.91) [11]. Additionally, Johnson et al. [10] reported moderate to high phenotypic correlations for these same traits (from 0.56 to 0.76). As these traits are highly genetically correlated, genetically selecting for skin temperature measured at any of the locations evaluated in this study should result in similar genetic progress on all of them due to indirect genetic responses.

A significant genomic region located on chromosome 2 was associated with vaginal temperature measured at 800 h. The genes harboring this region included *RASA1* (Ras GTPase-Activating Protein 1), a regulator of blood vessel and lymphatic vessel growth in adult mice and humans. *RASA1* induced-deficiency results in a lymphatic vessel disorder characterized by hyperplasia and leakage [32], which can affect the ability to vasodilate and dissipate excess body heat through the skin. Another gene found in the significant genomic region for T_{V8h} was *LYSMD3* (LysM Domain Containing 3). This gene plays a crucial role in the innate immune response by recognizing chitin and fungal spores, mediating the production of cytokines, and promoting early inflammatory responses in human lung epithelial cells [33]. For T_{Vall}, the candidate gene *AKAP7* (A-kinase Anchoring Protein 7), which encodes a protein kinase A-binding scaffolding molecule, was identified. This gene is crucial in cellular regulatory pathways during viral infections and influences neuroprotection by enhancing mitochondrial networks and

296 inhibiting apoptosis under glutamate-induced oxidative stress, being reported as a
297 cytoprotective factor, potentially preventing tissue damage during viral infections [34–
298 36]. Due to *AKAP7*'s cytoprotective functions, it might also contribute to preventing
299 tissue damage in HS conditions. Investigating the same population as in this study, Wen
300 et al. [37] used random regression models to analyze all automatically-recorded vaginal
301 temperature records as longitudinal traits. Wen et al. [37] identified two important
302 genomic regions on chromosomes 10 and 16, containing genes associated with immunity,
303 protein transport, and energy metabolism. However, in this study, we did not find these
304 same genomic regions and genes, which might be due to different modeling approaches
305 and the small effect size of the identified genomic regions.

306 It is well-known that heat shock proteins (HSP) play an important role in cell
307 survival under stress conditions, especially HS [38–40]. HSP protects cells from damage
308 by binding to unfolded or denatured proteins, preventing their aggregation and promoting
309 their refolding [41, 42]. In addition, HSP helps to restore protein structure and function,
310 ensuring that essential processes can continue despite the stress [41, 42]. HSP also acts in
311 the degradation of proteins that cannot be refolded properly and can interact with other
312 proteins and modulate their activity or stability, influencing various cellular processes
313 such as cell cycle progression and apoptosis [41]. HSP activities have been reported to
314 minimize HS-induced cellular death and improve thermotolerance in livestock [43] and
315 to regulate the immune response, including stimulatory and regulatory functions [44]. In
316 this study, we found genomic regions associated with T_{SS}, T_{RS}, and T_{TS} overlapping with
317 *HSBP1L1* (Heat Shock Factor Binding Protein 1 Like 1) and regions associated with EA
318 overlapping with the *HSP90AB1* (Heat Shock Protein 90 Alpha Family Class B Member
319 1) gene. *HSBP1L1* is presumed to suppress the heat shock factor transcription under
320 stress, suggesting that *HSBP1L1* may regulate cellular responses to stress and cellular

heat acclimation [45]. *HSP90AB1* encodes a member of the heat shock protein 90 family, a crucial protein for signal transduction, protein folding, and degradation, playing a significant role in maintaining protein stability and promoting cell survival, particularly under cellular stress [46]. Genetic variations in *HSP90AB1* have been linked to stress-induced mortality, heat tolerance, and productivity in animals [46].

One of the main responses to HS and mechanisms used for pigs to maintain their body temperature is increased RR, allowing them to dissipate heat through evaporation [4, 47, 48]. In the genomic windows around the two significant regions associated with RR we identified 63 genes, including *HSPA1L* (Heat Shock Protein Family A -Hsp70 - Member 1 Like), which encodes a 70kDa heat shock protein crucial for cellular and molecular responses to HS in livestock. *HSPA1L* ensures proper protein folding, unfolding, and refolding, having protective functions alongside other HSPs during HS events [49]. In the functional analyses, which includes all identified candidate genes for RR, a biological process related to protein refolding and cellular response to unfolded protein was revealed based on the GO analyses. Molecular functions of misfolded protein binding and amino acid binding were also identified, and these functions are linked to HSP activity.

It is already known that HS affects the immune response in pigs [50–52]. The genes found to overlap with the significant regions observed for T_{ES} include *BTBD17* (BTB domain containing 17), *PTPRE* (Protein Tyrosine Phosphatase Receptor Type E), and *ARNT2* (Aryl Hydrocarbon Receptor Nuclear Translocator 2). *BTBD17* has been reported to be involved in the negative regulation of viral genome replication and viral response [53, 54]. *PTPRE* has been shown to repress M2 macrophage activation and may have a critical role in regulating inflammatory responses and local homeostasis, particularly in the context of macrophage activation and function [55]. *ARNT2* regulates

346 immune-related genes, phagocytic cell differentiation, and lymphocyte activity [56]. A
347 polymorphism in *ARNT2* has been linked to reduced macrophage phagocytic activity,
348 impacting immunity, platelet activation, and phagocytosis in pigs [56]. Additionally, we
349 also found that the *NR1D1* (Nuclear Receptor Subfamily 1 Group D Member 1) gene
350 harbors genomic markers associated with T_{SS} and T_{RS}. *NR1D1* acts as a transcriptional
351 repressor and is required for establishing and maintaining body temperature rhythm in a
352 manner adaptable to environmental demands, allowing mammals to adapt to
353 environmental temperature changes [57].

354 Previous studies have reported that some anatomical characteristics, such as the
355 animal's surface area, hair density, and body mass, can affect the ability of the animal to
356 dissipate heat [23]. In this study we identified that regions associated with EA overlapping
357 with the *HSP90AB1* (Heat Shock Protein 90 Alpha Family Class B Member 1) gene that
358 encodes a member of the heat shock protein 90 family, as previously discussed.
359 Additionally, we found that regions associated with HD overlap with the gene *DOCK10*
360 (dedicator of cytokinesis 10). *DOCK10* is part of the dedicator of cytokinesis (DOCK)
361 family proteins, which are expressed at varying levels in lymphocytes and have diverse
362 effects on immune functions [58]. *DOCK10* influences the B cells development, which
363 play a crucial role in the adaptive immune response by producing antibodies [58].

364 In the functional genomic analyses, the molecular functions of intracellular
365 calcium activated chloride channel activity and chloride channel activity were found to
366 be associated with T_{ES}. The chloride anion plays a key role in regulating cellular
367 homeostasis, affecting diverse cellular functions, including reactive oxygen species levels
368 [59]. Oxidative stress stimulates calcium activated chloride channels [60–62], and
369 promotes cellular and mitochondrial oxidative damage [63]. In addition, the molecular
370 function of DNA replication origin binding was associate with T_{SS} and T_{RS} and the

biological process of centrosome cycle was associated with T_{TS}. These two GO terms are related to cell division and are affected by HS. HS can induce partial DNA re-replication and centrosome amplification in early S-phase cells [64]. Although HS causes centrosome degradation, HSP70 protects centrosome proteins from denaturation [65]. In the functional genomic analysis for RR, we identified two pathways: the pathway of *Staphylococcus aureus* infection and the pathway of complement and coagulation cascades. The latter is a proteolytic cascade in blood plasma and serves as a mediator of innate immunity, a nonspecific defense mechanism against pathogens [66–68].

Candidate genes with pleiotropic effects for heat stress-related traits in lactating sows

Pleiotropy is a well-known effect that occurs when a locus influences more than one trait [69, 70]. In cases of pleiotropy, if a gene has effects on more than one trait, the genetic variation associated with one trait may be correlated with the genetic variation of another trait, resulting in a genetic correlation between the two traits. Freitas et al. [11] reported high genetic correlations among skin temperature traits (> 0.78) and among vaginal temperature traits (> 0.75). Similarly, high genetic correlations were observed for RR with PS (0.87), with BCS measures (0.92), and with ear length and ear area (0.95). Additionally, low to moderately positive genetic correlations were observed between skin temperatures and vaginal temperatures (ranging from 0.25 to 0.76). Low genetic correlations were estimated between vaginal temperatures and BCS (from -0.01 to 0.06), while all other trait combinations were lowly genetically correlated [11].

Identifying candidate genes with pleiotropic effects is important to understand how a single gene can affect multiple traits and the common biological pathways involved in the expression of these traits. In GWAS studies, it is possible to identify the same

regions or genes affecting different traits, which is termed cross-phenotype associations, however these associations might not be pleiotropy [70]. Solovieff et al. [70] defined three categories of pleiotropy: biological pleiotropy, mediated pleiotropy, and spurious pleiotropy. Biological pleiotropy refers to a genetic variant that directly influences more than one trait [70, 71]. Mediated pleiotropy is when a variant directly affects a first phenotype that affects the second phenotype [70, 71]. Spurious pleiotropy can occur due to some sources of bias, identifying genes that are not truly pleiotropic [70, 71].

In this study, to identify the pleiotropy among the traits, we grouped them as skin surface temperature traits (T_{ES}, T_{SS}, T_{RS}, and T_{TS}), vaginal temperatures (T_{Vall}, T_{V4days}, T_{V8h}, T_{V12h}, T_{V16h}, and T_{V20h}), animal body temperatures (i.e., all skin surface and vaginal temperature traits), respiration traits (RR and PS), thermoregulatory indicators (i.e., all skin surface temperatures, vaginal temperatures, and respiration traits), anatomical traits (BCS_{cal}, BCS_{vis}, HD, BS, EA, and EL), and a combination of all traits.

A common genomic region located on chromosome 7 was associated with vaginal temperature, animal body temperatures, and thermoregulatory traits groups. This region comprised the genes *RCAN2* (Regulator of Calcineurin 2), *ENPP5* (Ectonucleotide Pyrophosphatase/Phosphodiesterase Family Member 5), *ENPP4* (Ectonucleotide Pyrophosphatase/Phosphodiesterase 4), *CLIC5* (Chloride Intracellular Channel 5), and *U6* (U6 small nuclear RNA). *ENPP5* and *ENPP4* belong to the ectonucleotide pyrophosphatase/phosphodiesterase (ENPP) family of genes encoding a group of proteins that have enzymatic activity involved in the hydrolysis of nucleotides [72]. Based on their sequence homology, *ENPP4* and *ENPP5* have been described as putative ENPP ectoenzymes [73]. The ectoenzymes are found on leukocytes and endothelial cells and play a crucial role in regulating leukocyte trafficking [74]. *RCAN2* is a gene that encodes a protein involved in the regulation of the calcineurin signaling pathway. This protein is

421 involved in many physiological processes by binding to the catalytic domain of
422 calcineurin A and inhibiting calcineurin-mediated nuclear translocation of the
423 transcription factor NFATC1 (nuclear factor of activated T cells 1) [75, 76]. Inactivation
424 of the *RCAN2* gene in mice reduced age- and diet-induced obesity by causing a reduction
425 in feed intake [77]. *CLIC5* encodes a member of the chloride intracellular channel (CLIC)
426 family of chloride ion channels that regulates chloride transport and interacts with the
427 cortical actin cytoskeleton in polarized epithelial cells [78]. *U6* is a small nuclear RNA
428 (snRNA) involved in catalytic steps of pre-mRNA splicing [79]. This common genomic
429 region identified for vaginal temperatures, animal body temperatures, and
430 thermoregulatory traits groups might be relevant for thermoregulatory indicators since
431 the genes annotated in this region are involved in immune response and in catalytic
432 activities to reduce cell damage caused by oxidative stress.

433 The candidate genes *MCTP1* (Multiple C2 And Transmembrane Domain
434 Containing 1), and *ELL2* (Elongation Factor for RNA Polymerase II 2), both located on
435 chromosome 2, were candidate genes for animal temperature traits that also presented
436 pleiotropic effects. *MCTP1* regulates endocytic recycling in central nervous system
437 neurons and synapses, and possibly cellular vesicle retrieval and oxidative stress [80],
438 which might influence HS response since it also causes cellular oxidative stress. *ELL2*
439 has been reported to contribute to prostate homeostasis and potentially acts as a tumor
440 suppressor in the development and progression of prostate cancer cells [81, 82].
441 Additionally, it regulates plasma cell gene expression, including immunoglobulin
442 production in plasma cells [83]. Therefore, it is possible that the *ELL2* gene may
443 influence immune response when the sows are under HS conditions.

444 We also annotated the protein-coding genes *NTN1* (Netrin-1) and *STX8* (Syntaxin
445 8) located on chromosome 12 for the thermoregulatory traits group. *NTN1* belongs to a

446 family of laminin-related secreted proteins and contributes to the regulation of
447 inflammation by influencing cell migration [84, 85]. *NTN1* is involved in immune
448 response modulation, regulation of inflammation, and leukocyte infiltration [84]. *STX8*
449 has been identified as a key player in the efficient sorting and trafficking of cytotoxic
450 molecules to functional lytic granules in cytotoxic T lymphocytes in humans [86]. Both
451 *NTN1* and *STX8* contribute significantly to the immune response, particularly in
452 combating pathogens through the actions of macrophages and cytotoxic T cells.

453 For the RR group of traits, the gene *AKAP7* located on chromosome 1 was
454 annotated. *AKAP7* is a gene encoding a protein kinase A-binding scaffolding molecule
455 associated with a cellular regulatory pathway during viral infections [34, 35]. In addition,
456 this gene promotes neuroprotection by enhancing mitochondrial networks and blocking
457 apoptosis in glutamate-induced oxidative stress [36]. According to Gusho et al. [34],
458 *AKAP7* may serve as a cytoprotective factor and potentially prevent tissue damage during
459 viral infections. Several candidate genes with pleiotropic effects for physiological
460 indicators of HS response in lactating sows were associated with immune response,
461 supporting the already reported effects of HS on immune responses [50–52].

462 The gene *TMEM161B* (Transmembrane Protein 161B), located on chromosome
463 2, was found to be a candidate gene with pleiotropic effects for skin temperature traits. In
464 zebrafish and mice, *TMEM161B* is linked with cardiac rhythm, preventing arrhythmic
465 calcium oscillations, and ensuring proper blood flow for the developing embryo [87].
466 Moreover, studies indicate that increasing vasodilatation elevates skin blood flow,
467 increasing skin temperature [88], which facilitates heat dissipation. In humans,
468 *TMEM161B* has been reported to regulate cerebral cortical gyration, Sonic Hedgehog
469 signaling, and ciliary structure in the developing central nervous system [89]. This gene
470 might be important under HS conditions, where the sympathetic nervous system

471 coordinates adjustments in cardiac rhythm and skin blood flow as response to thermal
472 challenges [90, 91]. The rate of skin blood flow is primarily determined by body
473 temperatures, and above an internal body temperature threshold for vasodilation, the
474 increase in skin blood flow is proportional to the increase in internal temperature
475 managing the impact of increased skin blood flow and heat transfer requirements on the
476 circulatory system [91, 92].

477 For the anatomical traits group, the candidate genes with pleiotropic effects found
478 included *ZMYND11* (Zinc finger MYND-type containing 11) and *DIP2C* (Disco
479 Interacting Protein 2 homolog C) located on chromosome 10, and *GDNF* (Glial Cell
480 Derived Neurotrophic Factor) and *CDH18* (Cadherin 18) on chromosome 16. *ZMYND11*,
481 a multidomain protein, modulates RNA polymerase activity and regulates splicing. This
482 gene was differentially regulated in response to thermal stress in sockeye and pink salmon
483 [93] and in chicken pituitary under heat stress [94]. *ZMYND11* has been associated with
484 neurodevelopmental disorders, global developmental delay, seizures, and hypotonia, and
485 it is a potential causative gene in complex neurodevelopmental phenotypes [95–97].
486 While the biological functions of *DIP2C* are not entirely clear, it may regulate neuronal
487 differentiation and early embryonic nervous development [98], as well as overall brain
488 development and function [99]. *GDNF* is essential for maintaining neuronal
489 morphological and neurochemical phenotypes, and protecting dopaminergic neurons
490 from toxic damage [100]. It has several positive effects on the nervous system, including
491 viability, proliferative activity, and migratory ability of cells [101]. *CDH18* has been
492 associated with neuropsychiatric disorders in humans [102] and tumor suppressors [103,
493 104]. The candidate genes with pleiotropic effect for anatomical traits influence nervous
494 system functions. The response to heat stress involves complex interactions between the
495 brain and various neurotransmitter systems [105]. Furthermore, prolonged exposure to

HS conditions can negatively affect central nervous system, leading to cognitive and neurological sequelae [106].

Implications and limitations

Understanding the genetic background of physiological and anatomical traits related to HS response is valuable for breeding programs aimed to improve HS resilience in pigs. In this study we identified many genomic regions associated with indicators of HS response in lactating sows, but the QTL presented small effect sizes indicating that the traits are highly polygenic. The candidate genes for indicators of HS response evaluated are associated with catalytic activities to reduce cell damage from oxidative stress and cellular mechanisms related to immune response. Furthermore, gene ontology terms and pathways involved in heat shock protein activities, immune response, and oxidative cellular stress were found, which inform biological mechanisms related to heat tolerance and resilience in pigs. Additionally, in this study we identified variants with potential pleiotropic effects and influence in multiple indicators of HS response in lactating sows. This information allows breeders to design programs that could maximize genetic gain across multiple traits for more comprehensive improvements in animal populations. The utilization of imputed whole-genome sequencing (WGS) enabled the identification of significant variants that were absent on the medium-density SNP array. Additionally, pleiotropic variants can be filtered and included in the SNP array [107], which would benefit breeding programs focusing on selecting animals with greater climatic resilience. However, further investigations are required to assess pleiotropy between HS response indicators and traits related to production and reproduction. This evaluation is crucial to determine the importance of these variants for other relevant traits.

520 The use of crossbred animals represents a limitation of this study, as different
521 genomic regions may be associated with the same indicators of HS response in purebred
522 populations. This discrepancy arises because allelic frequencies vary across populations
523 and breeds. Additionally, the dataset is not large, and the animals are from a single farm.
524 Therefore, caution should be taken when extrapolating findings from crossbred animals
525 to purebred populations, as the genetic background of the populations can significantly
526 influence the observed associations between genomic regions and HS response indicators.
527 In future studies, the incorporation of economically important traits associated
528 with reproductive and productive performance would allow the understanding of
529 pleiotropy between these traits and those related to HS response. This expanded
530 knowledge would provide valuable insights for creating selection indexes, enabling the
531 identification of animals that are not only more resilient to HS but also capable of
532 maintaining high productivity.
533

534 **Conclusions**

535 In this study we identified numerous genomic regions significantly associated
536 with indicators of HS response in lactating sows. The significant variants have small
537 effects, indicating the highly polygenic nature of the traits evaluated. The candidate genes
538 for physiological and anatomical indicators of HS response are associated with gene
539 ontology terms and pathways involved in heat shock proteins activities, immune
540 response, and oxidative cellular stress. The indicators of HS response exhibited
541 pleiotropic effects, suggesting that multiple genomic regions influence various
542 physiological and anatomical indicators of HS response. Many candidate genes with
543 potential pleiotropic effects are associated with catalytic activities to reduce cell damage
544 from oxidative stress and cellular mechanisms related to immune response were

identified, providing valuable insights for breeding programs aimed at improving HS resilience in pigs. The findings have significant implications for advancing breeding programs aimed at improving heat tolerance in pigs.

Materials and Methods

Animals and genotypes

The data used in this study was previously described by Johnson et al. [10] and Freitas et al. [11]. In summary, the phenotypes were collected from 1,645 multiparous lactating sows (Large White x Landrace cross) at a commercial sow farm located in Maple Hill, North Carolina, USA. A total of 1,639 sows were genotyped using the PorcineSNP50K (50,703 SNPs) Bead Chip (Illumina, San Diego, CA, USA). The quality control applied to the genotypes consisted of removing animals with a call rate lower than 0.80 and SNPs with a call rate lower than 0.90, and SNPs located on non-autosomal chromosomes. After quality control, 36,258 SNPs for 1,622 animals remained for further analyses. The genotypes were imputed to WGS containing 34,615,361 SNPs using the Swine Imputation (SWIM) Server [17]. The reference population consisted of 2,259 animals from various breeds, including 615 Landrace and 543 Large White, and 25 Landrace x Large White crossbred animals [17].

After genotype imputation, additional quality control was performed, removing variants with impute scores lower than 0.85, animals and SNPs with missing rates greater than 0.10, minor allele frequency (MAF) lower than 0.05, and extreme p-values for Hardy-Weinberg equilibrium tests lower than $1x10^{-15}$. Data from 7,065,922 SNPs for 1,622 animals remained for subsequent analyses. LD-based pruning was performed considering a pairwise correlation coefficient threshold of 0.90 between markers, and a

570 window size of 10 markers, with a step size of five markers, retaining 1,710,312 SNPs.
571 Some advantages of performing LD pruning are to reduce redundancy and confounding
572 factors that may interfere with statistical analyses and reduce the number of tests
573 performed improving the power of the analyses [108]. Genotyping data was pre-
574 processed using the Plink software [109].
575
576 **Phenotypic records**
577 The description of the phenotypes evaluated in this study are presented in Table
578 1. In summary, the thermoregulatory indicators of HS response phenotypes collected
579 were respiration rate (RR), ear skin temperature (T_{ES}), shoulder skin temperature (T_{SS}),
580 rump skin temperature (T_{RS}) tail skin temperature (T_{TS}), vaginal temperatures, and
581 panting score (PS). RR and skin surface temperatures were collected at 0800, 1200, 1600,
582 and 2000 h daily during a period of four consecutive days. Vaginal temperature was
583 automatically recorded in 10 min intervals over four days using calibrated thermochron
584 temperature recorders. This data was used to compute six traits in this study: whole data
585 measured at every 10 minutes (T_{Vall}), the average of the six records per hour
586 corresponding to 0800, 1200, 1600, and 2000 h during four days (T_{V4days}), and single
587 record corresponding to 0800, 1200, 1600, and 2000 h measured at the first day of
588 collection (T_{V8h}, T_{V12h}, T_{V16h}, and T_{V20h}, respectively). Panting score was collected during
589 four consecutive days at 15:30 hours and scored from 0 to 3 (0: if it was with closed
590 mouth and normal breathing; 1: closed mouth and rapid breathing; 2: open mouth and
591 rapid breathing; 3: open mouth and rapid breathing with obvious salivation).
592 We also collected phenotypes for sow anatomical traits that might influence on
593 the ability of the animal to dissipate metabolic heat. The traits measured include hair
594 density (HD), body condition score (BCS), body size (BS), ear length (EL), and ear area

595 (EA). HD was measured as a subjective visual score ranging from 0 to 2, being the score
596 0 = hairless or limited hair cover, 1 = normal or moderate hair cover, and 2 = sow with
597 greater than normal hair cover. BCS was evaluated using a sow caliper (BCS_{cal}) [110] and
598 it was also evaluated as a visual BCS (BCS_{vis}) considering five categories: 1 = emaciated,
599 2 = thin, and 3 = ideal, 4 = fat, and 5 = overly fat. The animals were also score into three
600 categories according to their BS as small, medium, or large. The descriptive statistics for
601 the traits used in this study are presented in Table 4. More details about the data collection
602 procedures are presented in Johnson et al. [10].

603 The phenotypes were pre-corrected for fixed effects to be used as input for the
604 GWAS analyses. The fixed effects for each trait were described by Freitas et al. [11]. In
605 summary, the fixed effects fitted for skin surface temperature (T_{ES}, T_{SS}, T_{RS}, and T_{TS}) and
606 RR were trait recorder; concatenation of week, day, and time of measurement; parity;
607 days in lactation; concatenation of barn type and room; and in-barn environmental
608 temperature as a linear covariate. For PS, the fixed effects were trait recorder;
609 concatenation of week and day of measurement; parity; days in lactation; concatenation
610 of barn type and room; and in-barn environmental temperature as a linear covariate. For
611 T_{Vall}, the fixed effects were the concatenation of week and day of measurement; parity;
612 concatenation of barn type and room; and in-barn environmental temperature as a linear
613 covariate. For T_{V4days}, the fixed effects were concatenation of week, day, and time of
614 measurement; parity; days in lactation; concatenation of barn type and room; and in-barn
615 environmental temperature as a linear covariate. For T_{V8h}, T_{V12h}, T_{V16h}, and T_{V20h}, the
616 fixed effects were the concatenation of week and day of measurement; parity; days in
617 lactation; concatenation of barn type and room; and in-barn environmental temperature
618 as a linear covariate. For HD, the fixed effects fitted were trait recorder and parity. For
619 BS, the fixed effects fitted were trait recorder, week of measurement, and parity. For

620 BCS_{cal} and BCS_{vis}, the fixed effect fitted were trait recorder, week of measurement, parity,
621 days in lactation, and concatenation of barn type and room. For EA and EL, the fixed
622 effects fitted were trait recorder and picture quality. For traits that presented repeated
623 measurements (i.e., the thermoregulatory traits: skin surface temperatures, vaginal
624 temperatures, RR, and PS), we computed the average adjusted phenotype to be used as
625 response variables for GWAS [111].
626

627 **Genome-wide association studies**

628 The GWAS was performed considering the WGS dataset using the leave-one-
629 chromosome-out approach on mixed linear model association analysis (MLMA-LOCO)
630 implemented in the GCTA software [112]. The model can be described as:

631 $$\mathbf{y} = \mathbf{1}\mu + \mathbf{X}b + \mathbf{Z}\mathbf{u} + \boldsymbol{\varepsilon},$$

632 Where $\mathbf{y}$ is the vector of pre-corrected phenotypes for each analyzed trait; $\mathbf{1}$ is a vector of
633 ones; μ is the overall mean; b is the fixed effect of each tested SNP; $\mathbf{X}$ is a vector
634 containing the genotype for SNP; $\mathbf{u}$ is the random vector of polygenic effect
635 with $\mathbf{u} \sim N(0, \mathbf{G}\sigma_u^2)$, where $\mathbf{G}$ is the genomic-based relationship matrix (GRM) as
636 previously described [112], σ_u^2 is the additive genetic variance; $\mathbf{Z}$ is the incidence matrix
637 for $\mathbf{u}$; and $\boldsymbol{\varepsilon}$ is a random vector of residual effects with $\boldsymbol{\varepsilon} \sim N(0, \mathbf{I}\sigma_\varepsilon^2)$, where $\mathbf{I}$ is an
638 identity matrix and σ_ε^2 is the residual variance.
639

640 **Table 4.** Descriptive statistics for continuous heat stress indicators in Landrace x Large White crossbred pig population.

Trait[1]	Number of animals	Number of observations	Mean	Minimum	Maximum	Coefficient of variation (%)
T_{ES}	1,381	21,411	36.70	32.50	40.70	2.92
T_{SS}	1,381	21,414	36.50	32.30	39.80	2.96
T_{RS}	1,381	21,414	37.20	33.60	39.90	2.47
T_{TS}	1,381	21,413	36.90	33.20	40.00	2.57
RR	1,381	21,360	73.00	12.00	172.00	38.74
PS	1,380	5,450	1.02	0	3	58.82
T_{Vall}	1,381	932,708	39.74	37.08	42.35	1.91
T_{V4days}	1,381	21,415	39.70	37.10	42.70	1.94
T_{V8h}	1,357	1,357	39.25	37.43	41.43	1.53
T_{V12h}	1,370	1,370	39.69	37.08	41.61	1.61
T_{V16h}	1,354	1,354	40.15	37.35	42.72	1.72
T_{V20h}	1,362	1,362	40.25	37.85	41.84	1.71

HD	1,151	1,151	2.04	1	3	31.37
BS	1,379	1,379	2.26	1	3	27,43
BCS_{cal}	1,361	1,361	6.93	1	10	29.15
BCS_{vis}	1,348	1,348	2.10	1	3	30.48
EA	705	705	309.01	183.23	487.86	17.37
EL	713	713	24.98	14.83	34.34	11,25

[1]T_{ES}: ear skin temperature (°C); T_{SS}: shoulder skin temperature (°C); T_{RS}: rump skin temperature (°C); T_{TS}: tail skin temperature (°C); RR: respiration rate (breaths per minute); PS: panting score; T_{Vall}: all measures (every 10 minutes) of vaginal temperatures (°C); T_{V4days}: average of the six records per hour corresponding to 08:00, 12:00, 16:00, and 20:00 hours during four days (°C); T_{V8h}: vaginal temperature measured on the first day at 8:00 (°C); T_{V12h}: vaginal temperature measured on the first day at 12:00 (°C); T_{V16h}: vaginal temperature measured on the first day at 16:00 (°C); T_{V16h}: vaginal temperature measured on the first day at 20:00 (°C); HD: hair density score; BS: body size; BCS_{cal}: body condition score using a sow caliper; BCS_{vis}: visual body condition score; EA: ear area (cm^2); EL: and ear length (cm). Data collection protocols have been described by Johnson et al. [10] and Freitas et al. [11].

641

642 The MLMA-LOCO approach is based on fitting a different genomic relationship
643 matrix (GRM) to account for population stratification for the association tests of each
644 chromosome by excluding the markers located on the chromosome where the tested SNP
645 are located when creating the GRM for that chromosome [113]. The inclusion of the
646 marker being tested in the GRM can reduce the statistical test power due to the double
647 fitting of the marker in the model: both as a fixed effect for association and as a random
648 effect as part of the GRM [113–115]. This phenomenon was termed "proximal
649 contamination" by Listgarten et al. [114], who demonstrated that a mixed linear model
650 excluding the marker from GRM is the mathematically correct approach and provided an
651 efficient algorithm for mixed linear model analysis.
652
653 **Adjustment for multiple testing**
654 To check if there was potential population stratification due to the population
655 structure, the genomic inflation factor (λ) [116] was evaluated, along with its 95%
656 confidence interval. Due to the multiple testing nature of the GWAS method employed
657 in this study, there is a cumulative probability of false-positive associated SNPs [117,
658 118]. In this sense, a Bonferroni correction at α = 0.05 for the genome-wise significance
659 level [119] was applied, by dividing α by the number of independent chromosome
660 segments (Me) to account for the dependence among tests due to LD. The Me was
661 calculated as proposed by Goddard et al. [120]:
662 $$Me = \frac{2NeLk}{\log(NeL)},$$
663 where Ne is the effective population size, which was computed as 85 according to
664 populational LD [121]; L is the average length of chromosome expressed in Morgan; and
665 k is the number of chromosomes. A SNP was considered as statistically significant if its
666 p-value was smaller than $0.05/Me$, which was equal to 1.21×10^{-6}.

667 **Pleiotropic effects**

668 The multiple-trait analysis proposed by Bolormaa et al. [18] allows to evaluate the
669 pleiotropy in groups of more than two traits. This approach is based on combining the
670 results from the single-trait association analyses to calculate a multi-trait statistic and it
671 has been demonstrated that the multi-trait approach proposed by them has a lower FDR
672 than a single trait analysis (at the same significance test p-value) [18, 122]. First, the
673 phenotypes were Cholesky-decorrelated because the Bolormaa et al. [18] approach was
674 originally proposed to perform meta-analysis, i.e., independent studies [19, 20]. Then, the
675 traits were grouped in seven different categories: skin surface temperature traits (i.e., T_{ES},
676 T_{SS}, T_{RS}, and T_{TS}), vaginal temperatures (i.e., T_{Vall}, T_{V4days}, T_{V8h}, T_{V12h}, T_{V16h}, and T_{V20h}),
677 animal temperatures (all skin surface and vaginal temperature traits), respiration traits
678 (i.e., RR and PS), thermoregulatory indicators (i.e., all skin surface and vaginal
679 temperature traits, RR and PS), anatomical traits (i.e., BCS_{cal}, BCS_{vis}, HD, BS, EA, and
680 EL), and all traits to evaluate the presence of pleiotropic effects in each trait group. The
681 null hypothesis tested states that the SNP does not affect any of the n traits in the group
682 based on the χ^2 with n degrees of freedom. The multi-trait statistics for each SNP was
683 calculated as presented by [18]:

684 $$\text{Multi-trait } \chi^2 = \boldsymbol{t}_i' \boldsymbol{V}^{-1} \boldsymbol{t}_i,$$

685 where $\boldsymbol{t}_i$ is a n x 1 vector of signed t-values for the i^{th} SNP across the n trait, $\boldsymbol{t}_i'$ is the
686 transpose of $\boldsymbol{t}_i$, and $\boldsymbol{V}^{-1}$ is the inverse of the n x n correlation matrix over all estimated
687 SNP effects. As this method presents a distribution associated to the χ^2 statistics, each
688 marker presents a statistic and a p-value to infer if the marker is significant or not for
689 pleiotropic effects for the group of traits evaluated. A Bonferroni correction was also
690 applied in the same way described for the GWAS, then a variant was considered with
691 significant pleiotropic effect if its p-value was smaller than 1.21×10^{-6}.

692 **Gene annotation and functional analyses**

693 Gene annotation was performed within a region of ±100 kb around the significant
694 SNPs using the GALLO package [123]. The annotated data for *Sus scrofa* from the
695 Ensembl database (www.ensembl.org/Sus_scrofa/Info/Index) were used in the analyses.
696 The web-based tool Database for Annotation, Visualization, and Integrated Discovery
697 (DAVID) [124, 125] was used for conducting Gene Ontology (GO) and KEGG pathway
698 enrichment ($P < 0.05$) analyses to identify biological processes, molecular functions,
699 cellular components, and biological pathways associated with the positional candidate
700 genes identified. DAVID is a web-based tool for gene-enrichment analysis that utilizes a
701 knowledge base aggregating information from various heterogeneous and widely
702 distributed public databases [125].

703

704 **References**

705 1. NOAA National Centers for Environmental Information. Monthly Global Climate
706 Report for Annual 2022. 2023.
707 2. Johnson JS. Heat stress: Impact on livestock well-being and productivity and mitigation
708 strategies to alleviate the negative effects. Animal Production Science.
709 2018;58:1404–13.
710 3. Ingram DL, Monteith JL, Mount LE. Heat loss and its control in pigs. Heat loss from
711 animals and man Assessment and Control. 1973;:235–54.
712 4. Renaudeau D, Collin A, Yahav S, De Basilio V, Gourdine JL, Collier RJ. Adaptation
713 to hot climate and strategies to alleviate heat stress in livestock production. In:
714 Animal. 2012. p. 707–28.
715 5. Misztal I. Breeding and genetics symposium: Resilience and lessons from studies in
716 genetics of heat stress. J Anim Sci. 2017;95:1780–7.

717 6. Tiezzi F, Brito LF, Howard J, Huang YJ, Gray K, Schwab C, et al. Genomics of Heat
718 Tolerance in Reproductive Performance Investigated in Four Independent
719 Maternal Lines of Pigs. Front Genet. 2020;11.
720 7. Freitas PHF, Johnson JS, Chen S, Oliveira HR, Tiezzi F, Lázaro SF, et al. Definition
721 of Environmental Variables and Critical Periods to Evaluate Heat Tolerance in
722 Large White Pigs Based on Single-Step Genomic Reaction Norms. Front Genet.
723 2021;12.
724 8. Dodd GR, Gray K, Huang Y, Fragomeni B. Single-Step GBLUP and GWAS Analyses
725 Suggests Implementation of Unweighted Two Trait Approach for Heat Stress in
726 Swine. Animals. 2022;12.
727 9. Ravagnolo O, Misztal I, Hoogenboom G. Genetic Component of Heat Stress in Dairy
728 Cattle, Development of Heat Index Function. J Dairy Sci. 2000;83:2120–5.
729 10. Johnson JS, Wen H, Freitas PHF, Maskal JM, Hartman SO, Byrd MK, et al.
730 Evaluating phenotypes associated with heat tolerance and identifying moderate
731 and severe heat stress thresholds in lactating sows housed in mechanically or
732 naturally ventilated barns during the summer under commercial conditions. J
733 Anim Sci. 2023. https://doi.org/10.1093/JAS/SKAD129.
734 11. Freitas PHF, Johnson JS, Wen H, Maskal JM, Tiezzi F, Maltecca C, et al. Genetic
735 parameters for automatically-measured vaginal temperature, respiration
736 efficiency, and other thermotolerance indicators measured on lactating sows under
737 heat stress conditions. Genetics Selection Evolution. 2023;55:1–14.
738 12. Visscher PM, Brown MA, McCarthy MI, Yang J. Five years of GWAS discovery.
739 Am J Hum Genet. 2012;90:7–24.
740 13. Freitas PHF, Johnson JS, Tiezzi F, Huang Y, Schinckel AP, Brito LF. Genomic
741 predictions and GWAS for heat tolerance in pigs based on reaction norm models

742 with performance records and data from public weather stations considering
743 alternative temperature thresholds. Journal of Animal Breeding and Genetics.
744 2023;00:1–21.
745 14. Kim K-S, Seibert JT, Edea Z, Graves KL, Kim E-S, Keating AF, et al.
746 Characterization of the acute heat stress response in gilts: III. Genome-wide
747 association studies of thermotolerance traits in pigs RUNNING HEAD: Genetic
748 control of heat stress response in gilts. 2018.
749 https://doi.org/10.1093/jas/sky131/4970896.
750 15. Stearns FW. One Hundred Years of Pleiotropy: A Retrospective. Genetics.
751 2010;186:767–73.
752 16. Solovieff N, Cotsapas C, Lee PH, Purcell SM, Smoller JW. Pleiotropy in complex
753 traits: challenges and strategies. Nature Reviews Genetics 2013 14:7.
754 2013;14:483–95.
755 17. Ding R, Savegnago R, Liu J, Long N, Tan C, Cai G, et al. The SWine IMputation
756 (SWIM) haplotype reference panel enables nucleotide resolution genetic mapping
757 in pigs. Communications Biology 2023 6:1. 2023;6:1–10.
758 18. Bolormaa S, Pryce JE, Reverter A, Zhang Y, Barendse W, Kemper K, et al. A Multi-
759 Trait, Meta-analysis for Detecting Pleiotropic Polymorphisms for Stature, Fatness
760 and Reproduction in Beef Cattle. PLoS Genet. 2014;10.
761 19. Xiang R, van den Berg I, MacLeod IM, Daetwyler HD, Goddard ME. Effect direction
762 meta-analysis of GWAS identifies extreme, prevalent and shared pleiotropy in a
763 large mammal. Communications Biology 2020 3:1. 2020;3:1–14.
764 20. Xiang R, MacLeod IM, Bolormaa S, Goddard ME. Genome-wide comparative
765 analyses of correlated and uncorrelated phenotypes identify major pleiotropic
766 variants in dairy cattle. Scientific Reports 2017 7:1. 2017;7:1–12.

767 21. Collier RJ, Baumgard LH, Zimbelman RB, Xiao Y. Heat stress: Physiology of
768 acclimation and adaptation. Animal Frontiers. 2019;9:12–9.
769 22. Ross JW, Hale BJ, Gabler NK, Rhoads RP, Keating AF, Baumgard LH. Physiological
770 consequences of heat stress in pigs. Anim Prod Sci. 2015;55:1381–90.
771 23. Sejian V, Bhatta R, Gaughan JB, Dunshea FR, Lacetera N. Review: Adaptation of
772 animals to heat stress. Animal. 2018;12:S431–44.
773 24. Shin J, Lee C. Statistical power for identifying nucleotide markers associated with
774 quantitative traits in genome-wide association analysis using a mixed model.
775 Genomics. 2015;105:1–4.
776 25. Khanzadeh H, Ghavi Hossein-Zadeh N, Ghovvati S. The statistical power of genome-
777 wide association studies for threshold traits with different frequencies of causal
778 variants. Genetica. 2022;150:51–7.
779 26. Sanchez MP, Govignon-Gion A, Croiseau P, Fritz S, Hozé C, Miranda G, et al.
780 Within-breed and multi-breed GWAS on imputed whole-genome sequence
781 variants reveal candidate mutations affecting milk protein composition in dairy
782 cattle. Genetics Selection Evolution. 2017;49:1–16.
783 27. Daetwyler HD, Capitan A, Pausch H, Stothard P, Van Binsbergen R, Brøndum RF,
784 et al. Whole-genome sequencing of 234 bulls facilitates mapping of monogenic
785 and complex traits in cattle. Nature Genetics 2014 46:8. 2014;46:858–65.
786 28. Van Den Berg S, Vandenplas J, Van Eeuwijk FA, Bouwman AC, Lopes MS,
787 Veerkamp RF. Imputation to whole-genome sequence using multiple pig
788 populations and its use in genome-wide association studies. Genetics Selection
789 Evolution. 2019;51:1–13.

790 29. Wu Y, Zheng Z, Visscher PM, Yang J. Quantifying the mapping precision of genome-
791 wide association studies using whole-genome sequencing data. Genome Biol.
792 2017;18:1–10.
793 30. Yang J, Weedon MN, Purcell S, Lettre G, Estrada K, Willer CJ, et al. Genomic
794 inflation factors under polygenic inheritance. European Journal of Human
795 Genetics 2011 19:7. 2011;19:807–12.
796 31. Hayes B. Overview of Statistical Methods for Genome-Wide Association Studies
797 (GWAS). In: Gondro C, van der Werf J, Hayes B, editors. Genome-Wide
798 Association Studies and Genomic Prediction. Totowa, NJ: Humana Press; 2013.
799 p. 149–69.
800 32. Lapinski PE, Kwon S, Lubeck BA, Wilkinson JE, Srinivasan RS, Sevick-Muraca E,
801 et al. RASA1 maintains the lymphatic vasculature in a quiescent functional state
802 in mice. Journal of Clinical Investigation. 2012;122:733–47.
803 33. He X, Howard BA, Liu Y, Squillace DL, Klein BS, Lawrence CB, et al. LYSMD3:
804 A mammalian pattern recognition receptor for chitin ll LYSMD3: A mammalian
805 pattern recognition receptor for chitin. CellReports. 2021;36:109392.
806 34. Gusho E, Jha BK, Zhang R, Weiss SR, H. Silverman R. 108 : Preventing activation
807 of the IFN inducible OAS-RNase L pathway by A-kinase anchoring protein 7
808 (AKAP7). Cytokine. 2013;63:268.
809 35. King CR, Cohen MJ, Fonseca GJ, Dirk BS, Dikeakos JD, Mymryk JS. Functional and
810 Structural Mimicry of Cellular Protein Kinase A Anchoring Proteins by a Viral
811 Oncoprotein. PLoS Pathog. 2016;12:e1005621.
812 36. Zhang J, Feng J, Ma D, Wang F, Wang Y, Li C, et al. Neuroprotective Mitochondrial
813 Remodeling by AKAP121/PKA Protects HT22 Cell from Glutamate-Induced
814 Oxidative Stress. Mol Neurobiol. 2019;56:1–22.

815 37. Wen H, Johnson JS, Freitas PHF, Maskal JM, Gloria LS, Araujo AC, et al.
816 Longitudinal genomic analyses of automatically-recorded vaginal temperature in
817 lactating sows under heat stress conditions based on random regression models.
818 Genetics Selection Evolution. 2023;55:1–19.
819 38. Richter K, Haslbeck M, Buchner J. The heat shock response: life on the verge of
820 death. Mol Cell. 2010;40 2:253–66.
821 39. Anckar J, Sistonen L. Regulation of HSF1 Function in the Heat Stress Response:
822 Implications in Aging and Disease. https://doi.org/101146/annurev-biochem-
823 060809-095203. 2011;80:1089–115.
824 40. Li GC, Li L, Liu RY, Rehman M, Lee WMF. Heat shock protein hsp70 protects cells
825 from thermal stress even after deletion of its ATP-binding domain. Proceedings
826 of the National Academy of Sciences. 1992;89:2036–40.
827 41. Beere HM. Stressed to Death: Regulation of Apoptotic Signaling Pathways by the
828 Heat Shock Proteins. Science's STKE. 2001;2001:1–1.
829 42. Chatterjee BK, Puri S, Sharma A, Pastor A, Chaudhuri TK, Chatterjee BK, et al.
830 Molecular Chaperones: Structure-Function Relationship and their Role in Protein
831 Folding. 2018;:181–218.
832 43. Dangi SS, Bharati J, Samad HA, Kumar Bhure S, Singh G, Prakash Maurya V, et al.
833 Expression Dynamics of Heat Shock Proteins (HSP) in Livestock under Thermal
834 Stress. Heat Shock Proteins. 2017;12:37–79.
835 44. Calderwood SK, Gong J, Murshid A. Extracellular HSPs: The complicated roles of
836 extracellular HSPs in immunity. Front Immunol. 2016;7 APR:187592.
837 45. Chen K, He Y, Liu Y, Yang X. Gene signature associated with neuro-endocrine
838 activity predicting prognosis of pancreatic carcinoma. Mol Genet Genomic Med.
839 2019;7:e00729.

840 46. Haase M, Fitze G. HSP90AB1: Helping the good and the bad. Gene. 2016;575:171–
841 86.
842 47. Brown-Brandl TM, Eigenberg RA, Nienaber JA, Kachman SD. Thermoregulatory
843 profile of a newer genetic line of pigs. Livest Prod Sci. 2001;71:253–60.
844 48. Gourdine JL, Rauw WM, Gilbert H, Poullet N. The Genetics of Thermoregulation in
845 Pigs: A Review. Frontiers in Veterinary Science. 2021;8.
846 49. Archana P, Aleena J, Pragna P, Vidya M, Abdul Niyas P, Bagath M, et al. Role of
847 heat shock proteins in livestock adaptation to heat stress. Journal of Dairy,
848 Veterinary & Animal Research. 2017;Volume 5 Issue 1.
849 50. Cui Y, Wang C, Hao Y, Gu X, Wang H. Chronic heat stress induces acute phase
850 responses and serum metabolome changes in finishing pigs. Animals. 2019;9.
851 51. Johnson JS, Maskal JM, Duttlinger AW, Kpodo KR, McConn BR, Byrd CJ, et al. In
852 utero heat stress alters the postnatal innate immune response of pigs. J Anim Sci.
853 2020;98:1–13.
854 52. Yu TY, Yong YH, Li JY, Fang B, Hu CY, Wu LY, et al. Proteomic study of
855 hypothalamus in pigs exposed to heat stress. BMC Vet Res. 2020;16.
856 53. Logsdon BA, Perumal TM, Daily K, Sieberts SK, Omberg L, Mangravite LM, et al.
857 O3-03-03: EPIGENOME-WIDE ASSOCIATION STUDIES IMPLICATE
858 GENES INVOLVED IN GLIAL CELL FUNCTION AND VIRAL RESPONSE
859 IN CEREBRAL WHITE MATTER HYPERINTENSITIES. Alzheimer's &
860 Dementia. 2018;14 7S_Part_19:P1015–6.
861 54. Chung O, Jung YE, Lee KW, An YJ, Kim J, Roh YR, et al. The Analyses of Cetacean
862 Virus-Responsive Genes Reveal Evolutionary Marks in Mucosal Immunity-
863 Associated Genes. Biochem Genet. 2022;60:2299–312.

55. Gerhart-Hines Z, Feng D, Emmett MJ, Everett LJ, Loro E, Briggs ER, et al. The nuclear receptor Rev-erbα controls circadian thermogenic plasticity. Nature. 2013;503:410–3.

56. Crespo-Piazuelo D, Ramayo-Caldas Y, González-Rodríguez O, Pascual M, Quintanilla R, Ballester M. A Co-Association Network Analysis Reveals Putative Regulators for Health-Related Traits in Pigs. Front Immunol. 2021;12:784978.

57. Gerhart-Hines Z, Feng D, Emmett MJ, Everett LJ, Loro E, Briggs ER, et al. The nuclear receptor Rev-erbα controls circadian thermogenic plasticity. Nature 2013 503:7476. 2013;503:410–3.

58. Chen Y, Chen Y, Yin W, Han H, Miller H, Li J, et al. The regulation of DOCK family proteins on T and B cells. J Leukoc Biol. 2021;109:383–94.

59. Valdivieso ÁG, Santa-Coloma TA. The chloride anion as a signalling effector. Biological Reviews. 2019;94:1839–56.

60. Averaimo S, Milton RH, Duchen MR, Mazzanti M. Chloride intracellular channel 1 (CLIC1): Sensor and effector during oxidative stress. FEBS Lett. 2010;584:2076–84.

61. Wills NK, Weng T, Mo L, Hellmich H, Yu A, Wang T, et al. Chloride channel expression in cultured human fetal RPE cells: response to oxidative stress. Invest Ophthalmol Vis Sci. 41 13:4247–55.

62. Jeulin C, Guadagnini R, Marano F. Oxidant stress stimulates Ca2+-activated chloride channels in the apical activated membrane of cultured nonciliated human nasal epithelial cells. Am J Physiol Lung Cell Mol Physiol. 2005;289 4 4 33-4:636–46.

63. Belhadj Slimen I, Najar T, Ghram A, Abdrrabba M. Heat stress effects on livestock: molecular, cellular and metabolic aspects, a review. J Anim Physiol Anim Nutr (Berl). 2016;100:401–12.

889 64. Petrova N V., Velichko AK, Razin S V., Kantidze OL. Early S-phase cell
890 hypersensitivity to heat stress. Cell Cycle. 2016;15:337–44.
891 65. Vertii A, Zimmerman W, Ivshina M, Doxsey S. Centrosome-intrinsic mechanisms
892 modulate centrosome integrity during fever. Mol Biol Cell. 2015;26:3451–63.
893 66. Oikonomopoulou K, Ricklin D, Ward PA, Lambris JD. Interactions between
894 coagulation and complement - Their role in inflammation. Semin Immunopathol.
895 2012;34:151–65.
896 67. Mathern DR, Heeger PS. Molecules great and small: The complement system.
897 Clinical Journal of the American Society of Nephrology. 2015;10:1636–50.
898 68. Bajic G, Degn SE, Thiel S, Andersen GR. Complement activation, regulation, and
899 molecular basis for complement-related diseases. EMBO J. 2015;34:2735–57.
900 69. Paaby AB, Rockman M V. The many faces of pleiotropy. Trends in Genetics.
901 2013;29:66–73.
902 70. Solovieff N, Cotsapas C, Lee PH, Purcell SM, Smoller JW. Pleiotropy in complex
903 traits: challenges and strategies. Nature Reviews Genetics 2013 14:7.
904 2013;14:483–95.
905 71. Hackinger S, Zeggini E. Statistical methods to detect pleiotropy in human complex
906 traits. Open Biol. 2017;7.
907 72. Borza R, Salgado-Polo F, Moolenaar WH, Perrakis A. Structure and function of the
908 ecto-nucleotide pyrophosphatase/ phosphodiesterase (ENPP) family: Tidying up
909 diversity. Journal of Biological Chemistry. 2022;298:101526.
910 73. Gijsbers R, Ceulemans H, Stalmans W, Bollen M. Structural and Catalytic
911 Similarities between Nucleotide Pyrophosphatases/Phosphodiesterases and
912 Alkaline Phosphatases. 2000. https://doi.org/10.1074/jbc.M007552200.

913 74. Salmi M, Jalkanen S. Ectoenzymes controlling leukocyte traffic. Eur J Immunol.
914 2012;42:284–92.
915 75. Serrano-Candelas E, Farré D, Aranguren-Ibáñez Á, Martínez-Høyer S, Pérez-Riba M.
916 The Vertebrate RCAN Gene Family: Novel Insights into Evolution, Structure and
917 Regulation. PLoS One. 2014;9:e85539.
918 76. Davies KJA, Ermak G, Rothermel BA, Pritchard M, Heitman J, Ahnn J, et al.
919 Renaming the DSCR1 / Adapt78 gene family as RCAN: regulators of calcineurin.
920 The FASEB Journal. 2007;21:3023–8.
921 77. Sun XY, Hayashi Y, Xu S, Kanou Y, Takagishi Y, Tang YP, et al. Inactivation of the
922 Rcan2 Gene in Mice Ameliorates the Age- and Diet-Induced Obesity by Causing
923 a Reduction in Food Intake. PLoS One. 2011;6:e14605.
924 78. Berryman M, Bretscher A. Identification of a novel member of the chloride
925 intracellular channel gene family (CLIC5) that associates with the actin
926 cytoskeleton of placental microvilli. Mol Biol Cell. 2000;11 5:1509–21.
927 79. Kandels-Lewis S, Séraphin B. Role of U6 snRNA in 5’ splice site selection. Science
928 (1979). 1993;262:2035–9.
929 80. Qiu L, Yu H, Liang F. Multiple C2 domains transmembrane protein 1 is expressed in
930 CNS neurons and possibly regulates cellular vesicle retrieval and oxidative stress.
931 J Neurochem. 2015;135:492–507.
932 81. Pascal LE, Masoodi KZ, Liu J, Qiu X, Song Q, Wang Y, et al. Conditional deletion
933 of ELL2 induces murine prostate intraepithelial neoplasia. J Endocrinol. 2017;235
934 2:123–36.
935 82. Wang Z, Pascal LE, Chandran UR, Chaparala S, Lv S, Ding H, et al. ELL2 Is Required
936 for the Growth and Survival of AR-Negative Prostate Cancer Cells. Cancer
937 Manag Res. 2020;12:4411–27.

938 83. Ghobrial A, Flick N, Daly R, Hoffman M, Milcarek C. ELL2 Influences Transcription
939 Elongation, Splicing, Ig Secretion and Growth. J Mucosal Immunol Res. 2019;3.
940 84. Xia X, Hu Z, Wang S, Yin K. Netrin-1: An emerging player in inflammatory diseases.
941 Cytokine Growth Factor Rev. 2022;64:46–56.
942 85. Ziegon L, Schlegel M. Netrin-1: A Modulator of Macrophage Driven Acute and
943 Chronic Inflammation. International Journal of Molecular Sciences 2022, Vol 23,
944 Page 275. 2021;23:275.
945 86. Bhat SS, Friedmann KS, Knörck A, Hoxha C, Leidinger P, Backes C, et al. Syntaxin
946 8 is required for efficient lytic granule trafficking in cytotoxic T lymphocytes.
947 Biochimica et Biophysica Acta (BBA) - Molecular Cell Research.
948 2016;1863:1653–64.
949 87. Koopman CD, de Angelis J, Iyer SP, Verkerk AO, Silva J Da, Berecki G, et al. The
950 zebrafish grime mutant uncovers an evolutionarily conserved role for Tmem161b
951 in the control of cardiac rhythm. Proceedings of the National Academy of
952 Sciences. 2021;118.
953 88. Chou T-H, Coyle EF. Cardiovascular responses to hot skin at rest and during exercise.
954 2022. https://doi.org/10.1080/23328940.2022.2109931.
955 89. Akula SK, Marciano JH, Lim Y, Exposito-Alonso D, Hylton NK, Hwang GH, et al.
956 TMEM161B regulates cerebral cortical gyration, Sonic Hedgehog signaling, and
957 ciliary structure in the developing central nervous system. Proc Natl Acad Sci U
958 S A. 2023;120.
959 90. Charkoudian N. Skin Blood Flow in Adult Human Thermoregulation: How It Works,
960 When It Does Not, and Why. Mayo Clin Proc. 2003;78:603–12.
961 91. Ootsuka Y, Tanaka M. Control of cutaneous blood flow by central nervous system.
962 Temperature. 2015;2:392–405.

963 92. Nadel ER, Cafarelli E, Roberts MF, Wenger CB. Circulatory regulation during
964 exercise in different ambient temperatures. J Appl Physiol Respir Environ Exerc
965 Physiol. 1979;46:430–7.
966 93. Akbarzadeh A, Günther OP, Houde AL, Li S, Ming TJ, Jeffries KM, et al. Developing
967 specific molecular biomarkers for thermal stress in salmonids. BMC Genomics.
968 2018;19:1–28.
969 94. Pritchett EM, Van Goor A, Schneider BK, Young M, Lamont SJ, Schmidt CJ.
970 Chicken pituitary transcriptomic responses to acute heat stress. Mol Biol Rep.
971 2023;50:5233–46.
972 95. Tumiene B, Čiuladaitė, Preikšaitienė E, Mameniškienė R, Utkus A, Kučinskas V.
973 Phenotype comparison confirms ZMYND11 as a critical gene for 10p15.3
974 microdeletion syndrome. J Appl Genet. 2017;58:467–74.
975 96. Moskowitz AM, Belnap N, Siniard AL, Szelinger S, Claasen AM, Richholt RF, et al.
976 A de novo missense mutation in ZMYND11 is associated with global
977 developmental delay, seizures, and hypotonia. Cold Spring Harb Mol Case Stud.
978 2016;2:a000851.
979 97. Yates TM, Drucker M, Barnicoat A, Low K, Gerkes EH, Fry AE, et al. ZMYND11-
980 related syndromic intellectual disability: 16 patients delineating and expanding
981 the phenotypic spectrum. Hum Mutat. 2020;41:1042–50.
982 98. Yao M, Su P, Li Z, Cui X, Yang Q, Xing X, et al. Knockout of Dip2c in murine ES
983 cell line IBMSe001-B-1 by CRISPR/Cas9 genome editing technology. Stem Cell
984 Res. 2021;53:102236.
985 99. Oo ZM, Adlat S, Sah RK, Myint MZZ, Hayel F, Chen Y, et al. Brain transcriptome
986 study through CRISPR/Cas9 mediated mouse Dip2c gene knock-out. Gene.
987 2020;758:144975.

988 100. De Tassigny XD anglemont, Pascual A, Lopez-Barneo J. GDNF-based therapies,
989 GDNF-producing interneurons, and trophic support of the dopaminergic
990 nigrostriatal pathway. Implications for parkinson's disease. Front Neuroanat.
991 2015;9 FEB:1–15.
992 101. Revishchin A V., Parshina V V., Pavlova G V. [The role of glial cell line-derived
993 neurotrophic factor isoforms in human glial tumors]. Zh Vopr Neirokhir Im N N
994 Burdenko. 2022;86:106–12.
995 102. Redies C, Hertel N, Hübner CA. Cadherins and neuropsychiatric disorders. Brain
996 Res. 2012;1470:130–44.
997 103. Bai YH, Zhan YB, Yu B, Wang WW, Wang L, Zhou JQ, et al. A Novel Tumor-
998 Suppressor, CDH18, Inhibits Glioma Cell Invasiveness Via UQCRC2 and
999 Correlates with the Prognosis of Glioma Patients. Cell Physiol Biochem.
1000 2018;48:1755–70.
1001 104. Zhao B, Wu J, Cha X, Mao G, Shi H, Fei S, et al. Effect of COP1 in Promoting the
1002 Tumorigenesis of Gastric Cancer by Down-Regulation of CDH18 via PI3K/AKT
1003 Signal Pathway. Anal Cell Pathol (Amst). 2023;2023.
1004 105. Nybo L. Exercise and heat stress: cerebral challenges and consequences. Prog Brain
1005 Res. 2007;162:29–43.
1006 106. Walter EJ, Carraretto M. The neurological and cognitive consequences of
1007 hyperthermia. Crit Care. 2016;20:1–8.
1008 107. Xiang R, MacLeod IM, Daetwyler HD, de Jong G, O'Connor E, Schrooten C, et al.
1009 Genome-wide fine-mapping identifies pleiotropic and functional variants that
1010 predict many traits across global cattle populations. Nature Communications 2021
1011 12:1. 2021;12:1–13.

1012 108. Weale ME. Quality control for genome-wide association studies. Methods in
1013 Molecular Biology. 2010;628:341–72.
1014 109. Purcell S, Neale B, Todd-Brown K, Thomas L, Ferreira MAR, Bender D, et al.
1015 PLINK: a tool set for whole-genome association and population-based linkage
1016 analyses. Am J Hum Genet. 2007;81:559–75.
1017 110. Knauer MT, Baitinger DJ. The Sow Body Condition Caliper. Appl Eng Agric.
1018 2015;31:175–8.
1019 111. Sahana G, Cai Z, Sanchez MP, Bouwman AC, Boichard D. Invited review: Good
1020 practices in genome-wide association studies to identify candidate sequence
1021 variants in dairy cattle. J Dairy Sci. 2023;106:5218–41.
1022 112. Yang J, Lee SH, Goddard ME, Visscher PM. GCTA: A tool for genome-wide
1023 complex trait analysis. Am J Hum Genet. 2011;88:76–82.
1024 113. Yang J, Zaitlen NA, Goddard ME, Visscher PM, Price AL. Advantages and pitfalls
1025 in the application of mixed-model association methods. Nature Genetics 2014
1026 46:2. 2014;46:100–6.
1027 114. Listgarten J, Lippert C, Kadie CM, Davidson RI, Eskin E, Heckerman D. Improved
1028 linear mixed models for genome-wide association studies. Nature Methods 2012
1029 9:6. 2012;9:525–6.
1030 115. Lippert C, Listgarten J, Liu Y, Kadie CM, Davidson RI, Heckerman D. FaST linear
1031 mixed models for genome-wide association studies. Nature Methods 2011 8:10.
1032 2011;8:833–5.
1033 116. van den Berg S, Vandenplas J, van Eeuwijk FA, Lopes MS, Veerkamp RF.
1034 Significance testing and genomic inflation factor using high-density genotypes or
1035 whole-genome sequence data. Journal of Animal Breeding and Genetics.
1036 2019;136:418–29.

1037 117. Balding DJ. A tutorial on statistical methods for population association studies.
1038 Nature Reviews Genetics 2006 7:10. 2006;7:781–91.
1039 118. Alghamdi J, Padmanabhan S. Fundamentals of complex trait genetics and
1040 association studies. Handbook of Pharmacogenomics and Stratified Medicine.
1041 2014;1:235–57.
1042 119. Li X, Buitenhuis AJ, Lund MS, Li C, Sun D, Zhang Q, et al. Joint genome-wide
1043 association study for milk fatty acid traits in Chinese and Danish Holstein
1044 populations. J Dairy Sci. 2015;98:8152–63.
1045 120. Goddard ME, Hayes BJ, Meuwissen THE. Using the genomic relationship matrix to
1046 predict the accuracy of genomic selection. Journal of Animal Breeding and
1047 Genetics. 2011;128:409–21.
1048 121. Corbin LJ, Liu AYH, Bishop SC, Woolliams JA. Estimation of historical effective
1049 population size using linkage disequilibria with marker data. Journal of Animal
1050 Breeding and Genetics. 2012;129:257–70.
1051 122. Bolormaa S, Hayes BJ, van der Werf JHJ, Pethick D, Goddard ME, Daetwyler HD.
1052 Detailed phenotyping identifies genes with pleiotropic effects on body
1053 composition. BMC Genomics. 2016;17:1–21.
1054 123. Fonseca PAS, Suárez-Vega A, Marras G, Cánovas Á. GALLO: An R package for
1055 genomic annotation and integration of multiple data sources in livestock for
1056 positional candidate loci. Gigascience. 2020;9:1–9.
1057 124. Huang DW, Sherman BT, Lempicki RA. Systematic and integrative analysis of large
1058 gene lists using DAVID bioinformatics resources. Nat Protoc. 2009;4:44–57.
1059 125. Sherman BT, Hao M, Qiu J, Jiao X, Baseler MW, Lane HC, et al. DAVID: a web
1060 server for functional enrichment analysis and functional annotation of gene lists
1061 (2021 update). Nucleic Acids Res. 2022;50:W216–21.

1062 **Supplementary Information**

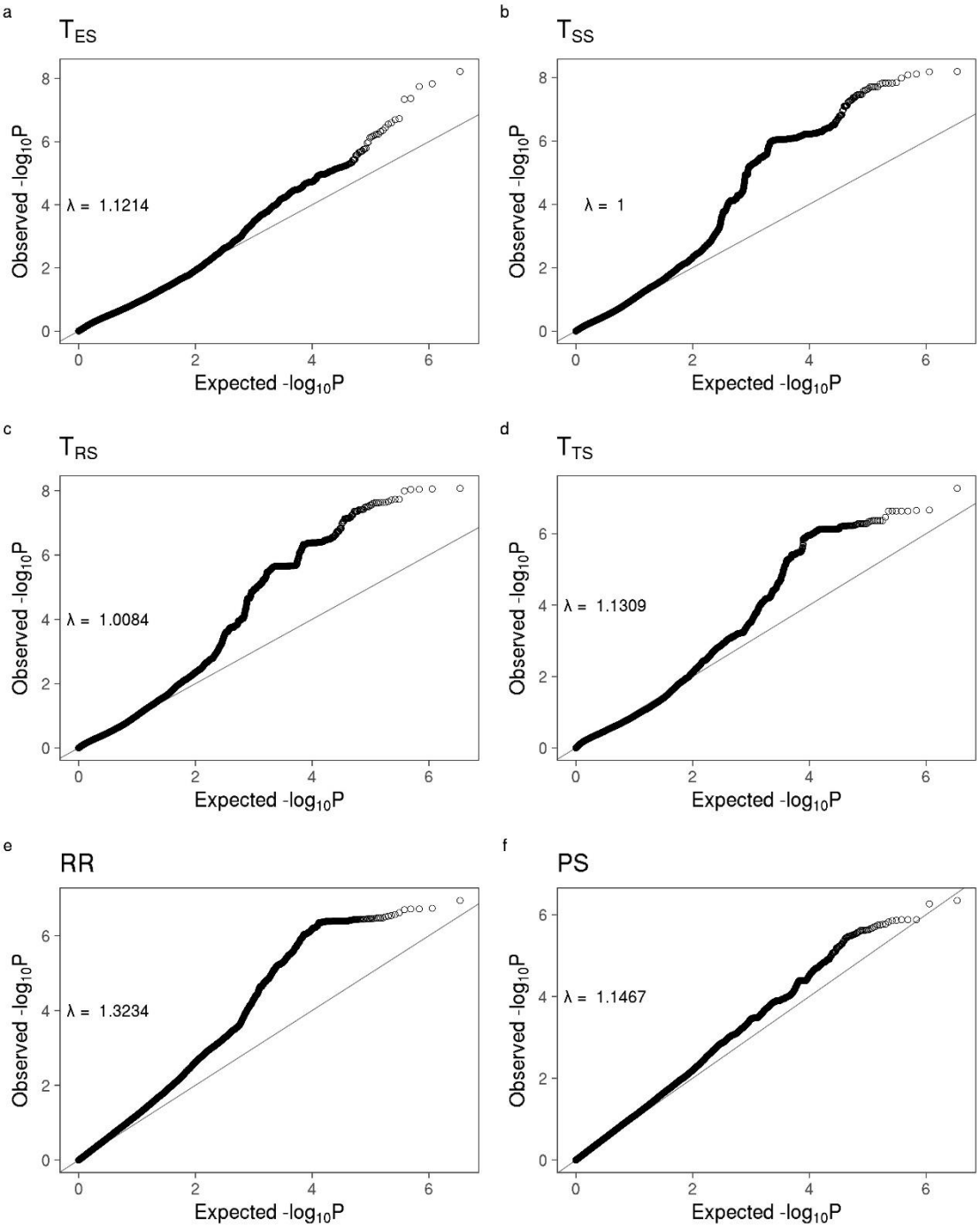

1063

1064 **Figure S1.** Quantile-quantile (QQ) plot of genome-wide association study for skin

1065 temperatures, respiration rate and panting score.

1066 -log10(p-values) for ear skin temperature (T_{ES}; **a**), shoulder skin temperature (T_{SS}; **b**),

1067 rump skin temperature (T_{RS}; **c**), tail skin temperature (T_{TS}; **d**), respiration rate (RR; **e**),

1068 and panting score (PS; **f**). Genome-wide significance level is shown in a red line.

1069

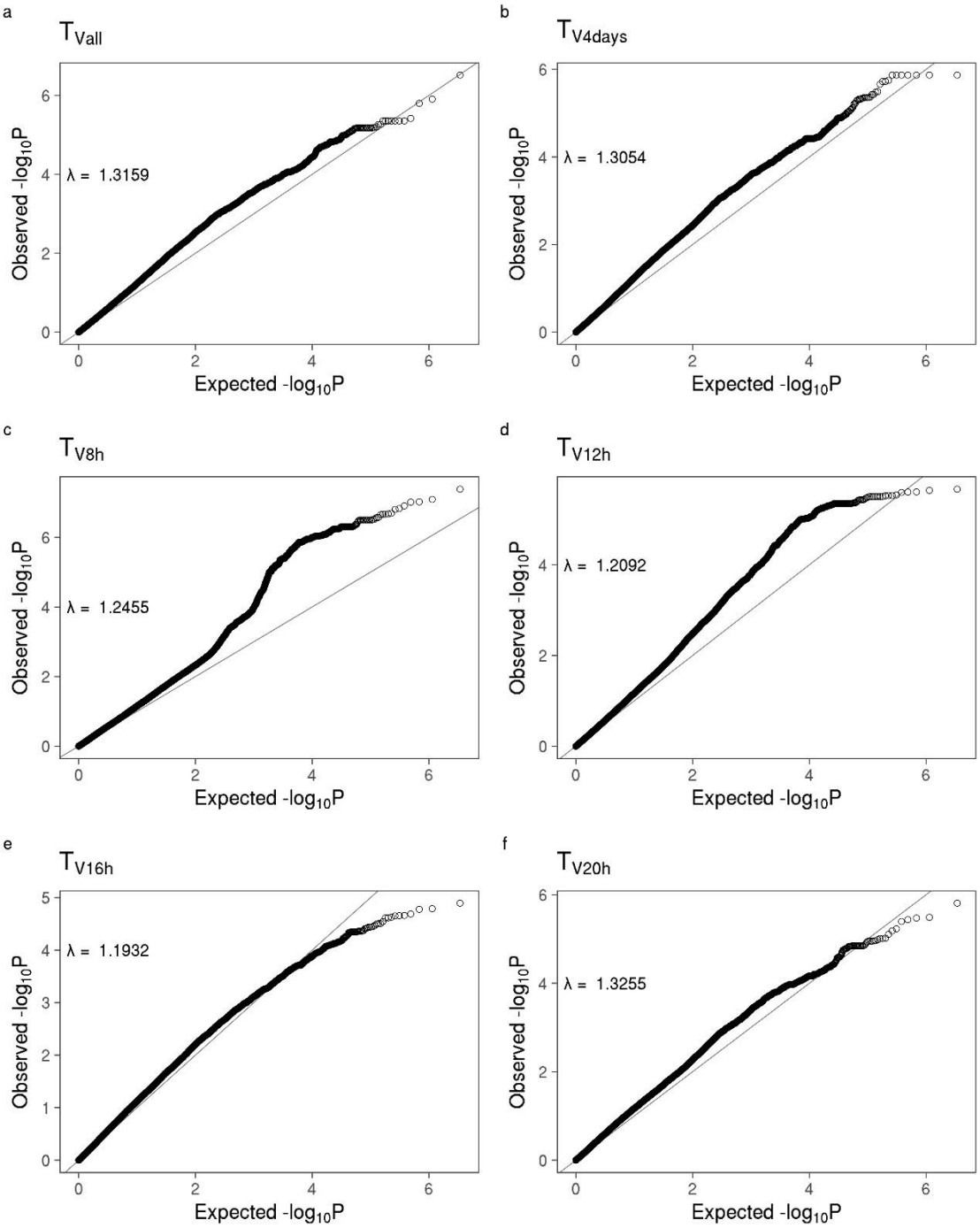

1070

1071 **Figure S2.** Quantile-quantile (QQ) plot of genome-wide association study for vaginal

1072 temperatures using whole genome sequence data.

1073 -log10(p-values) for all measures (every 10 minutes) of vaginal temperatures for four

1074 days (TV_{all}; **a**), four-time measures of vaginal temperatures for four days (T_{V4days}; **b**),

1075 vaginal temperature measured on the first day at 8:00 (T_{V8h}; **c**), at 12:00 (T_{V12h}; **d**), at

16:00 (T_{V16h}; **e**), and at 20:00 (T_{V20h}; **f**). Genome-wide significance level is shown in a red line.

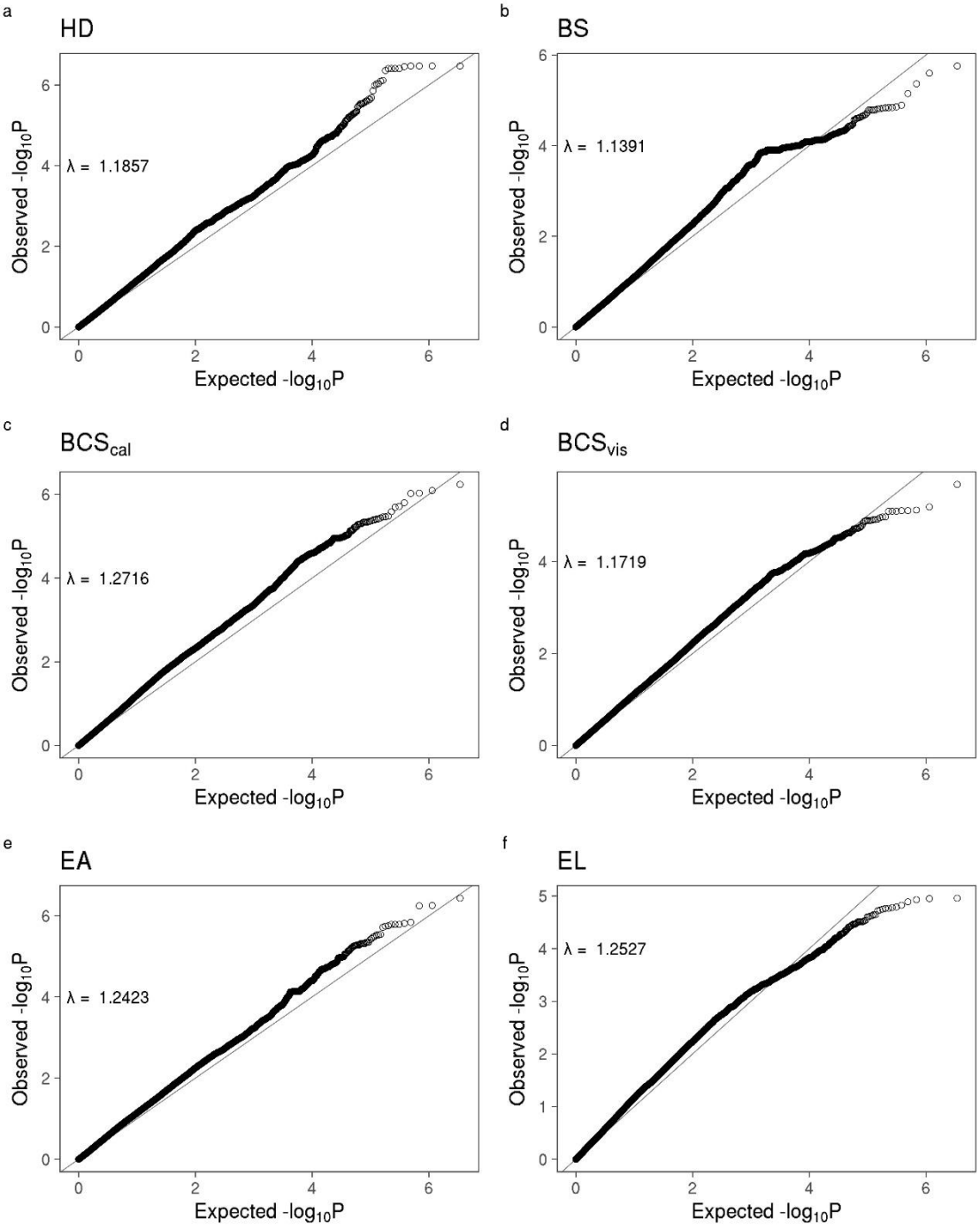

Figure S3. Quantile-quantile (QQ) plot of genome-wide association study for anatomical traits using whole genome sequence data.

1082 -log10(p-values) for hair density (HD; **a**), body size (BS; **b**), body condition score using
1083 a sow caliper (BCS_{cal}; **c**) and visual (BCS_{vis}; **d**), ear area (EA; **e**), and ear length (EL; **f**).
1084 Genome-wide significance level shown in a red line.
1085
1086 **Table S1.** Variants significantly associated with indicators of heat stress response in
1087 lactating sows

Trait	Chr	SNP	Position (bp)	Effect size	SE	p-value
T_{ES}	2	2_21729683_G	21,729,683	-1.14	0.22	0.00000028
T_{ES}	5	5_83314673_C	83,314,673	-1.56	0.30	0.00000025
T_{ES}	5	5_83647158_C	83,647,158	-1.19	0.24	0.00000103
T_{ES}	5	5_85914808_T	85,914,808	-1.59	0.27	0.00000001
T_{ES}	5	5_85980407_T	85,980,407	-1.50	0.27	0.00000002
T_{ES}	5	5_86004239_T	86,004,239	-1.43	0.26	0.00000005
T_{ES}	5	5_86011234_C	86,011,234	-1.44	0.26	0.00000004
T_{ES}	5	5_86026067_A	86,026,067	-1.51	0.27	0.00000001
T_{ES}	5	5_86030190_T	86,030,190	-1.31	0.25	0.00000020
T_{ES}	5	5_86033079_C	86,033,079	-1.32	0.25	0.00000019
T_{ES}	7	7_49276927_A	49,276,927	-1.43	0.29	0.00000075
T_{ES}	7	7_49440363_A	49,440,363	-1.44	0.29	0.00000066
T_{ES}	7	7_49527342_G	49,527,342	-1.46	0.29	0.00000059
T_{ES}	7	7_49584578_T	49,584,578	-1.45	0.29	0.00000071
T_{ES}	12	12_6808169_A	6,808,169	-1.54	0.31	0.00000049
T_{ES}	12	12_7330820_C	7,330,820	-1.16	0.23	0.00000062
T_{ES}	14	14_137210716_G	137,210,716	-1.39	0.27	0.00000044
T_{ES}	16	16_22801074_C	22,801,074	-1.14	0.23	0.00000110
T_{ES}	16	16_22804340_T	22,804,340	-1.20	0.24	0.00000058

T_{ES}	17	17_28358400_A	28,358,400	-1.56	0.31	0.00000036
T_{RS}	1	1_10473872_A	10,473,872	-0.78	0.15	0.00000026
T_{RS}	1	1_10505848_T	10,505,848	-0.76	0.15	0.00000042
T_{RS}	2	2_95628544_A	95,628,544	-0.76	0.15	0.00000035
T_{RS}	2	2_105870529_AC	105,870,529	-0.82	0.15	0.00000010
T_{RS}	2	2_106932589_C	106,932,589	-0.70	0.14	0.00000078
T_{RS}	2	2_106934370_A	106,934,370	-0.70	0.14	0.00000081
T_{RS}	2	2_106936039_A	106,936,039	-0.70	0.14	0.00000081
T_{RS}	2	2_106936870_G	106,936,870	-0.70	0.14	0.00000081
T_{RS}	2	2_106939546_C	106,939,546	-0.70	0.14	0.00000081
T_{RS}	2	2_106941818_T	106,941,818	-0.70	0.14	0.00000081
T_{RS}	2	2_106942263_T	106,942,263	-0.70	0.14	0.00000083
T_{RS}	2	2_106942836_C	106,942,836	-0.70	0.14	0.00000081
T_{RS}	2	2_106945457_G	106,945,457	-0.70	0.14	0.00000081
T_{RS}	2	2_106950249_T	106,950,249	-0.70	0.14	0.00000081
T_{RS}	2	2_106950790_C	106,950,790	-0.70	0.14	0.00000081
T_{RS}	2	2_106953486_C	106,953,486	-0.70	0.14	0.00000081
T_{RS}	2	2_106955955_T	106,955,955	-0.70	0.14	0.00000081
T_{RS}	2	2_106962610_C	106,962,610	-0.70	0.14	0.00000081
T_{RS}	2	2_106973729_G	106,973,729	-0.70	0.14	0.00000081
T_{RS}	2	2_106981316_A	106,981,316	-0.70	0.14	0.00000081
T_{RS}	2	2_106992942_T	106,992,942	-0.70	0.14	0.00000090
T_{RS}	2	2_106998524_G	106,998,524	-0.73	0.14	0.00000040
T_{RS}	2	2_107002094_G	107,002,094	-0.70	0.14	0.00000090
T_{RS}	2	2_107004443_G	107,004,443	-0.70	0.14	0.00000090
T_{RS}	2	2_107013764_T	107,013,764	-0.70	0.14	0.00000091
T_{RS}	2	2_107015777_A	107,015,777	-0.70	0.14	0.00000091

T_{RS}	2	2_107029393_G	107,029,393	-0.70	0.14	0.00000091
T_{RS}	2	2_107035570_T	107,035,570	-0.70	0.14	0.00000091
T_{RS}	2	2_107036854_C	107,036,854	-0.70	0.14	0.00000091
T_{RS}	2	2_107047998_C	107,047,998	-0.70	0.14	0.00000091
T_{RS}	2	2_107051105_G	107,051,105	-0.70	0.14	0.00000091
T_{RS}	2	2_107054884_T	107,054,884	-0.70	0.14	0.00000091
T_{RS}	2	2_107063657_T	107,063,657	-0.71	0.14	0.00000093
T_{RS}	2	2_107090101_A	107,090,101	-0.70	0.14	0.00000083
T_{RS}	2	2_107098377_A	107,098,377	-0.70	0.14	0.00000083
T_{RS}	2	2_107103152_G	107,103,152	-0.70	0.14	0.00000083
T_{RS}	2	2_107106134_G	107,106,134	-0.70	0.14	0.00000083
T_{RS}	2	2_107117477_A	107,117,477	-0.70	0.14	0.00000083
T_{RS}	2	2_107119623_T	107,119,623	-0.70	0.14	0.00000083
T_{RS}	2	2_107120979_G	107,120,979	-0.70	0.14	0.00000083
T_{RS}	2	2_107124307_A	107,124,307	-0.70	0.14	0.00000085
T_{RS}	2	2_107127915_A	107,127,915	-0.70	0.14	0.00000083
T_{RS}	2	2_107131360_G	107,131,360	-0.70	0.14	0.00000083
T_{RS}	2	2_107132410_C	107,132,410	-0.70	0.14	0.00000083
T_{RS}	2	2_107133110_C	107,133,110	-0.70	0.14	0.00000082
T_{RS}	2	2_107133669_GGT	107,133,669	-0.70	0.14	0.00000083
T_{RS}	2	2_107134600_C	107,134,600	-0.70	0.14	0.00000083
T_{RS}	2	2_107135916_T	107,135,916	-0.70	0.14	0.00000083
T_{RS}	2	2_107136945_G	107,136,945	-0.73	0.14	0.00000049
T_{RS}	2	2_107141897_A	107,141,897	-0.69	0.14	0.00000094
T_{RS}	2	2_107145818_A	107,145,818	-0.69	0.14	0.00000094
T_{RS}	2	2_107149379_C	107,149,379	-0.69	0.14	0.00000094
T_{RS}	2	2_107152325_A	107,152,325	-0.69	0.14	0.00000094

T_{RS}	2	2_107179342_A	107,179,342	-0.69	0.14	0.00000095
T_{RS}	2	2_107268832_T	107,268,832	-0.69	0.14	0.00000094
T_{RS}	2	2_107269860_T	107,269,860	-0.69	0.14	0.00000115
T_{RS}	2	2_107270950_T	107,270,950	-0.69	0.14	0.00000096
T_{RS}	2	2_107274108_G	107,274,108	-0.69	0.14	0.00000084
T_{RS}	2	2_107289176_G	107,289,176	-0.69	0.14	0.00000090
T_{RS}	2	2_107290276_T	107,290,276	-0.69	0.14	0.00000094
T_{RS}	2	2_107295408_G	107,295,408	-0.69	0.14	0.00000096
T_{RS}	2	2_107300857_G	107,300,857	-0.69	0.14	0.00000094
T_{RS}	2	2_107308172_A	107,308,172	-0.69	0.14	0.00000094
T_{RS}	2	2_107315087_A	107,315,087	-0.69	0.14	0.00000084
T_{RS}	2	2_107320377_A	107,320,377	-0.69	0.14	0.00000084
T_{RS}	2	2_107347961_T	107,347,961	-0.69	0.14	0.00000086
T_{RS}	2	2_107349607_C	107,349,607	-0.70	0.14	0.00000080
T_{RS}	2	2_107351712_T	107,351,712	-0.69	0.14	0.00000084
T_{RS}	2	2_107356272_T	107,356,272	-0.69	0.14	0.00000084
T_{RS}	2	2_107357509_A	107,357,509	-0.69	0.14	0.00000084
T_{RS}	2	2_107358869_C	107,358,869	-0.69	0.14	0.00000084
T_{RS}	2	2_107360210_G	107,360,210	-0.69	0.14	0.00000084
T_{RS}	2	2_107364084_C	107,364,084	-0.69	0.14	0.00000094
T_{RS}	2	2_107367991_C	107,367,991	-0.69	0.14	0.00000094
T_{RS}	2	2_107368945_A	107,368,945	-0.71	0.14	0.00000061
T_{RS}	2	2_107369775_C	107,369,775	-0.69	0.14	0.00000094
T_{RS}	2	2_107371983_G	107,371,983	-0.69	0.14	0.00000094
T_{RS}	2	2_107376291_G	107,376,291	-0.69	0.14	0.00000094
T_{RS}	2	2_107376916_A	107,376,916	-0.69	0.14	0.00000096
T_{RS}	2	2_107392404_T	107,392,404	-0.69	0.14	0.00000094

T_{RS}	2	2_107393684_A	107,393,684	-0.69	0.14	0.00000094
T_{RS}	2	2_107395283_A	107,395,283	-0.70	0.14	0.00000097
T_{RS}	2	2_107395560_T	107,395,560	-0.69	0.14	0.00000094
T_{RS}	2	2_107396185_G	107,396,185	-0.69	0.14	0.00000094
T_{RS}	2	2_107408013_T	107,408,013	-0.69	0.14	0.00000096
T_{RS}	2	2_107416249_T	107,416,249	-0.69	0.14	0.00000094
T_{RS}	2	2_107418953_G	107,418,953	-0.69	0.14	0.00000094
T_{RS}	2	2_107420684_A	107,420,684	-0.69	0.14	0.00000094
T_{RS}	2	2_107422508_G	107,422,508	-0.69	0.14	0.00000094
T_{RS}	2	2_107427544_T	107,427,544	-0.69	0.14	0.00000084
T_{RS}	2	2_107430752_G	107,430,752	-0.69	0.14	0.00000114
T_{RS}	2	2_107431839_G	107,431,839	-0.69	0.14	0.00000094
T_{RS}	2	2_107442112_A	107,442,112	-0.70	0.14	0.00000097
T_{RS}	2	2_107444574_CTAAT	107,444,574	-0.69	0.14	0.00000094
T_{RS}	2	2_107446310_T	107,446,310	-0.69	0.14	0.00000094
T_{RS}	2	2_107447973_C	107,447,973	-0.69	0.14	0.00000094
T_{RS}	2	2_107452342_A	107,452,342	-0.69	0.14	0.00000094
T_{RS}	2	2_107459251_CTT	107,459,251	-0.69	0.14	0.00000094
T_{RS}	2	2_107475616_G	107,475,616	-0.69	0.14	0.00000094
T_{RS}	2	2_107476926_G	107,476,926	-0.69	0.14	0.00000096
T_{RS}	2	2_107490285_A	107,490,285	-0.69	0.14	0.00000094
T_{RS}	2	2_107492866_T	107,492,866	-0.69	0.14	0.00000094
T_{RS}	2	2_107495160_T	107,495,160	-0.69	0.14	0.00000094
T_{RS}	2	2_107496558_A	107,496,558	-0.69	0.14	0.00000094
T_{RS}	2	2_107500977_C	107,500,977	-0.69	0.14	0.00000100
T_{RS}	2	2_107503295_T	107,503,295	-0.69	0.14	0.00000096
T_{RS}	2	2_107505281_T	107,505,281	-0.69	0.14	0.00000094

T_{RS}	2	2_107506999_G	107,506,999	-0.69	0.14	0.00000094
T_{RS}	2	2_107509674_C	107,509,674	-0.69	0.14	0.00000097
T_{RS}	2	2_107511805_T	107,511,805	-0.69	0.14	0.00000097
T_{RS}	2	2_107512887_T	107,512,887	-0.69	0.14	0.00000094
T_{RS}	2	2_107515816_C	107,515,816	-0.69	0.14	0.00000094
T_{RS}	2	2_107517438_T	107,517,438	-0.69	0.14	0.00000094
T_{RS}	2	2_107522864_G	107,522,864	-0.69	0.14	0.00000098
T_{RS}	2	2_107528939_A	107,528,939	-0.69	0.14	0.00000107
T_{RS}	2	2_107531849_C	107,531,849	-0.69	0.14	0.00000107
T_{RS}	2	2_107539254_A	107,539,254	-0.69	0.14	0.00000107
T_{RS}	2	2_107542028_T	107,542,028	-0.69	0.14	0.00000107
T_{RS}	2	2_107544837_A	107,544,837	-0.69	0.14	0.00000107
T_{RS}	2	2_107546360_G	107,546,360	-0.69	0.14	0.00000107
T_{RS}	2	2_107549103_T	107,549,103	-0.69	0.14	0.00000107
T_{RS}	2	2_107552495_C	107,552,495	-0.69	0.14	0.00000107
T_{RS}	2	2_107553872_A	107,553,872	-0.69	0.14	0.00000107
T_{RS}	2	2_107556354_A	107,556,354	-0.69	0.14	0.00000109
T_{RS}	2	2_107557567_A	107,557,567	-0.69	0.14	0.00000115
T_{RS}	2	2_107558538_C	107,558,538	-0.69	0.14	0.00000109
T_{RS}	2	2_107567561_G	107,567,561	-0.69	0.14	0.00000108
T_{RS}	2	2_107568003_CTTATA	107,568,003	-0.69	0.14	0.00000108
T_{RS}	2	2_107574561_G	107,574,561	-0.69	0.14	0.00000109
T_{RS}	2	2_107579551_C	107,579,551	-0.69	0.14	0.00000112
T_{RS}	2	2_107581705_T	107,581,705	-0.69	0.14	0.00000108
T_{RS}	2	2_107583005_T	107,583,005	-0.69	0.14	0.00000108
T_{RS}	2	2_107583603_G	107,583,603	-0.69	0.14	0.00000105
T_{RS}	2	2_107585221_A	107,585,221	-0.69	0.14	0.00000109

T_{RS}	2	2_107590260_G	107,590,260	-0.69	0.14	0.00000109
T_{RS}	2	2_107598357_T	107,598,357	-0.69	0.14	0.00000109
T_{RS}	2	2_107598492_AT	107,598,492	-0.69	0.14	0.00000109
T_{RS}	2	2_107599530_T	107,599,530	-0.69	0.14	0.00000109
T_{RS}	2	2_107601138_A	107,601,138	-0.69	0.14	0.00000109
T_{RS}	2	2_107608655_C	107,608,655	-0.69	0.14	0.00000104
T_{RS}	2	2_107609128_C	107,609,128	-0.69	0.14	0.00000109
T_{RS}	2	2_107613505_A	107,613,505	-0.69	0.14	0.00000112
T_{RS}	2	2_107614716_A	107,614,716	-0.69	0.14	0.00000109
T_{RS}	2	2_107615112_A	107,615,112	-0.69	0.14	0.00000109
T_{RS}	2	2_107617118_A	107,617,118	-0.69	0.14	0.00000109
T_{RS}	2	2_107776212_G	107,776,212	-0.69	0.14	0.00000098
T_{RS}	2	2_107789107_T	107,789,107	-0.69	0.14	0.00000098
T_{RS}	2	2_107790702_T	107,790,702	-0.69	0.14	0.00000097
T_{RS}	2	2_107794698_G	107,794,698	-0.69	0.14	0.00000086
T_{RS}	2	2_107795264_T	107,795,264	-0.69	0.14	0.00000083
T_{RS}	2	2_107797401_C	107,797,401	-0.69	0.14	0.00000083
T_{RS}	2	2_107807043_C	107,807,043	-0.69	0.14	0.00000093
T_{RS}	2	2_107807975_A	107,807,975	-0.69	0.14	0.00000093
T_{RS}	2	2_107910486_T	107,910,486	-0.69	0.14	0.00000094
T_{RS}	2	2_107945395_A	107,945,395	-0.69	0.14	0.00000094
T_{RS}	2	2_107955743_G	107,955,743	-0.69	0.14	0.00000094
T_{RS}	2	2_107959085_G	107,959,085	-0.69	0.14	0.00000094
T_{RS}	2	2_107990888_G	107,990,888	-0.71	0.14	0.00000058
T_{RS}	2	2_107995112_G	107,995,112	-0.71	0.14	0.00000060
T_{RS}	2	2_108014629_T	108,014,629	-0.69	0.14	0.00000092
T_{RS}	2	2_108021121_C	108,021,121	-0.69	0.14	0.00000092

T_{RS}	2	2_108023057_G	108,023,057	-0.69	0.14	0.00000092
T_{RS}	2	2_108028603_A	108,028,603	-0.69	0.14	0.00000092
T_{RS}	2	2_108036168_C	108,036,168	-0.69	0.14	0.00000095
T_{RS}	2	2_108037667_T	108,037,667	-0.69	0.14	0.00000092
T_{RS}	2	2_108042151_C	108,042,151	-0.69	0.14	0.00000092
T_{RS}	2	2_108067180_G	108,067,180	-0.71	0.14	0.00000052
T_{RS}	2	2_108072314_C	108,072,314	-0.69	0.14	0.00000092
T_{RS}	2	2_108073986_T	108,073,986	-0.69	0.14	0.00000092
T_{RS}	2	2_108077954_T	108,077,954	-0.69	0.14	0.00000095
T_{RS}	2	2_108097687_T	108,097,687	-0.69	0.14	0.00000092
T_{RS}	2	2_108103554_A	108,103,554	-0.69	0.14	0.00000092
T_{RS}	2	2_108108338_G	108,108,338	-0.69	0.14	0.00000092
T_{RS}	2	2_108111514_T	108,111,514	-0.69	0.14	0.00000092
T_{RS}	2	2_108118538_AAAACC	108,118,538	-0.69	0.14	0.00000089
T_{RS}	2	2_108123055_C	108,123,055	-0.69	0.14	0.00000092
T_{RS}	2	2_108128267_G	108,128,267	-0.69	0.14	0.00000092
T_{RS}	2	2_108130080_T	108,130,080	-0.69	0.14	0.00000092
T_{RS}	2	2_108135243_G	108,135,243	-0.69	0.14	0.00000092
T_{RS}	2	2_108219460_A	108,219,460	-0.69	0.14	0.00000095
T_{RS}	2	2_108231523_A	108,231,523	-0.69	0.14	0.00000092
T_{RS}	2	2_108272377_A	108,272,377	-0.69	0.14	0.00000092
T_{RS}	2	2_108286267_C	108,286,267	-0.69	0.14	0.00000092
T_{RS}	2	2_108286951_T	108,286,951	-0.69	0.14	0.00000092
T_{RS}	2	2_108294151_C	108,294,151	-0.69	0.14	0.00000092
T_{RS}	2	2_108304856_A	108,304,856	-0.69	0.14	0.00000092
T_{RS}	2	2_108318031_A	108,318,031	-0.69	0.14	0.00000092
T_{RS}	2	2_108322931_T	108,322,931	-0.69	0.14	0.00000092

T_{RS}	2	2_108332035_A	108,332,035	-0.69	0.14	0.00000092
T_{RS}	2	2_108344329_C	108,344,329	-0.69	0.14	0.00000092
T_{RS}	2	2_108346595_A	108,346,595	-0.69	0.14	0.00000095
T_{RS}	2	2_108354775_A	108,354,775	-0.69	0.14	0.00000095
T_{RS}	2	2_108387224_T	108,387,224	-0.69	0.14	0.00000092
T_{RS}	2	2_108408656_G	108,408,656	-0.69	0.14	0.00000092
T_{RS}	2	2_108423172_C	108,423,172	-0.69	0.14	0.00000088
T_{RS}	2	2_108425902_A	108,425,902	-0.69	0.14	0.00000092
T_{RS}	2	2_108443155_T	108,443,155	-0.69	0.14	0.00000094
T_{RS}	2	2_108450783_A	108,450,783	-0.69	0.14	0.00000092
T_{RS}	2	2_108483514_A	108,483,514	-0.69	0.14	0.00000092
T_{RS}	2	2_108484938_A	108,484,938	-0.69	0.14	0.00000092
T_{RS}	2	2_108486895_T	108,486,895	-0.69	0.14	0.00000092
T_{RS}	2	2_108490424_T	108,490,424	-0.70	0.14	0.00000076
T_{RS}	2	2_108491610_C	108,491,610	-0.69	0.14	0.00000092
T_{RS}	2	2_108495649_C	108,495,649	-0.69	0.14	0.00000092
T_{RS}	2	2_108509159_A	108,509,159	-0.69	0.14	0.00000092
T_{RS}	2	2_108524254_A	108,524,254	-0.69	0.14	0.00000092
T_{RS}	2	2_108540375_T	108,540,375	-0.69	0.14	0.00000099
T_{RS}	2	2_108545167_C	108,545,167	-0.69	0.14	0.00000099
T_{RS}	2	2_108550589_A	108,550,589	-0.69	0.14	0.00000099
T_{RS}	2	2_108553390_C	108,553,390	-0.69	0.14	0.00000099
T_{RS}	2	2_108556350_A	108,556,350	-0.69	0.14	0.00000099
T_{RS}	2	2_108557290_C	108,557,290	-0.69	0.14	0.00000099
T_{RS}	2	2_108561587_A	108,561,587	-0.69	0.14	0.00000099
T_{RS}	2	2_108562819_A	108,562,819	-0.71	0.14	0.00000064
T_{RS}	2	2_108565782_G	108,565,782	-0.69	0.14	0.00000099

T_{RS}	2	2_108569393_C	108,569,393	-0.69	0.14	0.00000099
T_{RS}	2	2_108570576_T	108,570,576	-0.69	0.14	0.00000101
T_{RS}	2	2_108572011_C	108,572,011	-0.69	0.14	0.00000099
T_{RS}	2	2_108576308_T	108,576,308	-0.69	0.14	0.00000099
T_{RS}	2	2_108578293_T	108,578,293	-0.69	0.14	0.00000099
T_{RS}	2	2_108582214_A	108,582,214	-0.69	0.14	0.00000109
T_{RS}	2	2_108587197_G	108,587,197	-0.69	0.14	0.00000109
T_{RS}	2	2_108592559_T	108,592,559	-0.69	0.14	0.00000099
T_{RS}	2	2_108596851_A	108,596,851	-0.69	0.14	0.00000099
T_{RS}	2	2_108598914_G	108,598,914	-0.69	0.14	0.00000101
T_{RS}	2	2_108599460_G	108,599,460	-0.69	0.14	0.00000099
T_{RS}	2	2_108600360_T	108,600,360	-0.71	0.14	0.00000070
T_{RS}	2	2_108601609_A	108,601,609	-0.69	0.14	0.00000100
T_{RS}	2	2_108602492_C	108,602,492	-0.69	0.14	0.00000099
T_{RS}	2	2_108603657_A	108,603,657	-0.69	0.14	0.00000100
T_{RS}	2	2_108629684_C	108,629,684	-0.69	0.14	0.00000100
T_{RS}	2	2_108713184_C	108,713,184	-0.69	0.14	0.00000100
T_{RS}	2	2_108719660_G	108,719,660	-0.69	0.14	0.00000100
T_{RS}	2	2_108726026_G	108,726,026	-0.69	0.14	0.00000100
T_{RS}	2	2_108751375_A	108,751,375	-0.69	0.14	0.00000102
T_{RS}	2	2_108787359_C	108,787,359	-0.69	0.14	0.00000102
T_{RS}	2	2_108790809_G	108,790,809	-0.69	0.14	0.00000102
T_{RS}	2	2_108793947_T	108,793,947	-0.69	0.14	0.00000102
T_{RS}	2	2_108797545_G	108,797,545	-0.69	0.14	0.00000102
T_{RS}	2	2_108804251_A	108,804,251	-0.69	0.14	0.00000100
T_{RS}	2	2_108806409_G	108,806,409	-0.69	0.14	0.00000102
T_{RS}	2	2_108810693_A	108,810,693	-0.69	0.14	0.00000108

T_{RS}	2	2_108813282_G	108,813,282	-0.69	0.14	0.00000113
T_{RS}	2	2_108815253_A	108,815,253	-0.69	0.14	0.00000108
T_{RS}	2	2_108820038_C	108,820,038	-0.68	0.14	0.00000110
T_{RS}	2	2_108845528_C	108,845,528	-0.68	0.14	0.00000116
T_{RS}	2	2_108852710_C	108,852,710	-0.68	0.14	0.00000110
T_{RS}	2	2_108857627_G	108,857,627	-0.68	0.14	0.00000110
T_{RS}	2	2_108867347_C	108,867,347	-0.68	0.14	0.00000110
T_{RS}	2	2_108874785_C	108,874,785	-0.89	0.16	0.00000002
T_{RS}	2	2_108879308_G	108,879,308	-0.69	0.14	0.00000098
T_{RS}	2	2_108880060_G	108,880,060	-0.69	0.14	0.00000098
T_{RS}	2	2_108882897_C	108,882,897	-0.69	0.14	0.00000096
T_{RS}	2	2_108886141_C	108,886,141	-0.69	0.14	0.00000096
T_{RS}	2	2_108888087_G	108,888,087	-0.69	0.14	0.00000096
T_{RS}	2	2_108890634_C	108,890,634	-0.69	0.14	0.00000096
T_{RS}	2	2_108897983_C	108,897,983	-0.69	0.14	0.00000091
T_{RS}	2	2_108903430_C	108,903,430	-0.69	0.14	0.00000091
T_{RS}	2	2_108906146_A	108,906,146	-0.69	0.14	0.00000091
T_{RS}	2	2_108909055_T	108,909,055	-0.69	0.14	0.00000091
T_{RS}	2	2_108910451_C	108,910,451	-0.69	0.14	0.00000091
T_{RS}	2	2_108911128_C	108,911,128	-0.69	0.14	0.00000091
T_{RS}	2	2_108912659_T	108,912,659	-0.69	0.14	0.00000091
T_{RS}	2	2_108915836_G	108,915,836	-0.69	0.14	0.00000091
T_{RS}	2	2_108917749_G	108,917,749	-0.69	0.14	0.00000091
T_{RS}	2	2_108937183_G	108,937,183	-0.70	0.14	0.00000079
T_{RS}	2	2_108940146_G	108,940,146	-0.70	0.14	0.00000079
T_{RS}	2	2_108948208_C	108,948,208	-0.70	0.14	0.00000079
T_{RS}	2	2_108955810_T	108,955,810	-0.70	0.14	0.00000079

T_{RS}	2	2_108964268_G	108,964,268	-0.69	0.14	0.00000093
T_{RS}	2	2_108971202_G	108,971,202	-0.69	0.14	0.00000091
T_{RS}	2	2_108973447_A	108,973,447	-0.69	0.14	0.00000091
T_{RS}	2	2_108985411_G	108,985,411	-0.69	0.14	0.00000091
T_{RS}	2	2_108990486_G	108,990,486	-0.69	0.14	0.00000091
T_{RS}	2	2_108996255_T	108,996,255	-0.69	0.14	0.00000091
T_{RS}	2	2_108999239_A	108,999,239	-0.69	0.14	0.00000091
T_{RS}	2	2_109005900_T	109,005,900	-0.69	0.14	0.00000091
T_{RS}	2	2_109014457_C	109,014,457	-0.69	0.14	0.00000081
T_{RS}	2	2_109019845_G	109,019,845	-0.69	0.14	0.00000091
T_{RS}	2	2_109021495_T	109,021,495	-0.69	0.14	0.00000091
T_{RS}	2	2_109027613_C	109,027,613	-0.69	0.14	0.00000091
T_{RS}	2	2_109036928_C	109,036,928	-0.69	0.14	0.00000091
T_{RS}	2	2_109038473_A	109,038,473	-0.69	0.14	0.00000091
T_{RS}	2	2_109039404_T	109,039,404	-0.69	0.14	0.00000091
T_{RS}	2	2_109042851_G	109,042,851	-0.69	0.14	0.00000091
T_{RS}	2	2_109051350_A	109,051,350	-0.69	0.14	0.00000091
T_{RS}	2	2_109054101_C	109,054,101	-0.69	0.14	0.00000093
T_{RS}	2	2_109060083_G	109,060,083	-0.69	0.14	0.00000091
T_{RS}	2	2_109062401_C	109,062,401	-0.69	0.14	0.00000091
T_{RS}	2	2_109066877_C	109,066,877	-0.69	0.14	0.00000091
T_{RS}	2	2_109069778_C	109,069,778	-0.69	0.14	0.00000091
T_{RS}	2	2_109073289_G	109,073,289	-0.69	0.14	0.00000091
T_{RS}	2	2_109080084_C	109,080,084	-0.69	0.14	0.00000091
T_{RS}	2	2_109082169_T	109,082,169	-0.70	0.14	0.00000086
T_{RS}	2	2_109085847_G	109,085,847	-0.69	0.14	0.00000089
T_{RS}	2	2_109092467_A	109,092,467	-0.69	0.14	0.00000089

T_{RS}	2	2_109094257_A	109,094,257	-0.69	0.14	0.00000089
T_{RS}	2	2_109097351_A	109,097,351	-0.69	0.14	0.00000089
T_{RS}	2	2_109098799_G	109,098,799	-0.69	0.14	0.00000089
T_{RS}	2	2_109105204_T	109,105,204	-0.69	0.14	0.00000087
T_{RS}	2	2_109110747_C	109,110,747	-0.69	0.14	0.00000087
T_{RS}	2	2_109117624_G	109,117,624	-0.69	0.14	0.00000089
T_{RS}	2	2_109124043_G	109,124,043	-0.69	0.14	0.00000089
T_{RS}	2	2_109130665_G	109,130,665	-0.69	0.14	0.00000088
T_{RS}	2	2_109133585_T	109,133,585	-0.69	0.14	0.00000089
T_{RS}	2	2_109139065_T	109,139,065	-0.69	0.14	0.00000089
T_{RS}	2	2_109144047_T	109,144,047	-0.69	0.14	0.00000089
T_{RS}	2	2_109153271_A	109,153,271	-0.69	0.14	0.00000099
T_{RS}	2	2_109156427_C	109,156,427	-0.69	0.14	0.00000099
T_{RS}	2	2_109160103_A	109,160,103	-0.69	0.14	0.00000089
T_{RS}	2	2_109167405_G	109,167,405	-0.69	0.14	0.00000089
T_{RS}	2	2_109169950_C	109,169,950	-0.69	0.14	0.00000089
T_{RS}	2	2_109171869_T	109,171,869	-0.70	0.14	0.00000074
T_{RS}	2	2_109177073_T	109,177,073	-0.69	0.14	0.00000090
T_{RS}	2	2_109178990_G	109,178,990	-0.70	0.14	0.00000080
T_{RS}	2	2_109180737_G	109,180,737	-0.69	0.14	0.00000089
T_{RS}	2	2_109183757_G	109,183,757	-0.69	0.14	0.00000092
T_{RS}	2	2_109186004_C	109,186,004	-0.69	0.14	0.00000089
T_{RS}	2	2_109194877_G	109,194,877	-0.69	0.14	0.00000086
T_{RS}	2	2_109199582_T	109,199,582	-0.69	0.14	0.00000089
T_{RS}	2	2_109206314_C	109,206,314	-0.69	0.14	0.00000089
T_{RS}	2	2_109209859_A	109,209,859	-0.69	0.14	0.00000089
T_{RS}	2	2_109229351_A	109,229,351	-0.69	0.14	0.00000089

T_{RS}	2	2_109236257_G	109,236,257	-0.69	0.14	0.00000089
T_{RS}	2	2_109240370_A	109,240,370	-0.69	0.14	0.00000089
T_{RS}	2	2_109284720_T	109,284,720	-0.69	0.14	0.00000089
T_{RS}	2	2_109298358_G	109,298,358	-0.69	0.14	0.00000089
T_{RS}	2	2_109301550_A	109,301,550	-0.69	0.14	0.00000089
T_{RS}	2	2_109303388_A	109,303,388	-0.69	0.14	0.00000089
T_{RS}	2	2_109307908_T	109,307,908	-0.69	0.14	0.00000089
T_{RS}	2	2_109315697_A	109,315,697	-0.70	0.14	0.00000080
T_{RS}	2	2_109317165_G	109,317,165	-0.69	0.14	0.00000089
T_{RS}	2	2_109319635_G	109,319,635	-0.69	0.14	0.00000089
T_{RS}	2	2_109324124_T	109,324,124	-0.69	0.14	0.00000089
T_{RS}	2	2_109334810_A	109,334,810	-0.69	0.14	0.00000086
T_{RS}	2	2_109336625_G	109,336,625	-0.70	0.14	0.00000086
T_{RS}	2	2_109337801_TG	109,337,801	-0.69	0.14	0.00000089
T_{RS}	2	2_109340076_A	109,340,076	-0.69	0.14	0.00000089
T_{RS}	2	2_109342087_G	109,342,087	-0.69	0.14	0.00000089
T_{RS}	2	2_109345826_G	109,345,826	-0.69	0.14	0.00000089
T_{RS}	2	2_109348873_CA	109,348,873	-0.70	0.14	0.00000080
T_{RS}	2	2_109351016_G	109,351,016	-0.70	0.14	0.00000080
T_{RS}	2	2_109352808_T	109,352,808	-0.70	0.14	0.00000076
T_{RS}	2	2_109354957_A	109,354,957	-0.69	0.14	0.00000088
T_{RS}	2	2_109356706_TA	109,356,706	-0.69	0.14	0.00000089
T_{RS}	2	2_109376318_G	109,376,318	-0.69	0.14	0.00000089
T_{RS}	2	2_109378224_C	109,378,224	-0.69	0.14	0.00000089
T_{RS}	2	2_109381850_T	109,381,850	-0.69	0.14	0.00000089
T_{RS}	2	2_109387382_G	109,387,382	-0.69	0.14	0.00000089
T_{RS}	2	2_109391511_A	109,391,511	-0.70	0.14	0.00000073

T_{RS}	2	2_109393203_C	109,393,203	-0.69	0.14	0.00000089
T_{RS}	2	2_109398825_T	109,398,825	-0.69	0.14	0.00000089
T_{RS}	2	2_109401482_A	109,401,482	-0.69	0.14	0.00000089
T_{RS}	2	2_109404466_T	109,404,466	-0.69	0.14	0.00000089
T_{RS}	2	2_109409209_T	109,409,209	-0.69	0.14	0.00000089
T_{RS}	2	2_109412262_T	109,412,262	-0.69	0.14	0.00000089
T_{RS}	2	2_109414329_A	109,414,329	-0.69	0.14	0.00000089
T_{RS}	2	2_109417119_C	109,417,119	-0.69	0.14	0.00000089
T_{RS}	2	2_109420883_A	109,420,883	-0.69	0.14	0.00000089
T_{RS}	2	2_109426124_AT	109,426,124	-0.70	0.14	0.00000073
T_{RS}	2	2_109431246_A	109,431,246	-0.69	0.14	0.00000089
T_{RS}	2	2_109432676_C	109,432,676	-0.69	0.14	0.00000089
T_{RS}	2	2_109433857_G	109,433,857	-0.69	0.14	0.00000089
T_{RS}	2	2_109457251_G	109,457,251	-0.70	0.14	0.00000079
T_{RS}	2	2_109472448_T	109,472,448	-0.70	0.14	0.00000079
T_{RS}	2	2_109486215_A	109,486,215	-0.70	0.14	0.00000085
T_{RS}	2	2_109489747_T	109,489,747	-0.69	0.14	0.00000089
T_{RS}	2	2_109493245_T	109,493,245	-0.70	0.14	0.00000079
T_{RS}	2	2_109494921_T	109,494,921	-0.69	0.14	0.00000089
T_{RS}	2	2_109496806_G	109,496,806	-0.69	0.14	0.00000089
T_{RS}	2	2_109500312_T	109,500,312	-0.69	0.14	0.00000089
T_{RS}	2	2_109506437_G	109,506,437	-0.69	0.14	0.00000089
T_{RS}	2	2_109509472_T	109,509,472	-0.69	0.14	0.00000089
T_{RS}	2	2_109514560_T	109,514,560	-0.69	0.14	0.00000089
T_{RS}	2	2_109515476_T	109,515,476	-0.69	0.14	0.00000089
T_{RS}	2	2_109518190_C	109,518,190	-0.69	0.14	0.00000089
T_{RS}	2	2_109522926_G	109,522,926	-0.69	0.14	0.00000089

T_{RS}	2	2_109529642_C	109,529,642	-0.69	0.14	0.00000089
T_{RS}	2	2_109537303_C	109,537,303	-0.70	0.14	0.00000085
T_{RS}	2	2_109542572_T	109,542,572	-0.70	0.14	0.00000085
T_{RS}	2	2_109581998_C	109,581,998	-0.69	0.14	0.00000089
T_{RS}	2	2_109589218_T	109,589,218	-0.69	0.14	0.00000089
T_{RS}	2	2_109607761_G	109,607,761	-0.69	0.14	0.00000089
T_{RS}	2	2_109618695_G	109,618,695	-0.70	0.14	0.00000073
T_{RS}	2	2_109619382_C	109,619,382	-0.69	0.14	0.00000089
T_{RS}	2	2_109622303_T	109,622,303	-0.69	0.14	0.00000089
T_{RS}	2	2_109623869_T	109,623,869	-0.69	0.14	0.00000089
T_{RS}	2	2_109627942_C	109,627,942	-0.69	0.14	0.00000089
T_{RS}	2	2_109632757_GA	109,632,757	-0.69	0.14	0.00000089
T_{RS}	2	2_109639715_T	109,639,715	-0.69	0.14	0.00000087
T_{RS}	2	2_109641694_T	109,641,694	-0.69	0.14	0.00000089
T_{RS}	2	2_109659487_A	109,659,487	-0.69	0.14	0.00000089
T_{RS}	2	2_109711134_T	109,711,134	-0.69	0.14	0.00000088
T_{RS}	2	2_109719183_A	109,719,183	-0.69	0.14	0.00000088
T_{RS}	2	2_109733255_T	109,733,255	-0.69	0.14	0.00000088
T_{RS}	2	2_109743977_A	109,743,977	-0.69	0.14	0.00000089
T_{RS}	2	2_109751307_T	109,751,307	-0.69	0.14	0.00000088
T_{RS}	2	2_109753661_T	109,753,661	-0.69	0.14	0.00000088
T_{RS}	2	2_109759976_A	109,759,976	-0.69	0.14	0.00000088
T_{RS}	2	2_109761648_C	109,761,648	-0.69	0.14	0.00000088
T_{RS}	2	2_109765000_TAA	109,765,000	-0.69	0.14	0.00000088
T_{RS}	2	2_109848074_T	109,848,074	-0.69	0.14	0.00000090
T_{RS}	2	2_110001016_G	110,001,016	-0.70	0.14	0.00000085
T_{RS}	2	2_110138295_A	110,138,295	-0.69	0.14	0.00000089

T_{RS}	2	2_110143812_A	110,143,812	-0.69	0.14	0.00000087
T_{RS}	2	2_110148918_T	110,148,918	-0.69	0.14	0.00000087
T_{RS}	2	2_110153985_G	110,153,985	-0.70	0.14	0.00000077
T_{RS}	2	2_110159685_A	110,159,685	-0.70	0.14	0.00000072
T_{RS}	2	2_110165746_A	110,165,746	-0.70	0.14	0.00000077
T_{RS}	2	2_110170036_G	110,170,036	-0.70	0.14	0.00000077
T_{RS}	2	2_110173007_G	110,173,007	-0.69	0.14	0.00000087
T_{RS}	2	2_110185078_T	110,185,078	-0.70	0.14	0.00000083
T_{RS}	2	2_110191621_G	110,191,621	-0.69	0.14	0.00000087
T_{RS}	2	2_110203808_T	110,203,808	-0.70	0.14	0.00000083
T_{RS}	2	2_110212515_T	110,212,515	-0.70	0.14	0.00000083
T_{RS}	2	2_110213800_T	110,213,800	-0.69	0.14	0.00000087
T_{RS}	2	2_110216003_T	110,216,003	-0.69	0.14	0.00000087
T_{RS}	2	2_110219837_A	110,219,837	-0.69	0.14	0.00000087
T_{RS}	2	2_110224555_G	110,224,555	-0.69	0.14	0.00000087
T_{RS}	2	2_110228726_G	110,228,726	-0.69	0.14	0.00000087
T_{RS}	2	2_110234070_C	110,234,070	-0.69	0.14	0.00000087
T_{RS}	2	2_110235910_G	110,235,910	-0.69	0.14	0.00000087
T_{RS}	2	2_110238545_T	110,238,545	-0.69	0.14	0.00000087
T_{RS}	2	2_110242971_T	110,242,971	-0.69	0.14	0.00000087
T_{RS}	2	2_110245298_G	110,245,298	-0.69	0.14	0.00000087
T_{RS}	2	2_110246122_TC	110,246,122	-0.70	0.14	0.00000083
T_{RS}	2	2_110247919_A	110,247,919	-0.69	0.14	0.00000087
T_{RS}	2	2_110250945_G	110,250,945	-0.69	0.14	0.00000087
T_{RS}	2	2_110251872_T	110,251,872	-0.69	0.14	0.00000087
T_{RS}	2	2_110256944_C	110,256,944	-0.69	0.14	0.00000087
T_{RS}	2	2_110259121_G	110,259,121	-0.69	0.14	0.00000087

T_{RS}	2	2_110259859_CA	110,259,859	-0.69	0.14	0.00000087
T_{RS}	2	2_110261555_A	110,261,555	-0.69	0.14	0.00000087
T_{RS}	2	2_110261837_G	110,261,837	-0.69	0.14	0.00000087
T_{RS}	2	2_110264069_A	110,264,069	-0.69	0.14	0.00000087
T_{RS}	2	2_110265415_A	110,265,415	-0.69	0.14	0.00000087
T_{RS}	2	2_110265939_A	110,265,939	-0.69	0.14	0.00000087
T_{RS}	2	2_110270658_C	110,270,658	-0.69	0.14	0.00000087
T_{RS}	2	2_110273764_GA	110,273,764	-0.69	0.14	0.00000087
T_{RS}	2	2_110274573_G	110,274,573	-0.69	0.14	0.00000087
T_{RS}	2	2_110275571_A	110,275,571	-0.69	0.14	0.00000087
T_{RS}	2	2_110285906_A	110,285,906	-0.69	0.14	0.00000089
T_{RS}	2	2_110288165_G	110,288,165	-0.69	0.14	0.00000087
T_{RS}	2	2_110297428_A	110,297,428	-0.69	0.14	0.00000093
T_{RS}	2	2_110298779_C	110,298,779	-0.70	0.14	0.00000081
T_{RS}	2	2_110304800_C	110,304,800	-0.70	0.14	0.00000081
T_{RS}	2	2_110306269_T	110,306,269	-0.70	0.14	0.00000081
T_{RS}	2	2_110309071_T	110,309,071	-0.70	0.14	0.00000072
T_{RS}	2	2_110311150_T	110,311,150	-0.70	0.14	0.00000081
T_{RS}	2	2_110314183_T	110,314,183	-0.70	0.14	0.00000081
T_{RS}	2	2_110318959_T	110,318,959	-0.70	0.14	0.00000081
T_{RS}	2	2_110328547_A	110,328,547	-0.70	0.14	0.00000081
T_{RS}	2	2_110330660_A	110,330,660	-0.70	0.14	0.00000081
T_{RS}	2	2_110337123_C	110,337,123	-0.70	0.14	0.00000083
T_{RS}	2	2_110340871_A	110,340,871	-0.70	0.14	0.00000083
T_{RS}	2	2_110342638_C	110,342,638	-0.70	0.14	0.00000082
T_{RS}	2	2_110344660_T	110,344,660	-0.70	0.14	0.00000083
T_{RS}	2	2_110346400_T	110,346,400	-0.70	0.14	0.00000083

T_{RS}	2	2_110347280_G	110,347,280	-0.70	0.14	0.00000083
T_{RS}	2	2_110349373_G	110,349,373	-0.70	0.14	0.00000074
T_{RS}	2	2_110351204_T	110,351,204	-0.70	0.14	0.00000083
T_{RS}	2	2_110353189_T	110,353,189	-0.70	0.14	0.00000083
T_{RS}	2	2_110355730_A	110,355,730	-0.70	0.14	0.00000083
T_{RS}	2	2_110359557_A	110,359,557	-0.70	0.14	0.00000083
T_{RS}	2	2_110366268_T	110,366,268	-0.70	0.14	0.00000084
T_{RS}	2	2_110369910_G	110,369,910	-0.70	0.14	0.00000083
T_{RS}	2	2_110379301_A	110,379,301	-0.70	0.14	0.00000083
T_{RS}	2	2_110405926_C	110,405,926	-0.70	0.14	0.00000085
T_{RS}	2	2_110409856_T	110,409,856	-0.69	0.14	0.00000087
T_{RS}	2	2_110414175_T	110,414,175	-0.69	0.14	0.00000089
T_{RS}	2	2_110418166_A	110,418,166	-0.69	0.14	0.00000090
T_{RS}	2	2_110420052_A	110,420,052	-0.69	0.14	0.00000090
T_{RS}	2	2_110425839_G	110,425,839	-0.69	0.14	0.00000090
T_{RS}	2	2_110426288_C	110,426,288	-0.70	0.14	0.00000075
T_{RS}	2	2_110429015_A	110,429,015	-0.90	0.16	0.00000002
T_{RS}	2	2_110430707_C	110,430,707	-0.69	0.14	0.00000087
T_{RS}	2	2_110439198_G	110,439,198	-0.69	0.14	0.00000080
T_{RS}	2	2_110451805_G	110,451,805	-0.69	0.14	0.00000080
T_{RS}	2	2_110456968_A	110,456,968	-0.69	0.14	0.00000090
T_{RS}	2	2_110464275_C	110,464,275	-0.69	0.14	0.00000080
T_{RS}	2	2_110472495_G	110,472,495	-0.69	0.14	0.00000080
T_{RS}	2	2_110473260_T	110,473,260	-0.69	0.14	0.00000090
T_{RS}	2	2_110474079_A	110,474,079	-0.69	0.14	0.00000087
T_{RS}	2	2_110474688_T	110,474,688	-0.69	0.14	0.00000090
T_{RS}	2	2_110475610_A	110,475,610	-0.70	0.14	0.00000086

T_{RS}	2	2_110483088_G	110,483,088	-0.68	0.14	0.00000120
T_{RS}	2	2_110485848_A	110,485,848	-0.69	0.14	0.00000090
T_{RS}	2	2_110487566_A	110,487,566	-0.69	0.14	0.00000090
T_{RS}	2	2_110497477_A	110,497,477	-0.68	0.14	0.00000111
T_{RS}	2	2_110499801_T	110,499,801	-0.68	0.14	0.00000111
T_{RS}	2	2_110513650_A	110,513,650	-0.69	0.14	0.00000090
T_{RS}	2	2_110528617_G	110,528,617	-0.69	0.14	0.00000090
T_{RS}	2	2_110554169_C	110,554,169	-0.69	0.14	0.00000090
T_{RS}	2	2_110562085_G	110,562,085	-0.69	0.14	0.00000090
T_{RS}	2	2_110603275_T	110,603,275	-0.69	0.14	0.00000090
T_{RS}	2	2_110607093_C	110,607,093	-0.69	0.14	0.00000090
T_{RS}	2	2_110624072_C	110,624,072	-0.69	0.14	0.00000091
T_{RS}	2	2_110630554_A	110,630,554	-0.70	0.14	0.00000085
T_{RS}	2	2_110638910_A	110,638,910	-0.70	0.14	0.00000088
T_{RS}	2	2_110644098_A	110,644,098	-0.69	0.14	0.00000092
T_{RS}	2	2_110659980_G	110,659,980	-0.69	0.14	0.00000090
T_{RS}	2	2_110665397_A	110,665,397	-0.69	0.14	0.00000092
T_{RS}	2	2_110671695_T	110,671,695	-0.70	0.14	0.00000089
T_{RS}	2	2_110674874_A	110,674,874	-0.69	0.14	0.00000087
T_{RS}	2	2_110722516_T	110,722,516	-0.69	0.14	0.00000090
T_{RS}	2	2_110764699_A	110,764,699	-0.69	0.14	0.00000092
T_{RS}	2	2_111224692_G	111,224,692	-0.69	0.14	0.00000090
T_{RS}	2	2_111227658_C	111,227,658	-0.69	0.14	0.00000092
T_{RS}	2	2_111246753_G	111,246,753	-0.70	0.14	0.00000091
T_{RS}	2	2_111261753_G	111,261,753	-0.69	0.14	0.00000092
T_{RS}	2	2_111265312_G	111,265,312	-0.69	0.14	0.00000092
T_{RS}	2	2_111272852_G	111,272,852	-0.69	0.14	0.00000092

T_{RS}	2	2_111279928_C	111,279,928	-0.69	0.14	0.00000092
T_{RS}	2	2_111281195_T	111,281,195	-0.69	0.14	0.00000088
T_{RS}	2	2_111282478_G	111,282,478	-0.71	0.14	0.00000063
T_{RS}	2	2_111283581_C	111,283,581	-0.69	0.14	0.00000092
T_{RS}	2	2_111285827_C	111,285,827	-0.69	0.14	0.00000092
T_{RS}	2	2_111299450_C	111,299,450	-0.69	0.14	0.00000092
T_{RS}	2	2_111304613_C	111,304,613	-0.69	0.14	0.00000087
T_{RS}	2	2_111305215_T	111,305,215	-0.69	0.14	0.00000092
T_{RS}	2	2_111327616_T	111,327,616	-0.69	0.14	0.00000092
T_{RS}	2	2_111333628_A	111,333,628	-0.69	0.14	0.00000092
T_{RS}	2	2_111414402_G	111,414,402	-0.69	0.14	0.00000092
T_{RS}	2	2_111433729_A	111,433,729	-0.70	0.14	0.00000091
T_{RS}	2	2_111453837_C	111,453,837	-0.69	0.14	0.00000092
T_{RS}	2	2_111486280_C	111,486,280	-0.69	0.14	0.00000091
T_{RS}	2	2_111499010_T	111,499,010	-0.69	0.14	0.00000090
T_{RS}	2	2_111526432_T	111,526,432	-0.69	0.14	0.00000091
T_{RS}	2	2_111530117_A	111,530,117	-0.69	0.14	0.00000120
T_{RS}	2	2_111540064_A	111,540,064	-0.69	0.14	0.00000090
T_{RS}	2	2_111553832_T	111,553,832	-0.69	0.14	0.00000092
T_{RS}	2	2_111563782_T	111,563,782	-0.70	0.14	0.00000091
T_{RS}	2	2_111570691_A	111,570,691	-0.69	0.14	0.00000090
T_{RS}	2	2_111575072_C	111,575,072	-0.70	0.14	0.00000089
T_{RS}	2	2_111582096_C	111,582,096	-0.70	0.14	0.00000089
T_{RS}	2	2_111598537_T	111,598,537	-0.69	0.14	0.00000089
T_{RS}	2	2_111614754_A	111,614,754	-0.69	0.14	0.00000091
T_{RS}	2	2_111625296_T	111,625,296	-0.69	0.14	0.00000092
T_{RS}	2	2_111634116_C	111,634,116	-0.69	0.14	0.00000090

T_{RS}	2	2_111640538_AT	111,640,538	-0.69	0.14	0.00000092
T_{RS}	2	2_111653862_AC	111,653,862	-0.69	0.14	0.00000092
T_{RS}	2	2_111659996_C	111,659,996	-0.69	0.14	0.00000092
T_{RS}	2	2_111670922_T	111,670,922	-0.69	0.14	0.00000092
T_{RS}	2	2_111689615_C	111,689,615	-0.69	0.14	0.00000090
T_{RS}	2	2_111879130_A	111,879,130	-0.69	0.14	0.00000092
T_{RS}	2	2_112051005_C	112,051,005	-0.69	0.14	0.00000092
T_{RS}	2	2_112209797_C	112,209,797	-0.69	0.14	0.00000087
T_{RS}	2	2_112393581_A	112,393,581	-0.69	0.14	0.00000092
T_{RS}	2	2_127833178_CA	127,833,178	-0.82	0.16	0.00000020
T_{RS}	6	6_125351232_T	125,351,232	-0.65	0.13	0.00000097
T_{RS}	6	6_125363033_C	125,363,033	-0.65	0.13	0.00000093
T_{RS}	6	6_125423535_AT	125,423,535	-0.65	0.13	0.00000107
T_{RS}	6	6_125624301_A	125,624,301	-0.65	0.13	0.00000108
T_{RS}	6	6_125677183_G	125,677,183	-0.65	0.13	0.00000107
T_{RS}	6	6_125681046_A	125,681,046	-0.65	0.13	0.00000107
T_{RS}	6	6_125685780_T	125,685,780	-0.65	0.13	0.00000107
T_{RS}	6	6_126323755_T	126,323,755	-0.66	0.13	0.00000064
T_{RS}	6	6_126370928_C	126,370,928	-0.66	0.13	0.00000070
T_{RS}	6	6_126378278_C	126,378,278	-0.66	0.13	0.00000069
T_{RS}	6	6_126410208_A	126,410,208	-0.65	0.13	0.00000109
T_{RS}	6	6_126474592_C	126,474,592	-0.69	0.13	0.00000039
T_{RS}	6	6_126476281_G	126,476,281	-0.66	0.13	0.00000057
T_{RS}	6	6_126476632_C	126,476,632	-0.66	0.13	0.00000064
T_{RS}	6	6_126477305_T	126,477,305	-0.69	0.13	0.00000039
T_{RS}	6	6_126477611_T	126,477,611	-0.69	0.13	0.00000039
T_{RS}	6	6_126478166_G	126,478,166	-0.66	0.13	0.00000057

T_{RS}	6	6_126478747_A	126,478,747	-0.66	0.13	0.00000057
T_{RS}	6	6_126481016_A	126,481,016	-0.66	0.13	0.00000057
T_{RS}	6	6_126482451_C	126,482,451	-0.66	0.13	0.00000057
T_{RS}	6	6_126482907_C	126,482,907	-0.66	0.13	0.00000057
T_{RS}	6	6_126485179_C	126,485,179	-0.69	0.13	0.00000039
T_{RS}	6	6_126488352_G	126,488,352	-0.69	0.13	0.00000039
T_{RS}	6	6_126575162_GT	126,575,162	-0.66	0.13	0.00000062
T_{RS}	6	6_126577562_G	126,577,562	-0.66	0.13	0.00000062
T_{RS}	6	6_126578662_A	126,578,662	-0.66	0.13	0.00000062
T_{RS}	6	6_126601500_G	126,601,500	-0.66	0.13	0.00000062
T_{RS}	6	6_126631171_T	126,631,171	-0.66	0.13	0.00000062
T_{RS}	6	6_126632332_G	126,632,332	-0.66	0.13	0.00000062
T_{RS}	6	6_126633199_A	126,633,199	-0.66	0.13	0.00000062
T_{RS}	6	6_126634337_G	126,634,337	-0.66	0.13	0.00000062
T_{RS}	6	6_126662275_AAT	126,662,275	-0.66	0.13	0.00000069
T_{RS}	6	6_126665276_T	126,665,276	-0.68	0.13	0.00000039
T_{RS}	6	6_126665714_T	126,665,714	-0.68	0.13	0.00000039
T_{RS}	6	6_126666580_T	126,666,580	-0.68	0.13	0.00000039
T_{RS}	6	6_126724087_G	126,724,087	-0.66	0.13	0.00000062
T_{RS}	6	6_126725424_G	126,725,424	-0.66	0.13	0.00000062
T_{RS}	6	6_126727270_C	126,727,270	-0.66	0.13	0.00000062
T_{RS}	6	6_126728420_G	126,728,420	-0.67	0.13	0.00000054
T_{RS}	6	6_126728686_C	126,728,686	-0.66	0.13	0.00000061
T_{RS}	6	6_126729827_G	126,729,827	-0.66	0.13	0.00000061
T_{RS}	6	6_126730408_A	126,730,408	-0.66	0.13	0.00000061
T_{RS}	6	6_126731484_C	126,731,484	-0.66	0.13	0.00000067
T_{RS}	6	6_126733670_A	126,733,670	-0.66	0.13	0.00000061

T_{RS}	6	6_126735467_C	126,735,467	-0.66	0.13	0.00000061
T_{RS}	6	6_126736755_TA	126,736,755	-0.66	0.13	0.00000069
T_{RS}	6	6_126737653_C	126,737,653	-0.66	0.13	0.00000061
T_{RS}	6	6_126738247_G	126,738,247	-0.66	0.13	0.00000067
T_{RS}	6	6_126738949_A	126,738,949	-0.66	0.13	0.00000061
T_{RS}	6	6_126747420_T	126,747,420	-0.67	0.13	0.00000060
T_{RS}	6	6_126748183_A	126,748,183	-0.67	0.13	0.00000054
T_{RS}	6	6_126749607_G	126,749,607	-0.66	0.13	0.00000061
T_{RS}	6	6_126750237_G	126,750,237	-0.66	0.13	0.00000061
T_{RS}	6	6_126751419_G	126,751,419	-0.66	0.13	0.00000061
T_{RS}	6	6_126751957_T	126,751,957	-0.66	0.13	0.00000061
T_{RS}	6	6_126752672_T	126,752,672	-0.66	0.13	0.00000061
T_{RS}	6	6_126753030_C	126,753,030	-0.66	0.13	0.00000062
T_{RS}	6	6_126753798_T	126,753,798	-0.66	0.13	0.00000061
T_{RS}	6	6_126754630_ATG	126,754,630	-0.66	0.13	0.00000061
T_{RS}	6	6_126755064_A	126,755,064	-0.66	0.13	0.00000061
T_{RS}	6	6_126757311_T	126,757,311	-0.66	0.13	0.00000061
T_{RS}	6	6_126761793_C	126,761,793	-0.66	0.13	0.00000061
T_{RS}	6	6_126764805_C	126,764,805	-0.66	0.13	0.00000061
T_{RS}	6	6_126768885_T	126,768,885	-0.67	0.13	0.00000048
T_{RS}	6	6_126772138_G	126,772,138	-0.66	0.13	0.00000061
T_{RS}	6	6_126774358_G	126,774,358	-0.66	0.13	0.00000061
T_{RS}	6	6_126776774_T	126,776,774	-0.66	0.13	0.00000061
T_{RS}	6	6_126778794_C	126,778,794	-0.66	0.13	0.00000061
T_{RS}	6	6_126780782_A	126,780,782	-0.66	0.13	0.00000061
T_{RS}	6	6_126782541_G	126,782,541	-0.66	0.13	0.00000062
T_{RS}	6	6_126783493_G	126,783,493	-0.66	0.13	0.00000061

T_{RS}	6	6_126784068_A	126,784,068	-0.66	0.13	0.00000061
T_{RS}	6	6_126786160_C	126,786,160	-0.66	0.13	0.00000061
T_{RS}	6	6_126787243_G	126,787,243	-0.66	0.13	0.00000061
T_{RS}	6	6_126788619_A	126,788,619	-0.68	0.14	0.00000040
T_{RS}	6	6_126789115_A	126,789,115	-0.66	0.13	0.00000061
T_{RS}	6	6_126789921_C	126,789,921	-0.66	0.13	0.00000061
T_{RS}	6	6_126790338_T	126,790,338	-0.66	0.13	0.00000061
T_{RS}	6	6_126791096_T	126,791,096	-0.66	0.13	0.00000061
T_{RS}	6	6_126791424_C	126,791,424	-0.66	0.13	0.00000061
T_{RS}	6	6_126793508_A	126,793,508	-0.67	0.13	0.00000052
T_{RS}	6	6_126794442_C	126,794,442	-0.67	0.13	0.00000052
T_{RS}	6	6_126794827_C	126,794,827	-0.67	0.13	0.00000052
T_{RS}	6	6_126797223_A	126,797,223	-0.67	0.13	0.00000052
T_{RS}	6	6_126797804_G	126,797,804	-0.67	0.13	0.00000052
T_{RS}	6	6_126799210_G	126,799,210	-0.67	0.13	0.00000056
T_{RS}	6	6_126799521_T	126,799,521	-0.67	0.13	0.00000052
T_{RS}	6	6_126800182_T	126,800,182	-0.67	0.13	0.00000052
T_{RS}	6	6_126801179_A	126,801,179	-0.67	0.13	0.00000058
T_{RS}	6	6_126801935_TGAG	126,801,935	-0.67	0.13	0.00000052
T_{RS}	6	6_126802692_A	126,802,692	-0.66	0.13	0.00000061
T_{RS}	6	6_126803237_A	126,803,237	-0.66	0.13	0.00000061
T_{RS}	6	6_126803633_C	126,803,633	-0.66	0.13	0.00000061
T_{RS}	6	6_126804039_T	126,804,039	-0.66	0.13	0.00000061
T_{RS}	6	6_126805230_G	126,805,230	-0.69	0.14	0.00000033
T_{RS}	6	6_126806972_G	126,806,972	-0.66	0.13	0.00000067
T_{RS}	6	6_126807860_C	126,807,860	-0.66	0.13	0.00000061
T_{RS}	6	6_126808053_G	126,808,053	-0.66	0.13	0.00000061

T_{RS}	6	6_126808755_T	126,808,755	-0.66	0.13	0.00000067
T_{RS}	6	6_126938442_G	126,938,442	-0.66	0.13	0.00000092
T_{RS}	6	6_126945076_C	126,945,076	-0.66	0.13	0.00000062
T_{RS}	6	6_127016158_G	127,016,158	-0.66	0.13	0.00000064
T_{RS}	6	6_127019840_G	127,019,840	-0.65	0.13	0.00000096
T_{RS}	6	6_127026604_C	127,026,604	-0.65	0.13	0.00000089
T_{RS}	6	6_127822624_TC	127,822,624	-0.68	0.13	0.00000049
T_{RS}	6	6_128028279_C	128,028,279	-0.67	0.13	0.00000053
T_{RS}	6	6_128038925_T	128,038,925	-0.67	0.13	0.00000053
T_{RS}	6	6_128061017_A	128,061,017	-0.67	0.13	0.00000053
T_{RS}	6	6_128096745_C	128,096,745	-0.70	0.14	0.00000032
T_{RS}	6	6_128100653_G	128,100,653	-0.67	0.13	0.00000053
T_{RS}	6	6_128126009_G	128,126,009	-0.67	0.13	0.00000053
T_{RS}	6	6_128129541_T	128,129,541	-0.67	0.13	0.00000053
T_{RS}	6	6_128142382_T	128,142,382	-0.67	0.13	0.00000053
T_{RS}	6	6_128180187_A	128,180,187	-0.67	0.13	0.00000054
T_{RS}	6	6_128318719_G	128,318,719	-0.68	0.13	0.00000045
T_{RS}	6	6_128319274_T	128,319,274	-0.68	0.13	0.00000045
T_{RS}	6	6_128319571_T	128,319,571	-0.68	0.13	0.00000045
T_{RS}	6	6_128349869_G	128,349,869	-0.68	0.13	0.00000043
T_{RS}	6	6_128355756_A	128,355,756	-0.68	0.13	0.00000043
T_{RS}	6	6_128362537_G	128,362,537	-0.68	0.13	0.00000043
T_{RS}	6	6_128506422_C	128,506,422	-0.69	0.14	0.00000037
T_{RS}	6	6_128540069_C	128,540,069	-0.68	0.13	0.00000043
T_{RS}	6	6_128559926_A	128,559,926	-0.68	0.13	0.00000043
T_{RS}	6	6_128591630_C	128,591,630	-0.72	0.14	0.00000031
T_{RS}	6	6_128592787_C	128,592,787	-0.72	0.14	0.00000031

T_{RS}	6	6_128598015_TTTG	128,598,015	-0.72	0.14	0.00000031
T_{RS}	6	6_128599052_C	128,599,052	-0.72	0.14	0.00000031
T_{RS}	6	6_128601962_TG	128,601,962	-0.72	0.14	0.00000031
T_{RS}	6	6_128607655_CTT	128,607,655	-0.72	0.14	0.00000030
T_{RS}	6	6_128926928_G	128,926,928	-0.65	0.13	0.00000072
T_{RS}	6	6_128933859_C	128,933,859	-0.65	0.13	0.00000072
T_{RS}	6	6_128961716_A	128,961,716	-0.68	0.13	0.00000041
T_{RS}	6	6_128965216_T	128,965,216	-0.66	0.13	0.00000059
T_{RS}	6	6_128975440_T	128,975,440	-0.67	0.13	0.00000054
T_{RS}	6	6_128977429_A	128,977,429	-0.66	0.13	0.00000059
T_{RS}	6	6_128978075_A	128,978,075	-0.67	0.13	0.00000052
T_{RS}	6	6_128978615_T	128,978,615	-0.66	0.13	0.00000059
T_{RS}	6	6_128979492_G	128,979,492	-0.66	0.13	0.00000059
T_{RS}	6	6_128982015_G	128,982,015	-0.65	0.13	0.00000072
T_{RS}	6	6_128993429_AGTGAT	128,993,429	-0.67	0.13	0.00000035
T_{RS}	6	6_128994784_A	128,994,784	-0.66	0.13	0.00000059
T_{RS}	6	6_128998619_T	128,998,619	-0.65	0.13	0.00000072
T_{RS}	6	6_129005315_T	129,005,315	-0.66	0.13	0.00000058
T_{RS}	6	6_129006571_A	129,006,571	-0.67	0.13	0.00000052
T_{RS}	6	6_129007942_C	129,007,942	-0.65	0.13	0.00000072
T_{RS}	6	6_129009756_A	129,009,756	-0.66	0.13	0.00000059
T_{RS}	6	6_129026191_A	129,026,191	-0.66	0.13	0.00000059
T_{RS}	6	6_129027823_G	129,027,823	-0.66	0.13	0.00000059
T_{RS}	6	6_129068935_CT	129,068,935	-0.66	0.13	0.00000067
T_{RS}	6	6_129071477_T	129,071,477	-0.66	0.13	0.00000067
T_{RS}	6	6_129072081_TG	129,072,081	-0.66	0.13	0.00000066
T_{RS}	6	6_129106033_G	129,106,033	-0.67	0.13	0.00000051

T_{RS}	6	6_129108303_A	129,108,303	-0.66	0.13	0.00000067
T_{RS}	6	6_129112736_G	129,112,736	-0.66	0.13	0.00000067
T_{RS}	6	6_129117086_G	129,117,086	-0.66	0.13	0.00000067
T_{RS}	6	6_129131873_C	129,131,873	-0.66	0.13	0.00000059
T_{RS}	6	6_129139371_A	129,139,371	-0.65	0.13	0.00000072
T_{RS}	6	6_129149710_A	129,149,710	-0.65	0.13	0.00000072
T_{RS}	6	6_129150250_C	129,150,250	-0.65	0.13	0.00000072
T_{RS}	6	6_129192451_T	129,192,451	-0.65	0.13	0.00000072
T_{RS}	6	6_129210420_ATATTT	129,210,420	-0.65	0.13	0.00000072
T_{RS}	6	6_129220846_T	129,220,846	-0.66	0.13	0.00000059
T_{RS}	6	6_129225399_T	129,225,399	-0.66	0.13	0.00000059
T_{RS}	6	6_129279850_A	129,279,850	-0.66	0.13	0.00000066
T_{RS}	6	6_129285004_A	129,285,004	-0.66	0.13	0.00000059
T_{RS}	6	6_129287766_G	129,287,766	-0.65	0.13	0.00000064
T_{RS}	6	6_129290483_A	129,290,483	-0.67	0.13	0.00000049
T_{RS}	6	6_129292314_T	129,292,314	-0.65	0.13	0.00000070
T_{RS}	6	6_129298592_GA	129,298,592	-0.65	0.13	0.00000071
T_{RS}	6	6_129301918_C	129,301,918	-0.65	0.13	0.00000071
T_{RS}	6	6_129303560_A	129,303,560	-0.65	0.13	0.00000068
T_{RS}	6	6_129317770_C	129,317,770	-0.65	0.13	0.00000079
T_{RS}	6	6_129318237_C	129,318,237	-0.66	0.13	0.00000059
T_{RS}	6	6_129319267_A	129,319,267	-0.66	0.13	0.00000058
T_{RS}	6	6_129323259_G	129,323,259	-0.65	0.13	0.00000074
T_{RS}	6	6_129326462_TA	129,326,462	-0.66	0.13	0.00000062
T_{RS}	6	6_129331675_A	129,331,675	-0.66	0.13	0.00000059
T_{RS}	6	6_129331927_C	129,331,927	-0.65	0.13	0.00000071
T_{RS}	6	6_129332889_A	129,332,889	-0.65	0.13	0.00000071

T_{RS}	6	6_129334243_C	129,334,243	-0.65	0.13	0.00000070
T_{RS}	6	6_129338493_T	129,338,493	-0.65	0.13	0.00000069
T_{RS}	6	6_129348946_C	129,348,946	-0.65	0.13	0.00000077
T_{RS}	6	6_129357055_A	129,357,055	-0.65	0.13	0.00000064
T_{RS}	6	6_129363499_T	129,363,499	-0.65	0.13	0.00000072
T_{RS}	6	6_135196192_G	135,196,192	-0.75	0.15	0.00000081
T_{RS}	8	8_4906107_T	4,906,107	-0.70	0.13	0.00000024
T_{RS}	8	8_4911786_G	4,911,786	-0.69	0.14	0.00000037
T_{RS}	8	8_4913740_G	4,913,740	-0.62	0.13	0.00000113
T_{RS}	8	8_4914699_T	4,914,699	-0.78	0.14	0.00000006
T_{RS}	8	8_4914910_A	4,914,910	-0.70	0.13	0.00000021
T_{RS}	8	8_4915104_G	4,915,104	-0.88	0.15	0.00000001
T_{RS}	8	8_4916056_G	4,916,056	-0.65	0.13	0.00000088
T_{RS}	8	8_4917068_G	4,917,068	-0.66	0.13	0.00000058
T_{RS}	8	8_4917329_T	4,917,329	-0.67	0.13	0.00000060
T_{RS}	8	8_4917689_C	4,917,689	-0.75	0.14	0.00000015
T_{RS}	8	8_4918153_A	4,918,153	-0.75	0.14	0.00000015
T_{RS}	8	8_4919089_T	4,919,089	-0.66	0.13	0.00000087
T_{RS}	8	8_4919380_A	4,919,380	-0.77	0.14	0.00000008
T_{RS}	8	8_4919503_G	4,919,503	-0.67	0.13	0.00000077
T_{RS}	8	8_4920014_G	4,920,014	-0.65	0.13	0.00000097
T_{RS}	8	8_4920197_T	4,920,197	-0.65	0.13	0.00000118
T_{RS}	8	8_4928499_A	4,928,499	-0.73	0.14	0.00000031
T_{RS}	8	8_4935159_T	4,935,159	-0.66	0.13	0.00000091
T_{RS}	8	8_4960712_G	4,960,712	-0.76	0.15	0.00000016
T_{RS}	8	8_134856930_G	134,856,930	-0.76	0.15	0.00000043
T_{RS}	8	8_134857072_T	134,857,072	-0.93	0.16	0.00000001

T_{RS}	8	8_134857114_G	134,857,114	-0.77	0.15	0.00000040
T_{RS}	8	8_134860931_C	134,860,931	-0.77	0.15	0.00000033
T_{RS}	8	8_134974704_T	134,974,704	-0.67	0.13	0.00000067
T_{RS}	8	8_135028616_C	135,028,616	-0.65	0.13	0.00000100
T_{RS}	8	8_135049023_A	135,049,023	-0.65	0.13	0.00000119
T_{RS}	9	9_39195933_C	39,195,933	-0.78	0.15	0.00000011
T_{RS}	9	9_39424271_A	39,424,271	-0.77	0.15	0.00000012
T_{RS}	9	9_39453846_A	39,453,846	-0.75	0.14	0.00000016
T_{RS}	9	9_39457848_T	39,457,848	-0.76	0.14	0.00000016
T_{RS}	9	9_39461176_T	39,461,176	-0.76	0.14	0.00000016
T_{RS}	9	9_39464877_T	39,464,877	-0.75	0.14	0.00000019
T_{RS}	9	9_39476585_C	39,476,585	-0.73	0.14	0.00000025
T_{RS}	9	9_39486772_G	39,486,772	-0.74	0.14	0.00000024
T_{RS}	10	10_51412141_GAATT	51,412,141	-0.68	0.14	0.00000068
T_{RS}	10	10_51430474_A	51,430,474	-0.66	0.13	0.00000080
T_{RS}	10	10_51438887_T	51,438,887	-0.66	0.14	0.00000101
T_{RS}	10	10_51870599_A	51,870,599	-0.86	0.16	0.00000004
T_{RS}	10	10_51935344_A	51,935,344	-0.87	0.16	0.00000003
T_{RS}	10	10_51936602_CTCT	51,936,602	-0.87	0.16	0.00000003
T_{RS}	10	10_51971041_G	51,971,041	-0.87	0.16	0.00000003
T_{RS}	10	10_51972715_A	51,972,715	-0.87	0.16	0.00000003
T_{RS}	10	10_51974203_C	51,974,203	-0.87	0.16	0.00000003
T_{RS}	10	10_52218082_C	52,218,082	-0.86	0.16	0.00000004
T_{RS}	10	10_52219746_A	52,219,746	-0.86	0.16	0.00000004
T_{RS}	10	10_52220457_A	52,220,457	-0.86	0.16	0.00000004
T_{RS}	10	10_52221786_A	52,221,786	-0.88	0.16	0.00000003
T_{RS}	10	10_52234291_T	52,234,291	-0.88	0.16	0.00000003

T_{RS}	10	10_68726153_TC	68,726,153	-0.90	0.17	0.00000006
T_{RS}	10	10_68752585_G	68,752,585	-0.91	0.16	0.00000002
T_{RS}	10	10_68776792_G	68,776,792	-0.89	0.16	0.00000005
T_{RS}	10	10_68938360_A	68,938,360	-0.91	0.16	0.00000002
T_{RS}	10	10_68961807_A	68,961,807	-0.91	0.16	0.00000002
T_{RS}	10	10_69003765_C	69,003,765	-0.87	0.16	0.00000005
T_{RS}	10	10_69038207_C	69,038,207	-0.91	0.16	0.00000002
T_{RS}	10	10_69069560_C	69,069,560	-0.91	0.16	0.00000002
T_{RS}	10	10_69122246_A	69,122,246	-0.92	0.16	0.00000001
T_{RS}	10	10_69167156_A	69,167,156	-0.92	0.16	0.00000001
T_{RS}	10	10_69231514_G	69,231,514	-0.90	0.16	0.00000002
T_{RS}	10	10_69260687_T	69,260,687	-0.92	0.16	0.00000001
T_{RS}	10	10_69304512_G	69,304,512	-0.92	0.16	0.00000001
T_{RS}	10	10_69352432_T	69,352,432	-0.90	0.16	0.00000002
T_{RS}	11	11_16776240_G	16,776,240	-0.83	0.16	0.00000008
T_{RS}	11	11_16779060_T	16,779,060	-0.83	0.16	0.00000008
T_{RS}	11	11_16787987_T	16,787,987	-0.84	0.16	0.00000008
T_{RS}	11	11_16791246_G	16,791,246	-0.84	0.16	0.00000008
T_{RS}	11	11_16792168_G	16,792,168	-0.84	0.16	0.00000008
T_{RS}	11	11_17051800_G	17,051,800	-0.73	0.15	0.00000061
T_{RS}	12	12_22191109_G	22,191,109	-0.73	0.14	0.00000041
T_{RS}	13	13_17486172_T	17,486,172	-0.77	0.15	0.00000022
T_{RS}	13	13_17492441_G	17,492,441	-0.87	0.16	0.00000006
T_{RS}	13	13_17495603_T	17,495,603	-0.88	0.16	0.00000005
T_{RS}	13	13_17496040_T	17,496,040	-0.88	0.16	0.00000005
T_{RS}	13	13_188570697_G	188,570,697	-0.92	0.16	0.00000001
T_{RS}	13	13_188575484_G	188,575,484	-0.91	0.16	0.00000001

T_{RS}	13	13_188587036_G	188,587,036	-0.91	0.16	0.00000001
T_{RS}	13	13_188609481_C	188,609,481	-0.90	0.16	0.00000001
T_{RS}	13	13_188638189_G	188,638,189	-0.81	0.15	0.00000004
T_{RS}	15	15_104520179_C	104,520,179	-0.71	0.14	0.00000019
T_{RS}	16	16_64692816_G	64,692,816	-0.64	0.13	0.00000059
T_{SS}	1	1_10473872_A	10,473,872	-0.80	0.15	0.00000011
T_{SS}	1	1_10505848_T	10,505,848	-0.77	0.15	0.00000025
T_{SS}	2	2_105870529_AC	105,870,529	-0.79	0.15	0.00000025
T_{SS}	2	2_108874785_C	108,874,785	-0.85	0.16	0.00000006
T_{SS}	2	2_110429015_A	110,429,015	-0.87	0.16	0.00000004
T_{SS}	2	2_127833178_CA	127,833,178	-0.80	0.16	0.00000025
T_{SS}	6	6_125351232_T	125,351,232	-0.66	0.13	0.00000045
T_{SS}	6	6_125363033_C	125,363,033	-0.66	0.13	0.00000046
T_{SS}	6	6_125423535_AT	125,423,535	-0.66	0.13	0.00000055
T_{SS}	6	6_125624301_A	125,624,301	-0.66	0.13	0.00000056
T_{SS}	6	6_125677183_G	125,677,183	-0.66	0.13	0.00000055
T_{SS}	6	6_125681046_A	125,681,046	-0.66	0.13	0.00000055
T_{SS}	6	6_125685780_T	125,685,780	-0.66	0.13	0.00000055
T_{SS}	6	6_125897646_T	125,897,646	-0.64	0.13	0.00000075
T_{SS}	6	6_125898528_CA	125,898,528	-0.64	0.13	0.00000080
T_{SS}	6	6_125900303_C	125,900,303	-0.65	0.13	0.00000060
T_{SS}	6	6_125901642_T	125,901,642	-0.64	0.13	0.00000074
T_{SS}	6	6_125902634_G	125,902,634	-0.64	0.13	0.00000075
T_{SS}	6	6_125903844_A	125,903,844	-0.64	0.13	0.00000075
T_{SS}	6	6_125905114_A	125,905,114	-0.64	0.13	0.00000075
T_{SS}	6	6_125906106_A	125,906,106	-0.64	0.13	0.00000080
T_{SS}	6	6_125906724_CAT	125,906,724	-0.64	0.13	0.00000075

T_{SS}	6	6_125907463_T	125,907,463	-0.64	0.13	0.00000075
T_{SS}	6	6_125907755_G	125,907,755	-0.64	0.13	0.00000075
T_{SS}	6	6_125909608_G	125,909,608	-0.65	0.13	0.00000068
T_{SS}	6	6_125910779_A	125,910,779	-0.64	0.13	0.00000076
T_{SS}	6	6_125911593_T	125,911,593	-0.64	0.13	0.00000076
T_{SS}	6	6_125973610_G	125,973,610	-0.64	0.13	0.00000086
T_{SS}	6	6_125974068_G	125,974,068	-0.64	0.13	0.00000092
T_{SS}	6	6_125974611_A	125,974,611	-0.64	0.13	0.00000086
T_{SS}	6	6_125975911_A	125,975,911	-0.64	0.13	0.00000092
T_{SS}	6	6_125976295_T	125,976,295	-0.64	0.13	0.00000086
T_{SS}	6	6_125977595_A	125,977,595	-0.64	0.13	0.00000093
T_{SS}	6	6_126040757_G	126,040,757	-0.64	0.13	0.00000081
T_{SS}	6	6_126058296_G	126,058,296	-0.64	0.13	0.00000081
T_{SS}	6	6_126080515_A	126,080,515	-0.64	0.13	0.00000082
T_{SS}	6	6_126120130_A	126,120,130	-0.64	0.13	0.00000081
T_{SS}	6	6_126135107_G	126,135,107	-0.64	0.13	0.00000081
T_{SS}	6	6_126261437_G	126,261,437	-0.64	0.13	0.00000093
T_{SS}	6	6_126268918_G	126,268,918	-0.64	0.13	0.00000091
T_{SS}	6	6_126317299_ACT	126,317,299	-0.65	0.13	0.00000067
T_{SS}	6	6_126323755_T	126,323,755	-0.67	0.13	0.00000040
T_{SS}	6	6_126370928_C	126,370,928	-0.67	0.13	0.00000045
T_{SS}	6	6_126378278_C	126,378,278	-0.67	0.13	0.00000045
T_{SS}	6	6_126410208_A	126,410,208	-0.65	0.13	0.00000066
T_{SS}	6	6_126474592_C	126,474,592	-0.69	0.13	0.00000028
T_{SS}	6	6_126476281_G	126,476,281	-0.67	0.13	0.00000040
T_{SS}	6	6_126476632_C	126,476,632	-0.67	0.13	0.00000040
T_{SS}	6	6_126477305_T	126,477,305	-0.69	0.13	0.00000028

T_{SS}	6	6_126477611_T	126,477,611	-0.69	0.13	0.00000028
T_{SS}	6	6_126478166_G	126,478,166	-0.67	0.13	0.00000040
T_{SS}	6	6_126478747_A	126,478,747	-0.67	0.13	0.00000040
T_{SS}	6	6_126481016_A	126,481,016	-0.67	0.13	0.00000040
T_{SS}	6	6_126482451_C	126,482,451	-0.67	0.13	0.00000040
T_{SS}	6	6_126482907_C	126,482,907	-0.67	0.13	0.00000040
T_{SS}	6	6_126485179_C	126,485,179	-0.69	0.13	0.00000028
T_{SS}	6	6_126488352_G	126,488,352	-0.69	0.13	0.00000028
T_{SS}	6	6_126575162_GT	126,575,162	-0.67	0.13	0.00000042
T_{SS}	6	6_126577562_G	126,577,562	-0.67	0.13	0.00000042
T_{SS}	6	6_126578662_A	126,578,662	-0.67	0.13	0.00000042
T_{SS}	6	6_126601500_G	126,601,500	-0.67	0.13	0.00000042
T_{SS}	6	6_126631171_T	126,631,171	-0.67	0.13	0.00000042
T_{SS}	6	6_126632332_G	126,632,332	-0.67	0.13	0.00000042
T_{SS}	6	6_126633199_A	126,633,199	-0.67	0.13	0.00000042
T_{SS}	6	6_126634337_G	126,634,337	-0.67	0.13	0.00000042
T_{SS}	6	6_126662275_AAT	126,662,275	-0.67	0.13	0.00000042
T_{SS}	6	6_126665276_T	126,665,276	-0.68	0.13	0.00000031
T_{SS}	6	6_126665714_T	126,665,714	-0.68	0.13	0.00000031
T_{SS}	6	6_126666580_T	126,666,580	-0.68	0.13	0.00000031
T_{SS}	6	6_126724087_G	126,724,087	-0.67	0.13	0.00000042
T_{SS}	6	6_126725424_G	126,725,424	-0.67	0.13	0.00000042
T_{SS}	6	6_126727270_C	126,727,270	-0.67	0.13	0.00000042
T_{SS}	6	6_126728420_G	126,728,420	-0.68	0.13	0.00000039
T_{SS}	6	6_126728686_C	126,728,686	-0.67	0.13	0.00000041
T_{SS}	6	6_126729827_G	126,729,827	-0.67	0.13	0.00000041
T_{SS}	6	6_126730408_A	126,730,408	-0.67	0.13	0.00000041

T_{SS}	6	6_126731484_C	126,731,484	-0.67	0.13	0.00000042
T_{SS}	6	6_126733670_A	126,733,670	-0.67	0.13	0.00000041
T_{SS}	6	6_126735467_C	126,735,467	-0.67	0.13	0.00000041
T_{SS}	6	6_126736755_TA	126,736,755	-0.67	0.13	0.00000042
T_{SS}	6	6_126737653_C	126,737,653	-0.67	0.13	0.00000041
T_{SS}	6	6_126738247_G	126,738,247	-0.67	0.13	0.00000042
T_{SS}	6	6_126738949_A	126,738,949	-0.67	0.13	0.00000041
T_{SS}	6	6_126747420_T	126,747,420	-0.67	0.13	0.00000040
T_{SS}	6	6_126748183_A	126,748,183	-0.68	0.13	0.00000039
T_{SS}	6	6_126749607_G	126,749,607	-0.67	0.13	0.00000041
T_{SS}	6	6_126750237_G	126,750,237	-0.67	0.13	0.00000041
T_{SS}	6	6_126751419_G	126,751,419	-0.67	0.13	0.00000041
T_{SS}	6	6_126751957_T	126,751,957	-0.67	0.13	0.00000041
T_{SS}	6	6_126752672_T	126,752,672	-0.67	0.13	0.00000041
T_{SS}	6	6_126753030_C	126,753,030	-0.67	0.13	0.00000042
T_{SS}	6	6_126753798_T	126,753,798	-0.67	0.13	0.00000041
T_{SS}	6	6_126754630_ATG	126,754,630	-0.67	0.13	0.00000041
T_{SS}	6	6_126755064_A	126,755,064	-0.67	0.13	0.00000041
T_{SS}	6	6_126757311_T	126,757,311	-0.67	0.13	0.00000041
T_{SS}	6	6_126761793_C	126,761,793	-0.67	0.13	0.00000041
T_{SS}	6	6_126764805_C	126,764,805	-0.67	0.13	0.00000041
T_{SS}	6	6_126768885_T	126,768,885	-0.68	0.13	0.00000032
T_{SS}	6	6_126772138_G	126,772,138	-0.67	0.13	0.00000041
T_{SS}	6	6_126774358_G	126,774,358	-0.67	0.13	0.00000041
T_{SS}	6	6_126776774_T	126,776,774	-0.67	0.13	0.00000041
T_{SS}	6	6_126778794_C	126,778,794	-0.67	0.13	0.00000041
T_{SS}	6	6_126780782_A	126,780,782	-0.67	0.13	0.00000041

T_{SS}	6	6_126782541_G	126,782,541	-0.67	0.13	0.00000042
T_{SS}	6	6_126783493_G	126,783,493	-0.67	0.13	0.00000041
T_{SS}	6	6_126784068_A	126,784,068	-0.67	0.13	0.00000041
T_{SS}	6	6_126786160_C	126,786,160	-0.67	0.13	0.00000041
T_{SS}	6	6_126787243_G	126,787,243	-0.67	0.13	0.00000041
T_{SS}	6	6_126788619_A	126,788,619	-0.69	0.13	0.00000029
T_{SS}	6	6_126789115_A	126,789,115	-0.67	0.13	0.00000041
T_{SS}	6	6_126789921_C	126,789,921	-0.67	0.13	0.00000041
T_{SS}	6	6_126790338_T	126,790,338	-0.67	0.13	0.00000041
T_{SS}	6	6_126791096_T	126,791,096	-0.67	0.13	0.00000041
T_{SS}	6	6_126791424_C	126,791,424	-0.67	0.13	0.00000041
T_{SS}	6	6_126793508_A	126,793,508	-0.68	0.13	0.00000033
T_{SS}	6	6_126794442_C	126,794,442	-0.68	0.13	0.00000033
T_{SS}	6	6_126794827_C	126,794,827	-0.68	0.13	0.00000033
T_{SS}	6	6_126797223_A	126,797,223	-0.68	0.13	0.00000033
T_{SS}	6	6_126797804_G	126,797,804	-0.68	0.13	0.00000033
T_{SS}	6	6_126799210_G	126,799,210	-0.68	0.13	0.00000033
T_{SS}	6	6_126799521_T	126,799,521	-0.68	0.13	0.00000033
T_{SS}	6	6_126800182_T	126,800,182	-0.68	0.13	0.00000033
T_{SS}	6	6_126801179_A	126,801,179	-0.68	0.13	0.00000033
T_{SS}	6	6_126801935_TGAG	126,801,935	-0.68	0.13	0.00000033
T_{SS}	6	6_126802692_A	126,802,692	-0.67	0.13	0.00000041
T_{SS}	6	6_126803237_A	126,803,237	-0.67	0.13	0.00000041
T_{SS}	6	6_126803633_C	126,803,633	-0.67	0.13	0.00000041
T_{SS}	6	6_126804039_T	126,804,039	-0.67	0.13	0.00000041
T_{SS}	6	6_126805230_G	126,805,230	-0.69	0.13	0.00000025
T_{SS}	6	6_126806972_G	126,806,972	-0.67	0.13	0.00000042

T_{SS}	6	6_126807860_C	126,807,860	-0.67	0.13	0.00000041
T_{SS}	6	6_126808053_G	126,808,053	-0.67	0.13	0.00000041
T_{SS}	6	6_126808755_T	126,808,755	-0.67	0.13	0.00000042
T_{SS}	6	6_126938442_G	126,938,442	-0.66	0.13	0.00000060
T_{SS}	6	6_126945076_C	126,945,076	-0.67	0.13	0.00000042
T_{SS}	6	6_127016158_G	127,016,158	-0.67	0.13	0.00000040
T_{SS}	6	6_127019840_G	127,019,840	-0.66	0.13	0.00000056
T_{SS}	6	6_127026604_C	127,026,604	-0.66	0.13	0.00000052
T_{SS}	6	6_127822624_TC	127,822,624	-0.68	0.13	0.00000031
T_{SS}	6	6_128028279_C	128,028,279	-0.68	0.13	0.00000035
T_{SS}	6	6_128038925_T	128,038,925	-0.68	0.13	0.00000035
T_{SS}	6	6_128061017_A	128,061,017	-0.68	0.13	0.00000035
T_{SS}	6	6_128096745_C	128,096,745	-0.70	0.14	0.00000024
T_{SS}	6	6_128100653_G	128,100,653	-0.68	0.13	0.00000035
T_{SS}	6	6_128126009_G	128,126,009	-0.68	0.13	0.00000035
T_{SS}	6	6_128129541_T	128,129,541	-0.68	0.13	0.00000035
T_{SS}	6	6_128142382_T	128,142,382	-0.68	0.13	0.00000035
T_{SS}	6	6_128180187_A	128,180,187	-0.68	0.13	0.00000034
T_{SS}	6	6_128318719_G	128,318,719	-0.68	0.13	0.00000039
T_{SS}	6	6_128319274_T	128,319,274	-0.68	0.13	0.00000039
T_{SS}	6	6_128319571_T	128,319,571	-0.68	0.13	0.00000039
T_{SS}	6	6_128349869_G	128,349,869	-0.68	0.13	0.00000040
T_{SS}	6	6_128355756_A	128,355,756	-0.68	0.13	0.00000040
T_{SS}	6	6_128362537_G	128,362,537	-0.68	0.13	0.00000040
T_{SS}	6	6_128506422_C	128,506,422	-0.68	0.13	0.00000041
T_{SS}	6	6_128540069_C	128,540,069	-0.68	0.13	0.00000040
T_{SS}	6	6_128559926_A	128,559,926	-0.68	0.13	0.00000040

T_{SS}	6	6_128591630_C	128,591,630	-0.72	0.14	0.00000019
T_{SS}	6	6_128592787_C	128,592,787	-0.72	0.14	0.00000019
T_{SS}	6	6_128598015_TTTG	128,598,015	-0.72	0.14	0.00000019
T_{SS}	6	6_128599052_C	128,599,052	-0.72	0.14	0.00000019
T_{SS}	6	6_128601962_TG	128,601,962	-0.72	0.14	0.00000019
T_{SS}	6	6_128607655_CTT	128,607,655	-0.73	0.14	0.00000018
T_{SS}	6	6_128926928_G	128,926,928	-0.66	0.13	0.00000047
T_{SS}	6	6_128933859_C	128,933,859	-0.66	0.13	0.00000047
T_{SS}	6	6_128961716_A	128,961,716	-0.69	0.13	0.00000028
T_{SS}	6	6_128965216_T	128,965,216	-0.66	0.13	0.00000043
T_{SS}	6	6_128975440_T	128,975,440	-0.67	0.13	0.00000042
T_{SS}	6	6_128977429_A	128,977,429	-0.66	0.13	0.00000043
T_{SS}	6	6_128978075_A	128,978,075	-0.67	0.13	0.00000040
T_{SS}	6	6_128978615_T	128,978,615	-0.66	0.13	0.00000043
T_{SS}	6	6_128979492_G	128,979,492	-0.66	0.13	0.00000043
T_{SS}	6	6_128982015_G	128,982,015	-0.66	0.13	0.00000047
T_{SS}	6	6_128993429_AGTGAT	128,993,429	-0.67	0.13	0.00000031
T_{SS}	6	6_128994784_A	128,994,784	-0.66	0.13	0.00000043
T_{SS}	6	6_128998619_T	128,998,619	-0.66	0.13	0.00000047
T_{SS}	6	6_129005315_T	129,005,315	-0.66	0.13	0.00000043
T_{SS}	6	6_129006571_A	129,006,571	-0.67	0.13	0.00000040
T_{SS}	6	6_129007942_C	129,007,942	-0.66	0.13	0.00000047
T_{SS}	6	6_129009756_A	129,009,756	-0.66	0.13	0.00000043
T_{SS}	6	6_129026191_A	129,026,191	-0.66	0.13	0.00000043
T_{SS}	6	6_129027823_G	129,027,823	-0.66	0.13	0.00000043
T_{SS}	6	6_129068935_CT	129,068,935	-0.66	0.13	0.00000047
T_{SS}	6	6_129071477_T	129,071,477	-0.66	0.13	0.00000047

T_{SS}	6	6_129072081_TG	129,072,081	-0.66	0.13	0.00000045
T_{SS}	6	6_129106033_G	129,106,033	-0.67	0.13	0.00000039
T_{SS}	6	6_129108303_A	129,108,303	-0.66	0.13	0.00000047
T_{SS}	6	6_129112736_G	129,112,736	-0.66	0.13	0.00000047
T_{SS}	6	6_129117086_G	129,117,086	-0.66	0.13	0.00000047
T_{SS}	6	6_129131873_C	129,131,873	-0.67	0.13	0.00000036
T_{SS}	6	6_129139371_A	129,139,371	-0.66	0.13	0.00000047
T_{SS}	6	6_129149710_A	129,149,710	-0.66	0.13	0.00000047
T_{SS}	6	6_129150250_C	129,150,250	-0.66	0.13	0.00000047
T_{SS}	6	6_129192451_T	129,192,451	-0.66	0.13	0.00000047
T_{SS}	6	6_129210420_ATATTT	129,210,420	-0.66	0.13	0.00000047
T_{SS}	6	6_129220846_T	129,220,846	-0.67	0.13	0.00000038
T_{SS}	6	6_129225399_T	129,225,399	-0.67	0.13	0.00000038
T_{SS}	6	6_129279850_A	129,279,850	-0.66	0.13	0.00000047
T_{SS}	6	6_129285004_A	129,285,004	-0.67	0.13	0.00000038
T_{SS}	6	6_129287766_G	129,287,766	-0.66	0.13	0.00000050
T_{SS}	6	6_129290483_A	129,290,483	-0.67	0.13	0.00000041
T_{SS}	6	6_129292314_T	129,292,314	-0.66	0.13	0.00000046
T_{SS}	6	6_129298592_GA	129,298,592	-0.66	0.13	0.00000047
T_{SS}	6	6_129301918_C	129,301,918	-0.66	0.13	0.00000047
T_{SS}	6	6_129303560_A	129,303,560	-0.66	0.13	0.00000044
T_{SS}	6	6_129317770_C	129,317,770	-0.66	0.13	0.00000050
T_{SS}	6	6_129318237_C	129,318,237	-0.67	0.13	0.00000038
T_{SS}	6	6_129319267_A	129,319,267	-0.67	0.13	0.00000036
T_{SS}	6	6_129323259_G	129,323,259	-0.66	0.13	0.00000047
T_{SS}	6	6_129326462_TA	129,326,462	-0.67	0.13	0.00000039
T_{SS}	6	6_129331675_A	129,331,675	-0.67	0.13	0.00000038

T_{SS}	6	6_129331927_C	129,331,927	-0.66	0.13	0.00000047
T_{SS}	6	6_129332889_A	129,332,889	-0.66	0.13	0.00000047
T_{SS}	6	6_129334243_C	129,334,243	-0.66	0.13	0.00000046
T_{SS}	6	6_129338493_T	129,338,493	-0.66	0.13	0.00000045
T_{SS}	6	6_129348946_C	129,348,946	-0.66	0.13	0.00000050
T_{SS}	6	6_129357055_A	129,357,055	-0.66	0.13	0.00000043
T_{SS}	6	6_129363499_T	129,363,499	-0.66	0.13	0.00000046
T_{SS}	6	6_135196192_G	135,196,192	-0.80	0.15	0.00000010
T_{SS}	8	8_4906107_T	4,906,107	-0.69	0.13	0.00000024
T_{SS}	8	8_4911786_G	4,911,786	-0.68	0.13	0.00000041
T_{SS}	8	8_4914699_T	4,914,699	-0.77	0.14	0.00000007
T_{SS}	8	8_4914910_A	4,914,910	-0.69	0.13	0.00000021
T_{SS}	8	8_4915104_G	4,915,104	-0.87	0.15	0.00000001
T_{SS}	8	8_4916056_G	4,916,056	-0.64	0.13	0.00000118
T_{SS}	8	8_4917068_G	4,917,068	-0.66	0.13	0.00000062
T_{SS}	8	8_4917329_T	4,917,329	-0.66	0.13	0.00000058
T_{SS}	8	8_4917689_C	4,917,689	-0.74	0.14	0.00000015
T_{SS}	8	8_4918153_A	4,918,153	-0.74	0.14	0.00000015
T_{SS}	8	8_4919380_A	4,919,380	-0.77	0.14	0.00000007
T_{SS}	8	8_4919503_G	4,919,503	-0.65	0.13	0.00000111
T_{SS}	8	8_4928499_A	4,928,499	-0.72	0.14	0.00000035
T_{SS}	8	8_4960712_G	4,960,712	-0.75	0.14	0.00000017
T_{SS}	8	8_134857072_T	134,857,072	-0.89	0.16	0.00000006
T_{SS}	8	8_134860931_C	134,860,931	-0.73	0.15	0.00000118
T_{SS}	9	9_39195933_C	39,195,933	-0.81	0.15	0.00000003
T_{SS}	9	9_39424271_A	39,424,271	-0.80	0.14	0.00000003
T_{SS}	9	9_39453846_A	39,453,846	-0.77	0.14	0.00000007

T_{SS}	9	9_39457848_T	39,457,848	-0.77	0.14	0.00000007
T_{SS}	9	9_39461176_T	39,461,176	-0.77	0.14	0.00000007
T_{SS}	9	9_39464877_T	39,464,877	-0.76	0.14	0.00000009
T_{SS}	9	9_39476585_C	39,476,585	-0.75	0.14	0.00000010
T_{SS}	9	9_39486772_G	39,486,772	-0.75	0.14	0.00000009
T_{SS}	10	10_51403771_C	51,403,771	-0.64	0.13	0.00000104
T_{SS}	10	10_51412141_GAATT	51,412,141	-0.68	0.13	0.00000044
T_{SS}	10	10_51430474_A	51,430,474	-0.66	0.13	0.00000062
T_{SS}	10	10_51438887_T	51,438,887	-0.67	0.13	0.00000070
T_{SS}	10	10_51870599_A	51,870,599	-0.86	0.15	0.00000002
T_{SS}	10	10_51935344_A	51,935,344	-0.87	0.16	0.00000002
T_{SS}	10	10_51936602_CTCT	51,936,602	-0.87	0.16	0.00000002
T_{SS}	10	10_51971041_G	51,971,041	-0.87	0.16	0.00000002
T_{SS}	10	10_51972715_A	51,972,715	-0.87	0.16	0.00000002
T_{SS}	10	10_51974203_C	51,974,203	-0.87	0.16	0.00000002
T_{SS}	10	10_52218082_C	52,218,082	-0.86	0.15	0.00000003
T_{SS}	10	10_52219746_A	52,219,746	-0.86	0.15	0.00000003
T_{SS}	10	10_52220457_A	52,220,457	-0.86	0.15	0.00000003
T_{SS}	10	10_52221786_A	52,221,786	-0.87	0.16	0.00000002
T_{SS}	10	10_52234291_T	52,234,291	-0.88	0.16	0.00000002
T_{SS}	10	10_68726153_TC	68,726,153	-0.91	0.16	0.00000003
T_{SS}	10	10_68752585_G	68,752,585	-0.88	0.16	0.00000004
T_{SS}	10	10_68776792_G	68,776,792	-0.89	0.16	0.00000004
T_{SS}	10	10_68938360_A	68,938,360	-0.88	0.16	0.00000004
T_{SS}	10	10_68961807_A	68,961,807	-0.88	0.16	0.00000004
T_{SS}	10	10_69003765_C	69,003,765	-0.85	0.16	0.00000009
T_{SS}	10	10_69038207_C	69,038,207	-0.88	0.16	0.00000004

T_{SS}	10	10_69069560_C	69,069,560	-0.88	0.16	0.00000004
T_{SS}	10	10_69122246_A	69,122,246	-0.89	0.16	0.00000004
T_{SS}	10	10_69167156_A	69,167,156	-0.89	0.16	0.00000004
T_{SS}	10	10_69231514_G	69,231,514	-0.87	0.16	0.00000005
T_{SS}	10	10_69260687_T	69,260,687	-0.89	0.16	0.00000004
T_{SS}	10	10_69304512_G	69,304,512	-0.89	0.16	0.00000004
T_{SS}	10	10_69352432_T	69,352,432	-0.87	0.16	0.00000006
T_{SS}	11	11_16776240_G	16,776,240	-0.83	0.15	0.00000007
T_{SS}	11	11_16779060_T	16,779,060	-0.83	0.15	0.00000007
T_{SS}	11	11_16787987_T	16,787,987	-0.83	0.15	0.00000007
T_{SS}	11	11_16791246_G	16,791,246	-0.83	0.15	0.00000007
T_{SS}	11	11_16792168_G	16,792,168	-0.83	0.15	0.00000007
T_{SS}	11	11_17051800_G	17,051,800	-0.73	0.14	0.00000046
T_{SS}	12	12_22191109_G	22,191,109	-0.75	0.14	0.00000020
T_{SS}	13	13_17486172_T	17,486,172	-0.78	0.15	0.00000015
T_{SS}	13	13_17492441_G	17,492,441	-0.89	0.16	0.00000002
T_{SS}	13	13_17495603_T	17,495,603	-0.90	0.16	0.00000002
T_{SS}	13	13_17496040_T	17,496,040	-0.90	0.16	0.00000002
T_{SS}	13	13_17767850_T	17,767,850	-0.73	0.14	0.00000044
T_{SS}	13	13_188570697_G	188,570,697	-0.91	0.16	0.00000001
T_{SS}	13	13_188575484_G	188,575,484	-0.90	0.16	0.00000001
T_{SS}	13	13_188587036_G	188,587,036	-0.90	0.16	0.00000001
T_{SS}	13	13_188609481_C	188,609,481	-0.89	0.16	0.00000001
T_{SS}	13	13_188638189_G	188,638,189	-0.79	0.15	0.00000007
T_{SS}	13	13_204671997_G	204,671,997	-0.66	0.13	0.00000034
T_{SS}	15	15_104520179_C	104,520,179	-0.71	0.14	0.00000015
T_{TS}	4	4_72028076_A	72,028,076	-0.71	0.15	0.00000113

T_{TS}	4	4_72045767_G	72,045,767	-0.75	0.15	0.00000044
T_{TS}	6	6_125351232_T	125,351,232	-0.88	0.18	0.00000091
T_{TS}	6	6_125363033_C	125,363,033	-0.88	0.18	0.00000088
T_{TS}	6	6_125423535_AT	125,423,535	-0.88	0.18	0.00000093
T_{TS}	6	6_125624301_A	125,624,301	-0.88	0.18	0.00000094
T_{TS}	6	6_125677183_G	125,677,183	-0.88	0.18	0.00000093
T_{TS}	6	6_125681046_A	125,681,046	-0.88	0.18	0.00000093
T_{TS}	6	6_125685780_T	125,685,780	-0.88	0.18	0.00000093
T_{TS}	6	6_125900303_C	125,900,303	-0.87	0.18	0.00000103
T_{TS}	6	6_125909608_G	125,909,608	-0.87	0.18	0.00000107
T_{TS}	6	6_126317299_ACT	126,317,299	-0.87	0.18	0.00000103
T_{TS}	6	6_126323755_T	126,323,755	-0.89	0.18	0.00000074
T_{TS}	6	6_126370928_C	126,370,928	-0.88	0.18	0.00000081
T_{TS}	6	6_126378278_C	126,378,278	-0.88	0.18	0.00000081
T_{TS}	6	6_126410208_A	126,410,208	-0.87	0.18	0.00000107
T_{TS}	6	6_126474592_C	126,474,592	-0.92	0.18	0.00000043
T_{TS}	6	6_126476281_G	126,476,281	-0.89	0.18	0.00000074
T_{TS}	6	6_126476632_C	126,476,632	-0.89	0.18	0.00000074
T_{TS}	6	6_126477305_T	126,477,305	-0.92	0.18	0.00000043
T_{TS}	6	6_126477611_T	126,477,611	-0.92	0.18	0.00000043
T_{TS}	6	6_126478166_G	126,478,166	-0.89	0.18	0.00000074
T_{TS}	6	6_126478747_A	126,478,747	-0.89	0.18	0.00000074
T_{TS}	6	6_126481016_A	126,481,016	-0.89	0.18	0.00000074
T_{TS}	6	6_126482451_C	126,482,451	-0.89	0.18	0.00000074
T_{TS}	6	6_126482907_C	126,482,907	-0.89	0.18	0.00000073
T_{TS}	6	6_126485179_C	126,485,179	-0.92	0.18	0.00000043
T_{TS}	6	6_126488352_G	126,488,352	-0.92	0.18	0.00000043

T_{TS}	6	6_126575162_GT	126,575,162	-0.89	0.18	0.00000076
T_{TS}	6	6_126577562_G	126,577,562	-0.89	0.18	0.00000076
T_{TS}	6	6_126578662_A	126,578,662	-0.89	0.18	0.00000076
T_{TS}	6	6_126601500_G	126,601,500	-0.89	0.18	0.00000076
T_{TS}	6	6_126631171_T	126,631,171	-0.89	0.18	0.00000076
T_{TS}	6	6_126632332_G	126,632,332	-0.89	0.18	0.00000076
T_{TS}	6	6_126633199_A	126,633,199	-0.89	0.18	0.00000076
T_{TS}	6	6_126634337_G	126,634,337	-0.89	0.18	0.00000076
T_{TS}	6	6_126662275_AAT	126,662,275	-0.89	0.18	0.00000076
T_{TS}	6	6_126665276_T	126,665,276	-0.90	0.18	0.00000057
T_{TS}	6	6_126665714_T	126,665,714	-0.90	0.18	0.00000057
T_{TS}	6	6_126666580_T	126,666,580	-0.90	0.18	0.00000058
T_{TS}	6	6_126724087_G	126,724,087	-0.89	0.18	0.00000076
T_{TS}	6	6_126725424_G	126,725,424	-0.89	0.18	0.00000076
T_{TS}	6	6_126727270_C	126,727,270	-0.89	0.18	0.00000076
T_{TS}	6	6_126728420_G	126,728,420	-0.90	0.18	0.00000063
T_{TS}	6	6_126728686_C	126,728,686	-0.89	0.18	0.00000075
T_{TS}	6	6_126729827_G	126,729,827	-0.89	0.18	0.00000075
T_{TS}	6	6_126730408_A	126,730,408	-0.89	0.18	0.00000075
T_{TS}	6	6_126731484_C	126,731,484	-0.89	0.18	0.00000076
T_{TS}	6	6_126733670_A	126,733,670	-0.89	0.18	0.00000075
T_{TS}	6	6_126735467_C	126,735,467	-0.89	0.18	0.00000075
T_{TS}	6	6_126736755_TA	126,736,755	-0.89	0.18	0.00000076
T_{TS}	6	6_126737653_C	126,737,653	-0.89	0.18	0.00000075
T_{TS}	6	6_126738247_G	126,738,247	-0.89	0.18	0.00000076
T_{TS}	6	6_126738949_A	126,738,949	-0.89	0.18	0.00000075
T_{TS}	6	6_126747420_T	126,747,420	-0.89	0.18	0.00000080

T_{TS}	6	6_126748183_A	126,748,183	-0.90	0.18	0.00000063
T_{TS}	6	6_126749607_G	126,749,607	-0.89	0.18	0.00000075
T_{TS}	6	6_126750237_G	126,750,237	-0.89	0.18	0.00000075
T_{TS}	6	6_126751419_G	126,751,419	-0.89	0.18	0.00000075
T_{TS}	6	6_126751957_T	126,751,957	-0.89	0.18	0.00000075
T_{TS}	6	6_126752672_T	126,752,672	-0.89	0.18	0.00000075
T_{TS}	6	6_126753030_C	126,753,030	-0.89	0.18	0.00000076
T_{TS}	6	6_126753798_T	126,753,798	-0.89	0.18	0.00000075
T_{TS}	6	6_126754630_ATG	126,754,630	-0.89	0.18	0.00000075
T_{TS}	6	6_126755064_A	126,755,064	-0.89	0.18	0.00000075
T_{TS}	6	6_126757311_T	126,757,311	-0.89	0.18	0.00000075
T_{TS}	6	6_126761793_C	126,761,793	-0.89	0.18	0.00000075
T_{TS}	6	6_126764805_C	126,764,805	-0.89	0.18	0.00000075
T_{TS}	6	6_126768885_T	126,768,885	-0.90	0.18	0.00000055
T_{TS}	6	6_126772138_G	126,772,138	-0.89	0.18	0.00000075
T_{TS}	6	6_126774358_G	126,774,358	-0.89	0.18	0.00000075
T_{TS}	6	6_126776774_T	126,776,774	-0.89	0.18	0.00000075
T_{TS}	6	6_126778794_C	126,778,794	-0.89	0.18	0.00000075
T_{TS}	6	6_126780782_A	126,780,782	-0.89	0.18	0.00000075
T_{TS}	6	6_126782541_G	126,782,541	-0.89	0.18	0.00000076
T_{TS}	6	6_126783493_G	126,783,493	-0.89	0.18	0.00000075
T_{TS}	6	6_126784068_A	126,784,068	-0.89	0.18	0.00000075
T_{TS}	6	6_126786160_C	126,786,160	-0.89	0.18	0.00000075
T_{TS}	6	6_126787243_G	126,787,243	-0.89	0.18	0.00000075
T_{TS}	6	6_126788619_A	126,788,619	-0.92	0.18	0.00000045
T_{TS}	6	6_126789115_A	126,789,115	-0.89	0.18	0.00000075
T_{TS}	6	6_126789921_C	126,789,921	-0.89	0.18	0.00000075

T_{TS}	6	6_126790338_T	126,790,338	-0.89	0.18	0.00000075
T_{TS}	6	6_126791096_T	126,791,096	-0.89	0.18	0.00000075
T_{TS}	6	6_126791424_C	126,791,424	-0.89	0.18	0.00000075
T_{TS}	6	6_126793508_A	126,793,508	-0.90	0.18	0.00000060
T_{TS}	6	6_126794442_C	126,794,442	-0.90	0.18	0.00000060
T_{TS}	6	6_126794827_C	126,794,827	-0.90	0.18	0.00000060
T_{TS}	6	6_126797223_A	126,797,223	-0.90	0.18	0.00000060
T_{TS}	6	6_126797804_G	126,797,804	-0.90	0.18	0.00000060
T_{TS}	6	6_126799210_G	126,799,210	-0.90	0.18	0.00000062
T_{TS}	6	6_126799521_T	126,799,521	-0.90	0.18	0.00000060
T_{TS}	6	6_126800182_T	126,800,182	-0.90	0.18	0.00000060
T_{TS}	6	6_126801179_A	126,801,179	-0.90	0.18	0.00000060
T_{TS}	6	6_126801935_TGAG	126,801,935	-0.90	0.18	0.00000060
T_{TS}	6	6_126802692_A	126,802,692	-0.89	0.18	0.00000075
T_{TS}	6	6_126803237_A	126,803,237	-0.89	0.18	0.00000075
T_{TS}	6	6_126803633_C	126,803,633	-0.89	0.18	0.00000075
T_{TS}	6	6_126804039_T	126,804,039	-0.89	0.18	0.00000075
T_{TS}	6	6_126805230_G	126,805,230	-0.91	0.18	0.00000052
T_{TS}	6	6_126806972_G	126,806,972	-0.89	0.18	0.00000076
T_{TS}	6	6_126807860_C	126,807,860	-0.89	0.18	0.00000075
T_{TS}	6	6_126808053_G	126,808,053	-0.89	0.18	0.00000075
T_{TS}	6	6_126808755_T	126,808,755	-0.89	0.18	0.00000076
T_{TS}	6	6_126938442_G	126,938,442	-0.88	0.18	0.00000099
T_{TS}	6	6_126945076_C	126,945,076	-0.89	0.18	0.00000076
T_{TS}	6	6_127016158_G	127,016,158	-0.89	0.18	0.00000074
T_{TS}	6	6_127019840_G	127,019,840	-0.88	0.18	0.00000097
T_{TS}	6	6_127026604_C	127,026,604	-0.88	0.18	0.00000092

T_{TS}	6	6_127822624_TC	127,822,624	-0.91	0.18	0.00000046
T_{TS}	6	6_128028279_C	128,028,279	-0.91	0.18	0.00000053
T_{TS}	6	6_128038925_T	128,038,925	-0.91	0.18	0.00000053
T_{TS}	6	6_128061017_A	128,061,017	-0.91	0.18	0.00000053
T_{TS}	6	6_128096745_C	128,096,745	-0.94	0.18	0.00000035
T_{TS}	6	6_128100653_G	128,100,653	-0.91	0.18	0.00000053
T_{TS}	6	6_128126009_G	128,126,009	-0.91	0.18	0.00000053
T_{TS}	6	6_128129541_T	128,129,541	-0.91	0.18	0.00000053
T_{TS}	6	6_128142382_T	128,142,382	-0.91	0.18	0.00000053
T_{TS}	6	6_128180187_A	128,180,187	-0.91	0.18	0.00000053
T_{TS}	6	6_128318719_G	128,318,719	-0.90	0.18	0.00000062
T_{TS}	6	6_128319274_T	128,319,274	-0.90	0.18	0.00000062
T_{TS}	6	6_128319571_T	128,319,571	-0.90	0.18	0.00000062
T_{TS}	6	6_128349869_G	128,349,869	-0.91	0.18	0.00000060
T_{TS}	6	6_128355756_A	128,355,756	-0.91	0.18	0.00000060
T_{TS}	6	6_128362537_G	128,362,537	-0.91	0.18	0.00000060
T_{TS}	6	6_128506422_C	128,506,422	-0.91	0.18	0.00000065
T_{TS}	6	6_128540069_C	128,540,069	-0.91	0.18	0.00000060
T_{TS}	6	6_128559926_A	128,559,926	-0.91	0.18	0.00000060
T_{TS}	6	6_128591630_C	128,591,630	-0.98	0.19	0.00000023
T_{TS}	6	6_128592787_C	128,592,787	-0.98	0.19	0.00000023
T_{TS}	6	6_128598015_TTTG	128,598,015	-0.98	0.19	0.00000023
T_{TS}	6	6_128599052_C	128,599,052	-0.98	0.19	0.00000023
T_{TS}	6	6_128601962_TG	128,601,962	-0.98	0.19	0.00000023
T_{TS}	6	6_128607655_CTT	128,607,655	-0.98	0.19	0.00000022
T_{TS}	6	6_128926928_G	128,926,928	-0.86	0.18	0.00000110
T_{TS}	6	6_128933859_C	128,933,859	-0.86	0.18	0.00000110

T_{TS}	6	6_128961716_A	128,961,716	-0.90	0.18	0.00000065
T_{TS}	6	6_128965216_T	128,965,216	-0.87	0.18	0.00000099
T_{TS}	6	6_128975440_T	128,975,440	-0.88	0.18	0.00000089
T_{TS}	6	6_128977429_A	128,977,429	-0.87	0.18	0.00000099
T_{TS}	6	6_128978075_A	128,978,075	-0.88	0.18	0.00000083
T_{TS}	6	6_128978615_T	128,978,615	-0.87	0.18	0.00000099
T_{TS}	6	6_128979492_G	128,979,492	-0.87	0.18	0.00000100
T_{TS}	6	6_128982015_G	128,982,015	-0.86	0.18	0.00000110
T_{TS}	6	6_128993429_AGTGAT	128,993,429	-0.88	0.18	0.00000074
T_{TS}	6	6_128994784_A	128,994,784	-0.87	0.18	0.00000099
T_{TS}	6	6_128998619_T	128,998,619	-0.86	0.18	0.00000110
T_{TS}	6	6_129005315_T	129,005,315	-0.87	0.18	0.00000098
T_{TS}	6	6_129006571_A	129,006,571	-0.88	0.18	0.00000084
T_{TS}	6	6_129007942_C	129,007,942	-0.86	0.18	0.00000110
T_{TS}	6	6_129009756_A	129,009,756	-0.87	0.18	0.00000103
T_{TS}	6	6_129026191_A	129,026,191	-0.87	0.18	0.00000099
T_{TS}	6	6_129027823_G	129,027,823	-0.87	0.18	0.00000099
T_{TS}	6	6_129068935_CT	129,068,935	-0.87	0.18	0.00000115
T_{TS}	6	6_129071477_T	129,071,477	-0.87	0.18	0.00000115
T_{TS}	6	6_129072081_TG	129,072,081	-0.86	0.18	0.00000118
T_{TS}	6	6_129106033_G	129,106,033	-0.88	0.18	0.00000086
T_{TS}	6	6_129108303_A	129,108,303	-0.87	0.18	0.00000115
T_{TS}	6	6_129112736_G	129,112,736	-0.87	0.18	0.00000115
T_{TS}	6	6_129117086_G	129,117,086	-0.87	0.18	0.00000115
T_{TS}	6	6_129131873_C	129,131,873	-0.88	0.18	0.00000084
T_{TS}	6	6_129139371_A	129,139,371	-0.86	0.18	0.00000110
T_{TS}	6	6_129149710_A	129,149,710	-0.86	0.18	0.00000110

T_{TS}	6	6_129150250_C	129,150,250	-0.86	0.18	0.00000110
T_{TS}	6	6_129192451_T	129,192,451	-0.86	0.18	0.00000110
T_{TS}	6	6_129210420_ATATTT	129,210,420	-0.86	0.18	0.00000110
T_{TS}	6	6_129220846_T	129,220,846	-0.88	0.18	0.00000085
T_{TS}	6	6_129225399_T	129,225,399	-0.88	0.18	0.00000085
T_{TS}	6	6_129279850_A	129,279,850	-0.87	0.18	0.00000115
T_{TS}	6	6_129285004_A	129,285,004	-0.88	0.18	0.00000085
T_{TS}	6	6_129287766_G	129,287,766	-0.86	0.18	0.00000118
T_{TS}	6	6_129290483_A	129,290,483	-0.88	0.18	0.00000088
T_{TS}	6	6_129292314_T	129,292,314	-0.86	0.18	0.00000108
T_{TS}	6	6_129298592_GA	129,298,592	-0.86	0.18	0.00000109
T_{TS}	6	6_129301918_C	129,301,918	-0.86	0.18	0.00000109
T_{TS}	6	6_129303560_A	129,303,560	-0.87	0.18	0.00000104
T_{TS}	6	6_129317770_C	129,317,770	-0.87	0.18	0.00000110
T_{TS}	6	6_129318237_C	129,318,237	-0.88	0.18	0.00000084
T_{TS}	6	6_129319267_A	129,319,267	-0.88	0.18	0.00000084
T_{TS}	6	6_129323259_G	129,323,259	-0.86	0.18	0.00000112
T_{TS}	6	6_129326462_TA	129,326,462	-0.87	0.18	0.00000119
T_{TS}	6	6_129331675_A	129,331,675	-0.88	0.18	0.00000085
T_{TS}	6	6_129331927_C	129,331,927	-0.86	0.18	0.00000110
T_{TS}	6	6_129332889_A	129,332,889	-0.86	0.18	0.00000110
T_{TS}	6	6_129334243_C	129,334,243	-0.86	0.18	0.00000117
T_{TS}	6	6_129338493_T	129,338,493	-0.86	0.18	0.00000113
T_{TS}	6	6_129348946_C	129,348,946	-0.87	0.18	0.00000106
T_{TS}	6	6_129357055_A	129,357,055	-0.87	0.18	0.00000102
T_{TS}	6	6_129363499_T	129,363,499	-0.86	0.18	0.00000111
T_{TS}	15	15_25570481_T	25,570,481	-0.92	0.18	0.00000022

T_{TS}	15	15_25570891_C	25,570,891	-1.01	0.19	0.00000005
RR	7	7_23843264_G	23,843,264	-2.30	0.46	0.00000070
RR	7	7_23886397_G	23,886,397	-2.23	0.46	0.00000114
RR	7	7_23892506_C	23,892,506	-2.24	0.46	0.00000115
RR	7	7_23905782_G	23,905,782	-2.24	0.46	0.00000089
RR	7	7_23913884_T	23,913,884	-2.24	0.46	0.00000102
RR	7	7_23919566_T	23,919,566	-2.23	0.46	0.00000112
RR	7	7_23936480_C	23,936,480	-2.43	0.47	0.00000019
RR	7	7_23945958_G	23,945,958	-2.48	0.47	0.00000011
RR	7	7_24051539_C	24,051,539	-2.35	0.46	0.00000024
RR	7	7_39351307_C	39,351,307	-2.60	0.52	0.00000059
RR	7	7_39355266_C	39,355,266	-2.56	0.52	0.00000095
RR	8	8_79518715_T	79,518,715	2.85	0.58	0.00000106
RR	8	8_79522877_A	79,522,877	2.88	0.58	0.00000082
RR	8	8_79530183_A	79,530,183	2.88	0.58	0.00000082
RR	8	8_79532515_A	79,532,515	2.88	0.58	0.00000082
RR	8	8_79534072_T	79,534,072	2.88	0.58	0.00000082
RR	8	8_79535545_T	79,535,545	2.87	0.58	0.00000086
RR	8	8_79538654_C	79,538,654	2.85	0.58	0.00000095
RR	8	8_79539013_A	79,539,013	2.83	0.58	0.00000112
RR	8	8_79540101_T	79,540,101	2.87	0.58	0.00000082
RR	8	8_79545451_A	79,545,451	2.88	0.58	0.00000082
RR	8	8_79549027_G	79,549,027	2.88	0.58	0.00000082
RR	8	8_79554168_A	79,554,168	2.88	0.58	0.00000082
RR	8	8_79558744_A	79,558,744	2.95	0.59	0.00000051
RR	8	8_79561407_A	79,561,407	2.88	0.58	0.00000082
RR	8	8_79630035_A	79,630,035	2.83	0.58	0.00000112

RR	8	8_79635229_A	79,635,229	2.83	0.58	0.00000112
RR	8	8_79658971_G	79,658,971	2.82	0.58	0.00000118
RR	8	8_79664431_C	79,664,431	2.84	0.58	0.00000117
RR	8	8_79669879_C	79,669,879	2.85	0.58	0.00000092
RR	8	8_79674675_T	79,674,675	2.86	0.58	0.00000081
RR	8	8_79678124_A	79,678,124	2.83	0.58	0.00000102
RR	8	8_79680311_T	79,680,311	2.84	0.58	0.00000083
RR	8	8_79684982_T	79,684,982	2.81	0.58	0.00000103
RR	8	8_79688500_C	79,688,500	2.84	0.57	0.00000075
RR	8	8_79690595_A	79,690,595	2.83	0.57	0.00000086
RR	8	8_79693509_AT	79,693,509	2.84	0.58	0.00000080
RR	8	8_79909652_G	79,909,652	2.93	0.58	0.00000040
RR	8	8_80358650_G	80,358,650	2.70	0.56	0.00000120
RR	8	8_80401982_A	80,401,982	3.17	0.65	0.00000096
RR	8	8_80430101_A	80,430,101	3.28	0.65	0.00000039
RR	8	8_80437485_G	80,437,485	3.19	0.64	0.00000057
RR	8	8_80448311_A	80,448,311	3.16	0.64	0.00000068
RR	8	8_80461727_C	80,461,727	3.92	0.78	0.00000055
RR	8	8_80462738_G	80,462,738	3.84	0.77	0.00000067
RR	8	8_80469777_G	80,469,777	3.19	0.64	0.00000056
RR	8	8_80470676_G	80,470,676	3.98	0.79	0.00000042
RR	8	8_80471691_A	80,471,691	3.16	0.64	0.00000068
RR	8	8_80473435_T	80,473,435	3.15	0.64	0.00000074
RR	8	8_80475642_G	80,475,642	3.29	0.64	0.00000029
RR	8	8_80477234_T	80,477,234	3.19	0.64	0.00000056
RR	8	8_80477908_G	80,477,908	3.19	0.64	0.00000056
RR	8	8_80478830_T	80,478,830	3.18	0.64	0.00000060

RR	8	8_80481645_AT	80,481,645	3.83	0.77	0.00000062
RR	8	8_80492107_A	80,492,107	3.29	0.68	0.00000112
RR	8	8_80509831_G	80,509,831	3.92	0.80	0.00000094
RR	8	8_80673033_A	80,673,033	3.32	0.68	0.00000113
RR	8	8_80674817_T	80,674,817	3.49	0.69	0.00000035
RR	8	8_80677037_A	80,677,037	3.37	0.68	0.00000070
RR	8	8_80678894_C	80,678,894	3.37	0.68	0.00000070
RR	8	8_80679218_A	80,679,218	3.39	0.68	0.00000064
RR	8	8_80680241_T	80,680,241	3.39	0.68	0.00000064
RR	8	8_80680582_G	80,680,582	3.39	0.68	0.00000064
RR	8	8_80681227_A	80,681,227	3.39	0.68	0.00000061
RR	8	8_80682336_G	80,682,336	3.39	0.68	0.00000064
RR	8	8_80683197_A	80,683,197	3.43	0.68	0.00000045
RR	8	8_80683844_T	80,683,844	3.39	0.68	0.00000064
RR	8	8_80684841_C	80,684,841	3.42	0.68	0.00000048
RR	8	8_80688592_G	80,688,592	3.40	0.68	0.00000062
RR	8	8_80689590_G	80,689,590	3.35	0.68	0.00000082
RR	8	8_80689919_CACT	80,689,919	3.37	0.68	0.00000068
RR	8	8_80693076_A	80,693,076	3.34	0.68	0.00000094
RR	8	8_80696944_T	80,696,944	3.48	0.68	0.00000030
RR	8	8_80699562_T	80,699,562	3.41	0.68	0.00000056
RR	8	8_80727453_A	80,727,453	3.28	0.66	0.00000077
RR	8	8_80734740_C	80,734,740	3.29	0.67	0.00000083
RR	8	8_80806197_T	80,806,197	4.16	0.85	0.00000090
RR	8	8_80807661_G	80,807,661	4.14	0.85	0.00000102
RR	8	8_80808919_T	80,808,919	3.47	0.71	0.00000121
RR	8	8_80809566_A	80,809,566	4.25	0.85	0.00000055

RR	8	8_80809640_G	80,809,640	3.47	0.71	0.00000121
RR	8	8_80809838_CT	80,809,838	4.25	0.85	0.00000055
RR	8	8_80810376_T	80,810,376	3.47	0.71	0.00000121
RR	8	8_80811062_C	80,811,062	4.28	0.86	0.00000057
RR	8	8_80819917_G	80,819,917	3.47	0.71	0.00000121
RR	8	8_80841211_GT	80,841,211	4.24	0.87	0.00000107
RR	8	8_80843941_T	80,843,941	4.27	0.87	0.00000090
RR	8	8_80874951_G	80,874,951	4.59	0.89	0.00000027
RR	8	8_80878477_G	80,878,477	4.32	0.88	0.00000091
RR	8	8_80879644_G	80,879,644	4.42	0.88	0.00000043
RR	8	8_80913041_G	80,913,041	4.35	0.89	0.00000111
RR	8	8_80920355_A	80,920,355	3.53	0.71	0.00000071
RR	8	8_80928564_G	80,928,564	4.48	0.91	0.00000076
RR	8	8_80930376_A	80,930,376	4.48	0.91	0.00000076
RR	8	8_80936350_G	80,936,350	4.41	0.88	0.00000059
RR	8	8_80939825_G	80,939,825	4.43	0.88	0.00000052
RR	8	8_80966843_C	80,966,843	4.69	0.94	0.00000067
RR	8	8_81092365_C	81,092,365	4.73	0.94	0.00000055
RR	8	8_81155471_A	81,155,471	4.63	0.94	0.00000091
RR	8	8_81163081_C	81,163,081	4.63	0.94	0.00000091
RR	8	8_81164213_G	81,164,213	4.63	0.94	0.00000091
RR	8	8_81173969_C	81,173,969	4.63	0.94	0.00000092
RR	8	8_81236896_T	81,236,896	4.70	0.94	0.00000060
RR	8	8_81240491_G	81,240,491	4.59	0.94	0.00000109
RR	8	8_81266264_T	81,266,264	4.63	0.94	0.00000091
RR	8	8_81269516_G	81,269,516	4.63	0.94	0.00000091
RR	8	8_81283977_C	81,283,977	4.59	0.94	0.00000109

RR	8	8_81284565_C	81,284,565	4.63	0.94	0.00000091
RR	8	8_81289607_G	81,289,607	4.63	0.94	0.00000091
RR	8	8_81290898_G	81,290,898	4.63	0.94	0.00000091
RR	8	8_81292062_T	81,292,062	4.63	0.94	0.00000091
RR	8	8_81294206_G	81,294,206	4.63	0.94	0.00000091
RR	8	8_81295235_A	81,295,235	4.62	0.94	0.00000091
RR	8	8_81299105_G	81,299,105	4.63	0.94	0.00000091
RR	8	8_81302722_G	81,302,722	4.63	0.94	0.00000088
RR	8	8_81303915_T	81,303,915	4.63	0.94	0.00000091
RR	8	8_81307145_A	81,307,145	4.63	0.94	0.00000088
RR	8	8_81310484_G	81,310,484	4.63	0.94	0.00000088
RR	8	8_81312125_A	81,312,125	4.63	0.94	0.00000088
RR	8	8_81313528_T	81,313,528	4.63	0.94	0.00000088
RR	8	8_81315021_A	81,315,021	4.78	0.94	0.00000041
RR	8	8_81317019_G	81,317,019	4.78	0.94	0.00000041
RR	8	8_81319178_T	81,319,178	4.78	0.94	0.00000041
RR	8	8_81320527_C	81,320,527	4.67	0.94	0.00000076
RR	8	8_81327224_C	81,327,224	4.78	0.94	0.00000041
RR	8	8_81328951_CT	81,328,951	4.63	0.94	0.00000091
RR	8	8_81330741_T	81,330,741	4.81	0.94	0.00000036
RR	8	8_81335069_A	81,335,069	4.81	0.94	0.00000036
RR	8	8_81336429_C	81,336,429	4.83	0.94	0.00000031
RR	8	8_81336711_G	81,336,711	4.81	0.94	0.00000036
RR	8	8_81338537_TCTAA	81,338,537	4.81	0.94	0.00000036
RR	8	8_81344792_C	81,344,792	4.81	0.94	0.00000036
RR	8	8_81346572_A	81,346,572	4.66	0.94	0.00000077
RR	8	8_81347747_C	81,347,747	4.81	0.94	0.00000036

RR	8	8_81348919_G	81,348,919	4.80	0.94	0.00000038
RR	8	8_81350197_A	81,350,197	4.80	0.94	0.00000038
RR	8	8_81354101_AG	81,354,101	4.80	0.94	0.00000038
RR	8	8_81356615_G	81,356,615	4.79	0.94	0.00000039
RR	8	8_81358701_T	81,358,701	4.79	0.94	0.00000039
RR	8	8_81362081_A	81,362,081	4.77	0.94	0.00000043
RR	8	8_81363330_G	81,363,330	4.77	0.94	0.00000043
RR	8	8_81363867_C	81,363,867	4.77	0.94	0.00000043
RR	8	8_81368176_TG	81,368,176	4.78	0.94	0.00000041
RR	8	8_81369114_A	81,369,114	4.78	0.94	0.00000041
RR	8	8_81373864_A	81,373,864	4.59	0.92	0.00000061
RR	8	8_81375124_G	81,375,124	4.78	0.94	0.00000041
RR	8	8_81377115_C	81,377,115	4.78	0.94	0.00000041
RR	8	8_81378296_C	81,378,296	4.78	0.94	0.00000041
RR	8	8_81379814_C	81,379,814	4.78	0.94	0.00000041
RR	8	8_81380617_C	81,380,617	4.75	0.94	0.00000050
RR	8	8_81381962_C	81,381,962	4.78	0.94	0.00000041
RR	8	8_81384059_CCTTT	81,384,059	4.78	0.94	0.00000041
RR	8	8_81385697_C	81,385,697	4.78	0.94	0.00000041
RR	8	8_81386399_A	81,386,399	4.78	0.94	0.00000041
RR	8	8_81390426_C	81,390,426	4.78	0.94	0.00000041
RR	8	8_81392199_A	81,392,199	4.78	0.94	0.00000041
RR	8	8_81393030_G	81,393,030	4.78	0.94	0.00000041
RR	8	8_81393551_C	81,393,551	4.63	0.94	0.00000088
RR	8	8_81395661_C	81,395,661	4.78	0.94	0.00000041
RR	8	8_81396133_AGTGTT	81,396,133	4.55	0.92	0.00000079
RR	8	8_81396944_A	81,396,944	4.78	0.94	0.00000041

RR	8	8_81397717_G	81,397,717	4.78	0.94	0.00000041
RR	8	8_81398308_G	81,398,308	4.78	0.94	0.00000041
RR	8	8_81400157_C	81,400,157	4.78	0.94	0.00000041
RR	8	8_81401899_G	81,401,899	4.78	0.94	0.00000041
RR	8	8_81404143_G	81,404,143	4.78	0.94	0.00000041
RR	8	8_81407689_GAC	81,407,689	4.78	0.94	0.00000041
RR	8	8_81409926_T	81,409,926	4.59	0.92	0.00000061
RR	8	8_81410305_T	81,410,305	4.63	0.94	0.00000088
RR	8	8_81412417_C	81,412,417	4.77	0.94	0.00000043
RR	8	8_81414165_A	81,414,165	4.77	0.94	0.00000043
RR	8	8_81419728_T	81,419,728	4.59	0.92	0.00000061
RR	8	8_81421309_T	81,421,309	4.87	0.96	0.00000041
RR	8	8_81421800_A	81,421,800	4.90	0.96	0.00000036
RR	8	8_81422231_C	81,422,231	4.87	0.96	0.00000041
RR	8	8_81422714_T	81,422,714	4.92	0.97	0.00000041
RR	8	8_81423371_C	81,423,371	4.72	0.96	0.00000095
RR	8	8_81423749_A	81,423,749	4.87	0.96	0.00000041
RR	8	8_81424899_T	81,424,899	4.87	0.96	0.00000041
RR	8	8_81425522_T	81,425,522	4.87	0.96	0.00000041
RR	8	8_81425957_A	81,425,957	4.87	0.96	0.00000041
RR	8	8_81426302_G	81,426,302	4.87	0.96	0.00000041
RR	8	8_81426681_G	81,426,681	4.87	0.96	0.00000041
RR	8	8_81426998_A	81,426,998	4.87	0.96	0.00000041
RR	8	8_81428787_A	81,428,787	4.86	0.96	0.00000043
RR	8	8_81435134_A	81,435,134	4.67	0.94	0.00000061
RR	8	8_81438040_A	81,438,040	4.87	0.96	0.00000041
RR	8	8_81439251_T	81,439,251	5.02	0.96	0.00000019

RR	8	8_81440919_G	81,440,919	4.63	0.94	0.00000088
RR	8	8_81442397_A	81,442,397	4.87	0.96	0.00000041
RR	8	8_81443695_G	81,443,695	4.67	0.94	0.00000061
RR	8	8_81444906_A	81,444,906	4.76	0.96	0.00000077
RR	8	8_81446758_C	81,446,758	5.03	0.96	0.00000019
RR	8	8_81449093_G	81,449,093	4.88	0.96	0.00000039
RR	8	8_81457629_A	81,457,629	4.87	0.96	0.00000041
RR	8	8_81458793_T	81,458,793	4.87	0.96	0.00000041
RR	8	8_81459648_C	81,459,648	4.86	0.96	0.00000045
RR	8	8_81460138_C	81,460,138	4.87	0.96	0.00000041
RR	8	8_81460944_G	81,460,944	4.87	0.96	0.00000041
RR	8	8_81462839_C	81,462,839	4.87	0.96	0.00000041
RR	8	8_81466173_G	81,466,173	4.87	0.96	0.00000041
RR	8	8_81469502_T	81,469,502	4.77	0.94	0.00000033
RR	8	8_81470812_C	81,470,812	4.77	0.94	0.00000034
RR	8	8_81474708_G	81,474,708	4.91	0.96	0.00000035
RR	8	8_81476346_T	81,476,346	4.87	0.96	0.00000041
RR	8	8_81477234_G	81,477,234	4.87	0.96	0.00000041
RR	8	8_81477867_T	81,477,867	4.65	0.94	0.00000079
RR	8	8_81478479_A	81,478,479	4.77	0.94	0.00000033
RR	8	8_81479392_G	81,479,392	4.87	0.96	0.00000041
RR	8	8_81481496_G	81,481,496	4.87	0.96	0.00000041
RR	8	8_81484673_G	81,484,673	4.87	0.96	0.00000041
RR	8	8_81488326_G	81,488,326	4.87	0.96	0.00000041
RR	8	8_81489749_A	81,489,749	4.87	0.96	0.00000041
RR	8	8_81490996_G	81,490,996	4.87	0.96	0.00000041
RR	8	8_81495316_G	81,495,316	4.87	0.96	0.00000041

RR	8	8_81497003_T	81,497,003	4.87	0.96	0.00000041
RR	8	8_81499092_G	81,499,092	4.87	0.96	0.00000041
RR	8	8_81500923_T	81,500,923	4.87	0.96	0.00000041
RR	8	8_81505260_C	81,505,260	4.61	0.94	0.00000084
RR	8	8_81511606_G	81,511,606	4.67	0.94	0.00000061
RR	8	8_81513419_T	81,513,419	4.67	0.94	0.00000061
RR	8	8_81515686_A	81,515,686	4.67	0.94	0.00000061
RR	8	8_81516525_A	81,516,525	4.87	0.96	0.00000041
RR	8	8_81517435_AACAT	81,517,435	4.67	0.94	0.00000061
RR	8	8_81519923_A	81,519,923	4.67	0.94	0.00000061
RR	8	8_81523977_T	81,523,977	4.87	0.96	0.00000041
RR	8	8_81525049_G	81,525,049	4.67	0.94	0.00000061
RR	8	8_81525766_TA	81,525,766	4.77	0.94	0.00000033
RR	8	8_81527422_C	81,527,422	4.87	0.96	0.00000041
RR	8	8_81528942_T	81,528,942	4.87	0.96	0.00000041
RR	8	8_81530451_A	81,530,451	4.92	0.97	0.00000041
RR	8	8_81531775_G	81,531,775	4.89	0.96	0.00000038
RR	8	8_81532568_C	81,532,568	4.87	0.96	0.00000041
RR	8	8_81533131_A	81,533,131	4.86	0.96	0.00000043
RR	8	8_81536004_A	81,536,004	4.86	0.96	0.00000043
RR	8	8_81537795_G	81,537,795	4.76	0.96	0.00000079
RR	8	8_81538048_G	81,538,048	4.86	0.96	0.00000043
RR	8	8_81538907_G	81,538,907	4.86	0.96	0.00000045
RR	8	8_81541831_G	81,541,831	4.86	0.96	0.00000045
RR	8	8_81546958_T	81,546,958	4.77	0.94	0.00000035
RR	8	8_81549837_G	81,549,837	4.76	0.94	0.00000036
RR	8	8_81550500_A	81,550,500	4.76	0.94	0.00000036

RR	8	8_81551917_G	81,551,917	4.76	0.94	0.00000036
RR	8	8_81561170_T	81,561,170	4.76	0.94	0.00000036
RR	8	8_81563767_T	81,563,767	4.76	0.94	0.00000036
RR	8	8_81564660_A	81,564,660	4.76	0.94	0.00000035
RR	8	8_81566514_C	81,566,514	4.86	0.96	0.00000045
RR	8	8_81568886_G	81,568,886	4.86	0.96	0.00000045
RR	8	8_81569897_A	81,569,897	4.86	0.96	0.00000045
RR	8	8_81570976_G	81,570,976	4.86	0.96	0.00000045
RR	8	8_81573631_T	81,573,631	4.86	0.96	0.00000045
RR	8	8_81575573_T	81,575,573	4.86	0.96	0.00000045
RR	8	8_81577658_C	81,577,658	4.86	0.96	0.00000043
RR	8	8_81578697_G	81,578,697	4.86	0.96	0.00000045
RR	8	8_81579807_G	81,579,807	4.86	0.96	0.00000043
RR	8	8_81580621_A	81,580,621	4.72	0.94	0.00000047
RR	8	8_81581418_C	81,581,418	4.76	0.94	0.00000036
RR	8	8_81581597_G	81,581,597	4.86	0.96	0.00000045
RR	8	8_81582661_T	81,582,661	4.76	0.94	0.00000036
RR	8	8_81583943_C	81,583,943	4.86	0.96	0.00000045
RR	8	8_81585662_G	81,585,662	5.02	0.96	0.00000020
RR	8	8_81585863_A	81,585,863	4.86	0.96	0.00000045
RR	8	8_81586715_A	81,586,715	4.89	0.96	0.00000034
RR	8	8_81587033_C	81,587,033	4.86	0.96	0.00000043
RR	8	8_81588480_A	81,588,480	4.86	0.96	0.00000043
RR	8	8_81590164_G	81,590,164	4.76	0.96	0.00000079
PS	9	9_470047_A	470,047	0.09	0.02	0.00000045
PS	9	9_481970_G	481,970	0.09	0.02	0.00000054
T_{Vall}	1	1_32189900_T	32,189,900	0.10	0.02	0.00000031

T_{V8h}	2	2_86854220_G	86,854,220	-0.19	0.04	0.00000063
T_{V8h}	2	2_94855585_G	94,855,585	-0.21	0.04	0.00000022
T_{V8h}	2	2_94938876_A	94,938,876	-0.21	0.04	0.00000022
T_{V8h}	2	2_94984869_T	94,984,869	-0.20	0.04	0.00000057
T_{V8h}	2	2_94991762_A	94,991,762	-0.20	0.04	0.00000057
T_{V8h}	2	2_95014810_C	95,014,810	-0.20	0.04	0.00000058
T_{V8h}	2	2_95096326_C	95,096,326	-0.20	0.04	0.00000057
T_{V8h}	2	2_95223027_A	95,223,027	-0.21	0.04	0.00000012
T_{V8h}	2	2_95266233_T	95,266,233	-0.20	0.04	0.00000032
T_{V8h}	2	2_95286846_T	95,286,846	-0.20	0.04	0.00000032
T_{V8h}	2	2_95298258_T	95,298,258	-0.20	0.04	0.00000032
T_{V8h}	2	2_95303987_T	95,303,987	-0.20	0.04	0.00000022
T_{V8h}	2	2_95317254_A	95,317,254	-0.20	0.04	0.00000032
T_{V8h}	2	2_95320233_G	95,320,233	-0.20	0.04	0.00000032
T_{V8h}	2	2_95336608_A	95,336,608	-0.20	0.04	0.00000032
T_{V8h}	2	2_95342861_C	95,342,861	-0.20	0.04	0.00000031
T_{V8h}	2	2_95352071_T	95,352,071	-0.20	0.04	0.00000032
T_{V8h}	2	2_95363953_TG	95,363,953	-0.20	0.04	0.00000032
T_{V8h}	2	2_95366187_G	95,366,187	-0.20	0.04	0.00000032
T_{V8h}	2	2_95435801_ACT	95,435,801	-0.20	0.04	0.00000020
T_{V8h}	2	2_95446118_A	95,446,118	-0.20	0.04	0.00000032
T_{V8h}	2	2_95500013_C	95,500,013	-0.20	0.04	0.00000032
T_{V8h}	2	2_95549933_C	95,549,933	-0.21	0.04	0.00000004
T_{V8h}	2	2_95679479_C	95,679,479	-0.18	0.03	0.00000010
T_{V8h}	2	2_95770145_C	95,770,145	-0.18	0.03	0.00000021
T_{V8h}	2	2_95859076_T	95,859,076	-0.18	0.03	0.00000016
T_{V8h}	2	2_95941838_C	95,941,838	-0.17	0.03	0.00000089

T_{V8h}	2	2_95953423_C	95,953,423	-0.19	0.04	0.00000008
T_{V8h}	2	2_96027967_T	96,027,967	-0.17	0.03	0.00000087
T_{V8h}	2	2_96041647_T	96,041,647	-0.17	0.03	0.00000087
T_{V8h}	2	2_96077373_C	96,077,373	-0.17	0.03	0.00000100
T_{V8h}	2	2_96137988_T	96,137,988	-0.17	0.03	0.00000100
T_{V8h}	2	2_96190298_A	96,190,298	-0.17	0.03	0.00000087
T_{V8h}	2	2_96197993_T	96,197,993	-0.17	0.03	0.00000087
T_{V8h}	2	2_96249140_G	96,249,140	-0.17	0.03	0.00000087
T_{V8h}	2	2_96349263_G	96,349,263	-0.17	0.03	0.00000091
T_{V8h}	2	2_96372331_G	96,372,331	-0.17	0.03	0.00000091
T_{V8h}	2	2_96417792_T	96,417,792	-0.17	0.03	0.00000098
T_{V8h}	2	2_96440983_G	96,440,983	-0.17	0.03	0.00000097
T_{V8h}	2	2_96490360_G	96,490,360	-0.17	0.03	0.00000075
T_{V8h}	2	2_96515110_A	96,515,110	-0.17	0.03	0.00000069
T_{V8h}	2	2_96579517_C	96,579,517	-0.17	0.03	0.00000071
T_{V8h}	2	2_96645000_G	96,645,000	-0.17	0.03	0.00000072
T_{V8h}	2	2_96681918_C	96,681,918	-0.16	0.03	0.00000108
T_{V8h}	2	2_96689798_C	96,689,798	-0.17	0.03	0.00000072
T_{V8h}	2	2_96715847_C	96,715,847	-0.17	0.03	0.00000072
T_{V8h}	2	2_96753503_T	96,753,503	-0.17	0.03	0.00000072
T_{V8h}	2	2_96763009_G	96,763,009	-0.16	0.03	0.00000104
T_{V8h}	2	2_96852755_G	96,852,755	-0.17	0.03	0.00000086
T_{V8h}	2	2_96953410_T	96,953,410	-0.17	0.03	0.00000059
T_{V8h}	2	2_96960117_G	96,960,117	-0.17	0.03	0.00000094
T_{V8h}	2	2_96969360_A	96,969,360	-0.16	0.03	0.00000101
T_{V8h}	2	2_96980275_T	96,980,275	-0.16	0.03	0.00000101
T_{V8h}	2	2_97012732_G	97,012,732	-0.16	0.03	0.00000101

T_{V8h}	2	2_97018425_A	97,018,425	-0.17	0.03	0.00000057
T_{V8h}	2	2_97022117_T	97,022,117	-0.16	0.03	0.00000101
T_{V8h}	2	2_97033798_A	97,033,798	-0.17	0.03	0.00000051
T_{V8h}	2	2_97042799_C	97,042,799	-0.16	0.03	0.00000101
T_{V8h}	2	2_97057093_T	97,057,093	-0.17	0.03	0.00000057
T_{V8h}	2	2_97065405_A	97,065,405	-0.17	0.03	0.00000057
T_{V8h}	2	2_97069345_A	97,069,345	-0.16	0.03	0.00000097
T_{V8h}	2	2_97087835_T	97,087,835	-0.17	0.03	0.00000057
T_{V8h}	2	2_97097010_G	97,097,010	-0.16	0.03	0.00000104
T_{V8h}	2	2_97108989_G	97,108,989	-0.17	0.03	0.00000057
T_{V8h}	2	2_97112649_T	97,112,649	-0.17	0.03	0.00000061
T_{V8h}	2	2_97120477_G	97,120,477	-0.17	0.03	0.00000057
T_{V8h}	2	2_97135146_C	97,135,146	-0.17	0.03	0.00000053
T_{V8h}	2	2_97160510_A	97,160,510	-0.17	0.03	0.00000057
T_{V8h}	2	2_97163311_T	97,163,311	-0.17	0.03	0.00000057
T_{V8h}	2	2_97171427_C	97,171,427	-0.17	0.03	0.00000057
T_{V8h}	2	2_97174617_G	97,174,617	-0.16	0.03	0.00000104
T_{V8h}	2	2_97196645_C	97,196,645	-0.17	0.03	0.00000059
T_{V8h}	2	2_97208065_T	97,208,065	-0.17	0.03	0.00000057
T_{V8h}	2	2_97213766_A	97,213,766	-0.17	0.03	0.00000050
T_{V8h}	2	2_97217701_G	97,217,701	-0.17	0.03	0.00000050
T_{V8h}	2	2_97220184_G	97,220,184	-0.17	0.03	0.00000050
T_{V8h}	2	2_97221728_G	97,221,728	-0.17	0.03	0.00000050
T_{V8h}	2	2_97222435_A	97,222,435	-0.17	0.03	0.00000050
T_{V8h}	2	2_97225469_T	97,225,469	-0.16	0.03	0.00000090
T_{V8h}	2	2_97228017_A	97,228,017	-0.17	0.03	0.00000046
T_{V8h}	2	2_97231098_C	97,231,098	-0.16	0.03	0.00000090

T_{V8h}	2	2_97234661_G	97,234,661	-0.18	0.03	0.00000027
T_{V8h}	2	2_97242170_T	97,242,170	-0.17	0.03	0.00000050
T_{V8h}	2	2_97243893_A	97,243,893	-0.17	0.03	0.00000050
T_{V8h}	2	2_97250083_T	97,250,083	-0.17	0.03	0.00000050
T_{V8h}	2	2_97251933_C	97,251,933	-0.17	0.03	0.00000050
T_{V8h}	2	2_97252908_C	97,252,908	-0.17	0.03	0.00000050
T_{V8h}	2	2_97254942_C	97,254,942	-0.17	0.03	0.00000050
T_{V8h}	2	2_97256112_C	97,256,112	-0.17	0.03	0.00000050
T_{V8h}	2	2_97287033_A	97,287,033	-0.17	0.03	0.00000050
T_{V8h}	2	2_97290691_A	97,290,691	-0.17	0.03	0.00000050
T_{V8h}	2	2_97298155_C	97,298,155	-0.17	0.03	0.00000050
T_{V8h}	2	2_97301292_G	97,301,292	-0.17	0.03	0.00000042
T_{V8h}	2	2_97304972_G	97,304,972	-0.17	0.03	0.00000050
T_{V8h}	2	2_97311698_T	97,311,698	-0.16	0.03	0.00000090
T_{V8h}	2	2_97321472_A	97,321,472	-0.17	0.03	0.00000050
T_{V8h}	2	2_97328947_A	97,328,947	-0.17	0.03	0.00000064
T_{V8h}	2	2_97336293_G	97,336,293	-0.17	0.03	0.00000050
T_{V8h}	2	2_97357185_C	97,357,185	-0.17	0.03	0.00000050
T_{V8h}	2	2_97508070_T	97,508,070	-0.16	0.03	0.00000090
T_{V8h}	2	2_97546945_C	97,546,945	-0.16	0.03	0.00000091
T_{V8h}	2	2_97560134_A	97,560,134	-0.16	0.03	0.00000090
T_{V8h}	2	2_97607971_G	97,607,971	-0.16	0.03	0.00000090
T_{V8h}	2	2_97614899_A	97,614,899	-0.16	0.03	0.00000091
T_{V8h}	2	2_97637824_A	97,637,824	-0.17	0.03	0.00000050
T_{V8h}	2	2_97653371_G	97,653,371	-0.16	0.03	0.00000091
T_{V8h}	2	2_97680472_C	97,680,472	-0.16	0.03	0.00000091
T_{V8h}	2	2_97710223_A	97,710,223	-0.16	0.03	0.00000091

T_{V8h}	2	2_97822905_T	97,822,905	-0.16	0.03	0.00000096
T_{V8h}	2	2_97832251_C	97,832,251	-0.16	0.03	0.00000096
T_{V8h}	2	2_97845730_A	97,845,730	-0.16	0.03	0.00000096
T_{V8h}	2	2_97867049_G	97,867,049	-0.16	0.03	0.00000111
T_{V8h}	2	2_97869210_A	97,869,210	-0.16	0.03	0.00000096
T_{V8h}	2	2_97873249_G	97,873,249	-0.16	0.03	0.00000111
T_{V8h}	2	2_97874102_A	97,874,102	-0.16	0.03	0.00000111
T_{V8h}	2	2_97875213_A	97,875,213	-0.16	0.03	0.00000111
T_{V8h}	2	2_97877797_G	97,877,797	-0.16	0.03	0.00000111
T_{V8h}	2	2_97902246_T	97,902,246	-0.16	0.03	0.00000111
T_{V8h}	2	2_97904673_G	97,904,673	-0.16	0.03	0.00000111
T_{V8h}	2	2_97906592_G	97,906,592	-0.16	0.03	0.00000111
T_{V8h}	2	2_97908251_C	97,908,251	-0.16	0.03	0.00000096
T_{V8h}	2	2_97909292_T	97,909,292	-0.16	0.03	0.00000111
T_{V8h}	2	2_97910031_T	97,910,031	-0.16	0.03	0.00000111
T_{V8h}	2	2_97910332_G	97,910,332	-0.16	0.03	0.00000111
T_{V8h}	2	2_97915351_G	97,915,351	-0.16	0.03	0.00000111
T_{V8h}	2	2_97916298_C	97,916,298	-0.16	0.03	0.00000096
T_{V8h}	2	2_97921767_G	97,921,767	-0.16	0.03	0.00000111
T_{V8h}	2	2_97933494_G	97,933,494	-0.16	0.03	0.00000111
T_{V8h}	2	2_97946519_G	97,946,519	-0.16	0.03	0.00000111
T_{V8h}	2	2_97955673_C	97,955,673	-0.16	0.03	0.00000099
T_{V8h}	2	2_97979364_A	97,979,364	-0.16	0.03	0.00000111
T_{V8h}	2	2_97982465_C	97,982,465	-0.18	0.03	0.00000030
T_{V8h}	2	2_97990500_A	97,990,500	-0.17	0.03	0.00000058
T_{V8h}	2	2_97997629_G	97,997,629	-0.16	0.03	0.00000096
T_{V8h}	2	2_98213679_T	98,213,679	-0.17	0.03	0.00000077

T_{V8h}	2	2_98619839_T	98,619,839	-0.18	0.03	0.00000015
T_{V8h}	2	2_99041870_G	99,041,870	-0.16	0.03	0.00000120
T_{V8h}	2	2_99069820_A	99,069,820	-0.16	0.03	0.00000120
T_{V8h}	2	2_99492485_C	99,492,485	-0.18	0.04	0.00000069
T_{V8h}	2	2_99515035_A	99,515,035	-0.16	0.03	0.00000112
T_{V8h}	2	2_99523542_C	99,523,542	-0.16	0.03	0.00000120
T_{V8h}	2	2_99531694_T	99,531,694	-0.16	0.03	0.00000120
T_{V8h}	2	2_99573010_T	99,573,010	-0.16	0.03	0.00000116
T_{V8h}	2	2_99577410_A	99,577,410	-0.17	0.03	0.00000027
T_{V8h}	2	2_99599185_C	99,599,185	-0.16	0.03	0.00000120
T_{V8h}	2	2_99712712_G	99,712,712	-0.16	0.03	0.00000120
T_{V8h}	2	2_99777237_A	99,777,237	-0.17	0.03	0.00000064
T_{V8h}	2	2_99784035_A	99,784,035	-0.16	0.03	0.00000116
T_{V8h}	2	2_99798826_T	99,798,826	-0.17	0.03	0.00000037
T_{V8h}	2	2_99803416_G	99,803,416	-0.16	0.03	0.00000095
T_{V8h}	2	2_99845424_C	99,845,424	-0.16	0.03	0.00000082
T_{V8h}	2	2_99852196_T	99,852,196	-0.17	0.03	0.00000045
T_{V8h}	2	2_99899912_T	99,899,912	-0.16	0.03	0.00000082
T_{V8h}	2	2_99925883_C	99,925,883	-0.16	0.03	0.00000082
T_{V8h}	2	2_99932721_A	99,932,721	-0.16	0.03	0.00000082
T_{V8h}	2	2_99940212_C	99,940,212	-0.16	0.03	0.00000082
T_{V8h}	2	2_99957731_A	99,957,731	-0.17	0.03	0.00000059
T_{V8h}	2	2_99963247_G	99,963,247	-0.18	0.03	0.00000010
T_{V8h}	2	2_99968868_T	99,968,868	-0.17	0.03	0.00000042
T_{V8h}	2	2_99969778_A	99,969,778	-0.16	0.03	0.00000079
T_{V8h}	2	2_99974267_T	99,974,267	-0.16	0.03	0.00000082
T_{V8h}	2	2_99981114_A	99,981,114	-0.16	0.03	0.00000077

T_{V8h}	2	2_99984716_G	99,984,716	-0.16	0.03	0.00000082
T_{V8h}	2	2_99995475_T	99,995,475	-0.16	0.03	0.00000082
T_{V8h}	2	2_99998822_C	99,998,822	-0.17	0.03	0.00000075
T_{V8h}	2	2_100001754_T	100,001,754	-0.16	0.03	0.00000082
T_{V8h}	2	2_100004010_A	100,004,010	-0.16	0.03	0.00000082
T_{V8h}	2	2_100037326_C	100,037,326	-0.16	0.03	0.00000089
T_{V8h}	2	2_100063240_G	100,063,240	-0.16	0.03	0.00000089
T_{V8h}	2	2_100073946_G	100,073,946	-0.17	0.03	0.00000049
T_{V8h}	2	2_100074384_G	100,074,384	-0.16	0.03	0.00000089
T_{V8h}	2	2_100079909_T	100,079,909	-0.16	0.03	0.00000091
T_{V8h}	2	2_100089417_T	100,089,417	-0.16	0.03	0.00000091
T_{V8h}	2	2_100096616_C	100,096,616	-0.17	0.03	0.00000033
T_{V8h}	2	2_100099506_G	100,099,506	-0.16	0.03	0.00000091
T_{V8h}	2	2_100100558_G	100,100,558	-0.16	0.03	0.00000091
T_{V8h}	2	2_100103987_T	100,103,987	-0.16	0.03	0.00000091
T_{V8h}	2	2_100105589_A	100,105,589	-0.16	0.03	0.00000091
T_{V8h}	2	2_100110228_C	100,110,228	-0.16	0.03	0.00000091
T_{V8h}	2	2_100111808_C	100,111,808	-0.16	0.03	0.00000091
T_{V8h}	2	2_100114851_G	100,114,851	-0.16	0.03	0.00000091
T_{V8h}	2	2_100116879_C	100,116,879	-0.16	0.03	0.00000091
T_{V8h}	2	2_100119761_C	100,119,761	-0.16	0.03	0.00000091
T_{V8h}	2	2_100121238_C	100,121,238	-0.16	0.03	0.00000091
T_{V8h}	2	2_100127129_G	100,127,129	-0.16	0.03	0.00000091
T_{V8h}	2	2_100127811_T	100,127,811	-0.16	0.03	0.00000091
T_{V8h}	2	2_100129766_C	100,129,766	-0.17	0.03	0.00000050
T_{V8h}	2	2_100134231_CGTTGT	100,134,231	-0.16	0.03	0.00000120
T_{V8h}	2	2_100137687_T	100,137,687	-0.16	0.03	0.00000091

T_{V8h}	2	2_100140880_C	100,140,880	-0.16	0.03	0.00000115
T_{V8h}	2	2_100144080_A	100,144,080	-0.16	0.03	0.00000115
T_{V8h}	2	2_100146841_A	100,146,841	-0.16	0.03	0.00000115
T_{V8h}	2	2_100241628_C	100,241,628	-0.17	0.03	0.00000084
T_{V8h}	2	2_100292635_T	100,292,635	-0.16	0.03	0.00000100
T_{V8h}	2	2_100326888_A	100,326,888	-0.16	0.03	0.00000100
T_{V8h}	2	2_100350673_A	100,350,673	-0.17	0.03	0.00000079
T_{V8h}	2	2_100369091_G	100,369,091	-0.16	0.03	0.00000100
T_{V8h}	2	2_100545358_C	100,545,358	-0.16	0.03	0.00000109
T_{V8h}	2	2_100777051_ACTG	100,777,051	-0.17	0.03	0.00000094
T_{V8h}	2	2_100819761_T	100,819,761	-0.17	0.03	0.00000094
T_{V8h}	2	2_100913881_T	100,913,881	-0.17	0.03	0.00000062
T_{V8h}	2	2_100948637_G	100,948,637	-0.17	0.03	0.00000076
T_{V8h}	2	2_102014302_C	102,014,302	-0.17	0.03	0.00000110
T_{V8h}	2	2_102034366_T	102,034,366	-0.17	0.03	0.00000110
T_{V8h}	2	2_102039175_A	102,039,175	-0.17	0.03	0.00000107
T_{V8h}	2	2_102057570_C	102,057,570	-0.17	0.03	0.00000110
T_{V8h}	2	2_102064911_T	102,064,911	-0.17	0.03	0.00000110
T_{V8h}	2	2_102069888_A	102,069,888	-0.17	0.03	0.00000110
T_{V8h}	2	2_102072694_C	102,072,694	-0.17	0.03	0.00000110
T_{V8h}	2	2_102087838_A	102,087,838	-0.17	0.03	0.00000110
T_{V8h}	2	2_102133556_T	102,133,556	-0.17	0.03	0.00000110
T_{V8h}	2	2_102136773_G	102,136,773	-0.17	0.03	0.00000110
T_{V8h}	2	2_102142621_T	102,142,621	-0.17	0.03	0.00000110
T_{V8h}	2	2_102145110_A	102,145,110	-0.17	0.03	0.00000066
T_{V8h}	2	2_102148280_T	102,148,280	-0.17	0.03	0.00000066
T_{V8h}	2	2_102168428_T	102,168,428	-0.17	0.03	0.00000110

T_{V8h}	2	2_102204874_G	102,204,874	-0.17	0.03	0.00000082
T_{V8h}	2	2_102222267_G	102,222,267	-0.18	0.04	0.00000056
T_{V8h}	2	2_102387102_A	102,387,102	-0.17	0.03	0.00000115
T_{V8h}	2	2_102387566_T	102,387,566	-0.17	0.03	0.00000115
T_{V8h}	2	2_102392475_T	102,392,475	-0.17	0.03	0.00000115
T_{V8h}	2	2_102400157_G	102,400,157	-0.17	0.03	0.00000115
T_{V8h}	2	2_102430205_G	102,430,205	-0.17	0.04	0.00000073
T_{V8h}	2	2_102438092_A	102,438,092	-0.17	0.03	0.00000120
T_{V8h}	2	2_102471418_C	102,471,418	-0.17	0.03	0.00000102
T_{V8h}	2	2_102474625_T	102,474,625	-0.17	0.03	0.00000094
T_{V8h}	2	2_102483852_T	102,483,852	-0.17	0.03	0.00000102
T_{V8h}	2	2_102489498_G	102,489,498	-0.17	0.03	0.00000090
HD	2	2_2677442_A	2,677,442	-0.18	0.04	0.00000104
HD	7	7_17063229_G	17,063,229	0.15	0.03	0.00000080
HD	15	15_126575680_C	126,575,680	0.21	0.04	0.00000039
HD	15	15_126576120_A	126,576,120	0.21	0.04	0.00000039
HD	15	15_126576736_C	126,576,736	0.21	0.04	0.00000039
HD	15	15_126578009_A	126,578,009	0.21	0.04	0.00000035
HD	15	15_126578571_C	126,578,571	0.21	0.04	0.00000034
HD	15	15_126579790_T	126,579,790	0.20	0.04	0.00000077
HD	15	15_126580989_C	126,580,989	0.21	0.04	0.00000034
HD	15	15_126581768_A	126,581,768	0.21	0.04	0.00000034
HD	15	15_126582362_G	126,582,362	0.21	0.04	0.00000034
HD	15	15_126586302_C	126,586,302	0.21	0.04	0.00000039
HD	15	15_126602850_T	126,602,850	0.21	0.04	0.00000092
HD	15	15_126607437_T	126,607,437	0.22	0.04	0.00000044
HD	15	15_126609737_A	126,609,737	0.21	0.04	0.00000095

BCS_{cal}	13	13_131195060_A	131,195,060	-0.46	0.09	0.00000095
BCS_{cal}	13	13_131198219_T	131,198,219	-0.46	0.09	0.00000094
BCS_{cal}	13	13_131200333_A	131,200,333	-0.48	0.10	0.00000058
BCS_{cal}	13	13_131201128_C	131,201,128	-0.47	0.10	0.00000081
EA	7	7_39303762_A	39,303,762	15.36	3.07	0.00000057
EA	7	7_39305689_A	39,305,689	15.72	3.09	0.00000037
EA	7	7_39306371_C	39,306,371	17.81	3.56	0.00000056

Table S2. Gene annotation for the significant variants for indicators of heat stress response in lactating sows

Trait	Chr	Position (bp)	Gene ID	Gene name
BCS_{cal}	13	131,195,060 - 131,200,333	*ENSSSCG00000031356*	*HES1*
BCS_{cal}	13	131,195,060 - 131,200,333	*ENSSSCG00000039561*	
BCS_{cal}	13	131,195,060 - 131,200,333	*ENSSSCG00000034990*	
BCS_{cal}	13	131,195,060 - 131,200,333	*ENSSSCG00000054894*	
EA	7	39,303,762 - 39,306,371	*ENSSSCG00000040047*	*TMEM151B*
EA	7	39,303,762 - 39,306,371	*ENSSSCG00000001705*	*TCTE1*
EA	7	39,303,762 - 39,306,371	*ENSSSCG00000001706*	*AARS2*
EA	7	39,303,762 - 39,306,371	*ENSSSCG00000039903*	*SPATS1*
EA	7	39,303,762 - 39,306,371	*ENSSSCG00000001708*	*CDC5L*
EA	7	39,303,762 - 39,306,371	*ENSSSCG00000001700*	*SLC29A1*
EA	7	39,303,762 - 39,306,371	*ENSSSCG00000001701*	*HSP90AB1*
EA	7	39,303,762 - 39,306,371	*ENSSSCG00000001702*	*SLC35B2*
EA	7	39,303,762 - 39,306,371	*ENSSSCG00000001703*	*NFKBIE*
EA	7	39,303,762 - 39,306,371	*ENSSSCG00000053910*	*MYMX*
EA	7	39,303,762 - 39,306,371	*ENSSSCG00000041884*	

HD	2	2,677,442	*ENSSSCG00000062960*	
HD	2	2,677,442	*ENSSSCG00000058263*	
HD	7	17,063,229	*ENSSSCG00000049691*	
HD	15	126,575,680 - 126,609,737	*ENSSSCG00000016237*	*DOCK10*
PS	9	470,047 - 481,970	*ENSSSCG00000014575*	
PS	9	470,047 - 481,970	*ENSSSCG00000014577*	*TMEM9B*
PS	9	470,047 - 481,970	*ENSSSCG00000033335*	*AKIP1*
PS	9	470,047 - 481,970	*ENSSSCG00000051028*	
PS	9	470,047 - 481,970	*ENSSSCG00000059660*	
PS	9	470,047 - 481,970	*ENSSSCG00000059027*	
PS	9	470,047 - 481,970	*ENSSSCG00000044344*	
PS	9	470,047 - 481,970	*ENSSSCG00000014570*	*NRIP3*
RR	7	23,843,264	*ENSSSCG00000001409*	*PRRC2A*
RR	7	23,843,264	*ENSSSCG00000001410*	*BAG6*
RR	7	23,843,264	*ENSSSCG00000001411*	*APOM*
RR	7	23,843,264	*ENSSSCG00000001413*	*GPANK1*
RR	7	24,051,539	*ENSSSCG00000001424*	*SKIC2*
RR	7	24,051,539	*ENSSSCG00000001425*	*DXO*
RR	7	24,051,539	*ENSSSCG00000001426*	*STK19*
RR	7	24,051,539	*ENSSSCG00000001427*	*C4A*
RR	7	24,051,539	*ENSSSCG00000001428*	*CYP21A2*
RR	7	24,051,539	*ENSSSCG00000023611*	*TNXB*
RR	7	23,843,264 - 23,886,397	*ENSSSCG00000001414*	*CSNK2B*
RR	7	23,843,264 - 23,886,397	*ENSSSCG00000062414*	*LY6G5B*
RR	7	23,843,264 - 23,892,506	*ENSSSCG00000001416*	*LY6G5C*
RR	7	23,843,264 - 23,913,884	*ENSSSCG00000034923*	*ABHD16A*
RR	7	23,843,264 - 23,919,566	*ENSSSCG00000033590*	*LY6G6F*

RR	7	23,843,264 - 23,919,566	*ENSSSCG00000036566*	*LY6G6C*
RR	7	23,843,264 - 23,919,566	*ENSSSCG00000040885*	
RR	7	23,843,264 - 23,919,566	*ENSSSCG00000060949*	*LY6G6D*
RR	7	23,843,264 - 23,936,480	*ENSSSCG00000034664*	*MPIG6B*
RR	7	23,843,264 - 23,945,958	*ENSSSCG00000022712*	*SNORD52*
RR	7	23,843,264 - 23,945,958	*ENSSSCG00000029160*	
RR	7	23,843,264 - 23,945,958	*ENSSSCG00000030368*	*HSPA1L*
RR	7	23,843,264 - 23,945,958	*ENSSSCG00000035596*	*MSH5*
RR	7	23,843,264 - 23,945,958	*ENSSSCG00000036796*	*VWA7*
RR	7	23,843,264 - 23,945,958	*ENSSSCG00000038950*	*VARS1*
RR	7	23,843,264 - 23,945,958	*ENSSSCG00000039021*	*LSM2*
RR	7	23,843,264 - 23,945,958	*ENSSSCG00000039071*	
RR	7	23,843,264 - 23,945,958	*ENSSSCG00000040506*	*SNORD48*
RR	7	23,843,264 - 23,945,958	*ENSSSCG00000044205*	
RR	7	23,843,264 - 23,945,958	*ENSSSCG00000044572*	
RR	7	23,843,264 - 23,945,958	*ENSSSCG00000046056*	
RR	7	23,843,264 - 23,945,958	*ENSSSCG00000061053*	*SAPCD1*
RR	7	23,886,397 - 24,051,539	*ENSSSCG00000001418*	*NEU1*
RR	7	23,886,397 - 24,051,539	*ENSSSCG00000001419*	*SLC44A4*
RR	7	23,886,397 - 24,051,539	*ENSSSCG00000001420*	*EHMT2*
RR	7	23,905,782 - 24,051,539	*ENSSSCG00000001421*	*ZBTB12*
RR	7	23,905,782 - 24,051,539	*ENSSSCG00000001422*	*C2*
RR	7	23,936,480 - 24,051,539	*ENSSSCG00000024914*	*CFB*
RR	7	23,945,958 - 24,051,539	*ENSSSCG00000001423*	*NELFE*
RR	7	23843264 - 23936480	*ENSSSCG00000038514*	*DDAH2*
RR	7	39,351,307	*ENSSSCG00000001702*	*SLC35B2*
RR	7	39,351,307 - 39,355,266	*ENSSSCG00000001703*	*NFKBIE*

RR	7	39,351,307 - 39,355,266	*ENSSSCG00000001705*	*TCTE1*
RR	7	39,351,307 - 39,355,266	*ENSSSCG00000001706*	*AARS2*
RR	7	39,351,307 - 39,355,266	*ENSSSCG00000001708*	*CDC5L*
RR	7	39,351,307 - 39,355,266	*ENSSSCG00000040047*	*TMEM151B*
RR	7	39,351,307 - 39,355,266	*ENSSSCG00000041884*	
RR	7	39,351,307 - 39,355,266	*ENSSSCG00000059458*	
RR	7	39351307 - 39355266	*ENSSSCG00000039903*	*SPATS1*
RR	7	39351307 - 39355266	*ENSSSCG00000057783*	
RR	8	80,358,650	*ENSSSCG00000060000*	
RR	8	79,518,715 - 79,561,407	*ENSSSCG00000035623*	*IQCM*
RR	8	79,518,715 - 79,561,407	*ENSSSCG00000055701*	
RR	8	79,518,715 - 79,635,229	*ENSSSCG00000050872*	
RR	8	79,518,715 - 79,669,879	*ENSSSCG00000055186*	
RR	8	80,358,650 - 80,481,645	*ENSSSCG00000043522*	
RR	8	80,358,650 - 80,734,740	*ENSSSCG00000037766*	*NR3C2*
RR	8	80,673,033 - 81,092,365	*ENSSSCG00000009029*	*ARHGAP10*
RR	8	81,092,365 - 81,173,969	*ENSSSCG00000009030*	*PRMT9*
RR	8	81,092,365 - 81,236,896	*ENSSSCG00000030044*	*TMEM184C*
RR	8	81,092,365 - 81,240,491	*ENSSSCG00000046523*	
RR	8	81,155,471 - 81,375,124	*ENSSSCG00000009031*	*EDNRA*
RR	8	81,390,426 - 81,590,164	*ENSSSCG00000054066*	
T_{ES}	2	21,729,683	*ENSSSCG00000013286*	*LRRC4C*
T_{ES}	5	83,314,673	*ENSSSCG00000000873*	*ANO4*
T_{ES}	5	83,647,158	*ENSSSCG00000000874*	*GAS2L3*
T_{ES}	5	83,647,158	*ENSSSCG00000000875*	*NR1H4*
T_{ES}	5	83,647,158	*ENSSSCG00000038946*	*SLC17A8*
T_{ES}	5	83,647,158	*ENSSSCG00000047401*	

T_{ES}	5	85,914,808 - 86,033,079	*ENSSSCG00000047567*	
T_{ES}	7	49,276,927 - 49,527,342	*ENSSSCG00000040288*	*ARNT2*
T_{ES}	7	49,527,342 - 49,584,578	*ENSSSCG00000001782*	*ABHD17C*
T_{ES}	7	49,527,342 - 49,584,578	*ENSSSCG00000038929*	*CEMIP*
T_{ES}	7	49,440,363 - 49,584,578	*ENSSSCG00000057483*	
T_{ES}	7	49,276,927 - 49,440,363	*ENSSSCG00000055731*	*U6*
T_{ES}	12	6,808,169	*ENSSSCG00000017239*	*RPL38*
T_{ES}	12	6,808,169	*ENSSSCG00000017238*	*TTYH2*
T_{ES}	12	6,808,169	*ENSSSCG00000040989*	*GPRC5C*
T_{ES}	12	6,808,169	*ENSSSCG00000027923*	*GPR142*
T_{ES}	12	6,808,169	*ENSSSCG00000059713*	*BTBD17*
T_{ES}	12	6,808,169	*ENSSSCG00000021724*	*KIF19*
T_{ES}	12	6,808,169	*ENSSSCG00000024357*	*DNAI2*
T_{ES}	14	137,210,716	*ENSSSCG00000010755*	*PTPRE*
T_{ES}	14	137,210,716	*ENSSSCG00000026302*	
T_{ES}	16	22,801,074 - 22,804,340	*ENSSSCG00000016846*	*WDR70*
T_{ES}	17	28,358,400	*ENSSSCG00000038858*	*CFAP61*
T_{ES}	17	28,358,400	*ENSSSCG00000026506*	*RALGAPA2*
T_{ES}	17	28,358,400	*ENSSSCG00000062159*	*INSM1*
T_{ES}	17	28,358,400	*ENSSSCG00000046267*	
T_{RS}	1	10473872 - 10505848	*ENSSSCG00000056648*	
T_{RS}	1	10473872 - 10505848	*ENSSSCG00000061773*	
T_{RS}	1	10,473,872 - 10,505,848	*ENSSSCG00000045185*	*ssc-mir-9857*
T_{RS}	2	108,874,785	*ENSSSCG00000014186*	
T_{RS}	2	127,833,178	*ENSSSCG00000053601*	
T_{RS}	2	127,833,178	*ENSSSCG00000054233*	
T_{RS}	2	108,874,785	*ENSSSCG00000049923*	

T_{RS}	2	105,870,529	*ENSSSCG00000054777*	
T_{RS}	6	135,196,192	*ENSSSCG00000035582*	*GIPC2*
T_{RS}	6	135,196,192	*ENSSSCG00000003766*	*DNAJB4*
T_{RS}	6	135,196,192	*ENSSSCG00000003771*	*FUBP1*
T_{RS}	6	135,196,192	*ENSSSCG00000050806*	
T_{RS}	6	135,196,192	*ENSSSCG00000055126*	*U6*
T_{RS}	6	135,196,192	*ENSSSCG00000018423*	*U6*
T_{RS}	6	128,607,655	*ENSSSCG00000003754*	
T_{RS}	6	128,028,279 - 128,061,017	*ENSSSCG00000005778*	*HSBP1L1*
T_{RS}	6	128,028,279 - 128,061,017	*ENSSSCG00000005777*	*TXNL4A*
T_{RS}	6	125,897,646 - 126,135,107	*ENSSSCG00000003749*	*PIK3C3*
T_{RS}	6	127,822,624	*ENSSSCG00000005780*	*KCNG2*
T_{RS}	6	127,822,624 - 128,038,925	*ENSSSCG00000023171*	*SLC66A2*
T_{RS}	6	128,028,279 - 128,126,009	*ENSSSCG00000038475*	
T_{RS}	6	128,028,279 - 128,180,187	*ENSSSCG00000038632*	*ADNP2*
T_{RS}	6	128,096,745 - 128,349,869	*ENSSSCG00000023376*	*PARD6G*
T_{RS}	6	128,540,069 - 128,607,655	*ENSSSCG00000003753*	
T_{RS}	6	128,926,928 - 128,933,859	*ENSSSCG00000003755*	*MCOLN2*
T_{RS}	6	128,926,928 - 129,027,823	*ENSSSCG00000003756*	*LPAR3*
T_{RS}	6	128,961,716 - 129,210,420	*ENSSSCG00000003757*	*SSX2IP*
T_{RS}	6	128,975,440 - 129,150,250	*ENSSSCG00000044786*	
T_{RS}	6	129,106,033 - 129,303,560	*ENSSSCG00000003758*	*CTBS*
T_{RS}	6	129,106,033 - 129,338,493	*ENSSSCG00000029882*	*SPATA1*
T_{RS}	6	129,149,710 - 129,348,946	*ENSSSCG00000053185*	*GNG5*
T_{RS}	6	129,192,451 - 129,363,499	*ENSSSCG00000022145*	*RPF1*
T_{RS}	6	129,279,850 - 129,363,499	*ENSSSCG00000026532*	*DNASE2B*
T_{RS}	6	129,298,592 - 129,363,499	*ENSSSCG00000026005*	*SAMD13*

T_{RS}	6	129,301,918 - 129,363,499	*ENSSSCG00000044862*	
T_{RS}	6	126,040,757 - 126,135,107	*ENSSSCG00000037233*	
T_{RS}	6	128,506,422 - 128,607,655	*ENSSSCG00000060282*	
T_{RS}	6	125,685,780	*ENSSSCG00000055429*	
T_{RS}	6	126,631,171 - 126,808,755	*ENSSSCG00000057422*	
T_{RS}	6	127,822,624	*ENSSSCG00000055983*	
T_{RS}	6	128038925 - 128180187	*ENSSSCG00000063496*	
T_{RS}	6	128,061,017 - 128,180,187	*ENSSSCG00000055757*	
T_{RS}	6	128,318,719 - 128,362,537	*ENSSSCG00000063050*	
T_{RS}	6	129,279,850 - 129,363,499	*ENSSSCG00000022206*	*UOX*
T_{RS}	8	134,857,072 - 134,860,931	*ENSSSCG00000009233*	*GPAT3*
T_{RS}	8	134857072 - 134860931	*ENSSSCG00000056871*	
T_{RS}	8	4,960,712	*ENSSSCG00000035020*	*STK32B*
T_{RS}	8	4,906,107 - 4,960,712	*ENSSSCG00000032637*	*EVC*
T_{RS}	8	4,906,107 - 4,960,712	*ENSSSCG00000024399*	*EVC2*
T_{RS}	9	39,195,933	*ENSSSCG00000015016*	*POU2AF1*
T_{RS}	9	39,195,933	*ENSSSCG00000015020*	*BTG4*
T_{RS}	9	39,195,933	*ENSSSCG00000015021*	*HOATZ*
T_{RS}	9	39,424,271	*ENSSSCG00000015022*	*LAYN*
T_{RS}	9	39,424,271 - 39,486,772	*ENSSSCG00000032941*	*SIK2*
T_{RS}	9	39,424,271 - 39,486,772	*ENSSSCG00000029538*	*PPP2R1B*
T_{RS}	9	39,453,846 - 39,486,772	*ENSSSCG00000015023*	*ALG9*
T_{RS}	9	39,195,933	*ENSSSCG00000023071*	*ssc-mir-34c-1*
T_{RS}	10	68,726,153 - 68,776,792	*ENSSSCG00000011162*	
T_{RS}	10	68,726,153 - 69,231,514	*ENSSSCG00000011163*	*DIP2C*
T_{RS}	10	69,069,560 - 69,352,432	*ENSSSCG00000011166*	*ZMYND11*
T_{RS}	10	68,726,153 - 68,752,585	*ENSSSCG00000052560*	

T_{RS}	10	68,726,153 - 68,776,792	*ENSSSCG00000042778*	
T_{RS}	10	68,726,153 - 68,776,792	*ENSSSCG00000056287*	
T_{RS}	10	51,870,599	*ENSSSCG00000030662*	*PTF1A*
T_{RS}	10	51,870,599 - 51,974,203	*ENSSSCG00000011077*	*MSRB2*
T_{RS}	10	51,870,599 - 51,974,203	*ENSSSCG00000011078*	*ARMC3*
T_{RS}	10	52,218,082 - 52,234,291	*ENSSSCG00000011079*	*PIP4K2A*
T_{RS}	10	52,218,082 - 52,234,291	*ENSSSCG00000045344*	
T_{RS}	10	51,403,771 - 51,438,887	*ENSSSCG00000057337*	
T_{RS}	10	51403771 - 51438887	*ENSSSCG00000062689*	
T_{RS}	10	51,403,771 - 51,438,887	*ENSSSCG00000053398*	
T_{RS}	10	51,412,141 - 51,438,887	*ENSSSCG00000063450*	
T_{RS}	10	52,218,082 - 52,234,291	*ENSSSCG00000018307*	*U6*
T_{RS}	11	16,776,240 - 16,792,168	*ENSSSCG00000047857*	*C13orf42*
T_{RS}	11	16,776,240 - 16,792,168	*ENSSSCG00000024765*	
T_{RS}	11	16,776,240 - 16,792,168	*ENSSSCG00000024385*	*RNASEH2B*
T_{RS}	11	17,051,800	*ENSSSCG00000009387*	*DLEU7*
T_{RS}	11	17,051,800	*ENSSSCG00000042045*	
T_{RS}	11	17,051,800	*ENSSSCG00000057141*	
T_{RS}	11	17,051,800	*ENSSSCG00000052173*	
T_{RS}	11	17,051,800	*ENSSSCG00000053383*	
T_{RS}	12	22,191,109	*ENSSSCG00000017471*	*CDC6*
T_{RS}	12	22,191,109	*ENSSSCG00000017479*	*WIPF2*
T_{RS}	12	22,191,109	*ENSSSCG00000017478*	*RAPGEFL1*
T_{RS}	12	22,191,109	*ENSSSCG00000017477*	*CASC3*
T_{RS}	12	22,191,109	*ENSSSCG00000052038*	
T_{RS}	12	22,191,109	*ENSSSCG00000017476*	*MSL1*
T_{RS}	12	22,191,109	*ENSSSCG00000036933*	*NR1D1*

T_{RS}	12	22,191,109	*ENSSSCG00000035969*	*THRA*
T_{RS}	13	204,671,997	*ENSSSCG00000012074*	
T_{RS}	13	204,671,997	*ENSSSCG00000012075*	*FAM3B*
T_{RS}	13	204,671,997	*ENSSSCG00000060594*	
T_{RS}	13	17,486,172 - 17,496,040	*ENSSSCG00000011229*	*STT3B*
T_{RS}	13	17,767,850	*ENSSSCG00000011230*	*OSBPL10*
T_{RS}	13	17,767,850	*ENSSSCG00000041659*	
T_{RS}	15	104,520,179	*ENSSSCG00000016093*	
T_{RS}	15	104,520,179	*ENSSSCG00000016094*	*BZW1*
T_{RS}	15	104,520,179	*ENSSSCG00000016095*	*CLK1*
T_{RS}	15	104,520,179	*ENSSSCG00000016096*	*PPIL3*
T_{RS}	15	104,520,179	*ENSSSCG00000039654*	*NIF3L1*
T_{RS}	15	104,520,179	*ENSSSCG00000016098*	*ORC2*
T_{RS}	15	104,520,179	*ENSSSCG00000060625*	
T_{SS}	2	95,628,544	*ENSSSCG00000014148*	*TMEM161B*
T_{SS}	2	95,628,544	*ENSSSCG00000061590*	
T_{SS}	2	95,628,544	*ENSSSCG00000053188*	
T_{SS}	2	95,628,544	*ENSSSCG00000051977*	
T_{SS}	2	107,776,212 - 107,959,085	*ENSSSCG00000014182*	*SLCO4C1*
T_{SS}	2	107,910,486 - 108,111,514	*ENSSSCG00000014183*	*SLCO6A1*
T_{SS}	2	108,067,180 - 108,272,377	*ENSSSCG00000054435*	
T_{SS}	2	108219460 - 108629684	*ENSSSCG00000014184*	*PAM*
T_{SS}	2	108,483,514 - 108,629,684	*ENSSSCG00000025287*	*GIN1*
T_{SS}	2	108,486,895 - 108,790,809	*ENSSSCG00000024999*	*PPIP5K2*
T_{SS}	2	108,713,184 - 108,852,710	*ENSSSCG00000038779*	*MACIR*
T_{SS}	2	108,810,693 - 109,062,401	*ENSSSCG00000014186*	
T_{SS}	2	108,948,208 - 109,156,427	*ENSSSCG00000014187*	*NUDT12*

T_{SS}	2	127,833,178	*ENSSSCG00000053601*	
T_{SS}	2	127,833,178	*ENSSSCG00000054233*	
T_{SS}	2	106,932,589 - 106,945,457	*ENSSSCG00000035539*	*ST8SIA4*
T_{SS}	2	108,713,184 - 108,903,430	*ENSSSCG00000049923*	
T_{SS}	2	105,870,529	*ENSSSCG00000054777*	
T_{SS}	2	106,932,589 - 107,004,443	*ENSSSCG00000042228*	
T_{SS}	2	107,268,832 - 107,452,342	*ENSSSCG00000045323*	
T_{SS}	2	107,945,395 - 108,130,080	*ENSSSCG00000053934*	
T_{SS}	2	108,629,684 - 108,806,409	*ENSSSCG00000042485*	
T_{SS}	2	108,964,268 - 109,160,103	*ENSSSCG00000053824*	
T_{SS}	2	108,964,268 - 109,160,103	*ENSSSCG00000058497*	
T_{SS}	2	109,005,900 -109,199,582	*ENSSSCG00000062896*	
T_{SS}	2	109,005,900 - 109,206,314	*ENSSSCG00000055779*	
T_{SS}	2	109080084 - 109284720	*ENSSSCG00000057887*	
T_{SS}	2	109,110,747 - 109,307,908	*ENSSSCG00000058355*	
T_{SS}	2	109,209,859 - 109,409,209	*ENSSSCG00000055932*	
T_{SS}	2	109,284,720 - 109,472,448	*ENSSSCG00000059317*	
T_{SS}	2	109,352,808 - 109,542,572	*ENSSSCG00000055792*	
T_{SS}	2	109,401,482 - 109,589,218	*ENSSSCG00000061911*	
T_{SS}	2	109,472,448 - 109,659,487	*ENSSSCG00000057965*	
T_{SS}	2	109,486,215 - 109,659,487	*ENSSSCG00000053102*	
T_{SS}	2	109,500,312 - 109,659,487	*ENSSSCG00000058010*	
T_{SS}	2	109,522,926 - 109,719,183	*ENSSSCG00000062992*	
T_{SS}	2	110,224,555 - 110,420,052	*ENSSSCG00000023111*	*U6*
T_{SS}	2	108,272,377 - 108,425,902	*ENSSSCG00000045807*	*U2*
T_{SS}	2	111,563,782 - 111,689,615	*ENSSSCG00000049466*	
T_{SS}	2	111,299,450 - 111,499,010	*ENSSSCG00000056998*	

T_{SS}	2	111,414,402 - 111,553,832	*ENSSSCG00000054209*	
T_{SS}	2	111,433,729 - 111,625,296	*ENSSSCG00000054276*	
T_{SS}	2	111,486,280 - 111,670,922	*ENSSSCG00000058903*	
T_{SS}	2	111,570,691 - 111,689,615	*ENSSSCG00000062919*	
T_{SS}	2	111,625,296 - 111,689,615	*ENSSSCG00000060138*	
T_{SS}	2	111,640,538 - 111,689,615	*ENSSSCG00000043847*	
T_{SS}	2	112,051,005	*ENSSSCG00000056485*	
T_{SS}	2	112,209,797 - 112,393,581	*ENSSSCG00000062819*	
T_{SS}	2	112,393,581	*ENSSSCG00000059572*	
T_{SS}	2	112,393,581	*ENSSSCG00000053625*	
T_{SS}	2	112,393,581	*ENSSSCG00000044646*	
T_{SS}	12	22,191,109	*ENSSSCG00000017471*	*CDC6*
T_{SS}	12	22,191,109	*ENSSSCG00000017479*	*WIPF2*
T_{SS}	12	22,191,109	*ENSSSCG00000017478*	*RAPGEFL1*
T_{SS}	12	22,191,109	*ENSSSCG00000017477*	*CASC3*
T_{SS}	12	22,191,109	*ENSSSCG00000052038*	
T_{SS}	12	22,191,109	*ENSSSCG00000017476*	*MSL1*
T_{SS}	12	22,191,109	*ENSSSCG00000036933*	*NR1D1*
T_{SS}	12	22,191,109	*ENSSSCG00000035969*	*THRA*
T_{SS}	16	64,692,816	*ENSSSCG00000017046*	*EBF1*
T_{SS}	16	64,692,816	*ENSSSCG00000061376*	
T_{SS}	1	10,473,872 - 10,505,848	*ENSSSCG00000056648*	
T_{SS}	1	10,473,872 - 10,505,848	*ENSSSCG00000061773*	
T_{SS}	1	10,473,872 - 10,505,848	*ENSSSCG00000045185*	*ssc-mir-9857*
T_{SS}	6	135,196,192	*ENSSSCG00000035582*	*GIPC2*
T_{SS}	6	135,196,192	*ENSSSCG00000003766*	*DNAJB4*
T_{SS}	6	135,196,192	*ENSSSCG00000003771*	*FUBP1*

T_{SS}	6	135,196,192	*ENSSSCG00000050806*	
T_{SS}	6	135,196,192	*ENSSSCG00000055126*	*U6*
T_{SS}	6	135,196,192	*ENSSSCG00000018423*	*U6*
T_{SS}	6	128,607,655	*ENSSSCG00000003754*	
T_{SS}	6	128,028,279 - 128,061,017	*ENSSSCG00000005778*	*HSBP1L1*
T_{SS}	6	128,028,279 - 128,061,017	*ENSSSCG00000005777*	*TXNL4A*
T_{SS}	6	127,822,624	*ENSSSCG00000005780*	*KCNG2*
T_{SS}	6	127,822,624 - 128,038,925	*ENSSSCG00000023171*	*SLC66A2*
T_{SS}	6	128,028,279 - 128,126,009	*ENSSSCG00000038475*	
T_{SS}	6	128,028,279 - 128,180,187	*ENSSSCG00000038632*	*ADNP2*
T_{SS}	6	128,096,745 - 128,349,869	*ENSSSCG00000023376*	*PARD6G*
T_{SS}	6	128,540,069 - 128,607,655	*ENSSSCG00000003753*	
T_{SS}	6	128,926,928 - 128,933,859	*ENSSSCG00000003755*	*MCOLN2*
T_{SS}	6	128,926,928 - 129,027,823	*ENSSSCG00000003756*	*LPAR3*
T_{SS}	6	128,961,716 - 129,210,420	*ENSSSCG00000003757*	*SSX2IP*
T_{SS}	6	128,975,440 - 129,150,250	*ENSSSCG00000044786*	
T_{SS}	6	129,106,033 - 129,303,560	*ENSSSCG00000003758*	*CTBS*
T_{SS}	6	129,106,033 - 129,338,493	*ENSSSCG00000029882*	*SPATA1*
T_{SS}	6	129,149,710 - 129,348,946	*ENSSSCG00000053185*	*GNG5*
T_{SS}	6	129,192,451 - 129,363,499	*ENSSSCG00000022145*	*RPF1*
T_{SS}	6	129,279,850 - 129,363,499	*ENSSSCG00000026532*	*DNASE2B*
T_{SS}	6	129,298,592 - 129,363,499	*ENSSSCG00000026005*	*SAMD13*
T_{SS}	6	129,301,918 - 129,363,499	*ENSSSCG00000044862*	
T_{SS}	6	128,506,422 - 128,607,655	*ENSSSCG00000060282*	
T_{SS}	6	125,685,780	*ENSSSCG00000055429*	
T_{SS}	6	126,631,171 - 126,808,755	*ENSSSCG00000057422*	
T_{SS}	6	127,822,624	*ENSSSCG00000055983*	

T_{SS}	6	128,038,925 - 128,180,187	*ENSSSCG00000063496*	
T_{SS}	6	128,061,017 - 128,180,187	*ENSSSCG00000055757*	
T_{SS}	6	128,318,719 - 128,362,537	*ENSSSCG00000063050*	
T_{SS}	6	129,279,850 - 129,363,499	*ENSSSCG00000022206*	*UOX*
T_{SS}	8	134,856,930 - 135,049,023	*ENSSSCG00000009233*	*GPAT3*
T_{SS}	8	134,974,704 - 135,049,023	*ENSSSCG00000009234*	*ABRAXAS1*
T_{SS}	8	134,974,704 - 135,049,023	*ENSSSCG00000038042*	*MRPS18C*
T_{SS}	8	134,974,704 - 135,049,023	*ENSSSCG00000009236*	*HELQ*
T_{SS}	8	135,028,616 - 135,049,023	*ENSSSCG00000051849*	
T_{SS}	8	135,049,023	*ENSSSCG00000009238*	*COQ2*
T_{SS}	8	134,856,930 - 134,860,931	*ENSSSCG00000056871*	
T_{SS}	8	134,974,704 - 135,049,023	*ENSSSCG00000047350*	
T_{SS}	8	135,028,616 - 135,049,023	*ENSSSCG00000047440*	
T_{SS}	8	135,028,616 - 135,049,023	*ENSSSCG00000009237*	*HPSE*
T_{SS}	8	4,960,712	*ENSSSCG00000035020*	*STK32B*
T_{SS}	8	4,906,107 - 4,960,712	*ENSSSCG00000032637*	*EVC*
T_{SS}	8	4,906,107 - 4,960,712	*ENSSSCG00000024399*	*EVC2*
T_{SS}	9	39,195,933	*ENSSSCG00000015016*	*POU2AF1*
T_{SS}	9	39,195,933	*ENSSSCG00000015020*	*BTG4*
T_{SS}	9	39,195,933	*ENSSSCG00000015021*	*HOATZ*
T_{SS}	9	39,424,271	*ENSSSCG00000015022*	*LAYN*
T_{SS}	9	39,424,271 - 39,486,772	*ENSSSCG00000032941*	*SIK2*
T_{SS}	9	39,424,271 - 39,486,772	*ENSSSCG00000029538*	*PPP2R1B*
T_{SS}	9	39,453,846 - 39,486,772	*ENSSSCG00000015023*	*ALG9*
T_{SS}	9	39,195,933	*ENSSSCG00000023071*	*ssc-mir-34c-1*
T_{SS}	10	68,726,153 - 68,776,792	*ENSSSCG00000011162*	
T_{SS}	10	68,726,153 - 69,231,514	*ENSSSCG00000011163*	*DIP2C*

T_{SS}	10	69,069,560 - 69,352,432	*ENSSSCG00000011166*	*ZMYND11*
T_{SS}	10	68,726,153 - 68,752,585	*ENSSSCG00000052560*	
T_{SS}	10	68,726,153 - 68,776,792	*ENSSSCG00000042778*	
T_{SS}	10	68,726,153 - 68,776,792	*ENSSSCG00000056287*	
T_{SS}	10	51,870,599	*ENSSSCG00000030662*	*PTF1A*
T_{SS}	10	51,870,599 - 51,974,203	*ENSSSCG00000011077*	*MSRB2*
T_{SS}	10	51,870,599 - 51,974,203	*ENSSSCG00000011078*	*ARMC3*
T_{SS}	10	52,218,082 - 52,234,291	*ENSSSCG00000011079*	*PIP4K2A*
T_{SS}	10	52,218,082 - 52,234,291	*ENSSSCG00000045344*	
T_{SS}	10	51,412,141 - 51,438,887	*ENSSSCG00000057337*	
T_{SS}	10	51,412,141 - 51,438,887	*ENSSSCG00000062689*	
T_{SS}	10	51,412,141 - 51,438,887	*ENSSSCG00000053398*	
T_{SS}	10	51,412,141 - 51,438,887	*ENSSSCG00000063450*	
T_{SS}	10	52,218,082 - 52,234,291	*ENSSSCG00000018307*	*U6*
T_{SS}	11	16,776,240 - 16,792,168	*ENSSSCG00000047857*	*C13orf42*
T_{SS}	11	16,776,240 - 16,792,168	*ENSSSCG00000024765*	
T_{SS}	11	16,776,240 - 16,792,168	*ENSSSCG00000024385*	*RNASEH2B*
T_{SS}	11	17,051,800	*ENSSSCG00000009387*	*DLEU7*
T_{SS}	11	17,051,800	*ENSSSCG00000042045*	
T_{SS}	11	17,051,800	*ENSSSCG00000057141*	
T_{SS}	11	17,051,800	*ENSSSCG00000052173*	
T_{SS}	11	17,051,800	*ENSSSCG00000053383*	
T_{SS}	13	17,486,172 - 17,496,040	*ENSSSCG00000011229*	*STT3B*
T_{SS}	15	104,520,179	*ENSSSCG00000016093*	
T_{SS}	15	104,520,179	*ENSSSCG00000016094*	*BZW1*
T_{SS}	15	104,520,179	*ENSSSCG00000016095*	*CLK1*
T_{SS}	15	104,520,179	*ENSSSCG00000016096*	*PPIL3*

T_{SS}	15	104,520,179	*ENSSSCG00000039654*	*NIF3L1*
T_{SS}	15	104,520,179	*ENSSSCG00000016098*	*ORC2*
T_{SS}	15	104,520,179	*ENSSSCG00000060625*	
T_{TS}	6	128,607,655	*ENSSSCG00000003754*	
T_{TS}	6	128,028,279 - 128,061,017	*ENSSSCG00000005778*	*HSBP1L1*
T_{TS}	6	128,028,279 - 128,061,017	*ENSSSCG00000005777*	*TXNL4A*
T_{TS}	6	125,900,303 - 125,909,608	*ENSSSCG00000003749*	*PIK3C3*
T_{TS}	6	127,822,624	*ENSSSCG00000005780*	*KCNG2*
T_{TS}	6	127,822,624 - 128,038,925	*ENSSSCG00000023171*	*SLC66A2*
T_{TS}	6	128,028,279 - 128,126,009	*ENSSSCG00000038475*	
T_{TS}	6	128,028,279 - 128,180,187	*ENSSSCG00000038632*	*ADNP2*
T_{TS}	6	128,096,745 - 128,349,869	*ENSSSCG00000023376*	*PARD6G*
T_{TS}	6	128,540,069 - 128,607,655	*ENSSSCG00000003753*	
T_{TS}	6	128,926,928 - 128,933,859	*ENSSSCG00000003755*	*MCOLN2*
T_{TS}	6	128,926,928 - 129,027,823	*ENSSSCG00000003756*	*LPAR3*
T_{TS}	6	128,961,716 - 129,210,420	*ENSSSCG00000003757*	*SSX2IP*
T_{TS}	6	128,975,440 - 129,150,250	*ENSSSCG00000044786*	
T_{TS}	6	129,106,033 - 129,303,560	*ENSSSCG00000003758*	*CTBS*
T_{TS}	6	129,106,033 - 129,338,493	*ENSSSCG00000029882*	*SPATA1*
T_{TS}	6	129,149,710 - 129,348,946	*ENSSSCG00000053185*	*GNG5*
T_{TS}	6	129,192,451 - 129,363,499	*ENSSSCG00000022145*	*RPF1*
T_{TS}	6	129,279,850 - 129,363,499	*ENSSSCG00000026532*	*DNASE2B*
T_{TS}	6	129,298,592 - 129,363,499	*ENSSSCG00000026005*	*SAMD13*
T_{TS}	6	129,301,918 - 129,363,499	*ENSSSCG00000044862*	
T_{TS}	6	128,506,422 - 128,607,655	*ENSSSCG00000060282*	
T_{TS}	6	125,685,780	*ENSSSCG00000055429*	
T_{TS}	6	126,631,171 - 126,808,755	*ENSSSCG00000057422*	

T_{TS}	6	127,822,624	*ENSSSCG00000055983*	
T_{TS}	6	128,038,925 - 128,180,187	*ENSSSCG00000063496*	
T_{TS}	6	128,061,017 - 128,180,187	*ENSSSCG00000055757*	
T_{TS}	6	128,318,719 - 128,362,537	*ENSSSCG00000063050*	
T_{TS}	6	129,279,850 - 129,363,499	*ENSSSCG00000022206*	*UOX*
T_{TS}	15	25,570,481 - 25,570,891	*ENSSSCG00000050390*	
T_{TS}	15	25,570,481 - 25,570,891	*ENSSSCG00000040701*	*GYPC*
T_{TS}	15	25,570,481 - 25,570,891	*ENSSSCG00000060468*	
T_{TS}	15	25,570,481 - 25,570,891	*ENSSSCG00000061010*	
T_{TS}	4	72,028,076 - 72,045,767	*ENSSSCG00000025087*	*ASPH*
T_{TS}	4	72,028,076 -72,045,767	*ENSSSCG00000006230*	*CLVS1*
T_{V8h}	2	99,041,870 - 99,069,820	*ENSSSCG00000046245*	
T_{V8h}	2	97,508,070 - 97,680,472	*ENSSSCG00000014151*	*CETN3*
T_{V8h}	2	97,546,945 - 97,710,223	*ENSSSCG00000014152*	*MBLAC2*
T_{V8h}	2	97,560,134 - 97,710,223	*ENSSSCG00000026233*	
T_{V8h}	2	97,607,971 - 97,710,223	*ENSSSCG00000024193*	*LYSMD3*
T_{V8h}	2	97,637,824 - 98,213,679	*ENSSSCG00000035025*	*ADGRV1*
T_{V8h}	2	98,619,839	*ENSSSCG00000056856*	
T_{V8h}	2	100,350,673 - 100,545,358	*ENSSSCG00000014157*	*NR2F1*
T_{V8h}	2	100,545,358 - 100,948,637	*ENSSSCG00000027608*	*FAM172A*
T_{V8h}	2	94,855,585 - 95,014,810	*ENSSSCG00000014146*	*RASA1*
T_{V8h}	2	94,938,876 - 95,096,326	*ENSSSCG00000014147*	*CCNH*
T_{V8h}	2	94,938,876 - 95,096,326	*ENSSSCG00000048763*	
T_{V8h}	2	95,549,933 - 95,770,145	*ENSSSCG00000014148*	*TMEM161B*
T_{V8h}	2	96,027,967 - 96,372,331	*ENSSSCG00000014149*	*MEF2C*
T_{V8h}	2	96,027,967 - 96,197,993	*ENSSSCG00000050823*	
T_{V8h}	2	95,014,810 - 95,096,326	*ENSSSCG00000052426*	

T_{V8h}	2	95,266,233 - 95,446,118	*ENSSSCG00000052480*
T_{V8h}	2	95,286,846 - 95,446,118	*ENSSSCG00000055619*
T_{V8h}	2	95,352,071 - 95,549,933	*ENSSSCG00000054377*
T_{V8h}	2	95,435,801 - 95,549,933	*ENSSSCG00000044415*
T_{V8h}	2	95,500,013 - 95,549,933	*ENSSSCG00000061590*
T_{V8h}	2	95,549,933 - 95,679,479	*ENSSSCG00000053188*
T_{V8h}	2	95,549,933 - 95,679,479	*ENSSSCG00000051977*
T_{V8h}	2	95,770,145 - 95,859,076	*ENSSSCG00000058079*
T_{V8h}	2	95,770,145 - 95,941,838	*ENSSSCG00000038476*
T_{V8h}	2	95,770,145 - 95,953,423	*ENSSSCG00000060814*
T_{V8h}	2	95,859,076 - 96,041,647	*ENSSSCG00000063280*
T_{V8h}	2	95,941,838 - 96,041,647	*ENSSSCG00000055379*
T_{V8h}	2	95,941,838 - 96,041,647	*ENSSSCG00000060171*
T_{V8h}	2	95,941,838 - 96,077,373	*ENSSSCG00000059644*
T_{V8h}	2	95,941,838 - 96,077,373	*ENSSSCG00000056869*
T_{V8h}	2	95,941,838 - 96,077,373	*ENSSSCG00000056397*
T_{V8h}	2	95,941,838 - 96,077,373	*ENSSSCG00000053066*
T_{V8h}	2	96,027,967 - 96,137,988	*ENSSSCG00000062861*
T_{V8h}	2	96,027,967 - 96,190,298	*ENSSSCG00000041042*
T_{V8h}	2	96,027,967 - 96,190,298	*ENSSSCG00000057405*
T_{V8h}	2	96,027,967 - 96,197,993	*ENSSSCG00000059257*
T_{V8h}	2	96,249,140 - 96,372,331	*ENSSSCG00000049322*
T_{V8h}	2	96,349,263 - 96,440,983	*ENSSSCG00000046941*
T_{V8h}	2	96,417,792 - 96,579,517	*ENSSSCG00000052751*
T_{V8h}	2	96,579,517 - 96,763,009	*ENSSSCG00000062254*
T_{V8h}	2	96,645,000 - 96,763,009	*ENSSSCG00000060605*
T_{V8h}	2	96,852,755 - 96,969,360	*ENSSSCG00000055741*

T_{V8h}	2	97,108,989 - 97,304,972	*ENSSSCG00000057810*
T_{V8h}	2	97,208,065 - 97,357,185	*ENSSSCG00000041572*
T_{V8h}	2	97,508,070 - 97,560,134	*ENSSSCG00000054994*
T_{V8h}	2	97,508,070 - 97,637,824	*ENSSSCG00000041183*
T_{V8h}	2	97,508,070 - 97,653,371	*ENSSSCG00000053092*
T_{V8h}	2	97,546,945 - 97,710,223	*ENSSSCG00000060756*
T_{V8h}	2	98,213,679	*ENSSSCG00000058343*
T_{V8h}	2	98,619,839	*ENSSSCG00000053095*
T_{V8h}	2	98,619,839	*ENSSSCG00000056205*
T_{V8h}	2	99,041,870 - 99,069,820	*ENSSSCG00000055008*
T_{V8h}	2	99,492,485	*ENSSSCG00000057995*
T_{V8h}	2	99,492,485 - 99,531,694	*ENSSSCG00000061085*
T_{V8h}	2	99,492,485 - 99,531,694	*ENSSSCG00000055903*
T_{V8h}	2	99,492,485 - 99,577,410	*ENSSSCG00000060099*
T_{V8h}	2	99,492,485 - 99,599,185	*ENSSSCG00000058507*
T_{V8h}	2	99,492,485 - 99,599,185	*ENSSSCG00000053794*
T_{V8h}	2	99,712,712 - 99,852,196	*ENSSSCG00000057162*
T_{V8h}	2	99,777,237 - 99,899,912	*ENSSSCG00000059147*
T_{V8h}	2	99,777,237 - 99,940,212	*ENSSSCG00000056823*
T_{V8h}	2	99,798,826 - 99,984,716	*ENSSSCG00000062174*
T_{V8h}	2	99,852,196 - 100,037,326	*ENSSSCG00000053056*
T_{V8h}	2	99,899,912 - 100,063,240	*ENSSSCG00000054919*
T_{V8h}	2	99,899,912 - 100,096,616	*ENSSSCG00000061177*
T_{V8h}	2	99,932,721 - 100,134,231	*ENSSSCG00000057342*
T_{V8h}	2	100,127,129 - 100,326,888	*ENSSSCG00000052594*
T_{V8h}	2	100,241,628 - 100,350,673	*ENSSSCG00000061981*
T_{V8h}	2	100,241,628 - 100,369,091	*ENSSSCG00000059319*

T_{V8h}	2	100,241,628 - 100,369,091	*ENSSSCG00000059056*	
T_{V8h}	2	100,913,881 - 100,948,637	*ENSSSCG00000014161*	*KIAA0825*
T_{V8h}	2	100,241,628 - 100,369,091	*ENSSSCG00000055599*	
T_{V8h}	2	100,241,628 - 100,369,091	*ENSSSCG00000056188*	
T_{V8h}	2	100,326,888 - 100,369,091	*ENSSSCG00000048883*	
T_{V8h}	2	100,326,888 - 100,369,091	*ENSSSCG00000061218*	
T_{V8h}	2	96,197,993 - 96,515,110	*ENSSSCG00000035571*	
T_{V8h}	2	100,241,628 - 100,369,091	*ENSSSCG00000051601*	
T_{V8h}	2	98,213,679 - 95,549,933	*ENSSSCG00000061809*	*U6*
T_{V8h}	2	96,027,967 -96,137,988	*ENSSSCG00000018888*	
T_{V8h}	2	102,014,302	*ENSSSCG00000025286*	*MCTP1*
T_{V8h}	2	102,014,302 - 102,148,280	*ENSSSCG00000026175*	*FAM81B*
T_{V8h}	2	102,014,302 - 102,222,267	*ENSSSCG00000014165*	
T_{V8h}	2	102,064,911 - 102,222,267	*ENSSSCG00000014139*	*ARSK*
T_{V8h}	2	102,145,110 - 102,222,267	*ENSSSCG00000014141*	*RFESD*
T_{V8h}	2	102,168,428 - 102,387,102	*ENSSSCG00000030114*	*SPATA9*
T_{V8h}	2	102,387,102 - 102,489,498	*ENSSSCG00000029805*	*RHOBTB3*
T_{V8h}	2	102,387,102 - 102,489,498	*ENSSSCG00000039731*	
T_{V8h}	2	102,430,205 - 102,489,498	*ENSSSCG00000014168*	*ELL2*
T_{V8h}	2	102,133,556 - 102,222,267	*ENSSSCG00000014140*	*GPR150*
T_{V8h}	2	86,854,220	*ENSSSCG00000034241*	
T_{V8h}	2	86,854,220	*ENSSSCG00000014101*	*AP3B1*
T_{Vall}	1	32,189,900 - 32,189,900	*ENSSSCG00000036790*	*AKAP7*

1092

1093 **Table S3.** Functional analysis for the genes annotated based on GWAs results using whole genome sequence data

Trait	Category	Term	Count	p-value	Genes
EA	Pathway	ssc04659: Th17 cell differentiation	2	0.0477	*HSP90AB1, NFKBIE*
RR	Biological process	GO:0042026 protein refolding	2	0.0322	*ENSSSCG00000029160, HSPA1L*
RR	Biological process	GO:0034620 cellular response to unfolded protein	2	0.0390	*ENSSSCG00000029160, HSPA1L*
RR	Biological process	GO:0007130 synaptonemal complex assembly	2	0.0412	*BAG6, EHMT2*
RR	Biological process	GO:0006402 mRNA catabolic process	2	0.0412	*LSM2, DXO*
RR	Biological process	GO:0051085 chaperone mediated protein folding requiring cofactor	2	0.0546	*ENSSSCG00000029160, HSPA1L*
RR	Biological process	GO:0006958 complement activation, classical pathway	2	0.0765	*C4A, C2*
RR	Cellular component	GO:0016020 membrane	6	0.0503	*SLC44A4, NEU1, ABHD16A, CYP21A2, BAG6, ENSSSCG00000039071*

					LY6G6D, ENSSSCG00000029160, HSPA1L, MPIG6B, SLC44A4, NEU1, PRRC2A, DXO, LY6G6F, EDNRA, NELFE, ENSSSCG00000039071, ENSSSCG00000040885
RR	Cellular component	GO:0005886 plasma membrane	13	0.0844	
RR	Molecular function	GO:0051787 misfolded protein binding	3	0.0010	*BAG6, ENSSSCG00000029160, HSPA1L*
RR	Molecular function	GO:0016597 amino acid binding	2	0.0171	*AARS2, DDAH2*
RR	Molecular function	GO:0002161 aminoacyl-tRNA editing activity	2	0.0214	*AARS2, VARS1*
RR	Molecular function	GO:0005496 steroid binding	2	0.0298	*CYP21A2, NR3C2*
RR	Molecular function	GO:0044183 protein binding involved in protein folding	2	0.0689	*ENSSSCG00000029160, HSPA1L*
RR	Molecular function	GO:0031072 heat shock protein binding	2	0.0729	*ENSSSCG00000029160, HSPA1L*
RR	Molecular function	GO:0031625 ubiquitin protein ligase binding	3	0.0852	*BAG6, ENSSSCG00000029160, HSPA1L*

RR	Pathway	ssc04610: Complement and coagulation cascades	3	0.0130	*CFB, C4A, C2*
RR	Pathway	ssc05150: Staphylococcus aureus infection	3	0.0169	*CFB, C4A, C2*
RR	Pathway	ssc03040: Spliceosome	3	0.0295	*LSM2, HSPA1L, CDC5L*
RR	Pathway	ssc00970: Aminoacyl-tRNA biosynthesis	2	0.0940	*AARS2, VARS1*
T_{ES}	Biological process	GO:0006821 chloride transport	2	0.0523	*ANO4, TTYH2*
T_{ES}	Biological process	GO:0007018 microtubule-based movement	2	0.0674	*KIF19, DNAI2*
T_{ES}	Biological process	GO:0007605 sensory perception of sound	2	0.0849	*CEMIP, RPL38*
T_{ES}	Molecular function	GO:0005229 intracellular calcium activated chloride channel activity	2	0.0182	*ANO4, TTYH2*
T_{ES}	Molecular function	GO:0003777 microtubule motor activity	2	0.0444	*KIF19, DNAI2*

		GO:0005254 chloride channel			
T_{ES}	Molecular function	activity	2	0.0454	*ANO4, TTYH2*
T_{RS}	Biological process	GO:0006486 protein glycosylation	3	0.0697	*STT3B, ST8SIA4, ALG9*
		GO:0098797 plasma membrane			
T_{RS}	Cellular component	protein complex	2	0.0308	*EVC2, EVC*
					NR1D1, THRA, ADNP2, NIF3L1, PIP4K2A,
					MRPS18C, ORC2, EBF1, NUDT12, CLK1, CDC6,
					SAMD13, PARD6G, EVC2, RNASEH2B, HSBP1L1,
T_{RS}	Cellular component	GO:0005634 nucleus	19	0.0387	*ABRAXAS1, HELQ, FUBP1*
		GO:0005763 mitochondrial small			
T_{RS}	Cellular component	ribosomal subunit	2	0.0736	*MRPS18C, ABRAXAS1*
		GO:0070181 small ribosomal			
T_{RS}	Molecular function	subunit rRNA binding	2	0.0271	*MRPS18C, ABRAXAS1*
		GO:0003688 DNA replication			
T_{RS}	Molecular function	origin binding	2	0.0437	*ORC2, CDC6*

					STT3B, COQ2, UOX, ALG9, NUDT12, ENSSSCG00000016093, GPAT3, ENSSSCG00000003754, ENSSSCG00000024765,
T_{RS}	Pathway	ssc01100:Metabolic pathways	11	0.0486	*PIP4K2A, HPSE*
T_{SS}	Biological process	GO:0006486 protein glycosylation	3	0.0697	*STT3B, ST8SIA4, ALG9*
T_{SS}	Cellular component	GO:0098797 plasma membrane protein complex	2	0.0308	*EVC2, EVC*
T_{SS}	Cellular component	GO:0005634 nucleus	19	0.0387	*NR1D1, THRA, ADNP2, NIF3L1, PIP4K2A, MRPS18C, ORC2, EBF1, NUDT12, CLK1, CDC6, SAMD13, PARD6G, EVC2, RNASEH2B, HSBP1L1, ABRAXAS1, HELQ, FUBP1*
T_{SS}	Cellular component	GO:0005763 mitochondrial small ribosomal subunit	2	0.0736	*MRPS18C, ABRAXAS1*
T_{SS}	Molecular function	GO:0070181 small ribosomal subunit rRNA binding	2	0.0271	*MRPS18C, ABRAXAS1*

T_{SS}	Molecular function	GO:0003688 DNA replication origin binding	2	0.0437	*ORC2, CDC6*
T_{TS}	Biological process	GO:0007098 centrosome cycle	2	0.0275	*SSX2IP, PARD6G*
T_{TS}	Cellular component	GO:0005777 peroxisome	2	0.0788	*UOX, PIK3C3*
T_{V8h}	Biological process	GO:0045944 positive regulation of transcription from RNA polymerase II promoter	3	0.0817	*MEF2C, AP3B1, NR2F1*

1094

CHAPTER 4: Genome-wide detection of copy number variation and association study with physiological and anatomical indicators of heat stress response in lactating sows

Abstract

Background: Indicators of heat stress (HS) response are heritable, but of polygenic nature and complex inheritance. In this context, copy number variation (CNV) are important genomic structural variation that could be linked to climatic adaptation by influencing the phenotypic variability of traits related to thermal stress and disease resistance in animals. Therefore, the primary objectives of this study were to detect CNVs and CNV regions (CNVRs) in pigs and explore their associations with physiological and anatomical indicators of HS response measured in crossbred (Large White x Landrace) lactating sows.

Results: A total of 4,184 autosomal genome CNVs (4,012 deletion and 172 duplication) were detected in 969. CNVRs were identified by merging CNVs with at least 1bp overlap, which enabled the identification of 236 autosomal CNVRs. Twelve CNVRs were shared by at least 5% of the population. These association analyses led to the identification of 15 CNVR significantly associated with ear skin temperature (T_{ES}), rump skin temperature (T_{RS}), tail skin temperature (T_{TS}) and vaginal temperature measured at 16:00 h (T_{V16h}). Two CNVRs were significantly associated with T_{ES}, one with T_{RS}, 12 with T_{TS}, and one with T_{V16h}. A total of 291 genes overlapped within the CNVRs associated with the traits. The functional analyses of the significant regions revealed genes associated with immune response that may influence climatic resilience in lactating sows. Additionally,

quantitative trait loci (QTL) overlapping with the CNVRs identified are related with meat and carcass traits, which are key economically relevant traits in the pig industry.

Conclusions: Various CNVs and CNVRs were identified in the genome of a crossbred pig population. Fifteen CNVRs were significantly associated with physiological and anatomical indicators of HS response in lactating sows. Several genes involved in immune and stress responses overlap with the CNVRs, suggesting that the identified CNVRs might climatic resilience in pigs during the lactation stage. The findings of this study contribute to the understanding of the genetic architecture of HS response in lactating sows.

Background

Copy number variation (CNV) are genomic structural variations of segments of DNA that are 1 kilobase (kb) or larger and are present at a variable copy number compared to a reference genome [1]. CNVs can be categorized into insertions, deletions, and duplications [1]. CNV is often considered a form of mutation that arises through replication defects, with transcription interfering with replication fork progression and stability, leading to increased mutation rates at highly transcribed loci [2]. However, CNV is a source of genetic variation that can modify the level of gene expression within and near the rearranged region, and consequently, resulting in phenotypic variability on the traits influenced by those genes [3]. Paudel et al. [4] reported CNV regions (CNVRs) in European wild boars, European domestics pigs, Asian wild boars and five Asian domestics pigs, which were enriched with genes related to sensory perception, neurological processes, and response to stimulus. These findings suggested that the CNVRs identified could be related to adaptation in the wild and behavioral changes during the pig domestication. Kumar et al. [5] evaluating Tharparkar cattle, an indicus

50 breed, reported genes within CNVRs potentially involved in biological processes related
51 to indigenous cattle's adaptability and disease resistance.

52 These studies are evidence that CNVs are involved in environmental adaptation
53 by regulating traits related to stress tolerance, disease resistance, and key physiological
54 functions [4, 6–10]. For instance, CNVs have been reported to be related to local
55 adaptation to cold water, temperature, and reproductive isolation in Capelin fish
56 (*Mallotus villosus*) populations [9], adaptation to high temperature and humidity in horses
57 [11], and in adaptation to tropical environments, including heat stress (HS), disease
58 resistance, and feed scarcity in cattle [12]. Although there are studies investigating CNVs
59 in pigs (e.g., [13–16]), there is lack of studies investigating the relationship between
60 CNVs and HS resilience in pigs, especially during lactation (one of the most
61 environmental sensitive stages of pig production).

62 Understanding the genetic background of HS response in pigs could provide
63 valuable insights for breeding more thermal resilient animals. This has become more
64 relevant in recent years due to global warming as HS directly affects animal welfare and
65 productivity [17]. Investigating the association of CNVs with physiological and
66 anatomical indicators of HS response could provide insights into the genetic mechanisms
67 underlying climatic resilience in pigs. Therefore, our primary objectives were to: 1) detect
68 copy number variations (CNVs) and copy number variation regions (CNVRs) in a
69 crossbred (Large White x Landrace) population, and 2) investigate the potential
70 associations between the identified CNVRs and various physiological and anatomical
71 indicators of HS response in lactating sows.

72

Results

Overview

We performed CNV detection based on data from 1,639 lactating sows genotyped using the PorcineSNP50K Bead Chip (Illumina, San Diego, CA, USA) using the PennCNV software [18]. CNVs with at least a 1 bp overlap were merged to define the CNVRs. We investigated the genes and quantitative trait loci (QTL) overlapping with CNVRs present in at least 5% of the population. Furthermore, we investigated the association of the CNVRs with physiological and anatomical indicators of HS response in lactating sows. The physiological indicators of HS evaluated were ear skin temperature (T_{ES}), shoulder skin temperature (T_{SS}), rump skin temperature (T_{RS}), tail skin temperature (T_{TS}), respiration rate (RR), panting score (PS), vaginal temperature automatically measured at every 10 minutes (T_{Vall}), the average of the six records per hour corresponding to 08:00, 12:00, 16:00, and 20:00 hours during four days (T_{V4days}), and single record corresponding to 08:00, 12:00, 16:00, and 20:00 hours measured at the first day of collection (T_{V8h}, T_{V12h}, T_{V16h}, T_{V20h}, respectively). The anatomical traits evaluated were hair density score (HD), body size score (BS), body condition score (BCS) using a sow caliper (BCS_{cal}), visual BCS (BCS_{vis}), ear length (EL), and ear area (EA).

CNV and CNVR detection

A total of 8,270 CNVs were detected in 1,485 samples for autosomal chromosomes. After the quality control, 4,184 CNVs (4,012 deletion and 172 duplication) for 969 animals remained for subsequent analyses. The number of CNVs in autosomal chromosomes per individual ranged from 1 to 17 with an average (SD) of 4.32 (2.86) CNVs per individual. The minimum number of CNVs per chromosome across all samples was 50, which was for chromosomes 7 and 18. On the other hand, the highest number of

CNVs per chromosome across all samples was observed in chromosome 15 (627 individual CNVs). The length of the CNVs ranged from 2,646 bp to 1,352,876 bp with an average (SD) length of 170,292.4 (137,912.2) bp.

All 4,184 CNVs remaining after quality control were used to infer CNVR by merging CNV with at least 1bp overlap. After merging, we observed 399 CNVRs. However, 163 CNVRs were removed from subsequent analyses due to being observed in only one sample. A total of 236 CNVRs (Table S1), including 201 CNVRs classified as loss type, 30 gain, and five mixed patterns (i.e., the same chromosomal segment was a deletion or duplication in different samples) (Figure 1). The length of the CNVRs ranged from 14,161 bp to 1,938,601 bp with an average (SD) length of 249,698.9 (276,298.7) bp. The lowest number of CNVR per chromosome was observed for chromosome 18, which presented four CNVRs covering 1.18% of the chromosome. The chromosome 2 had the highest number of CNVRs per chromosome (n = 26) covering 3.56% of its length (Table 1). The chromosome 11 presented the highest CNVR coverage of a chromosome sequence (5.62%) with 14 CNVRs. The total number of CNVRs inferred in the autosomal chromosomes covered 58,928,942 bp, which corresponds to 2.60% of the pig autosomal genome size. At least 5% (80 animals) of the population studied shared 12 CNVRs (Table 2).

Table 1. Summary of copy number variation regions (CNVRs) detected in autosomal chromosomes

Chr[a]	Chr length (bp)	Number of CNVR	CNVR length (bp)	Coverage (%)[b]
chr1	274,330,532	25	3,803,364	1.39
chr2	151,935,994	26	5,410,473	3.56

chr3	132,848,913	11	2,826,150	2.13
chr4	130,910,915	11	2,692,015	2.06
chr5	104,526,007	16	4,931,129	4.72
chr6	170,843,587	6	2,055,133	1.20
chr7	121,844,099	9	1,812,412	1.49
chr8	138,966,237	8	1,165,734	0.84
chr9	139,512,083	13	1,729,061	1.24
chr10	69,359,453	7	1,224,889	1.77
chr11	79,169,978	14	4,452,633	5.62
chr12	61,602,749	9	3,044,686	4.94
chr13	208,334,590	21	5,224,056	2.51
chr14	141,755,446	20	6,463,588	4.56
chr15	140,412,725	19	5,833,526	4.15
chr16	79,944,280	12	4,002,490	5.01
chr17	63,494,081	5	1,599,001	2.52
chr18	55,982,971	4	658,602	1.18
Total	**2,265,774,640**	**236**	**58,928,942**	**2.60**

[a]Chromosome

[b]Percentage of the chromosome covered by the copy number variation regions.

119 **Table 2.** Copy number variation regions in autosomal chromosomes observed in at least
120 5% of the population

CNVR[a]	**Chr[b]**	**Start (bp)**	**End (bp)**	**Type**	**N[c]**
CNVR21	2	1,111	632,707	Loss	202
CNVR68	6	1,033,257	1,281,226	Loss	101

CNVR72	6	132,124,953	132,543,418	Mixed	139
CNVR82	8	123,960,362	124,128,258	Loss	95
CNVR101	11	46,563,594	46,642,716	Loss	90
CNVR103	11	59,735,869	61,470,768	Mixed	203
CNVR109	12	60,100	1,998,701	Mixed	93
CNVR122	13	194,665,680	196,342,442	Loss	108
CNVR149	14	151,966,127	153,374,972	Loss	80
CNVR150	15	9,519,813	10,711,345	Loss	245
CNVR151	15	12,597,728	12,844,713	Loss	80
CNVR174	17	2,202,762	2,730,970	Loss	184

[a]Copy number variation region

[b]Chromosome

[c]Number of animals with the CNVR

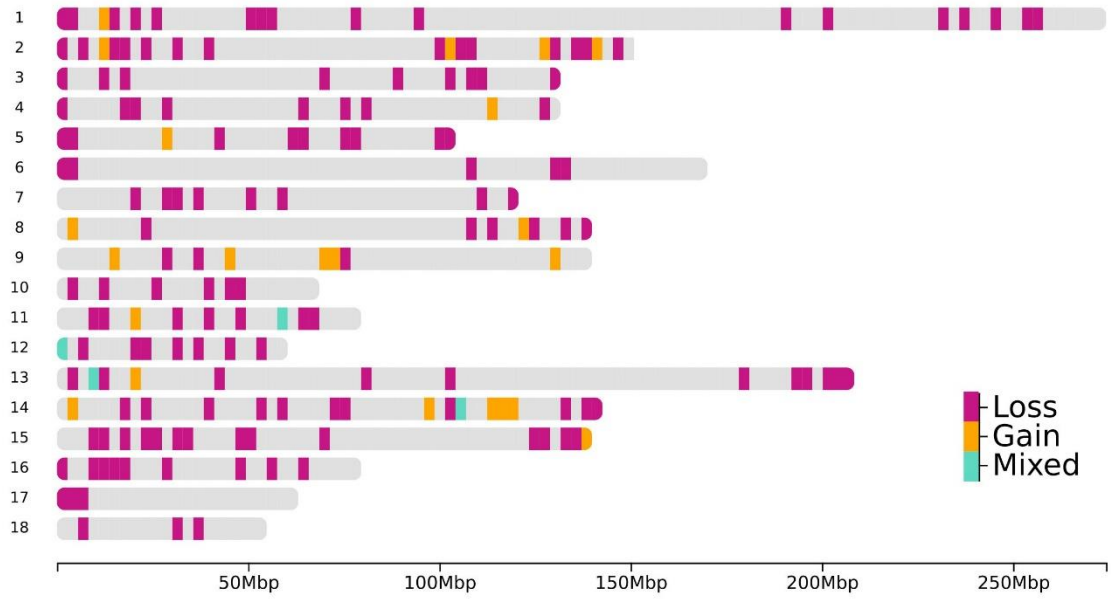

Figure 1. Distribution of copy number variation regions (loss, gain, and mixed type) across autosomal chromosomes

125 After identifying the CNVRs present in at least 5% of the population, we
126 performed gene and QTL annotation of these genomic regions. Three genes and 10 QTL
127 were annotated for CNVR150 (n = 245), nine genes and 38 QTL for CNVR103 (n = 203),
128 53 genes and 143 QTL for CNVR21 (n = 202), two genes and 20 QTL for CNVR174 (n
129 = 184), three genes and 26 QTL for CNVR72 (n = 139), 20 genes and six QTL for
130 CNVR122 (n = 108), five genes and three QTL for CNVR68 (n = 101), no genes and 22
131 QTL for CNVR82 (n = 95), 86 genes and 89 QTL for CNVR109 (n = 93), one gene and
132 18 QTL for CNVR101 (n = 90), no genes and four QTL for CNVR149 (n = 80), two
133 genes and nine QTL for CNVR151 (n = 80) (Table 3, Table S2). These genes were used
134 to perform functional analyses. Four significant ($P < 0.05$) gene ontology terms (three
135 biological processes and one molecular function) and one pathway were identified for
136 CNVR21. Six significant ($P < 0.05$) gene ontology terms (one biological process, two
137 cellular components, and three molecular functions), and one metabolic pathway were
138 identified for CNVR109 (Table 3).
139 In the QTL enrichment analyses, the significance of QTL representativeness was
140 determined by looking at annotated QTL overlapping with the investigated regions. The
141 number of QTL annotated for each type or trait within candidate regions were compared
142 to the numbers in the reference database [19]. QTL enrichment analyses were conducted
143 individually for each CNVR, resulting in the identification of 102 enriched QTL, with 65
144 QTL categorized under meat and carcass traits and 26 QTL classified in the health traits
145 category (Table S3). Twenty-three, one, 14, 11, 11, 4, 12, 3, 4, 5, 6, and 8 QTL were
146 enriched for CNVR21, CNVR68, CNVR72, CNVR82, CNVR101, CNVR103,
147 CNVR109, CNVR122, CNVR149, CNVR150, CNVR151, and CNVR174, respectively.
148

149 **Table 3.** Functional analyses of CNVRs detected in at least 5% of the population

CNVR	Category	Term	p-value	Genes
CNVR21	Biological process	GO:1900029 positive regulation of ruffle assembly	0.0158	*EPS8L2, HRAS*
	Biological process	GO:0007165 signal transduction	0.0161	*HPIDD1, RASSF7, HRAS, SCT, SIGIRR*
	Biological process	GO:0005975 carbohydrate metabolic process	0.0339	*CHID1, TALDO1, PGGHG*
	Cellular component	GO:0005887 integral component of plasma membrane	0.0772	*TSPAN4, IFITM5, CDHR5, DRD4, CD151*
	Molecular function	GO:0050839 cell adhesion molecule binding	0.0452	*PKP3, CDHR5*
	KEGG_PATHWAY	ssc05016: Huntington disease	0.0212	*PSMD13, AP2A2, ENSSSCG00000059584, COX8H*
	KEGG_PATHWAY	ssc04714: Thermogenesis	0.0751	*COX8H, HRAS, PNPLA2*
CNVR109	Biological process	GO:0005997 xylulose metabolic process	0.0096	*DCXR, CBR2*
	Biological process	GO:1900026 positive regulation of substrate adhesion-dependent cell spreading	0.0984	*P4HB, RAC3*
	Cellular component	GO:0005856 cytoskeleton	0.0089	*ACTG1, BAIAP2, FSCN2, P4HB, RAC3*
	Cellular component	GO:0032585 multivesicular body membrane	0.0375	*CHMP6, HGS*
	Molecular function	GO:0050038 L-xylulose reductase (NADP+) activity	0.0063	*DCXR, CBR2*
	Molecular function	GO:0102193 protein-ribulosamine 3-kinase activity	0.0063	*FN3KRP, FN3K*
	Molecular function	GO:0004090 carbonyl reductase (NADPH) activity	0.0251	*DCXR, CBR2*
	Molecular function	GO:0044877 macromolecular complex binding	0.064	*CEP131, CHMP6, RPTOR*

Molecular function	GO:0016301 kinase activity	0.0858	*FN3KRP, HGS, FN3K*
KEGG_PATHWAY	ssc04520: Adherens junction	0.044	*ACTG1, BAIAP2, RAC3*
KEGG_PATHWAY	ssc05135: Yersinia infection	0.0947	*ACTG1, BAIAP2, RAC3*

150

151

Association between CNVR and physiological and anatomical indicators of HS response in lactating sows

A total of 52 CNVRs, shared by at least 1% of the population, were used to perform the association analysis. These analyses led to the identification of 15 CNVR significantly associated with T_{ES}, T_{RS}, T_{TS}, and T_{V16h} (Table 4). Two CNVRs were significantly associated with T_{ES}, one with T_{RS}, 12 with T_{TS}, and one with T_{V16h}. CNVR23 were significantly associated with both T_{RS} and T_{TS}.

Table 4. Copy number variation regions (CNVRs) associated with physiological and anatomical indicators of HS response

Trait[a]	CNVR	Chr[b]	Start (bp)	End (bp)	Type	b[c]	SE	p-value
T_{ES}	CNVR72	6	132,124,953	132,543,418	Mixed	0.4985	0.2314	0.0009
	CNVR152	15	24,371,978	24,804,276	Loss	1.2835	0.3491	<0.0001
T_{RS}	CNVR23	2	6,179,112	6,495,647	Loss	0.1672	0.0838	<0.0001
T_{TS}	CNVR21	2	1,111	632,707	Loss	-0.0177	0.0433	0.0003
	CNVR23	2	6,179,112	6,495,647	Loss	0.0905	0.1054	<0.0001
	CNVR48	4	1,155,293	1,388,468	Loss	-0.0083	0.0749	<0.0001
	CNVR52	4	126,897,791	127,521,733	Loss	-0.0522	0.1119	0.0007
	CNVR65	5	77,179,466	77,352,621	Loss	-0.0483	0.1306	0.0001
	CNVR105	11	67,375,641	67,671,825	Loss	0.0582	0.1304	<0.0001
	CNVR109	12	60,100	1,998,701	Mixed	-0.0229	0.0616	0.0001
	CNVR134	14	38,219,290	38,645,949	Loss	0.1107	0.1342	<0.0001
	CNVR138	14	74,176,726	74,990,114	Loss	-0.0397	0.1214	0.0001
	CNVR147	14	140,199,680	140,419,493	Loss	0.0391	0.1552	<0.0001

	CNVR167	16	10,588,133	11,083,680	Loss	-0.0382	0.0913	0.0003
	CNVR173	16	85,407,012	86,024,383	Loss	-0.0443	0.1386	0.0001
T_{V16h}	CNVR133	14	16,993,535	17,333,398	Loss	0.1972	0.0789	0.0009

[a]T_{ES}: ear skin surface temperature; T_{RS}: rump skin surface temperature; T_{TS}: tail skin surface temperature; T_{V16h}: vaginal temperature measured on the first day at 16:00.

[b]Chr: chromosome

[c]Effect size

A total of 291 genes were annotated to overlap with the significantly associated CNVRs (Table S5). Nine genes overlapped with the CNVRs significantly associated with T_{ES}, while 27 genes overlapped with those associated with T_{RS}. Additionally, 254 genes overlapped with the CNVRs significantly associated with T_{TS}, and 1 gene overlapped with the CNVR significantly associated with T_{V16h}. The genes annotated within these significant CNVRs were subjected to functional analysis, revealing five significant gene ontology terms (four cellular components and one molecular function) for T_{RS}, 11 significant gene ontology terms (three biological processes, one cellular component, and seven molecular functions) and four significant pathways for T_{TS} (Table 5). Additionally, a total of 771 QTL overlapped with the CNVRs that were significantly associated with T_{ES}, T_{RS}, T_{TS}, and T_{V16h} (Table S6). Subsequently, QTL enrichment was performed using the QTLs annotated for these significant CNVRs, resulting in the identification of a total of 69 enriched QTLs (Table S7).

Discussion

Copy number variation are sources of genetic variation that influence gene expression within and near the modified regions, altering phenotypes and generating phenotypic variety [3]. The gene expression is generally increased in genes found in

181 higher copy CNVs and decreased in genes found in lower copy CNVs [20]. Furthermore,
182 through structural changes in the genome, CNVs can lead to the expansion of gene
183 families and the creation of new genes, especially by accumulation of recent duplications
184 in CNV regions [21]. The CNVs are heritable when present in germline cells [22, 23].
185 Since CNVs affect the phenotypes, their frequency and distribution within a population
186 can be influenced by both natural and artificial selection [24, 25].

187 The influence of CNV in the gene functions impacts phenotypes and potentially
188 conferring resilience to specific environmental challenges [4, 9, 10]. The identification
189 and genome-wide association study of CNVs provide valuable insights into the genetic
190 background of resilience and adaptation to specific environmental conditions. In this
191 study, we investigate the potential role of the most shared CNVRs, and we also identified
192 CNVRs associated with HS response.

193 **Copy number variation and CNVRs**

194 We identified 4,184 CNVs and 236 CNVRs after applying quality control to
195 reduce the number of potential false positive results. The number of CNVRs identified in
196 this study is in the range reported by previous studies in pigs. Using the Illumina Porcine
197 SNP60 BeadChip (Illumina Inc., San Diego, CA, USA) for CNVR detection, 170 CNVRs
198 (7 losses, 161 gains, and 2 mixed) were identified in 293 Large White pigs [26]; 249
199 CNVRs (70 losses, 43 gains, and 136 mixed) were detected in 585 Large White X Minzhu
200 pigs [27]; 348 CNVRs (243 losses, 88 gains, and 17 mixed) were observed in 302 animals
201 representing ten Chinese pig breeds [28]. Using the Illumina Porcine SNP50 BeadChip
202 (Illumina Inc., San Diego, CA, USA), Qiu et al. [29] identified 953 CNVRs (376 losses,
203 388 gains, and 189 mixed) in 5,928 Duroc pigs. Staffuza et al. [14] identified 425 CNVRs
204 (342 losses, 19 gains and 64 mixed) in 3,520 Duroc pigs genotyped using Porcine SNP80
205 BeadChip (Illumina Inc., San Diego, CA, USA). Also using the Illumina Porcine SNP80

206 BeadChip, Wang et al. [30] detected 312 CNVRs in 1,199 Large White pigs (184 losses,
207 66 gains, and 62 mixed). A total of 140 CNVRs identified in this study overlapped with
208 CNVRs reported in previous studies (Table S8). Specifically, 132 CNVRs overlapped
209 with those reported by Stafuzza et al. [14], 64 CNVRs overlapped with those identified
210 by Wang et al. [30], and 72 CNVRs overlapped with those reported by Qiu et al. [29].
211 Notably, while the majority of CNVRs are commonly reported as deleterious in several
212 studies in pigs (e.g., [13, 14, 16, 28, 30, 31]), ranging from 28.11 to 80.47% of the CNVs.
213 In our study, a higher proportion of deletions was observed, accounting for 85% of
214 identified CNVRs.

215 The variation in the number of identified CNVRs in different studies can be
216 attributed to the population-specific characteristics associated with CNVs [13, 32, 33].
217 These variations are sources of both interindividual differences and variations between
218 breeds [32]. Furthermore, differences in the genotyping or sequencing platforms and
219 methods employed (such as Comparative Genomic Hybridization, SNP-array, and Next
220 Generation Sequencing), the methodologies and software used for the analyses, quality
221 control, the density of genotyping SNP panels, and variations in sample size can
222 contribute to the observed differences in the identification of CNVs and CNVRs among
223 pig populations [34–36]. The proportion of the autosomal genome covered by CNVRs
224 (2.60%) observed in this study aligns with values reported in the literature on pigs, which
225 ranged from 0.36 to 10.90% [14, 27–30]. The observed variation in genome coverage
226 across studies can be explained by the different SNP panels used. The choice of SNP
227 panels has the potential to impact the sensitivity of CNV detection, such as the sensitivity
228 in detecting small CNVs [37].

229 In our study, we found twelve CNVRs shared by at least 5% of the population,
230 which are harbored by 184 genes. The frequency and distribution of CNVs among

231 individuals within a population can also be influenced by both natural and artificial
232 selection [24, 25]. Consequently, the most common CNVRs in a population may be
233 associated with traits undergoing selection and adaptation. Studying these most inherited
234 CNVs and CNVRs provides insights into genetic variation and offers valuable
235 information about their importance and how they might affect traits of interest.

236 In this study, we identified genes within the most common CNVRs associated
237 with responses to cellular oxidative stress and immune reactions, indicating that the
238 identified CNVRs may regulate biological processes related to adaptation and HS
239 resilience. Among the identified genes implicated in oxidative stress and immune
240 responses were *SOD1* (Superoxide dismutase 1), *IRF7* (Interferon regulatory factor 7),
241 and *SIGIRR* (Single Ig and TIR domain containing). *SOD1* acts as the first line of defense
242 against oxidative damage by controlling reactive oxygen species (ROS) levels during
243 mitochondrial respiration, thereby maintaining cellular homeostasis [38]. *IRF7*,
244 expressed in immune cells, regulates type I and III interferon production against viral
245 infections, acting in immune modulation [39, 40]. *SIGIRR* acts as a key negative regulator
246 in bacterial infection-induced inflammation, suppressing proinflammatory responses and
247 providing resistance against various infections by modulating immune responses [41, 42].

248 In the functional analysis, we identified Gene Ontology (GO) terms that are
249 pertinent to both cell and tissue integrity, particularly in their functions within the cell
250 response to stress. Additionally, we found GO terms linked to cellular energy production,
251 essential for sustaining fundamental cellular processes. Together, these identified GO
252 terms are involved in the survival and resilience of cells and tissues, aiding them in coping
253 with cellular damage induced by stress. Furthermore, suggestive ($P < 0.10$) KEGG
254 pathways were identified, including thermogenesis for CNVR21 and the Yersinia
255 infection pathway for CNVR109. These metabolic pathways suggest the potential

functions of CNVRs in adapting to thermal stress and enhancing resilience against diseases.

Sixty-five out of the 102 enriched QTLs are related to meat and carcass traits. Notably, CNVR21 showed enriched QTLs associated with backfat and carcass weight. CNVR72 presented enriched QTLs linked to muscle content, while CNVR109 presented enriched QTLs related to fatty acids ratio. These findings suggest that these specific CNVRs may influence meat quality in pigs. Across all CNVRs, 27 enriched QTLs classified as health-related were identified, with most of them being associated with immune response, which also highlight that the CNVRs identified might influence pigs' adaptation and resilience.

CNVR associated with physiological and anatomical indicators of HS response in lactating sows

The variance components and genetic parameters for the traits evaluated in this study have been previously reported by Freitas et al. [43]. Skin temperatures (i.e., T_{ES}, T_{SS}, T_{RS}, and T_{TS}), RR, and PS exhibited low heritability estimates, ranging from 0.04 to 0.06. Vaginal temperatures (i.e., T_{Vall}, T_{V4days}, T_{V8h} T_{V12h}, T_{V16h}, and T_{V20h}) are moderately heritable, with estimates ranging from 0.15 to 0.29. Hui et al. [44] reported estimates ranging from 0.14 to 0.20 throughout the day when studying vaginal temperature as longitudinal traits using a random regression model. Anatomical traits (i.e., BCS_{cal}, BCS_{vis}, HD, BS, EA, and EL) showed moderate to high heritability, ranging from 0.25 to 0.40 [43]. The heritability of traits represents the contribution of additive genetic variance to phenotypic variation. Genomic structural variations, such as CNVs, may elucidate a portion of trait heritability by influencing gene expressions and subsequently impacting phenotypic variability [3]. Investigating the functions of these genomic alterations

provides valuable insights into understanding inheritance patterns and the variability of phenotypes within populations.

We identified 15 CNVRs significantly associated with T_{ES}, T_{RS}, T_{TS}, and T_{V16h}. These regions overlap with a total of 291 genes, many of which are involved in immune response. Notably, pigs under HS conditions experience increased body temperature [45, 46]. Elevated body temperatures generally promote the activation of immune cells, while reduced temperatures inhibit these processes [47]. CNVR152, which was associated with T_{ES}, includes the genes *STEAP3* (STEAP3 metalloreductase) and *MARCO* (Macrophage receptor with collagenous structure). *STEAP3* is involved in the maintenance of iron homeostasis and modulation of immune responses in macrophages. *MARCO* acts in the innate immune system by binding and removing bacteria and has been implicated in actin cytoskeleton rearrangements [48]. It has also been shown that *MARCO* modulates the induction of T cell responses, indicating its function in adaptive immunity [48].

The CNVR23, associated with both T_{RS} and T_{TS}, comprises the gene *CTSW* (Cathepsin W), which encodes a protein of the cathepsin family. Cathepsin W is exclusively expressed in $CD8^+$ T cells and natural killer cells [49–51], making it an important factor in immune responses. The CNVR52, also associated with T_{TS}, contains the gene *LRRC8C* (Leucine rich repeat containing 8 VRAC subunit C), which is an essential component of the volume-regulated anion channel in T cells [52]. *LRRC8C* regulates T cell proliferation, apoptosis, function, cell cycle progression, survival, calcium ions influx, and cytokine production [52]. Additionally, the CNVR52 also comprises the genes *GBP1* (Guanylate binding protein 1), *GBP2* (Guanylate binding protein 2), and *GBP5* (Guanylate binding protein 5). Guanylate-binding proteins mediate innate immune response against a wide range of intracellular pathogens, including viruses, bacteria, and protozoa [53].

306 The CNVR48, which was associated with T_{TS}, overlaps with the genes *LY6E*
307 (Lymphocyte antigen 6 family member E), *LY6H* (Lymphocyte antigen 6 family member
308 H), and *LY6L* (Lymphocyte antigen 6 family member L), all of which are members of the
309 lymphocyte antigen-6 gene family and are involved in immune cells [54, 55]. *LY6E* is
310 expressed in peripheral B-cells, immature T-cells, activated T cells, thymus stromal cells,
311 and macrophages [54]. In contrast, *LY6H* is expressed in the brain and has been associated
312 with poor overall survival of renal clear cell carcinoma and pancreatic ductal
313 adenocarcinoma [54]. *LY6L* is involved in the differentiation and signaling of
314 lymphocytes [55]. These proteins are essential for the proper functioning and regulation
315 of immune cells, contributing to the body's defense against pathogens and diseases [54,
316 55]. The CNVR109, associated with T_{TS}, overlaps with the gene *AATK* (Apoptosis
317 associated tyrosine kinase). *AATK*, crucial for host defense against viral infection, inhibits
318 viral replication and is associated with inflammatory responses, playing a protective role
319 in cellular stress induced by viral infection, and contributing to the regulation of cell
320 differentiation, growth, and apoptosis [56, 57].

321 Additionally, the CNVRs associated with T_{RS}, and T_{TS} comprise genes involved
322 in oxidative stress response and apoptosis. The CNVR23, associated with both T_{RS} and
323 T_{TS}, overlaps with the genes *SART1* (Spliceosome associated factor 1, recruiter of
324 U4/U6.U5 tri-snRNP) and *FOSL1* (FOS like 1, AP-1 transcription factor subunit). The
325 *SART1* gene has been shown to have several functions inducing cell cycle arrest and
326 apoptosis [58]. *FOSL1* is involved in cell growth and cell death in various physiological
327 and pathological conditions [59]. The CNVR21, associated with T_{TS}, contains the gene
328 *SIRT3* (Sirtuin 3) and *TALDO1* (Transaldolase 1). *SIRT3*, a key regulator of mitochondrial
329 oxidative stress, contributes to cellular adaptation by deacetylating substrates involved in
330 ROS production and detoxification, protecting cells from oxidative damage [60, 61].

TALDO1 functions to maintain cellular redox equilibrium, preserve the cellular redox equilibrium, and is involved in eliminating oxygen radicals, acting in the oxidative stress response and apoptosis [62].

The CNVR133, associated with T_{V16h}, overlap with the gene *GALNTL6* (Polypeptide N-acetylgalactosaminyltransferase like 6). *GALNTL6* is primarily expressed in the gastrointestinal tract and is involved in the production of short-chain fatty acids in the intestines, which are important for anti-inflammatory and resynthesis functions [63, 64]. In humans, *GALNTL6* has been associated with power performance, particularly in anaerobic exercises, enhancing fitness and overall health in athletes [63]. The *GALNTL6* gene has also been associated with resistance to gastrointestinal parasites in sheep [64, 65]. Then, the results from this study, combined with the previous studies associating *GALNTL6* with endurance in sports in humans and resistance to gastrointestinal parasites in sheep, suggest that this gene might be involved in biological mechanisms in the resilience to stress factors.

The functional analyses, using the genes annotated for associated CNVRs with T_{ES}, T_{RS}, T_{TS}, and T_{V16h}, identified GO terms that are related to both cell and tissue integrity, particularly in their functions within the cell response to stress. Additionally, GO terms associated with glucose metabolism and cellular energy production, essential for cellular functions, were found. These identified GO terms collectively contribute to the response to cellular stress and cell survival. Metabolic pathways of amino acids biosynthesis and thermogenesis were identified for T_{TS}, suggesting the potential functions of CNVRs associated with T_{TS} in protein synthesis and heat stress response.

The CNVRs associated with T_{ES}, T_{RS}, T_{TS}, and T_{V16h} presented enriched QTL related to immune response: Interleukin-8 level, C3c concentration, Phagocytic activity, CD4-negative and CD8-positive leukocyte percentage. These findings suggest that the

CNVRs associated with skin and vaginal temperature traits also influence other aspects of the immune response. Additionally, enriched QTL associated with meat quality, such as muscle pH and meat color, were observed on CNVRs associated with T_{ES}, T_{RS}, and T_{TS}. Notably, exposure to HS has a recognized negative impact on meat quality, particularly on meat color and pH [66, 67].

Implications and limitations

The findings of this study offer valuable insights into the impact of CNVs in pigs. Notably, several genes involved to immune and stress responses were identified within the most frequently occurring CNVRs in the population. This implies a potentially important role of these CNVRs in adaptation. The CNVRs may result in animals that are more resilient to stress factors such as diseases and HS. Moreover, the CNVRs identified in this study may also impact other economically relevant traits. QTLs related to meat and carcass traits were identified within the most frequent CNVRs, suggesting an influence on production traits. Additionally, the CNVRs associated with skin and vaginal temperatures, which are physiological indicators of HS response, in lactating sows comprise genes and QTLs related to immune response, indicating a potential influence on the response to HS and adaptation in pigs.

Nevertheless, this study has some limitations. The number of animals used for CNV detection is relatively small while a higher number of samples are desirable to reduce the probability of false-positive CNVs. A larger dataset would also improve the power to detect associations between the CNVRs and the traits evaluated. of a medium-density SNP panel; a higher marker density could enhance the detection of short CNVs and potentially reduce the number of false-positive CNVs [37].

Conclusions

This study aimed to investigate CNVs and CNVRs in the genome of crossbred sows (Large White x Landrace) and their associations with physiological and anatomical indicators of HS response in lactating sows. Various CNVs and CNVRs were identified, with the most common CNVRs containing genes involved in responses to cellular oxidative stress and immune reactions. This suggests that these CNVRs may regulate biological processes related to adaptation and resilience to HS. Fifteen CNVRs were significantly associated with indicators of heat stress response in lactating sows, comprising genes with immune functions, which are essential processes in the HS response. Several genes and QTL involved in immune and stress responses were identified within the CNVRs, indicating that these CNVRs might influence adaptation and resilience to heat stress. Additionally, QTL overlapping with the CNVRs identified are related to meat and carcass traits, which are economically relevant traits for the pig industry.

Materials and Methods

Animals and genotypes

The data used in this study was previously described by Johnson et al. [68] and Freitas et al. [43]. In summary, the phenotypes were collected from 1,645 multiparous lactating sows (Large White x Landrace cross) at a commercial sow farm in Maple Hill, North Carolina, USA. A total of 1,639 sows were genotyped using PorcineSNP50K (50,703 SNPs) Bead Chip (Illumina, San Diego, CA, USA). Quality control was performed to remove samples with poor quality and to reduce false-positive CNV detection. First, the genotypes with GenCall scores lower than 0.15 were assumed as missing. SNPs located on non-autosomal chromosomes and SNPs with unknown or

406 duplicated positions were removed. SNPs and samples with call rate lower than 90% were
407 also removed. A total of 46,580 SNPs for 1,613 animals remained for subsequent
408 analyses.
409
410 **Phenotypes**
411 The phenotypes used in this study have been previously described by Freitas et al.
412 [43] and Johnson et al. [68]. The phenotypes recorded included respiration rate (RR), ear
413 skin temperature (T_{ES}), shoulder skin temperature (T_{SS}), rump skin temperature (T_{RS}) tail
414 skin temperature (T_{TS}), vaginal temperatures, and panting score (PS). Six distinct traits
415 were obtained for vaginal temperature, based on automatically records: T_{Vall}
416 (measurements at each 10-minute interval), T_{V4days} (average of six records per hour at
417 0800 h, 1200 h, 1600 h, and 2000 h over four days), and single records at 0800 h, 1200
418 h, 1600 h, and 2000 h on the first day (T_{V8h}, T_{V12h}, T_{V16h}, and T_{V20h}). Additionally, the
419 phenotypes included anatomical traits: hair density (HD), body condition score using a
420 sow caliper (BCS_{cal}) [69] and visual body condition score (BCS_{vis}), body size (BS), ear
421 length (EL), and ear area (EA). More details about data collection are available in Johnson
422 et al. [68].
423 The phenotypes were pre-corrected for fixed effect, which were described for
424 Freitas et al. [43]. Traits that presented repeated measurements had the average of the
425 adjusted phenotype computed and used as response variable for the CNVR association
426 analysis [70].
427
428 **CNV detection and CNVR identification**
429 Individual-based CNV detection was performed using the PennCNV software
430 [18], which is based on hidden Markov model and incorporates multiple sources of

information to obtain accurate CNV detection, such as distance between SNPs, log R ratio (LRR), B allele frequency (BAF), and population frequency of the B allele (PBF). LRR is a normalized intensity value and an allelic intensity ratio measurement to compare the observed normalized intensity of a subject sample to the expected intensity based on the observed allelic ratio [71]. BAF is a measurement used in SNP array analysis to determine the allelic intensity ratio of the B allele [71]. The LRR and BAF were exported from Illumina GenomeStudio software (Illumina Inc., San Diego, CA, USA). PBF was calculated from the BAF value of each SNP in all samples using compile_pbf.pl pipeline from the PennCNV software. We also performed an adjustment for genomic waves using the flag *–gcmodel* in the PennCNV software. Genomic waves refer to a signal noise related to the guanine-cytosine content in the genome, which interferes in the CNV detection and might increase false-positive CNV. The porcine *gcmodel* was generated by calculating the guanine-cytosine content in the porcine genome in a region of 500 Kb around each SNP and based on a regression model [72].

After CNV calling, a sample-based quality control was performed to reduce false-positive CNV detection. The quality control consisted of removing CNVs with less than three consecutive SNPs, BAF drift lower than 0.01, standard deviation of LRR greater than 0.40, minimum length of 1Kb, maximum length of 5000Kb bp, and GC wave factor lower than 0.10 (after genomic waves were corrected by guanine-cytosine content).

The CNVR were determined by merging the raw CNVs that overlapped by at least 1 bp within each region, using the *mergeBed* option of the BEDtools suite tool [73]. After the merging, CNVRs presented in only one animal were removed. Although there is a possibility that a CNVs exist within the loci reported in only one animal, they may constitute rare cases; nonetheless, considering CNVRs found in two or more animals can reduce the false-positive rate [31]. Another reason for removing CNVRs discovered in a

single individual is because some CNVs may be somatic rather than germline, which would make them not heritable [22, 23]. CNVRs were classified as losses when an animal exhibited a deletion in a chromosomal segment, gains for repeated chromosomal regions (i.e., duplication), and mixed when both deletions and duplications were identified in the same genomic region for different individuals.

Association analysis

The association analyses were performed considering the CNVR identified in the autosomal chromosomes that were observed in at least 1% of the population. To verify if the CNVRs identified were associated with the pre-adjusted phenotypes, the following model, previously described by Benfica et al. [74], was fitted:

$$\mathbf{y} = \mathbf{X}\mathrm{b} + \mathbf{Z}\mathbf{u} + \boldsymbol{\varepsilon},$$

Where $\mathbf{y}$ is the vector of pre-corrected phenotypes for each analyzed trait; b is the fixed effect of the CNVR tested for association, $\mathbf{X}$ is a vector containing the genotype score for the tested CNVR, which was coded as -1, 0, or 1 if the CNV on the tested region was a deletion, absent or a duplication in the individual; $\mathbf{u}$ is the random vector of polygenic effect with $\mathbf{u} \sim \mathrm{N}(0, \mathbf{G}\sigma_u^2)$, where $\mathbf{G}$ is the genomic-based relationship matrix computed according to the method proposed by VanRaden [75], σ_u^2 is the additive genomic variance of polygenic effects; $\mathbf{Z}$ is the incidence matrix for $\mathbf{u}$; and $\boldsymbol{\varepsilon}$ is a random vector of residual effects with $\boldsymbol{\varepsilon} \sim \mathrm{N}(0, \mathbf{I}\sigma_\varepsilon^2)$, where $\mathbf{I}$ is an identity matrix, and σ_ε^2 is the residual variance. The variance components were previously estimated fitting the above-described model excluding the CNVR as fixed effect. The variance components estimation and the CNVR effect size estimation were performed using BLUPF90+ program [76].

The model adjusted provided the effect size ($\hat{\beta}$) and standard error (SE) for each CNVR, which were used to compute the statistic t ($t = \hat{\beta}/SE$). Then, the p-values were

obtained assuming the t-distribution with $n-2$ degrees of freedom, where n is the sample size (i.e., the number of animals used to obtain the CNVR effect for each pre-adjusted phenotype). To check if there was potential stratification due to the population structure, the genomic inflation factor (λ) [77] was evaluated, along with its 95% confidence interval. Due to the multiple-test, a Bonferroni correction at α = 0.05 genome-wise significance level was applied, by dividing α by the number of CNVRs to account for dependence among tests.

Gene annotation and functional analyses

Genes and QTLs that overlapped with CNVRs present in at least 5% of the population were annotated. CNVRs that were significantly associated with the pre-adjusted phenotypes had also genes and QTL annotated.

The gene and QTL annotation in these regions was performed using the GALLO R package [19], utilizing data for Sus scrofa sourced from the Ensembl database (www.ensembl.org/Sus_scrofa/Info/Index). Additionally, the PigQTL database (www.animalgenome.org/cgi-bin/QTLdb/SS/index) was used as a resource for obtaining previously reported QTL information. To test the significance of the QTL representativeness, it was performed a QTL enrichment analysis using GALLO package. This analysis is based on a hypergeometric test approach, where the number of QTLs annotated within the candidate regions for each QTL type is compared with the observed number of QTLs in the reference database. The Database for Annotation, Visualization, and Integrated Discovery (DAVID) [78, 79] was used for conducting Gene Ontology (GO) and KEGG pathway enrichment ($P < 0.05$) analyses to identify biological processes, molecular functions, cellular components, and biological pathways associated with the positional candidate genes identified.

References

1. Feuk L, Carson AR, Scherer SW. Structural variation in the human genome. Nature Reviews Genetics 2006 7:2. 2006;7:85–97.

2. Hastings PJ, Lupski JR, Rosenberg SM, Ira G. Mechanisms of change in gene copy number. Nature Reviews Genetics 2009 10:8. 2009;10:551–64.

3. Henrichsen CN, Chaignat E, Reymond A. Copy number variants, diseases and gene expression. Hum Mol Genet. 2009;18:R1–8.

4. Paudel Y, Madsen O, Megens HJ, Frantz LAF, Bosse M, Bastiaansen JWM, et al. Evolutionary dynamics of copy number variation in pig genomes in the context of adaptation and domestication. BMC Genomics. 2013;14.

5. Kumar H, Panigrahi M, Saravanan KA, Rajawat D, Parida S, Bhushan B, et al. Genome-wide detection of copy number variations in Tharparkar cattle. Anim Biotechnol. 2023;34:448–55.

6. Hull RM, Cruz C, Jack C V., Houseley J. Environmental change drives accelerated adaptation through stimulated copy number variation. PLoS Biol. 2017;15.

7. Lauer S, Avecilla G, Spealman P, Sethia G, Brandt N, Levy SF, et al. Single-cell copy number variant detection reveals the dynamics and diversity of adaptation. PLoS Biol. 2018;16.

8. Iskow RC, Gokcumen O, Lee C. Exploring the role of copy number variants in human adaptation. Trends in Genetics. 2012;28:245–57.

9. Cayuela H, Dorant Y, Mérot C, Laporte M, Normandeau E, Gagnon-Harvey S, et al. Thermal adaptation rather than demographic history drives genetic structure inferred by copy number variants in a marine fish. Mol Ecol. 2021;30:1624–41.

529 10. Wang MD, Dzama K, Rees DJG, Muchadeyi FC. Tropically adapted cattle of Africa:
530 Perspectives on potential role of copy number variations. Animal Genetics.
531 2016;47:154–64.
532 11. Wang M, Liu Y, Bi X, Ma H, Zeng G, Guo J, et al. Genome-Wide Detection of Copy
533 Number Variants in Chinese Indigenous Horse Breeds and Verification of CNV-
534 Overlapped Genes Related to Heat Adaptation of the Jinjiang Horse. Genes
535 (Basel). 2022;13:603.
536 12. Wang MD, Dzama K, Rees DJG, Muchadeyi FC. Tropically adapted cattle of Africa:
537 perspectives on potential role of copy number variations. Anim Genet.
538 2016;47:154–64.
539 13. Chen C, Qiao R, Wei R, Guo Y, Ai H, Ma J, et al. A comprehensive survey of copy
540 number variation in 18 diverse pig populations and identification of candidate
541 copy number variable genes associated with complex traits. BMC Genomics.
542 2012;13:1–10.
543 14. Stafuzza NB, Silva RMDO, Fragomeni BDO, Masuda Y, Huang Y, Gray K, et al. A
544 genome-wide single nucleotide polymorphism and copy number variation
545 analysis for number of piglets born alive. BMC Genomics 2019 20:1. 2019;20:1–
546 11.
547 15. Dong K, Pu Y, Yao N, Shu G, Liu X, He X, et al. Copy number variation detection
548 using SNP genotyping arrays in three Chinese pig breeds. Anim Genet.
549 2015;46:101–9.
550 16. Qian R, Xie F, Zhang W, Kong JJ, Zhou X, Wang C, et al. Genome-wide detection
551 of CNV regions between Anqing six-end-white and Duroc pigs. Mol Cytogenet.
552 2023;16:1–9.

553 17. Johnson JS. Heat stress: Impact on livestock well-being and productivity and
554 mitigation strategies to alleviate the negative effects. Animal Production Science.
555 2018;58:1404–13.
556 18. Wang K, Li M, Hadley D, Liu R, Glessner J, Grant SFA, et al. PennCNV: An
557 integrated hidden Markov model designed for high-resolution copy number
558 variation detection in whole-genome SNP genotyping data. Genome Res.
559 2007;17:1665–74.
560 19. Fonseca PAS, Suárez-Vega A, Marras G, Cánovas Á. GALLO: An R package for
561 genomic annotation and integration of multiple data sources in livestock for
562 positional candidate loci. Gigascience. 2020;9:1–9.
563 20. Orozco LD, Cokus SJ, Ghazalpour A, Ingram-Drake L, Wang S, van Nas A, et al.
564 Copy number variation influences gene expression and metabolic traits in mice.
565 Hum Mol Genet. 2009;18:4118–29.
566 21. Juan D, Rico D, Marques-Bonet T, Fernández-Capetillo Ó, Valencia A. Late-
567 replicating CNVs as a source of new genes. Biol Open. 2013;2:1402–11.
568 22. Bruder CEG, Piotrowski A, Gijsbers AACJ, Andersson R, Erickson S, Diaz De Ståhl
569 T, et al. Phenotypically Concordant and Discordant Monozygotic Twins Display
570 Different DNA Copy-Number-Variation Profiles.
571 https://doi.org/10.1016/j.ajhg.2007.12.011.
572 23. Piotrowski A, Bruder CEG, Andersson R, De Ståhl TD, Menzel U, Sandgren J, et al.
573 Somatic mosaicism for copy number variation in differentiated human tissues.
574 Hum Mutat. 2008;29:1118–24.
575 24. Hou Y, Liu GE, Bickhart DM, Cardone MF, Wang K, Kim E soo, et al. Genomic
576 characteristics of cattle copy number variations. BMC Genomics. 2011;12:1–11.

577 25. Lye ZN, Purugganan MD. Copy Number Variation in Domestication. Trends Plant
578 Sci. 2019;24:352–65.
579 26. Schiavo G, Dolezal MA, Scotti E, Bertolini F, Calò DG, Galimberti G, et al. Copy
580 number variants in Italian Large White pigs detected using high-density single
581 nucleotide polymorphisms and their association with back fat thickness. Anim
582 Genet. 2014;45:745–9.
583 27. Wang J, Wang H, Jiang J, Kang H, Feng X, Zhang Q, et al. Identification of Genome-
584 Wide Copy Number Variations among Diverse Pig Breeds Using SNP
585 Genotyping Arrays. PLoS One. 2013;8:e68683.
586 28. Wang Y, Tang Z, Sun Y, Wang H, Wang C, Yu S, et al. Analysis of Genome-Wide
587 Copy Number Variations in Chinese Indigenous and Western Pig Breeds by 60 K
588 SNP Genotyping Arrays. PLoS One. 2014;9:e106780.
589 29. Qiu Y, Ding R, Zhuang Z, Wu J, Yang M, Zhou S, et al. Genome-wide detection of
590 CNV regions and their potential association with growth and fatness traits in
591 Duroc pigs. BMC Genomics. 2021;22:1–16.
592 30. Wang Y, Zhang T, Wang C. Detection and analysis of genome-wide copy number
593 variation in the pig genome using an 80 K SNP Beadchip. Journal of Animal
594 Breeding and Genetics. 2020;137:166–76.
595 31. Fadista J, Nygaard M, Holm LE, Thomsen B, Bendixen C. A Snapshot of CNVs in
596 the Pig Genome. PLoS One. 2008;3:e3916.
597 32. Pierce MD, Dzama K, Muchadeyi FC. Genetic diversity of seven cattle breeds
598 inferred using copy number variations. Front Genet. 2018;9 MAY:340644.
599 33. Hou Y, Liu GE, Bickhart DM, Matukumalli LK, Li C, Song J, et al. Genomic regions
600 showing copy number variations associate with resistance or susceptibility to

601 gastrointestinal nematodes in Angus cattle. Funct Integr Genomics. 2012;12:81–
602 92.
603 34. Duan J, Zhang JG, Deng HW, Wang YP. CNV-TV: A robust method to discover copy
604 number variation from short sequencing reads. BMC Bioinformatics. 2013;14:1–
605 12.
606 35. Zhao M, Wang Q, Wang Q, Jia P, Zhao Z. Computational tools for copy number
607 variation (CNV) detection using next-generation sequencing data: Features and
608 perspectives. BMC Bioinformatics. 2013;14:1–16.
609 36. Redon R, Ishikawa S, Fitch KR, Feuk L, Perry GH, Andrews TD, et al. Global
610 variation in copy number in the human genome. Nature 2006 444:7118.
611 2006;444:444–54.
612 37. Bernardini L, Alesi V, Loddo S, Novelli A, Bottillo I, Battaglia A, et al. High-
613 resolution SNP arrays in mental retardation diagnostics: how much do we gain?
614 European Journal of Human Genetics 2010 18:2. 2009;18:178–85.
615 38. Eleutherio ECA, Silva Magalhães RS, de Araújo Brasil A, Monteiro Neto JR, de
616 Holanda Paranhos L. SOD1, more than just an antioxidant. Arch Biochem
617 Biophys. 2021;697:108701.
618 39. Ning S, Pagano JS, Barber GN. IRF7: activation, regulation, modification and
619 function. Genes & Immunity 2011 12:6. 2011;12:399–414.
620 40. Ma W, Huang G, Wang Z, Wang L, Gao Q. IRF7: role and regulation in immunity
621 and autoimmunity. Front Immunol. 2023;14.
622 41. Giannoudaki E, Stefanska AM, Lawler H, Leon G, Hernandez Santana YE, Hassan
623 N, et al. SIGIRR Negatively Regulates IL-36–Driven Psoriasiform Inflammation
624 and Neutrophil Infiltration in the Skin. The Journal of Immunology.
625 2021;207:651–60.

626 42. Al-Kuhlani M, Lambert G, Pal S, de la Maza L, Ojcius DM. Immune response against
627 Chlamydia trachomatis via toll-like receptors is negatively regulated by SIGIRR.
628 PLoS One. 2020;15:e0230718.
629 43. Freitas PHF, Johnson JS, Wen H, Maskal JM, Tiezzi F, Maltecca C, et al. Genetic
630 parameters for automatically-measured vaginal temperature, respiration
631 efficiency, and other thermotolerance indicators measured on lactating sows under
632 heat stress conditions. Genetics Selection Evolution. 2023;55:1–14.
633 44. Wen H, Johnson JS, Freitas PHF, Maskal JM, Gloria LS, Araujo AC, et al.
634 Longitudinal genomic analyses of automatically-recorded vaginal temperature in
635 lactating sows under heat stress conditions based on random regression models.
636 Genetics Selection Evolution. 2023;55:1–19.
637 45. Yu TY, Yong YH, Li JY, Fang B, Hu CY, Wu LY, et al. Proteomic study of
638 hypothalamus in pigs exposed to heat stress. BMC Vet Res. 2020;16.
639 46. Cervantes M, Cota M, Arce N, Castillo G, Avelar E, Espinoza S, et al. Effect of heat
640 stress on performance and expression of selected amino acid and glucose
641 transporters, HSP90, leptin and ghrelin in growing pigs. J Therm Biol.
642 2016;59:69–76.
643 47. Coiffard B, Diallo AB, Mezouar S, Leone M, Mege JL. A Tangled Threesome:
644 Circadian Rhythm, Body Temperature Variations, and the Immune System.
645 Biology 2021, Vol 10, Page 65. 2021;10:65.
646 48. Komine H, Kuhn L, Matsushita N, Mulé JJ, Pilon-Thomas S. Examination of
647 MARCO Activity on Dendritic Cell Phenotype and Function Using a Gene
648 Knockout Mouse. PLoS One. 2013;8:e67795.
649 49. Li J, Chen Z, Kim G, Luo J, Hori S, Wu C. Cathepsin W restrains peripheral regulatory
650 T cells for mucosal immune quiescence. Sci Adv. 2023;9.

651 50. Stoeckle C, Gouttefangeas C, Hammer M, Weber E, Melms A, Tolosa E. Cathepsin
652 W expressed exclusively in CD8+ T cells and NK cells, is secreted during target
653 cell killing but is not essential for cytotoxicity in human CTLs. Exp Hematol.
654 2009;37:266–75.
655 51. Linnevers C, Smeekens SP, Brömme D. Human cathepsin W, a putative cysteine
656 protease predominantly expressed in CD8+ T-lymphocytes. FEBS Lett.
657 1997;405:253–9.
658 52. Concepcion AR, Wagner LE, Zhu J, Tao AY, Yang J, Khodadadi-Jamayran A, et al.
659 The volume-regulated anion channel LRRC8C suppresses T cell function by
660 regulating cyclic dinucleotide transport and STING–p53 signaling. Nature
661 Immunology 2022 23:2. 2022;23:287–302.
662 53. Praefcke GJK. Regulation of innate immune functions by guanylate-binding proteins.
663 International Journal of Medical Microbiology. 2018;308:237–45.
664 54. Upadhyay G. Emerging Role of Lymphocyte Antigen-6 Family of Genes in Cancer
665 and Immune Cells. Front Immunol. 2019;10:819.
666 55. Lee PY, Wang J-X, Parisini E, Dascher CC, Nigrovic PA. Ly6 family proteins in
667 neutrophil biology. J Leukoc Biol. 2013;94:585–94.
668 56. Jacovetti C, Jimenez V, Ayuso E, Laybutt R, Peyot ML, Prentki M, et al. Contribution
669 of Intronic miR-338–3p and Its Hosting Gene AATK to Compensatory β-Cell
670 Mass Expansion. Molecular Endocrinology. 2015;29:693–702.
671 57. Zhao L, Song R, Liu Y. Glycolytic metabolite phosphoenolpyruvate protects host
672 from viral infection through promoting AATK expression. Eur J Immunol.
673 2023;53:2350536.

674 58. Hosokawa M, Kadota R, Shichijo S, Itoh K, Dmitriev I, Krasnykh V, et al. Cell Cycle
675 Arrest and Apoptosis Induced by SART-1 Gene Transduction. Anticancer Res.
676 2005;25:1983–90.
677 59. Yao T, Zhang L, Fu Y, Yao L, Zhou C, Chen G. Saikosaponin-d Alleviates Renal
678 Inflammation and Cell Apoptosis in a Mouse Model of Sepsis via
679 TCF7/FOSL1/Matrix Metalloproteinase 9 Inhibition. Mol Cell Biol. 2021;41.
680 60. Bause AS, Haigis MC. SIRT3 regulation of mitochondrial oxidative stress. Exp
681 Gerontol. 2013;48:634–9.
682 61. Tseng AHH, Shieh SS, Wang DL. SIRT3 deacetylates FOXO3 to protect
683 mitochondria against oxidative damage. Free Radic Biol Med. 2013;63:222–34.
684 62. Samland AK, Sprenger GA. Transaldolase: From biochemistry to human disease. Int
685 J Biochem Cell Biol. 2009;41:1482–94.
686 63. Ramírez JD, Álvarez-Herms J, Castañeda-Babarro A, Larruskain J, de la Piscina XR,
687 Borisov O V., et al. The GALNTL6 Gene rs558129 Polymorphism Is Associated
688 With Power Performance. J Strength Cond Res. 2020;34:3031–6.
689 64. Pratap R, Chennuru S, Krovvidi S, Chitithoti J, Pentala RK. Putative SNPs in Ovar-
690 DRB1 and GALNTL6 Genes Conferring Susceptibility to Natural Infection of
691 Haemonchus Contortus in Southern Indian Sheep. Acta Parasitol. 2024;69:583–
692 90.
693 65. Al Kalaldeh M, Gibson J, Lee SH, Gondro C, Van Der Werf JHJ. Detection of
694 genomic regions underlying resistance to gastrointestinal parasites in Australian
695 sheep. Genetics Selection Evolution. 2019;51:1–18.
696 66. Gonzalez-Rivas PA, Chauhan SS, Ha M, Fegan N, Dunshea FR, Warner RD. Effects
697 of heat stress on animal physiology, metabolism, and meat quality: A review.
698 Meat Science. 2020;162.

699 67. Zhang M, Dunshea FR, Warner RD, DiGiacomo K, Osei-Amponsah R, Chauhan SS.
700 Impacts of heat stress on meat quality and strategies for amelioration: a review.
701 International Journal of Biometeorology 2020 64:9. 2020;64:1613–28.
702 68. Johnson JS, Wen H, Freitas PHF, Maskal JM, Hartman SO, Byrd MK, et al.
703 Evaluating phenotypes associated with heat tolerance and identifying moderate
704 and severe heat stress thresholds in lactating sows housed in mechanically or
705 naturally ventilated barns during the summer under commercial conditions. J
706 Anim Sci. 2023. https://doi.org/10.1093/JAS/SKAD129.
707 69. Knauer MT, Baitinger DJ. The Sow Body Condition Caliper. Appl Eng Agric.
708 2015;31:175–8.
709 70. Sahana G, Cai Z, Sanchez MP, Bouwman AC, Boichard D. Invited review: Good
710 practices in genome-wide association studies to identify candidate sequence
711 variants in dairy cattle. J Dairy Sci. 2023;106:5218–41.
712 71. Peiffer DA, Le JM, Steemers FJ, Chang W, Jenniges T, Garcia F, et al. High-
713 resolution genomic profiling of chromosomal aberrations using Infinium whole-
714 genome genotyping. Genome Res. 2006;16:1136–48.
715 72. Diskin SJ, Li M, Hou C, Yang S, Glessner J, Hakonarson H, et al. Adjustment of
716 genomic waves in signal intensities from whole-genome SNP genotyping
717 platforms. Nucleic Acids Res. 2008;36:e126–e126.
718 73. Quinlan AR, Hall IM. BEDTools: A flexible suite of utilities for comparing genomic
719 features. Bioinformatics. 2010;26:841–2.
720 74. Benfica LF, Brito LF, do Bem RD, Mulim HA, Glessner J, Braga LG, et al. Genome-
721 wide association study between copy number variation and feeding behavior, feed
722 efficiency, and growth traits in Nellore cattle. BMC Genomics. 2024;25:1–11.

723 75. VanRaden PM. Efficient Methods to Compute Genomic Predictions. J Dairy Sci.
724 2008;91:4414–23.
725 76. Misztal I, Tsuruta S, Lourenco D, Aguilar I, Legarra A, Vitezica Z. Manual for
726 BLUPF90 family of programs. 2014.
727 77. van den Berg S, Vandenplas J, van Eeuwijk FA, Lopes MS, Veerkamp RF.
728 Significance testing and genomic inflation factor using high-density genotypes or
729 whole-genome sequence data. Journal of Animal Breeding and Genetics.
730 2019;136:418–29.
731 78. Huang DW, Sherman BT, Lempicki RA. Systematic and integrative analysis of large
732 gene lists using DAVID bioinformatics resources. Nat Protoc. 2009;4:44–57.
733 79. Sherman BT, Hao M, Qiu J, Jiao X, Baseler MW, Lane HC, et al. DAVID: a web
734 server for functional enrichment analysis and functional annotation of gene lists
735 (2021 update). Nucleic Acids Res. 2022;50:W216–21.
736

737 **Supplementary Information**

738 **Table S1.** Copy number regions (CNVRs) identified in crossbed (Large White x
739 Landrace) sows

Chr	Start (bp)	End (bp)	Type	Number of individuals
1	1,296,974	1,637,442	Deletion	3
1	2,530,735	2,908,940	Deletion	3
1	4,621,444	4,690,022	Deletion	5
1	11,012,998	11,037,437	Duplication	3
1	16,313,130	16,384,057	Deletion	2
1	20,559,479	21,017,894	Deletion	23
1	26,407,492	26,757,112	Deletion	24
1	51,426,350	51,531,316	Deletion	15
1	52,843,788	52,930,466	Deletion	4
1	53,876,081	54,033,593	Deletion	7
1	54,929,205	55,080,766	Deletion	3
1	77,402,476	77,616,272	Deletion	2
1	77,973,487	78,233,457	Deletion	4
1	95,974,585	96,084,318	Deletion	5
1	190,422,856	190,521,756	Deletion	4
1	202,674,735	202,726,828	Deletion	6
1	232,171,858	232,231,168	Deletion	2
1	236,249,595	236,578,086	Deletion	6
1	245,380,316	245,417,266	Deletion	3
1	252,505,713	252,561,815	Deletion	11
1	255,734,516	255,775,164	Deletion	4
1	257,570,160	257,629,372	Deletion	7
1	296,787,813	296,854,248	Duplication	2

1	307,493,558	307,591,248	Deletion	4
1	308,407,845	308,540,510	Deletion	2
2	1,111	632,707	Deletion	202
2	1,728,741	1,792,444	Deletion	13
2	6,179,112	6,495,647	Deletion	34
2	12,967,586	13,092,623	Duplication	5
2	16,086,308	16,113,694	Deletion	3
2	16,914,155	16,957,926	Deletion	2
2	24,340,490	24,950,665	Deletion	4
2	32,124,159	32,186,193	Deletion	2
2	38,779,149	39,302,035	Deletion	22
2	100,248,260	100,301,718	Deletion	2
2	102,222,805	102,440,993	Duplication	2
2	103,642,873	103,742,033	Duplication	6
2	106,076,632	106,307,761	Deletion	12
2	110,341,590	110,423,447	Deletion	3
2	128,709,091	128,737,978	Duplication	2
2	129,799,406	129,981,864	Deletion	70
2	130,241,255	130,487,175	Deletion	58
2	137,484,909	137,871,651	Deletion	6
2	139,079,932	139,475,283	Deletion	8
2	140,748,675	140,896,496	Deletion	2
2	142,820,672	142,848,459	Duplication	2
2	146,604,847	146,623,766	Deletion	2
2	152,624,944	152,666,109	Duplication	3
2	157,653,015	158,139,060	Deletion	7
2	158,549,163	158,748,978	Deletion	6

2	160,171,978	160,334,626	Deletion	2
3	60,993	905,589	Deletion	28
3	1,157,712	1,540,289	Deletion	9
3	1,775,581	1,803,026	Deletion	3
3	11,450,046	11,519,897	Deletion	11
3	17,333,664	17,509,970	Deletion	47
3	69,789,999	70,298,496	Deletion	17
3	91,123,979	91,245,955	Deletion	2
3	102,698,568	102,763,903	Deletion	3
3	109,671,997	109,874,139	Deletion	13
3	113,053,130	113,163,300	Deletion	12
3	131,539,745	131,857,000	Deletion	5
4	1,155,293	1,388,468	Deletion	61
4	17,865,227	18,008,464	Deletion	2
4	19,578,395	19,626,320	Deletion	2
4	27,913,643	28,349,829	Deletion	4
4	63,290,072	63,491,767	Deletion	2
4	73,783,788	74,095,578	Deletion	6
4	80,721,007	80,767,798	Deletion	22
4	114,089,519	114,170,369	Duplication	2
4	126,897,791	127,521,733	Deletion	28
4	127,645,367	127,879,136	Deletion	12
4	131,676,536	132,009,191	Deletion	2
5	2,847	285,237	Deletion	3
5	548,113	1,210,042	Deletion	11
5	2,006,549	2,052,182	Deletion	3
5	2,144,424	2,559,524	Deletion	7

5	2,935,602	3,182,357	Deletion	2
5	29,640,202	29,787,794	Duplication	7
5	43,930,930	44,283,450	Deletion	11
5	60,541,361	60,621,247	Deletion	3
5	63,917,069	64,229,196	Deletion	10
5	64,347,352	64,392,680	Deletion	9
5	64,630,743	65,275,886	Deletion	32
5	75,132,228	75,385,516	Deletion	3
5	77,179,466	77,352,621	Deletion	28
5	99,716,210	99,952,686	Deletion	9
5	102,574,608	103,063,418	Deletion	2
5	110,482,927	111,027,924	Deletion	4
6	1,033,257	1,281,226	Deletion	101
6	2,952,600	3,336,730	Deletion	3
6	109,789,591	109,870,440	Deletion	4
6	129,702,907	130,569,596	Deletion	4
6	132,124,953	132,543,418	Mixed	139
6	132,647,018	132,704,049	Deletion	3
7	20,072,507	20,159,272	Deletion	2
7	30,314,760	30,550,361	Deletion	2
7	31,976,416	32,267,617	Deletion	5
7	37,900,142	37,967,748	Deletion	2
7	50,084,357	50,518,151	Deletion	16
7	52,531,709	52,558,947	Deletion	2
7	58,397,650	58,558,358	Deletion	9
7	112,964,257	113,292,023	Deletion	6
7	119,492,726	119,674,459	Deletion	5

8	4,899,715	4,961,037	Duplication	2
8	23,033,602	23,328,747	Deletion	12
8	108,840,104	108,903,615	Deletion	9
8	114,376,195	114,407,527	Deletion	22
8	122,249,328	122,288,920	Duplication	2
8	123,960,362	124,128,258	Deletion	95
8	131,207,688	131,694,842	Deletion	9
8	137,114,772	137,134,554	Deletion	23
9	15,049,063	15,211,706	Duplication	2
9	28,988,041	29,017,662	Deletion	3
9	29,741,635	29,982,654	Duplication	2
9	36,476,118	36,559,391	Deletion	4
9	44,613,872	44,716,642	Duplication	12
9	70,390,277	70,600,386	Duplication	2
9	71,697,328	71,711,489	Duplication	3
9	75,705,239	75,933,190	Deletion	2
9	130,785,204	130,830,299	Duplication	2
9	142,876,725	142,950,929	Duplication	2
9	143,288,947	143,605,209	Deletion	78
9	147,684,933	147,854,813	Duplication	3
9	148,629,187	148,681,260	Deletion	6
10	5,204,072	5,514,795	Deletion	2
10	11,450,736	11,498,946	Deletion	5
10	26,374,455	26,498,920	Deletion	2
10	39,272,858	39,507,554	Deletion	3
10	41,330,545	41,453,824	Deletion	7
10	47,123,541	47,259,902	Deletion	10

10	48,034,226	48,281,381	Deletion	66
11	8,876,752	8,927,330	Deletion	3
11	11,663,909	11,724,233	Deletion	12
11	20,388,606	20,495,264	Duplication	10
11	31,699,569	31,766,588	Deletion	2
11	32,127,787	32,515,591	Deletion	2
11	40,013,884	40,160,781	Deletion	7
11	46,563,594	46,642,716	Deletion	90
11	47,243,159	47,452,970	Deletion	3
11	59,735,869	61,470,768	Mixed	203
11	64,479,055	65,142,186	Deletion	45
11	67,375,641	67,671,825	Deletion	20
11	82,421,180	82,763,129	Deletion	6
11	86,175,659	86,395,677	Deletion	4
11	86,708,117	86,796,356	Deletion	6
12	60,100	1,998,701	Mixed	93
12	6,034,340	6,161,500	Deletion	2
12	7,385,966	7,581,758	Duplication	3
12	20,647,202	20,687,946	Deletion	9
12	23,645,644	23,760,296	Deletion	2
12	31,975,933	32,074,865	Deletion	4
12	36,947,624	37,322,661	Deletion	13
12	46,257,013	46,339,202	Deletion	12
12	54,979,595	55,051,174	Deletion	3
13	5,074,753	5,203,420	Deletion	3
13	8,329,572	8,363,589	Mixed	2
13	12,386,754	12,485,442	Deletion	3

13	19,629,258	19,683,797	Duplication	2
13	41,749,852	41,820,811	Deletion	6
13	81,326,561	81,437,311	Deletion	3
13	102,306,232	102,458,997	Deletion	31
13	179,990,010	180,090,208	Deletion	8
13	194,292,500	194,386,412	Deletion	2
13	194,665,680	196,342,442	Deletion	108
13	196,810,429	197,241,857	Deletion	12
13	200,335,858	200,366,615	Deletion	5
13	200,765,190	201,339,708	Deletion	36
13	202,480,537	202,728,252	Deletion	5
13	202,925,976	203,079,047	Deletion	9
13	204,430,769	204,569,521	Deletion	2
13	204,734,507	204,819,522	Deletion	3
13	206,943,236	207,322,709	Deletion	3
13	209,713,551	209,761,484	Deletion	8
13	216,912,741	217,056,683	Deletion	3
13	218,141,951	218,612,146	Deletion	12
14	2,789,202	2,852,561	Duplication	2
14	16,993,535	17,333,398	Deletion	63
14	24,286,577	24,389,234	Deletion	2
14	38,219,290	38,645,949	Deletion	21
14	52,573,859	52,621,172	Deletion	5
14	58,074,274	58,206,487	Deletion	4
14	73,479,608	73,695,090	Deletion	5
14	74,176,726	74,990,114	Deletion	24
14	98,057,493	98,157,352	Duplication	4

14	102,480,650	102,988,071	Deletion	6
14	104,441,890	105,084,009	Mixed	54
14	113,376,632	113,445,546	Duplication	3
14	114,586,489	114,610,574	Duplication	3
14	118,345,379	118,395,858	Duplication	2
14	132,285,105	132,353,947	Deletion	4
14	136,444,819	137,178,653	Deletion	64
14	139,546,885	139,906,120	Deletion	7
14	140,199,680	140,419,493	Deletion	18
14	141,068,807	141,208,015	Deletion	8
14	151,966,127	153,374,972	Deletion	80
15	9,519,813	10,711,345	Deletion	245
15	12,597,728	12,844,713	Deletion	80
15	17,097,658	17,123,356	Deletion	2
15	24,371,978	24,804,276	Deletion	63
15	25,845,378	25,910,541	Deletion	4
15	30,831,468	31,122,672	Deletion	19
15	33,345,253	33,617,369	Deletion	10
15	48,845,490	49,845,075	Deletion	47
15	50,619,226	50,703,404	Deletion	4
15	69,448,740	69,693,811	Deletion	3
15	125,908,102	126,154,684	Deletion	2
15	126,439,963	127,295,381	Deletion	45
15	127,544,621	127,786,638	Deletion	2
15	134,842,540	134,994,861	Deletion	62
15	137,449,752	137,725,895	Deletion	2
15	138,365,140	138,453,739	Duplication	4

15	141,222,980	141,247,045	Deletion	12
15	154,198,036	154,217,738	Deletion	6
15	154,516,149	154,590,998	Deletion	4
16	2,294,773	2,931,783	Deletion	20
16	9,539,468	9,771,058	Deletion	5
16	10,588,133	11,083,680	Deletion	43
16	11,287,880	11,615,935	Deletion	2
16	14,404,612	14,706,916	Deletion	26
16	17,665,436	17,995,430	Deletion	4
16	18,347,402	18,376,590	Deletion	13
16	30,289,787	30,566,627	Deletion	3
16	47,246,973	47,457,841	Deletion	2
16	56,228,146	56,340,252	Deletion	2
16	64,441,004	64,872,621	Deletion	6
16	85,407,012	86,024,383	Deletion	22
17	2,202,762	2,730,970	Deletion	184
17	3,434,809	3,642,846	Deletion	5
17	4,055,697	4,468,083	Deletion	22
17	7,151,308	7,537,515	Deletion	14
17	67,540,904	67,605,067	Duplication	2
18	6,247,938	6,366,290	Deletion	2
18	32,234,894	32,451,272	Deletion	8
18	38,984,087	39,185,391	Deletion	32
18	59,478,274	59,600,842	Deletion	6

740

741

742 **Table S2.** Genes annotated for CNVRs present in at least 5% of the population

CNVR	Ensembl Gene ID	Gene Name	Gene Biotype
	ENSSSCG00000012844	*SLC25A22*	Protein coding
	ENSSSCG00000049665		Pseudogene
	ENSSSCG00000012843	*PIDD1*	Protein coding
	ENSSSCG00000012842	*RPLP2*	Protein coding
	ENSSSCG00000012836	*AP2A2*	Protein coding
	ENSSSCG00000012835		Protein coding
	ENSSSCG00000012847	*TALDO1*	Protein coding
	ENSSSCG00000012846	*GATD1*	Protein coding
	ENSSSCG00000012845	*CEND1*	Protein coding
	ENSSSCG00000060622		Protein coding
	ENSSSCG00000032436		Protein coding
CNVR21	*ENSSSCG00000038912*		Protein coding
	ENSSSCG00000014565		Protein coding
	ENSSSCG00000032591		Protein coding
	ENSSSCG00000033780	*B4GALNT4*	Protein coding
	ENSSSCG00000051760		Protein coding
	ENSSSCG00000027302	*PKP3*	Protein coding
	ENSSSCG00000024389	*SIGIRR*	Protein coding
	ENSSSCG00000024569	*ANO9*	Protein coding
	ENSSSCG00000037427	*PTDSS2*	Protein coding
	ENSSSCG00000032010	*RNH1*	Protein coding
	ENSSSCG00000031513	*HRAS*	Protein coding
	ENSSSCG00000027045	*LRRC56*	Protein coding

ENSSSCG00000030137	*LMNTD2*	Protein coding
ENSSSCG00000012854	*RASSF7*	Protein coding
ENSSSCG00000014554		Protein coding
ENSSSCG00000014555	*ODF3*	Protein coding
ENSSSCG00000014556	*BET1L*	Protein coding
ENSSSCG00000014557	*RIC8A*	Protein coding
ENSSSCG00000014558	*SIRT3*	Protein coding
ENSSSCG00000014559	*PSMD13*	Protein coding
ENSSSCG00000061991	*COX8H*	Protein coding
ENSSSCG00000014561	*NLRP6*	Protein coding
ENSSSCG00000025023	*PGGHG*	Protein coding
ENSSSCG00000040278	*IFITM5*	Protein coding
ENSSSCG00000012841	*PNPLA2*	Protein coding
ENSSSCG00000023933	*CRACR2B*	Protein coding
ENSSSCG00000012840	*CD151*	Protein coding
ENSSSCG00000059584		Protein coding
ENSSSCG00000012838	*TSPAN4*	Protein coding
ENSSSCG00000012837	*CHID1*	Protein coding
ENSSSCG00000029723	*PHRF1*	Protein coding
ENSSSCG00000012853	*IRF7*	Protein coding
ENSSSCG00000012852	*CDHR5*	Protein coding
ENSSSCG00000040951	*SCT*	Protein coding
ENSSSCG00000012851	*DRD4*	Protein coding
ENSSSCG00000012850	*DEAF1*	Protein coding
ENSSSCG00000044406	*TMEM80*	Protein coding

	ENSSSCG00000012848	*EPS8L2*	Protein coding
	ENSSSCG00000063023		lncRNA
	ENSSSCG00000038005		lncRNA
	ENSSSCG00000018538	*SNORA52*	snoRNA
	ENSSSCG00000019083		miRNA
	ENSSSCG00000035967	*ZC3H18*	Protein coding
	ENSSSCG00000040875	*ZFPM1*	Protein coding
CNVR68	*ENSSSCG00000053583*		Pseudogene
	ENSSSCG00000058880		lncRNA
	ENSSSCG00000063162		lncRNA
	ENSSSCG00000053778		lncRNA
CNVR72	*ENSSSCG00000059804*		lncRNA
	ENSSSCG00000060648		lncRNA
CNVR101	*ENSSSCG00000061075*		lncRNA
	ENSSSCG00000031946	*GPC5*	Protein coding
	ENSSSCG00000063520		lncRNA
	ENSSSCG00000054481		lncRNA
	ENSSSCG00000019902		miRNA
CNVR103	*ENSSSCG00000019897*	*ssc-mir-19a*	miRNA
	ENSSSCG00000018681		miRNA
	ENSSSCG00000019883	*MIR20A*	miRNA
	ENSSSCG00000018617	*ssc-mir-17*	miRNA
	ENSSSCG00000019535	*ssc-mir-18a*	miRNA
CNVR109	*ENSSSCG00000022317*	*SLC38A10*	Protein coding
	ENSSSCG00000039183	*NDUFAF8*	Protein coding

ENSSSCG00000028593	*TEPSIN*	Protein coding
ENSSSCG00000044039		Protein coding
ENSSSCG00000039807		Protein coding
ENSSSCG00000037364		Protein coding
ENSSSCG00000035852	*CSNK1D*	Protein coding
ENSSSCG00000024018	*SLC16A3*	Protein coding
ENSSSCG00000029553	*CCDC57*	Protein coding
ENSSSCG00000029944	*FASN*	Protein coding
ENSSSCG00000034696		Protein coding
ENSSSCG00000017137	*METRNL*	Protein coding
ENSSSCG00000034723	*PYCR1*	Protein coding
ENSSSCG00000040352	*DUS1L*	Protein coding
ENSSSCG00000033689	*GPS1*	Protein coding
ENSSSCG00000040385	*RFNG*	Protein coding
ENSSSCG00000035253	*MAFG*	Protein coding
ENSSSCG00000034695	*SIRT7*	Protein coding
ENSSSCG00000031851	*CBR2*	Protein coding
ENSSSCG00000039650	*PCYT2*	Protein coding
ENSSSCG00000039873	*DCXR*	Protein coding
ENSSSCG00000036973	*RAC3*	Protein coding
ENSSSCG00000040503	*LRRC45*	Protein coding
ENSSSCG00000049515		Protein coding
ENSSSCG00000040727	*ASPSCR1*	Protein coding
ENSSSCG00000039013	*NOTUM*	Protein coding
ENSSSCG00000027229	*B3GNTL1*	Protein coding

ENSSSCG00000017136	*TBCD*	Protein coding
ENSSSCG00000017135		Pseudogene
ENSSSCG00000017131	*FN3K*	Protein coding
ENSSSCG00000017134	*FN3KRP*	Protein coding
ENSSSCG00000053358	*RAB40B*	Protein coding
ENSSSCG00000017125	*FOXK2*	Protein coding
ENSSSCG00000017126	*NARF*	Protein coding
ENSSSCG00000017127	*CYBC1*	Protein coding
ENSSSCG00000017143	*CEP131*	Protein coding
ENSSSCG00000017128	*HEXD*	Protein coding
ENSSSCG00000032116	*OGFOD3*	Protein coding
ENSSSCG00000039849	*PVALEF*	Protein coding
ENSSSCG00000017141	*AATK*	Protein coding
ENSSSCG00000017142	*BAIAP2*	Protein coding
ENSSSCG00000017140	*CHMP6*	Protein coding
ENSSSCG00000017139	*RPTOR*	Protein coding
ENSSSCG00000032655	*ALYREF*	Protein coding
ENSSSCG00000035837	*NPB*	Protein coding
ENSSSCG00000035728		Protein coding
ENSSSCG00000034058	*ARHGDIA*	Protein coding
ENSSSCG00000039148	*P4HB*	Protein coding
ENSSSCG00000037039	*PPP1R27*	Protein coding
ENSSSCG00000039424	*MCRIP1*	Protein coding
ENSSSCG00000034891	*GCGR*	Protein coding
ENSSSCG00000033620	*SLC25A10*	Protein coding

ENSSSCG00000033148	*MRPL12*	Protein coding
ENSSSCG00000033082	*HGS*	Protein coding
ENSSSCG00000053661	*ARL16*	Protein coding
ENSSSCG00000034716	*CCDC137*	Protein coding
ENSSSCG00000033788	*OXLD1*	Protein coding
ENSSSCG00000053315	*PDE6G*	Protein coding
ENSSSCG00000031531	*TSPAN10*	Protein coding
ENSSSCG00000024235	*NPLOC4*	Protein coding
ENSSSCG00000029616	*FAAP100*	Protein coding
ENSSSCG00000052003	*FSCN2*	Protein coding
ENSSSCG00000028355	*ACTG1*	Protein coding
ENSSSCG00000023045	*BAHCC1*	Protein coding
ENSSSCG00000032974	*MYADML2*	Protein coding
ENSSSCG00000033221		Protein coding
ENSSSCG00000048083		lncRNA
ENSSSCG00000048182		lncRNA
ENSSSCG00000052544		lncRNA
ENSSSCG00000051633		lncRNA
ENSSSCG00000058976		lncRNA
ENSSSCG00000044226		lncRNA
ENSSSCG00000052239		lncRNA
ENSSSCG00000044793		lncRNA
ENSSSCG00000059540		lncRNA
ENSSSCG00000057304		lncRNA
ENSSSCG00000053087		lncRNA

	ENSSSCG00000055034		lncRNA
	ENSSSCG00000057060		lncRNA
	ENSSSCG00000062857		lncRNA
	ENSSSCG00000061157		lncRNA
	ENSSSCG00000057894		lncRNA
	ENSSSCG00000051900		lncRNA
	ENSSSCG00000051406		lncRNA
	ENSSSCG00000024675		miRNA
	ENSSSCG00000017133	*WDR45B*	Protein coding
CNVR122	*ENSSSCG00000012034*	*TIAM1*	Protein coding
	ENSSSCG00000021355	*SOD1*	Protein coding
	ENSSSCG00000021023	*SCAF4*	Protein coding
	ENSSSCG00000029392	*HUNK*	Protein coding
	ENSSSCG00000034229	*MIS18A*	Protein coding
	ENSSSCG00000040843		Protein coding
	ENSSSCG00000032024	*URB1*	Protein coding
	ENSSSCG00000021598	*EVA1C*	Protein coding
	ENSSSCG00000040827	*CFAP298*	Protein coding
	ENSSSCG00000012035	*SYNJ1*	Protein coding
	ENSSSCG00000012037	*PAXBP1*	Protein coding
	ENSSSCG00000047315		lncRNA
	ENSSSCG00000057126		lncRNA
	ENSSSCG00000055848		lncRNA
	ENSSSCG00000062329		lncRNA
	ENSSSCG00000058707		lncRNA

	ENSSSCG00000055435		lncRNA
	ENSSSCG00000050688		lncRNA
	ENSSSCG00000052840	*U6*	snRNA
	ENSSSCG00000023224	*U6*	snRNA
CNVR150	*ENSSSCG00000023746*	*LRP1B*	Protein coding
	ENSSSCG00000058664		lncRNA
	ENSSSCG00000054640		lncRNA
CNVR151	*ENSSSCG00000053710*		lncRNA
	ENSSSCG00000054110	*U6*	snRNA
CNVR174	*ENSSSCG00000038257*	*SGCZ*	Protein coding
	ENSSSCG00000020959	*ssc-mir-383*	miRNA

743

744 **Table S3.** Annoted QTL for autossomal copy number variation regions (CNVRs) shared

745 by at least 5% of the population

CNVR	**Chr**	**Start (bp)**	**End (bp)**	**QTL type**	**Name**
CNVR21	2	1,111	632,707	Meat and Carcass	Average backfat thickness
CNVR21	2	1,111	632,707	Meat and Carcass	Loin weight
CNVR21	2	1,111	632,707	Meat and Carcass	Loin and ham percentage in carcass
CNVR21	2	1,111	632,707	Meat and Carcass	Estimated carcass lean content
CNVR21	2	1,111	632,707	Meat and Carcass	Backfat weight
CNVR21	2	1,111	632,707	Meat and Carcass	Percentage of backfat and leaf fat in carcass
CNVR21	2	1,111	632,707	Meat and Carcass	Backfat thickness between 3rd and 4th rib
CNVR21	2	1,111	632,707	Meat and Carcass	Backfat at last rib

CNVR21	2	1,111	632,707	Reproduction	Teat number
CNVR21	2	1,111	632,707	Meat and Carcass	Average backfat thickness
CNVR21	2	1,111	632,707	Meat and Carcass	Ham percentage
CNVR21	2	1,111	632,707	Meat and Carcass	Loin percentage
CNVR21	2	1,111	632,707	Meat and Carcass	Lean meat percentage
CNVR21	2	1,111	632,707	Meat and Carcass	Backfat percentage
CNVR21	2	1,111	632,707	Meat and Carcass	Fat-cuts percentage
CNVR21	2	1,111	632,707	Meat and Carcass	Lean meat percentage
CNVR21	2	1,111	632,707	Meat and Carcass	Ham meat weight
CNVR21	2	1,111	632,707	Meat and Carcass	Lean meat + bone in ham + back
CNVR21	2	1,111	632,707	Meat and Carcass	Loin muscle area
CNVR21	2	1,111	632,707	Meat and Carcass	Average backfat thickness
CNVR21	2	1,111	632,707	Meat and Carcass	Heart weight
CNVR21	2	1,111	632,707	Meat and Carcass	Meat color
CNVR21	2	1,111	632,707	Meat and Carcass	Heart weight
CNVR21	2	1,111	632,707	Production	Average daily gain
CNVR21	2	1,111	632,707	Meat and Carcass	Muscle conductivity
CNVR21	2	1,111	632,707	Meat and Carcass	Head weight
CNVR21	2	1,111	632,707	Meat and Carcass	Backfat at tenth rib
CNVR21	2	1,111	632,707	Meat and Carcass	Backfat at last rib
CNVR21	2	1,111	632,707	Meat and Carcass	Average backfat thickness
CNVR21	2	1,111	632,707	Meat and Carcass	Loin muscle area
CNVR21	2	1,111	632,707	Meat and Carcass	Loin weight
CNVR21	2	1,111	632,707	Meat and Carcass	Backfat weight
CNVR21	2	1,111	632,707	Meat and Carcass	Backfat at last lumbar

CNVR21	2	1,111	632,707	Meat and Carcass	Backfat thickness between 3rd and 4th rib
CNVR21	2	1,111	632,707	Meat and Carcass	Lean meat percentage
CNVR21	2	1,111	632,707	Meat and Carcass	Average backfat thickness
CNVR21	2	1,111	632,707	Meat and Carcass	Backfat at last rib
CNVR21	2	1,111	632,707	Meat and Carcass	Backfat at last lumbar
CNVR21	2	1,111	632,707	Meat and Carcass	Backfat at tenth rib
CNVR21	2	1,111	632,707	Meat and Carcass	Average backfat thickness
CNVR21	2	1,111	632,707	Meat and Carcass	Backfat at tenth rib
CNVR21	2	1,111	632,707	Meat and Carcass	Backfat at last lumbar
CNVR21	2	1,111	632,707	Meat and Carcass	Backfat at last rib
CNVR21	2	1,111	632,707	Meat and Carcass	Loin muscle area
CNVR21	2	1,111	632,707	Meat and Carcass	muscle protein percentage
CNVR21	2	1,111	632,707	Meat and Carcass	Backfat at first rib
CNVR21	2	1,111	632,707	Meat and Carcass	backfat at P2 position
CNVR21	2	1,111	632,707	Meat and Carcass	Carcass length
CNVR21	2	1,111	632,707	Meat and Carcass	Lean meat percentage
CNVR21	2	1,111	632,707	Meat and Carcass	External fat on loin
CNVR21	2	1,111	632,707	Meat and Carcass	Muscle pH
CNVR21	2	1,111	632,707	Meat and Carcass	Muscle pH
CNVR21	2	1,111	632,707	Meat and Carcass	Muscle conductivity
CNVR21	2	1,111	632,707	Meat and Carcass	Muscle conductivity
CNVR21	2	1,111	632,707	Production	Average daily gain
CNVR21	2	1,111	632,707	Meat and Carcass	Muscle pH
CNVR21	2	1,111	632,707	Meat and Carcass	Carcass length
CNVR21	2	1,111	632,707	Meat and Carcass	Carcass weight (hot)
CNVR21	2	1,111	632,707	Meat and Carcass	Muscle pH

CNVR21	2	1,111	632,707	Meat and Carcass	Muscle conductivity
CNVR21	2	1,111	632,707	Meat and Carcass	Carcass weight (hot)
CNVR21	2	1,111	632,707	Meat and Carcass	Neck fat weight
CNVR21	2	1,111	632,707	Production	Feed conversion ratio
CNVR21	2	1,111	632,707	Meat and Carcass	Loin weight
CNVR21	2	1,111	632,707	Meat and Carcass	Carcass weight (hot)
CNVR21	2	1,111	632,707	Meat and Carcass	Ham weight
CNVR21	2	1,111	632,707	Meat and Carcass	Shoulder weight
CNVR21	2	1,111	632,707	Meat and Carcass	Shear firmness
CNVR21	2	1,111	632,707	Health	Segmented neutrophil number
CNVR21	2	1,111	632,707	Meat and Carcass	Cutlet weight
CNVR21	2	1,111	632,707	Meat and Carcass	Loin muscle area
CNVR21	2	1,111	632,707	Meat and Carcass	Fat to meat ratio
CNVR21	2	1,111	632,707	Production	Body weight
CNVR21	2	1,111	632,707	Meat and Carcass	Average backfat thickness
CNVR21	2	1,111	632,707	Health	O2 partial pressure
CNVR21	2	1,111	632,707	Health	Oxygen saturation
CNVR21	2	1,111	632,707	Exterior	Gait score (hind)
CNVR21	2	1,111	632,707	Health	Hemolytic complement activity (alternative pathway)
CNVR21	2	1,111	632,707	Health	Hemolytic complement activity (alternative pathway)
CNVR21	2	1,111	632,707	Health	Hemolytic complement activity (alternative pathway)
CNVR21	2	1,111	632,707	Health	C3c concentration
CNVR21	2	1,111	632,707	Health	C3c concentration
CNVR21	2	1,111	632,707	Health	C3c concentration

CNVR21	2	1,111	632,707	Health	Creatine kinase level
CNVR21	2	1,111	632,707	Meat and Carcass	Backfat at last rib
CNVR21	2	1,111	632,707	Production	Average daily gain
CNVR21	2	1,111	632,707	Meat and Carcass	Backfat at last rib
CNVR21	2	1,111	632,707	Meat and Carcass	Average backfat thickness
CNVR21	2	1,111	632,707	Meat and Carcass	Loin weight
CNVR21	2	1,111	632,707	Meat and Carcass	Average backfat thickness
CNVR21	2	1,111	632,707	Health	Interleukin-10 level
CNVR21	2	1,111	632,707	Health	Toll-like receptor 9 level
CNVR21	2	1,111	632,707	Production	Bone mineral content
CNVR21	2	1,111	632,707	Exterior	Osteochondrosis score
CNVR21	2	1,111	632,707	Meat and Carcass	Average backfat thickness
CNVR21	2	1,111	632,707	Meat and Carcass	Adipocyte diameter
CNVR21	2	1,111	632,707	Health	Actinobacillus pleuropneumoniae susceptibility
CNVR21	2	1,111	632,707	Meat and Carcass	Loin muscle depth
CNVR21	2	1,111	632,707	Meat and Carcass	Dressing percentage
CNVR21	2	1,111	632,707	Meat and Carcass	Monounsaturated fatty acid to polyunsaturated fatty acid ratio
CNVR21	2	1,111	632,707	Meat and Carcass	Linoleic acid content
CNVR21	2	1,111	632,707	Meat and Carcass	Polyunsaturated fatty acid content
CNVR21	2	1,111	632,707	Meat and Carcass	Oleic acid content
CNVR21	2	1,111	632,707	Meat and Carcass	Monounsaturated fatty acid content

CNVR21	2	1,111	632,707	Meat and Carcass	Polyunsaturated fatty acid to saturated fatty acid ratio
CNVR21	2	1,111	632,707	Meat and Carcass	Dressing percentage
CNVR21	2	1,111	632,707	Meat and Carcass	Monounsaturated fatty acid to polyunsaturated fatty acid ratio
CNVR21	2	1,111	632,707	Meat and Carcass	Linoleic acid content
CNVR21	2	1,111	632,707	Meat and Carcass	Polyunsaturated fatty acid content
CNVR21	2	1,111	632,707	Meat and Carcass	Oleic acid content
CNVR21	2	1,111	632,707	Meat and Carcass	Average backfat thickness
CNVR21	2	1,111	632,707	Meat and Carcass	Dressing percentage
CNVR21	2	1,111	632,707	Meat and Carcass	Average backfat thickness
CNVR21	2	1,111	632,707	Meat and Carcass	Lean meat percentage
CNVR21	2	1,111	632,707	Meat and Carcass	Monounsaturated fatty acid to polyunsaturated fatty acid ratio
CNVR21	2	1,111	632,707	Meat and Carcass	Linoleic acid content
CNVR21	2	1,111	632,707	Meat and Carcass	Polyunsaturated fatty acid content
CNVR21	2	1,111	632,707	Meat and Carcass	Polyunsaturated fatty acid to saturated fatty acid ratio
CNVR21	2	1,111	632,707	Meat and Carcass	Oleic acid content
CNVR21	2	1,111	632,707	Meat and Carcass	Cooking loss
CNVR21	2	1,111	632,707	Meat and Carcass	Dressing percentage
CNVR21	2	1,111	632,707	Meat and Carcass	Dressing percentage
CNVR21	2	1,111	632,707	Meat and Carcass	Average backfat thickness
CNVR21	2	1,111	632,707	Meat and Carcass	Lean meat percentage

CNVR21	2	1,111	632,707	Meat and Carcass	Monounsaturated fatty acid to polyunsaturated fatty acid ratio
CNVR21	2	1,111	632,707	Meat and Carcass	Linoleic acid content
CNVR21	2	1,111	632,707	Meat and Carcass	Polyunsaturated fatty acid content
CNVR21	2	1,111	632,707	Meat and Carcass	Oleic acid content
CNVR21	2	1,111	632,707	Meat and Carcass	Monounsaturated fatty acid content
CNVR21	2	1,111	632,707	Meat and Carcass	Backfat between 6th and 7th ribs
CNVR21	2	1,111	632,707	Meat and Carcass	Average backfat thickness
CNVR21	2	1,111	632,707	Meat and Carcass	Monounsaturated fatty acid to polyunsaturated fatty acid ratio
CNVR21	2	1,111	632,707	Meat and Carcass	Linoleic acid content
CNVR21	2	1,111	632,707	Meat and Carcass	Polyunsaturated fatty acid content
CNVR21	2	1,111	632,707	Meat and Carcass	Oleic acid content
CNVR21	2	1,111	632,707	Meat and Carcass	Polyunsaturated fatty acid to saturated fatty acid ratio
CNVR21	2	1,111	632,707	Meat and Carcass	Monounsaturated fatty acid content
CNVR21	2	1,111	632,707	Meat and Carcass eQTL	Fat androstenone level
CNVR21	2	1,111	632,707	Meat and Carcass eQTL	Fat androstenone level
CNVR21	2	1,111	632,707	Meat and Carcass eQTL	Fat androstenone level

CNVR21	2	1,111	632,707	Meat and Carcass	Dressing percentage
CNVR21	2	1,111	632,707	Meat and Carcass	Average backfat thickness
CNVR21	2	1,111	632,707	Meat and Carcass	Lean meat percentage
CNVR68	6	1,033,257	1,281,226	Meat and Carcass	Intramuscular fat content
CNVR68	6	1,033,257	1,281,226	Exterior	Vertebra number
CNVR68	6	1,033,257	1,281,226	Reproduction	Teat number
CNVR72	6	132,124,953	132,543,418	Health	Alkaline phosphatase activity
CNVR72	6	132,124,953	132,543,418	Reproduction	Teat number
CNVR72	6	132,124,953	132,543,418	Meat and Carcass	Shear force
CNVR72	6	132,124,953	132,543,418	Meat and Carcass	Intramuscular fat content
CNVR72	6	132,124,953	132,543,418	Health	Cholesterol level
CNVR72	6	132,124,953	132,543,418	Meat and Carcass	Intramuscular fat content
CNVR72	6	132,124,953	132,543,418	Reproduction	Teat number
CNVR72	6	132,124,953	132,543,418	Meat and Carcass	Backfat at tenth rib
CNVR72	6	132,124,953	132,543,418	Meat and Carcass	Backfat at last rib
CNVR72	6	132,124,953	132,543,418	Meat and Carcass	Shoulder meat weight
CNVR72	6	132,124,953	132,543,418	Meat and Carcass	Backfat at tenth rib
CNVR72	6	132,124,953	132,543,418	Meat and Carcass	Muscle moisture percentage
CNVR72	6	132,124,953	132,543,418	Meat and Carcass	Carcass temperature
CNVR72	6	132,124,953	132,543,418	Meat and Carcass	Muscle fat content
CNVR72	6	132,124,953	132,543,418	Meat and Carcass	muscle protein percentage
CNVR72	6	132,124,953	132,543,418	Meat and Carcass	Muscle moisture percentage
CNVR72	6	132,124,953	132,543,418	Meat and Carcass	Semimembranosus angle
CNVR72	6	132,124,953	132,543,418	Health	Body temperature
CNVR72	6	132,124,953	132,543,418	Exterior	Gait score (hind)
CNVR72	6	132,124,953	132,543,418	Meat and Carcass	Shoulder weight
CNVR72	6	132,124,953	132,543,418	Meat and Carcass	Shoulder weight

CNVR72	6	132,124,953	132,543,418	Meat and Carcass	Ham weight
CNVR72	6	132,124,953	132,543,418	Meat and Carcass	Muscle conductivity
CNVR72	6	132,124,953	132,543,418	Meat and Carcass	Intramuscular fat content
CNVR72	6	132,124,953	132,543,418	Meat and Carcass	Ham weight
CNVR72	6	132,124,953	132,543,418	Reproduction	Cryptorchidism
CNVR82	8	123,960,362	124,128,258	Reproduction	Litter size
CNVR82	8	123,960,362	124,128,258	Meat and Carcass	Loin muscle area
CNVR82	8	123,960,362	124,128,258	Health	Melanoma susceptibility
CNVR82	8	123,960,362	124,128,258	Meat and Carcass	Muscle pH
CNVR82	8	123,960,362	124,128,258	Meat and Carcass	Muscle moisture percentage
CNVR82	8	123,960,362	124,128,258	Reproduction	Litter size
CNVR82	8	123,960,362	124,128,258	Reproduction	Total number born alive
CNVR82	8	123,960,362	124,128,258	Meat and Carcass	Muscle moisture percentage
CNVR82	8	123,960,362	124,128,258	Meat and Carcass	Off-flavor score
CNVR82	8	123,960,362	124,128,258	Meat and Carcass	Cooking yield
CNVR82	8	123,960,362	124,128,258	Meat and Carcass	Meat color
CNVR82	8	123,960,362	124,128,258	Meat and Carcass	Fat area percentage in carcass
CNVR82	8	123,960,362	124,128,258	Meat and Carcass	Fat area percentage in carcass
CNVR82	8	123,960,362	124,128,258	Meat and Carcass	Fat area percentage in carcass
CNVR82	8	123,960,362	124,128,258	Meat and Carcass	Carcass weight (hot)
CNVR82	8	123,960,362	124,128,258	Health	Monocyte number
CNVR82	8	123,960,362	124,128,258	Health	CO2 partial pressure
CNVR82	8	123,960,362	124,128,258	Health	Oxygen saturation
CNVR82	8	123,960,362	124,128,258	Health	Sodium level
CNVR82	8	123,960,362	124,128,258	Reproduction	Age at puberty
CNVR82	8	123,960,362	124,128,258	Meat and Carcass	Loin muscle area
CNVR82	8	123,960,362	124,128,258	Health	Plateletcrit

CNVR101	11	46,563,594	46,642,716	Reproduction	Teat number
CNVR101	11	46,563,594	46,642,716	Meat and Carcass	Loin and neck meat weight
CNVR101	11	46,563,594	46,642,716	Meat and Carcass	Backfat at mid-back
CNVR101	11	46,563,594	46,642,716	Meat and Carcass	Loin muscle area
CNVR101	11	46,563,594	46,642,716	Meat and Carcass	Meat color
CNVR101	11	46,563,594	46,642,716	Exterior	Time spent drinking
CNVR101	11	46,563,594	46,642,716	Health	Body temperature
CNVR101	11	46,563,594	46,642,716	Health	Eosinophil number
CNVR101	11	46,563,594	46,642,716	Production	Body weight
CNVR101	11	46,563,594	46,642,716	Meat and Carcass	Percentage angular fibers
CNVR101	11	46,563,594	46,642,716	Meat and Carcass	Meat color
CNVR101	11	46,563,594	46,642,716	Meat and Carcass	Drip loss
CNVR101	11	46,563,594	46,642,716	Meat and Carcass	Percentage type I fibers
CNVR101	11	46,563,594	46,642,716	Reproduction	Nonfunctional nipples
CNVR101	11	46,563,594	46,642,716	Health	Haptoglobin concentration
CNVR101	11	46,563,594	46,642,716	Health	Interferon-gamma level
CNVR101	11	46,563,594	46,642,716	Health	Interferon-gamma level
CNVR101	11	46,563,594	46,642,716	Health	Interferon-gamma to interleukin-10 ratio
CNVR103	11	59,735,869	61,470,768	Meat and Carcass	Backfat at mid-back
CNVR103	11	59,735,869	61,470,768	Meat and Carcass	Loin muscle area
CNVR103	11	59,735,869	61,470,768	Meat and Carcass	Meat color
CNVR103	11	59,735,869	61,470,768	Exterior	Time spent drinking
CNVR103	11	59,735,869	61,470,768	Health	Body temperature
CNVR103	11	59,735,869	61,470,768	Health	Eosinophil number
CNVR103	11	59,735,869	61,470,768	Meat and Carcass	Meat color
CNVR103	11	59,735,869	61,470,768	Meat and Carcass	Drip loss

CNVR103	11	59,735,869	61,470,768	Meat and Carcass	Percentage type I fibers
CNVR103	11	59,735,869	61,470,768	Reproduction	Nonfunctional nipples
CNVR103	11	59,735,869	61,470,768	Meat and Carcass	Lean meat percentage
CNVR103	11	59,735,869	61,470,768	Meat and Carcass	Average backfat thickness
CNVR103	11	59,735,869	61,470,768	Production	Feed intake
CNVR103	11	59,735,869	61,470,768	Meat and Carcass	Backfat at last rib
CNVR103	11	59,735,869	61,470,768	Production	Average daily gain
CNVR103	11	59,735,869	61,470,768	Meat and Carcass	Double-bond index
CNVR103	11	59,735,869	61,470,768	Meat and Carcass	Muscle pH decline
CNVR103	11	59,735,869	61,470,768	Meat and Carcass	Muscle fat content
CNVR103	11	59,735,869	61,470,768	Meat and Carcass	Muscle moisture percentage
CNVR103	11	59,735,869	61,470,768	Meat and Carcass	Empty body lipid content
CNVR103	11	59,735,869	61,470,768	Reproduction	Number of stillborn
CNVR103	11	59,735,869	61,470,768	Meat and Carcass	Empty body lipid content
CNVR103	11	59,735,869	61,470,768	Meat and Carcass	Ham fat thickness
CNVR103	11	59,735,869	61,470,768	Reproduction	Nonfunctional nipples
CNVR103	11	59,735,869	61,470,768	Health	Toll-like receptor 9 level
CNVR103	11	59,735,869	61,470,768	Production	Average daily gain
CNVR103	11	59,735,869	61,470,768	Production	Body weight
CNVR103	11	59,735,869	61,470,768	Reproduction	Litter size
CNVR103	11	59,735,869	61,470,768	Reproduction	Litter size
CNVR103	11	59,735,869	61,470,768	Reproduction	Litter size
CNVR103	11	59,735,869	61,470,768	Meat and Carcass	Intramuscular fat content
CNVR103	11	59,735,869	61,470,768	Meat and Carcass	Intramuscular fat content
CNVR103	11	59,735,869	61,470,768	Meat and Carcass	Intramuscular fat content
CNVR103	11	59,735,869	61,470,768	Health	CD4-positive, CD8-positive leukocyte percentage

CNVR103	11	59,735,869	61,470,768	Production	Feed conversion ratio
CNVR103	11	59,735,869	61,470,768	Meat and Carcass	Intramuscular fat content
CNVR103	11	59,735,869	61,470,768	Meat and Carcass	Number of ribs
CNVR103	11	59,735,869	61,470,768	Meat and Carcass	Intramuscular fat content
CNVR109	12	60,100	1,998,701	Meat and Carcass	Backfat at tenth rib
CNVR109	12	60,100	1,998,701	Meat and Carcass	Backfat at mid-back
CNVR109	12	60,100	1,998,701	Exterior	Ear size
CNVR109	12	60,100	1,998,701	Meat and Carcass	Backfat at last rib
CNVR109	12	60,100	1,998,701	Health	Interleukin-10 level
CNVR109	12	60,100	1,998,701	Health	Toll-like receptor 9 level
CNVR109	12	60,100	1,998,701	Exterior	Vertebra number
CNVR109	12	60,100	1,998,701	Exterior	Thoracic vertebra number
CNVR109	12	60,100	1,998,701	Health	Actinobacillus pleuropneumoniae susceptibility
CNVR109	12	60,100	1,998,701	Health	Actinobacillus pleuropneumoniae susceptibility
CNVR109	12	60,100	1,998,701	Meat and Carcass	Myristic acid content
CNVR109	12	60,100	1,998,701	Meat and Carcass	Myristic acid content
CNVR109	12	60,100	1,998,701	Meat and Carcass	Myristic acid content
CNVR109	12	60,100	1,998,701	Meat and Carcass	Myristic acid content
CNVR109	12	60,100	1,998,701	Meat and Carcass	Myristic acid content
CNVR109	12	60,100	1,998,701	Production	Feed intake
CNVR109	12	60,100	1,998,701	Meat and Carcass	Arachidic acid content
CNVR109	12	60,100	1,998,701	Meat and Carcass	Palmitic acid to myristic acid ratio

CNVR109	12	60,100	1,998,701	Meat and Carcass	Myristic acid content
CNVR109	12	60,100	1,998,701	Meat and Carcass	Palmitic acid to myristic acid ratio
CNVR109	12	60,100	1,998,701	Meat and Carcass	Myristic acid content
CNVR109	12	60,100	1,998,701	Meat and Carcass	Myristic acid content
CNVR109	12	60,100	1,998,701	Meat and Carcass	Myristic acid content
CNVR109	12	60,100	1,998,701	Meat and Carcass	Intramuscular fat content
CNVR109	12	60,100	1,998,701	Meat and Carcass	Myristic acid content
CNVR109	12	60,100	1,998,701	Meat and Carcass	Palmitoleic acid content
CNVR109	12	60,100	1,998,701	Meat and Carcass	Stearic acid content
CNVR109	12	60,100	1,998,701	Meat and Carcass	cis-Vaccenic acid content
CNVR109	12	60,100	1,998,701	Meat and Carcass	Arachidic acid content
CNVR109	12	60,100	1,998,701	Meat and Carcass	Dihomo-gamma-linolenic acid content
CNVR109	12	60,100	1,998,701	Meat and Carcass	Arachidonic acid content
CNVR109	12	60,100	1,998,701	Meat and Carcass	Myristic acid content
CNVR109	12	60,100	1,998,701	Meat and Carcass	Drip loss
CNVR109	12	60,100	1,998,701	Meat and Carcass	Meat color
CNVR109	12	60,100	1,998,701	Meat and Carcass	Muscle pH
CNVR109	12	60,100	1,998,701	Meat and Carcass	Muscle pH
CNVR109	12	60,100	1,998,701	Meat and Carcass	Dressing percentage
CNVR109	12	60,100	1,998,701	Meat and Carcass	Average backfat thickness
CNVR109	12	60,100	1,998,701	Meat and Carcass	Loin weight
CNVR109	12	60,100	1,998,701	Production	Average daily gain
CNVR109	12	60,100	1,998,701	Production	Feed conversion ratio
CNVR109	12	60,100	1,998,701	Production	Feed intake
CNVR109	12	60,100	1,998,701	Production	Age at slaughter

CNVR109	12	60,100	1,998,701	Meat and Carcass	Palmitic acid to myristic acid ratio
CNVR109	12	60,100	1,998,701	Meat and Carcass	Oleic acid to palmitoleic acid ratio
CNVR109	12	60,100	1,998,701	Meat and Carcass	Muscle pH
CNVR109	12	60,100	1,998,701	Meat and Carcass	Meat color
CNVR109	12	60,100	1,998,701	Meat and Carcass	Palmitoleic acid content
CNVR109	12	60,100	1,998,701	Meat and Carcass	Palmitic acid content
CNVR109	12	60,100	1,998,701	Meat and Carcass	Palmitic acid content
CNVR109	12	60,100	1,998,701	Meat and Carcass	Palmitoleic acid content
CNVR109	12	60,100	1,998,701	Meat and Carcass	Palmitoleic acid to palmitic acid ratio
CNVR109	12	60,100	1,998,701	Meat and Carcass	Oleic acid to palmitoleic acid ratio
CNVR109	12	60,100	1,998,701	Meat and Carcass	Palmitic acid content
CNVR109	12	60,100	1,998,701	Meat and Carcass	Palmitoleic acid content
CNVR109	12	60,100	1,998,701	Meat and Carcass	Palmitoleic acid to palmitic acid ratio
CNVR109	12	60,100	1,998,701	Meat and Carcass	Oleic acid to palmitoleic acid ratio
CNVR109	12	60,100	1,998,701	Meat and Carcass	Oleic acid content
CNVR109	12	60,100	1,998,701	Meat and Carcass	Oleic acid content
CNVR109	12	60,100	1,998,701	Meat and Carcass	Myristic acid content
CNVR109	12	60,100	1,998,701	Meat and Carcass	Myristic acid content
CNVR109	12	60,100	1,998,701	Meat and Carcass	Palmitic acid to myristic acid ratio
CNVR109	12	60,100	1,998,701	Meat and Carcass	Oleic acid content

CNVR109	12	60,100	1,998,701	Meat and Carcass	Monounsaturated fatty acid content
CNVR109	12	60,100	1,998,701	Meat and Carcass	Monounsaturated fatty acid to saturated fatty acid ratio
CNVR109	12	60,100	1,998,701	Meat and Carcass	Fatty acid atherogenic index
CNVR109	12	60,100	1,998,701	Meat and Carcass	Fatty acid atherogenic index
CNVR109	12	60,100	1,998,701	Meat and Carcass	Double-bond index
CNVR109	12	60,100	1,998,701	Meat and Carcass	Unsaturated index
CNVR109	12	60,100	1,998,701	Meat and Carcass	Double-bond index
CNVR109	12	60,100	1,998,701	Meat and Carcass	Unsaturated index
CNVR109	12	60,100	1,998,701	Meat and Carcass	Average chain length
CNVR109	12	60,100	1,998,701	Meat and Carcass	Stearic acid to palmitic acid ratio
CNVR109	12	60,100	1,998,701	Meat and Carcass	Average chain length
CNVR109	12	60,100	1,998,701	Meat and Carcass	Stearic acid to palmitic acid ratio
CNVR109	12	60,100	1,998,701	Meat and Carcass	Eicosadienoic acid content
CNVR109	12	60,100	1,998,701	Meat and Carcass	Eicosadienoic acid content
CNVR109	12	60,100	1,998,701	Reproduction	Teat number
CNVR109	12	60,100	1,998,701	Meat and Carcass	Myristic acid content
CNVR109	12	60,100	1,998,701	Meat and Carcass	Palmitic acid content
CNVR109	12	60,100	1,998,701	Meat and Carcass	Palmitoleic acid content
CNVR109	12	60,100	1,998,701	Meat and Carcass	Oleic acid content
CNVR109	12	60,100	1,998,701	Meat and Carcass	cis-11-Eicosenoic acid content
CNVR109	12	60,100	1,998,701	Health	Interferon-gamma to interleukin-10 ratio

CNVR109	12	60,100	1,998,701	Meat and Carcass	Palmitic acid to myristic acid ratio
CNVR109	12	60,100	1,998,701	Meat and Carcass	Palmitic acid to myristic acid ratio
CNVR109	12	60,100	1,998,701	Health	Interferon-gamma to interleukin-10 ratio
CNVR109	12	60,100	1,998,701	Reproduction	Age at puberty
CNVR109	12	60,100	1,998,701	Meat and Carcass	Palmitic acid to myristic acid ratio
CNVR122	13	194,665,680	196,342,442	Health	Melanoma susceptibility
CNVR122	13	194,665,680	196,342,442	Reproduction	Teat number
CNVR122	13	194,665,680	196,342,442	Health	Hematocrit
CNVR122	13	194,665,680	196,342,442	Health	Hemoglobin
CNVR122	13	194,665,680	196,342,442	Health	Red blood cell count
CNVR122	13	194,665,680	196,342,442	Health	Leptospirosus susceptibility
CNVR149	14	151,966,127	153,374,972	Meat and Carcass	Number of muscle fibers per unit area
CNVR149	14	151,966,127	153,374,972	Meat and Carcass	Total muscle fiber number
CNVR149	14	151,966,127	153,374,972	Meat and Carcass	Diameter of type IIa muscle fibers
CNVR149	14	151,966,127	153,374,972	Meat and Carcass	Diameter of type IIb muscle fibers
CNVR150	15	9,519,813	10,711,345	Meat and Carcass	Loin muscle area
CNVR150	15	9,519,813	10,711,345	Meat and Carcass	Loin muscle area
CNVR150	15	9,519,813	10,711,345	Meat and Carcass	Meat color
CNVR150	15	9,519,813	10,711,345	Meat and Carcass	Cooking loss
CNVR150	15	9,519,813	10,711,345	Meat and Carcass	Shear force

CNVR150	15	9,519,813	10,711,345	Meat and Carcass	chew score
CNVR150	15	9,519,813	10,711,345	Health	CSFV antibody level
CNVR150	15	9,519,813	10,711,345	Meat and Carcass	Loin muscle area
CNVR150	15	9,519,813	10,711,345	Production	Body length
CNVR151	15	12,597,728	12,844,713	Meat and Carcass	Backfat between 6th and 7th ribs
CNVR151	15	12,597,728	12,844,713	Meat and Carcass	Loin muscle area
CNVR151	15	12,597,728	12,844,713	Meat and Carcass	Loin muscle area
CNVR151	15	12,597,728	12,844,713	Meat and Carcass	Meat color
CNVR151	15	12,597,728	12,844,713	Meat and Carcass	Cooking loss
CNVR151	15	12,597,728	12,844,713	Meat and Carcass	Shear force
CNVR151	15	12,597,728	12,844,713	Meat and Carcass	chew score
CNVR151	15	12,597,728	12,844,713	Health	CSFV antibody level
CNVR151	15	12,597,728	12,844,713	Exterior	Anal atresia
CNVR150	17	9,519,813	10,711,345	Meat and Carcass	Backfat between 6th and 7th ribs
CNVR174	17	2,202,762	2,730,970	Meat and Carcass	Shear force
CNVR174	17	2,202,762	2,730,970	Production	Body weight
CNVR174	17	2,202,762	2,730,970	Production	Body weight
CNVR174	17	2,202,762	2,730,970	Health	Segmented neutrophil number
CNVR174	17	2,202,762	2,730,970	Health	Eosinophil number
CNVR174	17	2,202,762	2,730,970	Health	Creatinine level
CNVR174	17	2,202,762	2,730,970	Health	Eosinophil number
CNVR174	17	2,202,762	2,730,970	Health	Eosinophil number
CNVR174	17	2,202,762	2,730,970	Health	Haptoglobin concentration
CNVR174	17	2,202,762	2,730,970	Meat and Carcass	Meat color
CNVR174	17	2,202,762	2,730,970	Meat and Carcass	Muscle pH

CNVR174	17	2,202,762	2,730,970	Meat and Carcass	Cooking loss
CNVR174	17	2,202,762	2,730,970	Meat and Carcass	Drip loss
CNVR174	17	2,202,762	2,730,970	Meat and Carcass	Thawing loss
CNVR174	17	2,202,762	2,730,970	Meat and Carcass	Intramuscular fat content
CNVR174	17	2,202,762	2,730,970	Meat and Carcass	Shear force
CNVR174	17	2,202,762	2,730,970	Health	Toll-like receptor 9 level
CNVR174	17	2,202,762	2,730,970	Health	Actinobacillus pleuropneumoniae susceptibility
CNVR174	17	2,202,762	2,730,970	Health	Actinobacillus pleuropneumoniae susceptibility
CNVR174	17	2,202,762	2,730,970	Meat and Carcass	Backfat at last rib

Table S4. Enriched QTL for autosomal copy number variation regions (CNVR)shared by at least 5% of the population

CNVR	QTL	N QTLs	Total annotated QTLs	P-value	QTL type
CNVR21	Average backfat thickness	15	143	<0.0001	Meat and Carcass
CNVR21	Backfat at last lumbar	3	143	0.0101	Meat and Carcass
CNVR21	Backfat at last rib	6	143	0.0071	Meat and Carcass
CNVR21	Backfat percentage	1	143	0.0285	Meat and Carcass
CNVR21	Backfat thickness between 3rd and 4th rib	2	143	0.0297	Meat and Carcass
CNVR21	Backfat weight	2	143	0.0387	Meat and Carcass
CNVR21	Bone mineral content	1	143	0.0169	Production

CNVR21	C3c concentration	3	143	0.0030	Health
CNVR21	Carcass weight (hot)	3	143	0.0221	Meat and Carcass
CNVR21	Cutlet weight	1	143	0.0169	Meat and Carcass
CNVR21	Dressing percentage	6	143	0.0093	Meat and Carcass
CNVR21	Heart weight	2	143	0.0405	Meat and Carcass
CNVR21	Hemolytic complement activity (alternative pathway)	3	143	0.0002	Health
CNVR21	Lean meat + bone in ham + back	1	143	0.0386	Meat and Carcass
CNVR21	Lean meat percentage	7	143	0.0013	Meat and Carcass
CNVR21	Linoleic acid content	5	143	0.0005	Meat and Carcass
CNVR21	Loin weight	4	143	0.0048	Meat and Carcass
CNVR21	Monounsaturated fatty acid to polyunsaturated fatty acid ratio	5	143	<0.0001	Meat and Carcass
CNVR21	Neck fat weight	1	143	0.0169	Meat and Carcass
CNVR21	Oxygen saturation	1	143	0.0285	Health
CNVR21	Polyunsaturated fatty acid content	5	143	0.0002	Meat and Carcass
CNVR21	Polyunsaturated fatty acid to saturated fatty acid ratio	3	143	0.0021	Meat and Carcass
CNVR21	Shear firmness	1	143	0.0169	Meat and Carcass
CNVR68	Vertebra number	1	3	0.0127	Exterior
CNVR72	Alkaline phosphatase activity	1	26	0.0384	Health
CNVR72	Backfat at tenth rib	2	26	0.0378	Meat and Carcass
CNVR72	Body temperature	1	26	0.0296	Health
CNVR72	Carcass temperature	1	26	0.0339	Meat and Carcass

CNVR72	Cryptorchidism	1	26	0.0339	Reproduction
CNVR72	Gait score (hind)	1	26	0.0339	Exterior
CNVR72	Ham weight	2	26	0.0296	Meat and Carcass
CNVR72	Intramuscular fat content	3	26	0.0390	Meat and Carcass
CNVR72	Muscle fat content	1	26	0.0339	Meat and Carcass
CNVR72	Muscle moisture percentage	2	26	0.0239	Meat and Carcass
CNVR72	muscle protein percentage	1	26	0.0378	Meat and Carcass
CNVR72	Semimembranosus angle	1	26	0.0296	Meat and Carcass
CNVR72	Shoulder meat weight	1	26	0.0339	Meat and Carcass
CNVR72	Shoulder weight	2	26	0.0239	Meat and Carcass
CNVR82	CO2 partial pressure	1	22	0.0094	Health
CNVR82	Cooking yield	1	22	0.0094	Meat and Carcass
CNVR82	Fat area percentage in carcass	3	22	<0.0001	Meat and Carcass
CNVR82	Litter size	2	22	0.0473	Reproduction
CNVR82	Loin muscle area	2	22	0.0473	Meat and Carcass
CNVR82	Monocyte number	1	22	0.0294	Health
CNVR82	Muscle moisture percentage	2	22	0.0088	Meat and Carcass
CNVR82	Off-flavor score	1	22	0.0294	Meat and Carcass
CNVR82	Oxygen saturation	1	22	0.0088	Health
CNVR82	Plateletcrit	1	22	0.0473	Health
CNVR82	Sodium level	1	22	0.0094	Health
CNVR101	Backfat at mid-back	1	18	0.0275	Meat and Carcass
CNVR101	Body temperature	1	18	0.0173	Health
CNVR101	Eosinophil number	1	18	0.0258	Health
CNVR101	Haptoglobin concentration	1	18	0.0258	Health
CNVR101	Interferon-gamma level	2	18	0.0010	Health

CNVR101	Interferon-gamma to interleukin-10 ratio	1	18	0.0173	Health
CNVR101	Loin and neck meat weight	1	18	0.0258	Meat and Carcass
CNVR101	Nonfunctional nipples	1	18	0.0312	Reproduction
CNVR101	Percentage angular fibers	1	18	0.0087	Meat and Carcass
CNVR101	Percentage type I fibers	1	18	0.0258	Meat and Carcass
CNVR101	Time spent drinking	1	18	0.0173	Exterior
CNVR103	Empty body lipid content	2	38	0.0028	Meat and Carcass
CNVR103	Intramuscular fat content	5	38	0.0263	Meat and Carcass
CNVR103	Nonfunctional nipples	2	38	0.0135	Reproduction
CNVR103	Time spent drinking	1	38	0.0479	Exterior
CNVR109	Arachidic acid content	2	89	0.0272	Meat and Carcass
CNVR109	Average chain length	2	89	0.0108	Meat and Carcass
CNVR109	Double-bond index	2	89	0.0108	Meat and Carcass
CNVR109	Eicosadienoic acid content	2	89	0.0108	Meat and Carcass
CNVR109	Fatty acid atherogenic index	2	89	0.0108	Meat and Carcass
CNVR109	Interferon-gamma to interleukin-10 ratio	2	89	0.0028	Health
CNVR109	Myristic acid content	14	89	<0.0001	Meat and Carcass
CNVR109	Oleic acid to palmitoleic acid ratio	3	89	0.0017	Meat and Carcass
CNVR109	Palmitic acid to myristic acid ratio	7	89	<0.0001	Meat and Carcass
CNVR109	Palmitoleic acid to palmitic acid ratio	2	89	0.0485	Meat and Carcass
CNVR109	Stearic acid to palmitic acid ratio	2	89	0.0251	Meat and Carcass

CNVR109	Unsaturated index	2	89	0.0034	Meat and Carcass
CNVR122	Hemoglobin	1	6	0.0237	Health
CNVR122	Leptospirosus susceptibility	1	6	0.0043	Health
CNVR122	Melanoma susceptibility	1	6	0.0237	Health
CNVR149	Diameter of type IIa muscle fibers	1	4	0.0019	Meat and Carcass
CNVR149	Diameter of type IIb muscle fibers	1	4	0.0019	Meat and Carcass
CNVR149	Number of muscle fibers per unit area	1	4	0.0028	Meat and Carcass
CNVR149	Total muscle fiber number	1	4	0.0019	Meat and Carcass
CNVR150	Backfat between 6th and 7th ribs	1	10	0.0096	Meat and Carcass
CNVR150	chew score	1	10	0.0096	Meat and Carcass
CNVR150	Cooking loss	1	10	0.0442	Meat and Carcass
CNVR150	CSFV antibody level	1	10	0.0096	Health
CNVR150	Loin muscle area	3	10	0.0018	Meat and Carcass
CNVR151	Anal atresia	1	9	0.0099	Exterior
CNVR151	Backfat between 6th and 7th ribs	1	9	0.0099	Meat and Carcass
CNVR151	chew score	1	9	0.0099	Meat and Carcass
CNVR151	Cooking loss	1	9	0.0332	Meat and Carcass
CNVR151	CSFV antibody level	1	9	0.0099	Health
CNVR151	Loin muscle area	2	9	0.0099	Meat and Carcass
CNVR174	Actinobacillus pleuropneumoniae susceptibility	2	20	0.0072	Health

CNVR174	Creatinine level	1	20	0.0225	Health
CNVR174	Eosinophil number	3	20	<0.0001	Health
CNVR174	Haptoglobin concentration	1	20	0.0280	Health
CNVR174	Segmented neutrophil number	1	20	0.0225	Health
CNVR174	Shear force	2	20	0.0225	Meat and Carcass
CNVR174	Thawing loss	1	20	0.0256	Meat and Carcass
CNVR174	Toll-like receptor 9 level	1	20	0.0225	Health

749

Table S5. Genes annotated for CNVRs associated with physiological and anatomical indicators of heat stress response

Trait	CNVR	CHR	Start (bp)	End (bp)	Ensembl Gene ID	Gene Name	Gene Biotype
T_{ES}	CNVR72	6	132,124,953	132,543,418	*ENSSSCG00000053778*		lncRNA
T_{ES}	CNVR72	6	132,124,953	132,543,418	*ENSSSCG00000053778*		lncRNA
T_{ES}	CNVR72	6	132,124,953	132,543,418	*ENSSSCG00000060648*		lncRNA
T_{ES}	CNVR152	15	24,371,978	24,804,276	*ENSSSCG00000031239*		protein_coding
T_{ES}	CNVR152	15	24,371,978	24,804,276	*ENSSSCG00000029304*	*STEAP3*	protein_coding
T_{ES}	CNVR152	15	24,371,978	24,804,276	*ENSSSCG00000015715*	*EN1*	protein_coding
T_{ES}	CNVR152	15	24,371,978	24,804,276	*ENSSSCG00000015716*	*MARCO*	protein_coding
T_{ES}	CNVR152	15	24,371,978	24,804,276	*ENSSSCG00000015717*	*C1QL2*	protein_coding
T_{ES}	CNVR152	15	24,371,978	24,804,276	*ENSSSCG00000055496*		lncRNA
T_{RS}	CNVR23	2	6,179,112	6,495,647	*ENSSSCG00000012963*	*SART1*	protein_coding
T_{RS}	CNVR23	2	6,179,112	6,495,647	*ENSSSCG00000012967*	*FOSL1*	protein_coding
T_{RS}	CNVR23	2	6,179,112	6,495,647	*ENSSSCG00000012969*	*FIBP*	protein_coding
T_{RS}	CNVR23	2	6,179,112	6,495,647	*ENSSSCG00000012970*	*CTSW*	protein_coding
T_{RS}	CNVR23	2	6,179,112	6,495,647	*ENSSSCG00000012964*	*TSGA10IP*	protein_coding

T_{RS}	CNVR23	2	6,179,112	6,495,647	*ENSSSCG00000012971*	*EFEMP2*	protein_coding
T_{RS}	CNVR23	2	6,179,112	6,495,647	*ENSSSCG00000012973*	*MUS81*	protein_coding
T_{RS}	CNVR23	2	6,179,112	6,495,647	*ENSSSCG00000012974*	*CFL1*	protein_coding
T_{RS}	CNVR23	2	6,179,112	6,495,647	*ENSSSCG00000012975*	*SNX32*	protein_coding
T_{RS}	CNVR23	2	6,179,112	6,495,647	*ENSSSCG00000012957*	*SF3B2*	protein_coding
T_{RS}	CNVR23	2	6,179,112	6,495,647	*ENSSSCG00000028015*	*GAL3ST3*	protein_coding
T_{RS}	CNVR23	2	6,179,112	6,495,647	*ENSSSCG00000012959*	*CATSPER1*	protein_coding
T_{RS}	CNVR23	2	6,179,112	6,495,647	*ENSSSCG00000012960*	*CST6*	protein_coding
T_{RS}	CNVR23	2	6,179,112	6,495,647	*ENSSSCG00000012961*	*BANF1*	protein_coding
T_{RS}	CNVR23	2	6,179,112	6,495,647	*ENSSSCG00000027334*	*EIF1AD*	protein_coding
T_{RS}	CNVR23	2	6,179,112	6,495,647	*ENSSSCG00000012965*	*DRAP1*	protein_coding
T_{RS}	CNVR23	2	6,179,112	6,495,647	*ENSSSCG00000012966*	*C11orf68*	protein_coding
T_{RS}	CNVR23	2	6,179,112	6,495,647	*ENSSSCG00000012968*	*CCDC85B*	protein_coding
T_{RS}	CNVR23	2	6,179,112	6,495,647	*ENSSSCG00000047888*		protein_coding
T_{RS}	CNVR23	2	6,179,112	6,495,647	*ENSSSCG00000053775*		lncRNA
T_{RS}	CNVR23	2	6,179,112	6,495,647	*ENSSSCG00000054679*		lncRNA

T_{RS}	CNVR23	2	6,179,112	6,495,647	*ENSSSCG00000062968*		lncRNA
T_{RS}	CNVR23	2	6,179,112	6,495,647	*ENSSSCG00000044139*		lncRNA
T_{RS}	CNVR23	2	6,179,112	6,495,647	*ENSSSCG00000046010*		lncRNA
T_{RS}	CNVR23	2	6,179,112	6,495,647	*ENSSSCG00000051003*		lncRNA
T_{RS}	CNVR23	2	6,179,112	6,495,647	*ENSSSCG00000048633*		lncRNA
T_{RS}	CNVR23	2	6,179,112	6,495,647	*ENSSSCG00000048776*		lncRNA
T_{TS}	CNVR21	2	1,111	632,707	*ENSSSCG00000012844*	*SLC25A22*	protein_coding
T_{TS}	CNVR21	2	1,111	632,707	*ENSSSCG00000049665*		pseudogene
T_{TS}	CNVR21	2	1,111	632,707	*ENSSSCG00000012843*	*PIDD1*	protein_coding
T_{TS}	CNVR21	2	1,111	632,707	*ENSSSCG00000012842*	*RPLP2*	protein_coding
T_{TS}	CNVR21	2	1,111	632,707	*ENSSSCG00000012836*	*AP2A2*	protein_coding
T_{TS}	CNVR21	2	1,111	632,707	*ENSSSCG00000012835*		protein_coding
T_{TS}	CNVR21	2	1,111	632,707	*ENSSSCG00000012847*	*TALDO1*	protein_coding
T_{TS}	CNVR21	2	1,111	632,707	*ENSSSCG00000012846*	*GATD1*	protein_coding
T_{TS}	CNVR21	2	1,111	632,707	*ENSSSCG00000012845*	*CEND1*	protein_coding
T_{TS}	CNVR21	2	1,111	632,707	*ENSSSCG00000060622*		protein_coding

T_{TS}	CNVR21	2	1,111	632,707	*ENSSSCG00000032436*		protein_coding
T_{TS}	CNVR21	2	1,111	632,707	*ENSSSCG00000038912*		protein_coding
T_{TS}	CNVR21	2	1,111	632,707	*ENSSSCG00000014565*		protein_coding
T_{TS}	CNVR21	2	1,111	632,707	*ENSSSCG00000032591*		protein_coding
T_{TS}	CNVR21	2	1,111	632,707	*ENSSSCG00000033780*	*B4GALNT4*	protein_coding
T_{TS}	CNVR21	2	1,111	632,707	*ENSSSCG00000051760*		protein_coding
T_{TS}	CNVR21	2	1,111	632,707	*ENSSSCG00000027302*	*PKP3*	protein_coding
T_{TS}	CNVR21	2	1,111	632,707	*ENSSSCG00000024389*	*SIGIRR*	protein_coding
T_{TS}	CNVR21	2	1,111	632,707	*ENSSSCG00000024569*	*ANO9*	protein_coding
T_{TS}	CNVR21	2	1,111	632,707	*ENSSSCG00000037427*	*PTDSS2*	protein_coding
T_{TS}	CNVR21	2	1,111	632,707	*ENSSSCG00000032010*	*RNH1*	protein_coding
T_{TS}	CNVR21	2	1,111	632,707	*ENSSSCG00000031513*	*HRAS*	protein_coding
T_{TS}	CNVR21	2	1,111	632,707	*ENSSSCG00000027045*	*LRRC56*	protein_coding
T_{TS}	CNVR21	2	1,111	632,707	*ENSSSCG00000030137*	*LMNTD2*	protein_coding
T_{TS}	CNVR21	2	1,111	632,707	*ENSSSCG00000012854*	*RASSF7*	protein_coding
T_{TS}	CNVR21	2	1,111	632,707	*ENSSSCG00000014554*		protein_coding

T_{TS}	CNVR21	2	1,111	632,707	*ENSSSCG00000014555*	*ODF3*	protein_coding
T_{TS}	CNVR21	2	1,111	632,707	*ENSSSCG00000014556*	*BET1L*	protein_coding
T_{TS}	CNVR21	2	1,111	632,707	*ENSSSCG00000014557*	*RIC8A*	protein_coding
T_{TS}	CNVR21	2	1,111	632,707	*ENSSSCG00000014558*	*SIRT3*	protein_coding
T_{TS}	CNVR21	2	1,111	632,707	*ENSSSCG00000014559*	*PSMD13*	protein_coding
T_{TS}	CNVR21	2	1,111	632,707	*ENSSSCG00000061991*	*COX8H*	protein_coding
T_{TS}	CNVR21	2	1,111	632,707	*ENSSSCG00000014561*	*NLRP6*	protein_coding
T_{TS}	CNVR21	2	1,111	632,707	*ENSSSCG00000025023*	*PGGHG*	protein_coding
T_{TS}	CNVR21	2	1,111	632,707	*ENSSSCG00000040278*	*IFITM5*	protein_coding
T_{TS}	CNVR21	2	1,111	632,707	*ENSSSCG00000012841*	*PNPLA2*	protein_coding
T_{TS}	CNVR21	2	1,111	632,707	*ENSSSCG00000023933*	*CRACR2B*	protein_coding
T_{TS}	CNVR21	2	1,111	632,707	*ENSSSCG00000012840*	*CD151*	protein_coding
T_{TS}	CNVR21	2	1,111	632,707	*ENSSSCG00000059584*		protein_coding
T_{TS}	CNVR21	2	1,111	632,707	*ENSSSCG00000012838*	*TSPAN4*	protein_coding
T_{TS}	CNVR21	2	1,111	632,707	*ENSSSCG00000012837*	*CHID1*	protein_coding
T_{TS}	CNVR21	2	1,111	632,707	*ENSSSCG00000029723*	*PHRF1*	protein_coding

T_{TS}	CNVR21	2	1,111	632,707	*ENSSSCG00000012853*	*IRF7*	protein_coding
T_{TS}	CNVR21	2	1,111	632,707	*ENSSSCG00000012852*	*CDHR5*	protein_coding
T_{TS}	CNVR21	2	1,111	632,707	*ENSSSCG00000040951*	*SCT*	protein_coding
T_{TS}	CNVR21	2	1,111	632,707	*ENSSSCG00000012851*	*DRD4*	protein_coding
T_{TS}	CNVR21	2	1,111	632,707	*ENSSSCG00000012850*	*DEAF1*	protein_coding
T_{TS}	CNVR21	2	1,111	632,707	*ENSSSCG00000044406*	*TMEM80*	protein_coding
T_{TS}	CNVR21	2	1,111	632,707	*ENSSSCG00000012848*	*EPS8L2*	protein_coding
T_{TS}	CNVR21	2	1,111	632,707	*ENSSSCG00000063023*		lncRNA
T_{TS}	CNVR21	2	1,111	632,707	*ENSSSCG00000038005*		lncRNA
T_{TS}	CNVR21	2	1,111	632,707	*ENSSSCG00000018538*	*SNORA52*	snoRNA
T_{TS}	CNVR21	2	1,111	632,707	*ENSSSCG00000019083*		miRNA
T_{TS}	CNVR23	2	6,179,112	6,495,647	*ENSSSCG00000012963*	*SART1*	protein_coding
T_{TS}	CNVR23	2	6,179,112	6,495,647	*ENSSSCG00000012967*	*FOSL1*	protein_coding
T_{TS}	CNVR23	2	6,179,112	6,495,647	*ENSSSCG00000012969*	*FIBP*	protein_coding
T_{TS}	CNVR23	2	6,179,112	6,495,647	*ENSSSCG00000012970*	*CTSW*	protein_coding
T_{TS}	CNVR23	2	6,179,112	6,495,647	*ENSSSCG00000012964*	*TSGA10IP*	protein_coding

T_{TS}	CNVR23	2	6,179,112	6,495,647	*ENSSSCG00000012971*	*EFEMP2*	protein_coding
T_{TS}	CNVR23	2	6,179,112	6,495,647	*ENSSSCG00000012973*	*MUS81*	protein_coding
T_{TS}	CNVR23	2	6,179,112	6,495,647	*ENSSSCG00000012974*	*CFL1*	protein_coding
T_{TS}	CNVR23	2	6,179,112	6,495,647	*ENSSSCG00000012975*	*SNX32*	protein_coding
T_{TS}	CNVR23	2	6,179,112	6,495,647	*ENSSSCG00000012957*	*SF3B2*	protein_coding
T_{TS}	CNVR23	2	6,179,112	6,495,647	*ENSSSCG00000028015*	*GAL3ST3*	protein_coding
T_{TS}	CNVR23	2	6,179,112	6,495,647	*ENSSSCG00000012959*	*CATSPER1*	protein_coding
T_{TS}	CNVR23	2	6,179,112	6,495,647	*ENSSSCG00000012960*	*CST6*	protein_coding
T_{TS}	CNVR23	2	6,179,112	6,495,647	*ENSSSCG00000012961*	*BANF1*	protein_coding
T_{TS}	CNVR23	2	6,179,112	6,495,647	*ENSSSCG00000027334*	*EIF1AD*	protein_coding
T_{TS}	CNVR23	2	6,179,112	6,495,647	*ENSSSCG00000012965*	*DRAP1*	protein_coding
T_{TS}	CNVR23	2	6,179,112	6,495,647	*ENSSSCG00000012966*	*C11orf68*	protein_coding
T_{TS}	CNVR23	2	6,179,112	6,495,647	*ENSSSCG00000012968*	*CCDC85B*	protein_coding
T_{TS}	CNVR23	2	6,179,112	6,495,647	*ENSSSCG00000047888*		protein_coding
T_{TS}	CNVR23	2	6,179,112	6,495,647	*ENSSSCG00000053775*		lncRNA
T_{TS}	CNVR23	2	6,179,112	6,495,647	*ENSSSCG00000054679*		lncRNA

T_{TS}	CNVR23	2	6,179,112	6,495,647	*ENSSSCG00000062968*		lncRNA
T_{TS}	CNVR23	2	6,179,112	6,495,647	*ENSSSCG00000044139*		lncRNA
T_{TS}	CNVR23	2	6,179,112	6,495,647	*ENSSSCG00000046010*		lncRNA
T_{TS}	CNVR23	2	6,179,112	6,495,647	*ENSSSCG00000051003*		lncRNA
T_{TS}	CNVR23	2	6,179,112	6,495,647	*ENSSSCG00000048633*		lncRNA
T_{TS}	CNVR23	2	6,179,112	6,495,647	*ENSSSCG00000048776*		lncRNA
T_{TS}	CNVR48	4	1,155,293	1,388,468	*ENSSSCG00000031563*		protein_coding
T_{TS}	CNVR48	4	1,155,293	1,388,468	*ENSSSCG00000060510*		protein_coding
T_{TS}	CNVR48	4	1,155,293	1,388,468	*ENSSSCG00000031205*		protein_coding
T_{TS}	CNVR48	4	1,155,293	1,388,468	*ENSSSCG00000040535*	*LY6E*	protein_coding
T_{TS}	CNVR48	4	1,155,293	1,388,468	*ENSSSCG00000034689*	*GPIHBP1*	protein_coding
T_{TS}	CNVR48	4	1,155,293	1,388,468	*ENSSSCG00000033353*	*LY6H*	protein_coding
T_{TS}	CNVR48	4	1,155,293	1,388,468	*ENSSSCG00000053802*	*LY6L*	protein_coding
T_{TS}	CNVR48	4	1,155,293	1,388,468	*ENSSSCG00000006958*	*TOP1MT*	protein_coding
T_{TS}	CNVR48	4	1,155,293	1,388,468	*ENSSSCG00000006959*	*ZNF696*	protein_coding
T_{TS}	CNVR48	4	1,155,293	1,388,468	*ENSSSCG00000039881*	*GLI4*	protein_coding

T_{TS}	CNVR48	4	1,155,293	1,388,468	*ENSSSCG00000044186*		lncRNA
T_{TS}	CNVR48	4	1,155,293	1,388,468	*ENSSSCG00000044784*		lncRNA
T_{TS}	CNVR52	4	126,897,791	127,521,733	*ENSSSCG00000006917*	*LRRC8C*	protein_coding
T_{TS}	CNVR52	4	126,897,791	127,521,733	*ENSSSCG00000037101*	*LRRC8B*	protein_coding
T_{TS}	CNVR52	4	126,897,791	127,521,733	*ENSSSCG00000058619*		protein_coding
T_{TS}	CNVR52	4	126,897,791	127,521,733	*ENSSSCG00000030801*		protein_coding
T_{TS}	CNVR52	4	126,897,791	127,521,733	*ENSSSCG00000062656*	*GBP5*	protein_coding
T_{TS}	CNVR52	4	126,897,791	127,521,733	*ENSSSCG00000063342*		protein_coding
T_{TS}	CNVR52	4	126,897,791	127,521,733	*ENSSSCG00000058709*		protein_coding
T_{TS}	CNVR52	4	126,897,791	127,521,733	*ENSSSCG00000006923*	*GBP2*	protein_coding
T_{TS}	CNVR52	4	126,897,791	127,521,733	*ENSSSCG00000024973*	*GBP1*	protein_coding
T_{TS}	CNVR52	4	126,897,791	127,521,733	*ENSSSCG00000006925*	*KYAT3*	protein_coding
T_{TS}	CNVR52	4	126,897,791	127,521,733	*ENSSSCG00000061560*		protein_coding
T_{TS}	CNVR52	4	126,897,791	127,521,733	*ENSSSCG00000058148*		lncRNA
T_{TS}	CNVR52	4	126,897,791	127,521,733	*ENSSSCG00000061208*		lncRNA
T_{TS}	CNVR52	4	126,897,791	127,521,733	*ENSSSCG00000051861*		lncRNA

T_{TS}	CNVR52	4	126,897,791	127,521,733	*ENSSSCG00000062190*		lncRNA
T_{TS}	CNVR52	4	126,897,791	127,521,733	*ENSSSCG00000059700*		lncRNA
T_{TS}	CNVR52	4	126,897,791	127,521,733	*ENSSSCG00000051720*	*U2*	snRNA
T_{TS}	CNVR65	5	77,179,466	77,352,621	*ENSSSCG00000060580*		lncRNA
T_{TS}	CNVR105	11	67,375,641	67,671,825	*ENSSSCG00000026863*	*FARP1*	protein_coding
T_{TS}	CNVR105	11	67,375,641	67,671,825	*ENSSSCG00000060810*		pseudogene
T_{TS}	CNVR105	11	67,375,641	67,671,825	*ENSSSCG00000009511*	*STK24*	protein_coding
T_{TS}	CNVR105	11	67,375,641	67,671,825	*ENSSSCG00000009513*	*SLC15A1*	protein_coding
T_{TS}	CNVR109	12	60,100	1,998,701	*ENSSSCG00000022317*	*SLC38A10*	protein_coding
T_{TS}	CNVR109	12	60,100	1,998,701	*ENSSSCG00000039183*	*NDUFAF8*	protein_coding
T_{TS}	CNVR109	12	60,100	1,998,701	*ENSSSCG00000028593*	*TEPSIN*	protein_coding
T_{TS}	CNVR109	12	60,100	1,998,701	*ENSSSCG00000044039*		protein_coding
T_{TS}	CNVR109	12	60,100	1,998,701	*ENSSSCG00000039807*		protein_coding
T_{TS}	CNVR109	12	60,100	1,998,701	*ENSSSCG00000037364*		protein_coding
T_{TS}	CNVR109	12	60,100	1,998,701	*ENSSSCG00000035852*	*CSNK1D*	protein_coding
T_{TS}	CNVR109	12	60,100	1,998,701	*ENSSSCG00000024018*	*SLC16A3*	protein_coding

T_{TS}	CNVR109	12	60,100	1,998,701	*ENSSSCG00000029553*	*CCDC57*	protein_coding
T_{TS}	CNVR109	12	60,100	1,998,701	*ENSSSCG00000029944*	*FASN*	protein_coding
T_{TS}	CNVR109	12	60,100	1,998,701	*ENSSSCG00000034696*		protein_coding
T_{TS}	CNVR109	12	60,100	1,998,701	*ENSSSCG00000017137*	*METRNL*	protein_coding
T_{TS}	CNVR109	12	60,100	1,998,701	*ENSSSCG00000034723*	*PYCR1*	protein_coding
T_{TS}	CNVR109	12	60,100	1,998,701	*ENSSSCG00000040352*	*DUS1L*	protein_coding
T_{TS}	CNVR109	12	60,100	1,998,701	*ENSSSCG00000033689*	*GPS1*	protein_coding
T_{TS}	CNVR109	12	60,100	1,998,701	*ENSSSCG00000040385*	*RFNG*	protein_coding
T_{TS}	CNVR109	12	60,100	1,998,701	*ENSSSCG00000035253*	*MAFG*	protein_coding
T_{TS}	CNVR109	12	60,100	1,998,701	*ENSSSCG00000034695*	*SIRT7*	protein_coding
T_{TS}	CNVR109	12	60,100	1,998,701	*ENSSSCG00000031851*	*CBR2*	protein_coding
T_{TS}	CNVR109	12	60,100	1,998,701	*ENSSSCG00000039650*	*PCYT2*	protein_coding
T_{TS}	CNVR109	12	60,100	1,998,701	*ENSSSCG00000039873*	*DCXR*	protein_coding
T_{TS}	CNVR109	12	60,100	1,998,701	*ENSSSCG00000036973*	*RAC3*	protein_coding
T_{TS}	CNVR109	12	60,100	1,998,701	*ENSSSCG00000040503*	*LRRC45*	protein_coding
T_{TS}	CNVR109	12	60,100	1,998,701	*ENSSSCG00000049515*		protein_coding

T_{TS}	CNVR109	12	60,100	1,998,701	*ENSSSCG00000040727*	*ASPSCR1*	protein_coding
T_{TS}	CNVR109	12	60,100	1,998,701	*ENSSSCG00000039013*	*NOTUM*	protein_coding
T_{TS}	CNVR109	12	60,100	1,998,701	*ENSSSCG00000027229*	*B3GNTL1*	protein_coding
T_{TS}	CNVR109	12	60,100	1,998,701	*ENSSSCG00000017136*	*TBCD*	protein_coding
T_{TS}	CNVR109	12	60,100	1,998,701	*ENSSSCG00000017135*		pseudogene
T_{TS}	CNVR109	12	60,100	1,998,701	*ENSSSCG00000017131*	*FN3K*	protein_coding
T_{TS}	CNVR109	12	60,100	1,998,701	*ENSSSCG00000017134*	*FN3KRP*	protein_coding
T_{TS}	CNVR109	12	60,100	1,998,701	*ENSSSCG00000053358*	*RAB40B*	protein_coding
T_{TS}	CNVR109	12	60,100	1,998,701	*ENSSSCG00000017125*	*FOXK2*	protein_coding
T_{TS}	CNVR109	12	60,100	1,998,701	*ENSSSCG00000017126*	*NARF*	protein_coding
T_{TS}	CNVR109	12	60,100	1,998,701	*ENSSSCG00000017127*	*CYBC1*	protein_coding
T_{TS}	CNVR109	12	60,100	1,998,701	*ENSSSCG00000017143*	*CEP131*	protein_coding
T_{TS}	CNVR109	12	60,100	1,998,701	*ENSSSCG00000017128*	*HEXD*	protein_coding
T_{TS}	CNVR109	12	60,100	1,998,701	*ENSSSCG00000032116*	*OGFOD3*	protein_coding
T_{TS}	CNVR109	12	60,100	1,998,701	*ENSSSCG00000039849*	*PVALEF*	protein_coding
T_{TS}	CNVR109	12	60,100	1,998,701	*ENSSSCG00000017141*	*AATK*	protein_coding

T_{TS}	CNVR109	12	60,100	1,998,701	*ENSSSCG00000017142*	*BAIAP2*	protein_coding
T_{TS}	CNVR109	12	60,100	1,998,701	*ENSSSCG00000017140*	*CHMP6*	protein_coding
T_{TS}	CNVR109	12	60,100	1,998,701	*ENSSSCG00000017139*	*RPTOR*	protein_coding
T_{TS}	CNVR109	12	60,100	1,998,701	*ENSSSCG00000032655*	*ALYREF*	protein_coding
T_{TS}	CNVR109	12	60,100	1,998,701	*ENSSSCG00000035837*	*NPB*	protein_coding
T_{TS}	CNVR109	12	60,100	1,998,701	*ENSSSCG00000035728*		protein_coding
T_{TS}	CNVR109	12	60,100	1,998,701	*ENSSSCG00000034058*	*ARHGDIA*	protein_coding
T_{TS}	CNVR109	12	60,100	1,998,701	*ENSSSCG00000039148*	*P4HB*	protein_coding
T_{TS}	CNVR109	12	60,100	1,998,701	*ENSSSCG00000037039*	*PPP1R27*	protein_coding
T_{TS}	CNVR109	12	60,100	1,998,701	*ENSSSCG00000039424*	*MCRIP1*	protein_coding
T_{TS}	CNVR109	12	60,100	1,998,701	*ENSSSCG00000034891*	*GCGR*	protein_coding
T_{TS}	CNVR109	12	60,100	1,998,701	*ENSSSCG00000033620*	*SLC25A10*	protein_coding
T_{TS}	CNVR109	12	60,100	1,998,701	*ENSSSCG00000033148*	*MRPL12*	protein_coding
T_{TS}	CNVR109	12	60,100	1,998,701	*ENSSSCG00000033082*	*HGS*	protein_coding
T_{TS}	CNVR109	12	60,100	1,998,701	*ENSSSCG00000053661*	*ARL16*	protein_coding
T_{TS}	CNVR109	12	60,100	1,998,701	*ENSSSCG00000034716*	*CCDC137*	protein_coding

T_{TS}	CNVR109	12	60,100	1,998,701	*ENSSSCG00000033788*	*OXLD1*	protein_coding
T_{TS}	CNVR109	12	60,100	1,998,701	*ENSSSCG00000053315*	*PDE6G*	protein_coding
T_{TS}	CNVR109	12	60,100	1,998,701	*ENSSSCG00000031531*	*TSPAN10*	protein_coding
T_{TS}	CNVR109	12	60,100	1,998,701	*ENSSSCG00000024235*	*NPLOC4*	protein_coding
T_{TS}	CNVR109	12	60,100	1,998,701	*ENSSSCG00000029616*	*FAAP100*	protein_coding
T_{TS}	CNVR109	12	60,100	1,998,701	*ENSSSCG00000052003*	*FSCN2*	protein_coding
T_{TS}	CNVR109	12	60,100	1,998,701	*ENSSSCG00000028355*	*ACTG1*	protein_coding
T_{TS}	CNVR109	12	60,100	1,998,701	*ENSSSCG00000023045*	*BAHCC1*	protein_coding
T_{TS}	CNVR109	12	60,100	1,998,701	*ENSSSCG00000032974*	*MYADML2*	protein_coding
T_{TS}	CNVR109	12	60,100	1,998,701	*ENSSSCG00000033221*		protein_coding
T_{TS}	CNVR109	12	60,100	1,998,701	*ENSSSCG00000048083*		lncRNA
T_{TS}	CNVR109	12	60,100	1,998,701	*ENSSSCG00000048182*		lncRNA
T_{TS}	CNVR109	12	60,100	1,998,701	*ENSSSCG00000052544*		lncRNA
T_{TS}	CNVR109	12	60,100	1,998,701	*ENSSSCG00000051633*		lncRNA
T_{TS}	CNVR109	12	60,100	1,998,701	*ENSSSCG00000058976*		lncRNA
T_{TS}	CNVR109	12	60,100	1,998,701	*ENSSSCG00000044226*		lncRNA

T_{TS}	CNVR109	12	60,100	1,998,701	*ENSSSCG00000052239*		lncRNA
T_{TS}	CNVR109	12	60,100	1,998,701	*ENSSSCG00000044793*		lncRNA
T_{TS}	CNVR109	12	60,100	1,998,701	*ENSSSCG00000059540*		lncRNA
T_{TS}	CNVR109	12	60,100	1,998,701	*ENSSSCG00000057304*		lncRNA
T_{TS}	CNVR109	12	60,100	1,998,701	*ENSSSCG00000053087*		lncRNA
T_{TS}	CNVR109	12	60,100	1,998,701	*ENSSSCG00000055034*		lncRNA
T_{TS}	CNVR109	12	60,100	1,998,701	*ENSSSCG00000057060*		lncRNA
T_{TS}	CNVR109	12	60,100	1,998,701	*ENSSSCG00000062857*		lncRNA
T_{TS}	CNVR109	12	60,100	1,998,701	*ENSSSCG00000061157*		lncRNA
T_{TS}	CNVR109	12	60,100	1,998,701	*ENSSSCG00000057894*		lncRNA
T_{TS}	CNVR109	12	60,100	1,998,701	*ENSSSCG00000051900*		lncRNA
T_{TS}	CNVR109	12	60,100	1,998,701	*ENSSSCG00000051406*		lncRNA
T_{TS}	CNVR109	12	60,100	1,998,701	*ENSSSCG00000024675*		miRNA
T_{TS}	CNVR109	12	60,100	1,998,701	*ENSSSCG00000017133*	*WDR45B*	protein_coding
T_{TS}	CNVR134	14	38,219,290	38,645,949	*ENSSSCG00000009869*	*LHX5*	protein_coding
T_{TS}	CNVR134	14	38,219,290	38,645,949	*ENSSSCG00000009870*	*SDSL*	protein_coding

T_{TS}	CNVR134	14	38,219,290	38,645,949	*ENSSSCG00000036865*	*SDS*	protein_coding
T_{TS}	CNVR134	14	38,219,290	38,645,949	*ENSSSCG00000009872*	*PLBD2*	protein_coding
T_{TS}	CNVR134	14	38,219,290	38,645,949	*ENSSSCG00000009873*	*DTX1*	protein_coding
T_{TS}	CNVR134	14	38,219,290	38,645,949	*ENSSSCG00000009874*	*RASAL1*	protein_coding
T_{TS}	CNVR134	14	38,219,290	38,645,949	*ENSSSCG00000009875*	*CFAP73*	protein_coding
T_{TS}	CNVR134	14	38,219,290	38,645,949	*ENSSSCG00000009876*	*DDX54*	protein_coding
T_{TS}	CNVR134	14	38,219,290	38,645,949	*ENSSSCG00000061641*		lncRNA
T_{TS}	CNVR134	14	38,219,290	38,645,949	*ENSSSCG00000056974*		lncRNA
T_{TS}	CNVR134	14	38,219,290	38,645,949	*ENSSSCG00000056447*		lncRNA
T_{TS}	CNVR134	14	38,219,290	38,645,949	*ENSSSCG00000053474*		lncRNA
T_{TS}	CNVR134	14	38,219,290	38,645,949	*ENSSSCG00000054937*		lncRNA
T_{TS}	CNVR138	14	74,176,726	74,990,114	*ENSSSCG00000010276*	*UNC5B*	protein_coding
T_{TS}	CNVR138	14	74,176,726	74,990,114	*ENSSSCG00000010277*	*SLC29A3*	protein_coding
T_{TS}	CNVR138	14	74,176,726	74,990,114	*ENSSSCG00000010278*		protein_coding
T_{TS}	CNVR138	14	74,176,726	74,990,114	*ENSSSCG00000038545*	*C10orf105*	protein_coding
T_{TS}	CNVR138	14	74,176,726	74,990,114	*ENSSSCG00000010280*		protein_coding

T_{TS}	CNVR138	14	74,176,726	74,990,114	*ENSSSCG00000037377*		protein_coding
T_{TS}	CNVR138	14	74,176,726	74,990,114	*ENSSSCG00000010281*	*PSAP*	protein_coding
T_{TS}	CNVR138	14	74,176,726	74,990,114	*ENSSSCG00000023662*	*CHST3*	protein_coding
T_{TS}	CNVR138	14	74,176,726	74,990,114	*ENSSSCG00000010283*	*SPOCK2*	protein_coding
T_{TS}	CNVR138	14	74,176,726	74,990,114	*ENSSSCG00000023130*	*ASCC1*	protein_coding
T_{TS}	CNVR138	14	74,176,726	74,990,114	*ENSSSCG00000040734*	*U6*	snRNA
T_{TS}	CNVR138	14	74,176,726	74,990,114	*ENSSSCG00000059909*		protein_coding
T_{TS}	CNVR147	14	140,199,680	140,419,493	*ENSSSCG00000024388*	*BNIP3*	protein_coding
T_{TS}	CNVR147	14	140,199,680	140,419,493	*ENSSSCG00000024633*	*JAKMIP3*	protein_coding
T_{TS}	CNVR147	14	140,199,680	140,419,493	*ENSSSCG00000053237*		lncRNA
T_{TS}	CNVR147	14	140,199,680	140,419,493	*ENSSSCG00000027988*		lncRNA
T_{TS}	CNVR147	14	140,199,680	140,419,493	*ENSSSCG00000045438*		lncRNA
T_{TS}	CNVR167	16	10,588,133	11,083,680	*ENSSSCG00000062495*		lncRNA
T_{TS}	CNVR167	16	10,588,133	11,083,680	*ENSSSCG00000054059*		lncRNA
T_{TS}	CNVR167	16	10,588,133	11,083,680	*ENSSSCG00000056095*		lncRNA
T_{TS}	CNVR167	16	10,588,133	11,083,680	*ENSSSCG00000044561*		lncRNA

T_{TS}	CNVR167	16	10,588,133	11,083,680	*ENSSSCG00000061683*	lncRNA
T_{TS}	CNVR167	16	10,588,133	11,083,680	*ENSSSCG00000051939*	lncRNA
T_{TS}	CNVR167	16	10,588,133	11,083,680	*ENSSSCG00000057614*	lncRNA
T_{TS}	CNVR167	16	10,588,133	11,083,680	*ENSSSCG00000052417*	lncRNA
T_{TS}	CNVR167	16	10,588,133	11,083,680	*ENSSSCG00000042836*	lncRNA
T_{TS}	CNVR167	16	10,588,133	11,083,680	*ENSSSCG00000045303*	lncRNA
T_{TS}	CNVR167	16	10,588,133	11,083,680	*ENSSSCG00000059280*	lncRNA
T_{TS}	CNVR167	16	10,588,133	11,083,680	*ENSSSCG00000052138*	lncRNA
T_{TS}	CNVR167	16	10,588,133	11,083,680	*ENSSSCG00000053822*	lncRNA
T_{TS}	CNVR167	16	10,588,133	11,083,680	*ENSSSCG00000063333*	lncRNA
T_{TS}	CNVR167	16	10,588,133	11,083,680	*ENSSSCG00000059876*	lncRNA
T_{TS}	CNVR167	16	10,588,133	11,083,680	*ENSSSCG00000059361*	lncRNA
T_{TS}	CNVR167	16	10,588,133	11,083,680	*ENSSSCG00000056593*	lncRNA
T_{TS}	CNVR167	16	10,588,133	11,083,680	*ENSSSCG00000056630*	lncRNA
T_{TS}	CNVR167	16	10,588,133	11,083,680	*ENSSSCG00000051141*	lncRNA
T_{TS}	CNVR167	16	10,588,133	11,083,680	*ENSSSCG00000053467*	lncRNA

T_{TS}	CNVR167	16	10,588,133	11,083,680	*ENSSSCG00000056905*		lncRNA
T_{TS}	CNVR167	16	10,588,133	11,083,680	*ENSSSCG00000042540*		lncRNA
T_{TS}	CNVR167	16	10,588,133	11,083,680	*ENSSSCG00000062613*		lncRNA
T_{TS}	CNVR167	16	10,588,133	11,083,680	*ENSSSCG00000058555*		lncRNA
T_{V16h}	CNVR133	14	16,993,535	17,333,398	*ENSSSCG00000021805*	*GALNTL6*	protein_coding

Table S6. Annoted QTL for autossomal CNVRs associated with physiological and anatomical indicators of heat stress response

Trait	CNVR	Chr	Start (bp)	End (bp)	QTL type	Name
T_{ES}	CNVR72	6	132,124,953	132,543,418	Health	Alkaline phosphatase activity
T_{ES}	CNVR72	6	132,124,953	132,543,418	Reproduction	Teat number
T_{ES}	CNVR72	6	132,124,953	132,543,418	Meat and Carcass	Shear force
T_{ES}	CNVR72	6	132,124,953	132,543,418	Meat and Carcass	Intramuscular fat content
T_{ES}	CNVR72	6	132,124,953	132,543,418	Health	Cholesterol level
T_{ES}	CNVR72	6	132,124,953	132,543,418	Meat and Carcass	Intramuscular fat content
T_{ES}	CNVR72	6	132,124,953	132,543,418	Reproduction	Teat number
T_{ES}	CNVR72	6	132,124,953	132,543,418	Meat and Carcass	Backfat at tenth rib

T_{ES}	CNVR72	6	132,124,953	132,543,418	Meat and Carcass	Backfat at last rib
T_{ES}	CNVR72	6	132,124,953	132,543,418	Meat and Carcass	Shoulder meat weight
T_{ES}	CNVR72	6	132,124,953	132,543,418	Meat and Carcass	Backfat at tenth rib
T_{ES}	CNVR72	6	132,124,953	132,543,418	Meat and Carcass	Muscle moisture percentage
T_{ES}	CNVR72	6	132,124,953	132,543,418	Meat and Carcass	Carcass temperature
T_{ES}	CNVR72	6	132,124,953	132,543,418	Meat and Carcass	Muscle fat content
T_{ES}	CNVR72	6	132,124,953	132,543,418	Meat and Carcass	muscle protein percentage
T_{ES}	CNVR72	6	132,124,953	132,543,418	Meat and Carcass	Muscle moisture percentage
T_{ES}	CNVR72	6	132,124,953	132,543,418	Meat and Carcass	Semimembranosus angle
T_{ES}	CNVR72	6	132,124,953	132,543,418	Health	Body temperature
T_{ES}	CNVR72	6	132,124,953	132,543,418	Exterior	Gait score (hind)
T_{ES}	CNVR72	6	132,124,953	132,543,418	Meat and Carcass	Shoulder weight
T_{ES}	CNVR72	6	132,124,953	132,543,418	Meat and Carcass	Shoulder weight
T_{ES}	CNVR72	6	132,124,953	132,543,418	Meat and Carcass	Ham weight
T_{ES}	CNVR72	6	132,124,953	132,543,418	Meat and Carcass	Muscle conductivity
T_{ES}	CNVR72	6	132,124,953	132,543,418	Meat and Carcass	Intramuscular fat content

T_{ES}	CNVR72	6	132,124,953	132,543,418	Meat and Carcass	Ham weight
T_{ES}	CNVR72	6	132,124,953	132,543,418	Reproduction	Cryptorchidism
T_{ES}	CNVR152	15	24,371,978	24,804,276	Meat and Carcass	Loin muscle area
T_{ES}	CNVR152	15	24,371,978	24,804,276	Meat and Carcass	Loin muscle area
T_{ES}	CNVR152	15	24,371,978	24,804,276	Meat and Carcass	Meat color
T_{ES}	CNVR152	15	24,371,978	24,804,276	Meat and Carcass	Cooking loss
T_{ES}	CNVR152	15	24,371,978	24,804,276	Meat and Carcass	Shear force
T_{ES}	CNVR152	15	24,371,978	24,804,276	Meat and Carcass	chew score
T_{ES}	CNVR152	15	24,371,978	24,804,276	Meat and Carcass	Shear force
T_{ES}	CNVR152	15	24,371,978	24,804,276	Meat and Carcass	Backfat at tenth rib
T_{ES}	CNVR152	15	24,371,978	24,804,276	Exterior	Hind leg conformation
T_{ES}	CNVR152	15	24,371,978	24,804,276	Exterior	Hind feet conformation
T_{ES}	CNVR152	15	24,371,978	24,804,276	Meat and Carcass	Shear force
T_{ES}	CNVR152	15	24,371,978	24,804,276	Reproduction	Corpus luteum number
T_{ES}	CNVR152	15	24,371,978	24,804,276	Health	Interleukin-8 level
T_{ES}	CNVR152	15	24,371,978	24,804,276	Health	Interleukin-8 level

T_{ES}	CNVR152	15	24,371,978	24,804,276	Health	Interleukin-8 level
T_{ES}	CNVR152	15	24,371,978	24,804,276	Exterior	Splay leg
T_{ES}	CNVR152	15	24,371,978	24,804,276	Exterior	Splay leg
T_{ES}	CNVR152	15	24,371,978	24,804,276	Meat and Carcass	Muscle pH
T_{ES}	CNVR152	15	24,371,978	24,804,276	Meat and Carcass	Muscle pH
T_{ES}	CNVR152	15	24,371,978	24,804,276	Meat and Carcass	Muscle pH
T_{ES}	CNVR152	15	24,371,978	24,804,276	Meat and Carcass	Muscle pH
T_{ES}	CNVR152	15	24,371,978	24,804,276	Meat and Carcass	Muscle pH
T_{ES}	CNVR152	15	24,371,978	24,804,276	Production	Feed intake
T_{ES}	CNVR152	15	24,371,978	24,804,276	Meat and Carcass	Muscle pH
T_{ES}	CNVR152	15	24,371,978	24,804,276	Meat and Carcass	Muscle pH
T_{ES}	CNVR152	15	24,371,978	24,804,276	Reproduction	Litter size
T_{ES}	CNVR152	15	24,371,978	24,804,276	Reproduction	Total number born alive
T_{ES}	CNVR152	15	24,371,978	24,804,276	Reproduction	Litter size
T_{RS}	CNVR23	2	6,179,112	6,495,647	Meat and Carcass	Average backfat thickness
T_{RS}	CNVR23	2	6,179,112	6,495,647	Meat and Carcass	Loin weight

T_{RS}	CNVR23	2	6,179,112	6,495,647	Meat and Carcass	Loin and ham percentage in carcass
T_{RS}	CNVR23	2	6,179,112	6,495,647	Meat and Carcass	Estimated carcass lean content
T_{RS}	CNVR23	2	6,179,112	6,495,647	Meat and Carcass	Backfat weight
T_{RS}	CNVR23	2	6,179,112	6,495,647	Meat and Carcass	Percentage of backfat and leaf fat in carcass
T_{RS}	CNVR23	2	6,179,112	6,495,647	Meat and Carcass	Backfat thickness between 3rd and 4th rib
T_{RS}	CNVR23	2	6,179,112	6,495,647	Meat and Carcass	Backfat at last rib
T_{RS}	CNVR23	2	6,179,112	6,495,647	Reproduction	Teat number
T_{RS}	CNVR23	2	6,179,112	6,495,647	Meat and Carcass	Average backfat thickness
T_{RS}	CNVR23	2	6,179,112	6,495,647	Meat and Carcass	Ham percentage
T_{RS}	CNVR23	2	6,179,112	6,495,647	Meat and Carcass	Loin percentage
T_{RS}	CNVR23	2	6,179,112	6,495,647	Meat and Carcass	Lean meat percentage
T_{RS}	CNVR23	2	6,179,112	6,495,647	Meat and Carcass	Backfat percentage
T_{RS}	CNVR23	2	6,179,112	6,495,647	Meat and Carcass	Fat-cuts percentage
T_{RS}	CNVR23	2	6,179,112	6,495,647	Meat and Carcass	Lean meat percentage
T_{RS}	CNVR23	2	6,179,112	6,495,647	Meat and Carcass	Ham meat weight
T_{RS}	CNVR23	2	6,179,112	6,495,647	Meat and Carcass	Lean meat + bone in ham + back

T_{RS}	CNVR23	2	6,179,112	6,495,647	Meat and Carcass	Loin muscle area
T_{RS}	CNVR23	2	6,179,112	6,495,647	Meat and Carcass	Average backfat thickness
T_{RS}	CNVR23	2	6,179,112	6,495,647	Meat and Carcass	Heart weight
T_{RS}	CNVR23	2	6,179,112	6,495,647	Meat and Carcass	Meat color
T_{RS}	CNVR23	2	6,179,112	6,495,647	Meat and Carcass	Heart weight
T_{RS}	CNVR23	2	6,179,112	6,495,647	Production	Average daily gain
T_{RS}	CNVR23	2	6,179,112	6,495,647	Meat and Carcass	Muscle conductivity
T_{RS}	CNVR23	2	6,179,112	6,495,647	Meat and Carcass	Head weight
T_{RS}	CNVR23	2	6,179,112	6,495,647	Meat and Carcass	Average backfat thickness
T_{RS}	CNVR23	2	6,179,112	6,495,647	Meat and Carcass	Backfat at last rib
T_{RS}	CNVR23	2	6,179,112	6,495,647	Meat and Carcass	Backfat at last lumbar
T_{RS}	CNVR23	2	6,179,112	6,495,647	Meat and Carcass	Backfat at tenth rib
T_{RS}	CNVR23	2	6,179,112	6,495,647	Meat and Carcass	Average backfat thickness
T_{RS}	CNVR23	2	6,179,112	6,495,647	Meat and Carcass	Backfat at tenth rib
T_{RS}	CNVR23	2	6,179,112	6,495,647	Meat and Carcass	Backfat at last lumbar
T_{RS}	CNVR23	2	6,179,112	6,495,647	Meat and Carcass	Backfat at last rib

T_{RS}	CNVR23	2	6,179,112	6,495,647	Meat and Carcass	Loin muscle area
T_{RS}	CNVR23	2	6,179,112	6,495,647	Meat and Carcass	muscle protein percentage
T_{RS}	CNVR23	2	6,179,112	6,495,647	Meat and Carcass	Backfat at first rib
T_{RS}	CNVR23	2	6,179,112	6,495,647	Meat and Carcass	backfat at P2 position
T_{RS}	CNVR23	2	6,179,112	6,495,647	Meat and Carcass	Carcass length
T_{RS}	CNVR23	2	6,179,112	6,495,647	Meat and Carcass	Lean meat percentage
T_{RS}	CNVR23	2	6,179,112	6,495,647	Meat and Carcass	External fat on loin
T_{RS}	CNVR23	2	6,179,112	6,495,647	Meat and Carcass	Muscle pH
T_{RS}	CNVR23	2	6,179,112	6,495,647	Meat and Carcass	Muscle pH
T_{RS}	CNVR23	2	6,179,112	6,495,647	Meat and Carcass	Muscle conductivity
T_{RS}	CNVR23	2	6,179,112	6,495,647	Meat and Carcass	Muscle conductivity
T_{RS}	CNVR23	2	6,179,112	6,495,647	Production	Average daily gain
T_{RS}	CNVR23	2	6,179,112	6,495,647	Meat and Carcass	Muscle pH
T_{RS}	CNVR23	2	6,179,112	6,495,647	Meat and Carcass	Carcass length
T_{RS}	CNVR23	2	6,179,112	6,495,647	Meat and Carcass	Carcass weight (hot)
T_{RS}	CNVR23	2	6,179,112	6,495,647	Meat and Carcass	Muscle pH

T_{RS}	CNVR23	2	6,179,112	6,495,647	Meat and Carcass	Muscle conductivity
T_{RS}	CNVR23	2	6,179,112	6,495,647	Meat and Carcass	Carcass weight (hot)
T_{RS}	CNVR23	2	6,179,112	6,495,647	Meat and Carcass	Neck fat weight
T_{RS}	CNVR23	2	6,179,112	6,495,647	Production	Feed conversion ratio
T_{RS}	CNVR23	2	6,179,112	6,495,647	Meat and Carcass	Loin weight
T_{RS}	CNVR23	2	6,179,112	6,495,647	Meat and Carcass	Carcass weight (hot)
T_{RS}	CNVR23	2	6,179,112	6,495,647	Meat and Carcass	Ham weight
T_{RS}	CNVR23	2	6,179,112	6,495,647	Meat and Carcass	Shoulder weight
T_{RS}	CNVR23	2	6,179,112	6,495,647	Meat and Carcass	Shear firmness
T_{RS}	CNVR23	2	6,179,112	6,495,647	Health	Segmented neutrophil number
T_{RS}	CNVR23	2	6,179,112	6,495,647	Meat and Carcass	Cutlet weight
T_{RS}	CNVR23	2	6,179,112	6,495,647	Meat and Carcass	Loin muscle area
T_{RS}	CNVR23	2	6,179,112	6,495,647	Meat and Carcass	Fat to meat ratio
T_{RS}	CNVR23	2	6,179,112	6,495,647	Production	Body weight
T_{RS}	CNVR23	2	6,179,112	6,495,647	Meat and Carcass	Average backfat thickness
T_{RS}	CNVR23	2	6,179,112	6,495,647	Health	O2 partial pressure

T_{RS}	CNVR23	2	6,179,112	6,495,647	Health	Oxygen saturation
T_{RS}	CNVR23	2	6,179,112	6,495,647	Exterior	Gait score (hind)
T_{RS}	CNVR23	2	6,179,112	6,495,647	Health	Hemolytic complement activity (alternative pathway)
T_{RS}	CNVR23	2	6,179,112	6,495,647	Health	Hemolytic complement activity (alternative pathway)
T_{RS}	CNVR23	2	6,179,112	6,495,647	Health	Hemolytic complement activity (alternative pathway)
T_{RS}	CNVR23	2	6,179,112	6,495,647	Health	C3c concentration
T_{RS}	CNVR23	2	6,179,112	6,495,647	Health	C3c concentration
T_{RS}	CNVR23	2	6,179,112	6,495,647	Health	C3c concentration
T_{RS}	CNVR23	2	6,179,112	6,495,647	Health	Creatine kinase level
T_{RS}	CNVR23	2	6,179,112	6,495,647	Meat and Carcass	Backfat at last rib
T_{RS}	CNVR23	2	6,179,112	6,495,647	Production	Average daily gain
T_{RS}	CNVR23	2	6,179,112	6,495,647	Meat and Carcass	Backfat at last rib
T_{RS}	CNVR23	2	6,179,112	6,495,647	Meat and Carcass	Average backfat thickness
T_{RS}	CNVR23	2	6,179,112	6,495,647	Health	Interleukin-10 level
T_{RS}	CNVR23	2	6,179,112	6,495,647	Health	Toll-like receptor 9 level
T_{RS}	CNVR23	2	6,179,112	6,495,647	Production	Bone mineral content

T_{RS}	CNVR23	2	6,179,112	6,495,647	Exterior	Osteochondrosis score
T_{RS}	CNVR23	2	6,179,112	6,495,647	Meat and Carcass	Average backfat thickness
T_{RS}	CNVR23	2	6,179,112	6,495,647	Meat and Carcass	Adipocyte diameter
T_{RS}	CNVR23	2	6,179,112	6,495,647	Health	Actinobacillus pleuropneumoniae susceptibility
T_{RS}	CNVR23	2	6,179,112	6,495,647	Meat and Carcass	Backfat between 6th and 7th ribs
T_{RS}	CNVR23	2	6,179,112	6,495,647	Meat and Carcass	Average backfat thickness
T_{RS}	CNVR23	2	6,179,112	6,495,647	Meat and Carcass	Lean meat percentage
T_{RS}	CNVR23	2	6,179,112	6,495,647	Meat and Carcass	Lean meat + bone in ham + back
T_{RS}	CNVR23	2	6,179,112	6,495,647	Meat and Carcass	Lean meat + bone in back
T_{RS}	CNVR23	2	6,179,112	6,495,647	Meat and Carcass	Backfat at last lumbar
T_{RS}	CNVR23	2	6,179,112	6,495,647	Meat and Carcass	Cooking loss
T_{RS}	CNVR23	2	6,179,112	6,495,647	Meat and Carcass	Meat color
T_{RS}	CNVR23	2	6,179,112	6,495,647	Meat and Carcass	Muscle pH
T_{RS}	CNVR23	2	6,179,112	6,495,647	Meat and Carcass	Knuckle ham weight
T_{RS}	CNVR23	2	6,179,112	6,495,647	Meat and Carcass	Fat protein content
T_{RS}	CNVR23	2	6,179,112	6,495,647	Meat and Carcass	NADP-malate dehydrogenase activity

T_{RS}	CNVR23	2	6,179,112	6,495,647	Meat and Carcass	Average backfat thickness
T_{RS}	CNVR23	2	6,179,112	6,495,647	Meat and Carcass	Abdominal fat weight
T_{RS}	CNVR23	2	6,179,112	6,495,647	Meat and Carcass	Backfat at first rib
T_{RS}	CNVR23	2	6,179,112	6,495,647	Meat and Carcass	Backfat at rump
T_{RS}	CNVR23	2	6,179,112	6,495,647	Meat and Carcass	Abdominal fat weight
T_{RS}	CNVR23	2	6,179,112	6,495,647	Meat and Carcass	Backfat at mid-back
T_{RS}	CNVR23	2	6,179,112	6,495,647	Meat and Carcass	Loin weight
T_{RS}	CNVR23	2	6,179,112	6,495,647	Meat and Carcass	Loin and neck meat weight
T_{RS}	CNVR23	2	6,179,112	6,495,647	Meat and Carcass	Palmitic acid content
T_{RS}	CNVR23	2	6,179,112	6,495,647	Meat and Carcass	cis-Vaccenic acid content
T_{RS}	CNVR23	2	6,179,112	6,495,647	Meat and Carcass	Linoleic acid content
T_{RS}	CNVR23	2	6,179,112	6,495,647	Meat and Carcass	Arachidonic acid content
T_{RS}	CNVR23	2	6,179,112	6,495,647	Meat and Carcass	Subcutaneous fat thickness
T_{RS}	CNVR23	2	6,179,112	6,495,647	Meat and Carcass	Myristic acid content
T_{RS}	CNVR23	2	6,179,112	6,495,647	Meat and Carcass	Palmitic acid content
T_{RS}	CNVR23	2	6,179,112	6,495,647	Meat and Carcass	Palmitoleic acid content

T_{RS}	CNVR23	2	6,179,112	6,495,647	Meat and Carcass	Linoleic acid content
T_{RS}	CNVR23	2	6,179,112	6,495,647	Meat and Carcass	Arachidonic acid content
T_{RS}	CNVR23	2	6,179,112	6,495,647	Meat and Carcass	Intramuscular fat content
T_{RS}	CNVR23	2	6,179,112	6,495,647	Meat and Carcass	Myristic acid content
T_{RS}	CNVR23	2	6,179,112	6,495,647	Meat and Carcass	Stearic acid content
T_{RS}	CNVR23	2	6,179,112	6,495,647	Meat and Carcass	Linoleic acid content
T_{RS}	CNVR23	2	6,179,112	6,495,647	Meat and Carcass	Arachidonic acid content
T_{RS}	CNVR23	2	6,179,112	6,495,647	Meat and Carcass	Fatty acid C20:3 to C18:2 ratio
T_{RS}	CNVR23	2	6,179,112	6,495,647	Meat and Carcass	Fatty acid C18:1 to C18:0 ratio
T_{RS}	CNVR23	2	6,179,112	6,495,647	Meat and Carcass	Fatty acid C20:3 to C18:2 ratio
T_{RS}	CNVR23	2	6,179,112	6,495,647	Meat and Carcass	Meat to fat ratio
T_{RS}	CNVR23	2	6,179,112	6,495,647	Meat and Carcass	Obesity index
T_{RS}	CNVR23	2	6,179,112	6,495,647	Meat and Carcass	Palmitic acid content
T_{RS}	CNVR23	2	6,179,112	6,495,647	Meat and Carcass	Oleic acid content
T_{RS}	CNVR23	2	6,179,112	6,495,647	Meat and Carcass	Monounsaturated fatty acid content
T_{TS}	CNVR21	2	1,111	632,707	Meat and Carcass	Average backfat thickness

T_{TS}	CNVR21	2	1,111	632,707	Meat and Carcass	Loin weight
T_{TS}	CNVR21	2	1,111	632,707	Meat and Carcass	Loin and ham percentage in carcass
T_{TS}	CNVR21	2	1,111	632,707	Meat and Carcass	Estimated carcass lean content
T_{TS}	CNVR21	2	1,111	632,707	Meat and Carcass	Backfat weight
T_{TS}	CNVR21	2	1,111	632,707	Meat and Carcass	Percentage of backfat and leaf fat in carcass
T_{TS}	CNVR21	2	1,111	632,707	Meat and Carcass	Backfat thickness between 3rd and 4th rib
T_{TS}	CNVR21	2	1,111	632,707	Meat and Carcass	Backfat at last rib
T_{TS}	CNVR21	2	1,111	632,707	Reproduction	Teat number
T_{TS}	CNVR21	2	1,111	632,707	Meat and Carcass	Average backfat thickness
T_{TS}	CNVR21	2	1,111	632,707	Meat and Carcass	Ham percentage
T_{TS}	CNVR21	2	1,111	632,707	Meat and Carcass	Loin percentage
T_{TS}	CNVR21	2	1,111	632,707	Meat and Carcass	Lean meat percentage
T_{TS}	CNVR21	2	1,111	632,707	Meat and Carcass	Backfat percentage
T_{TS}	CNVR21	2	1,111	632,707	Meat and Carcass	Fat-cuts percentage
T_{TS}	CNVR21	2	1,111	632,707	Meat and Carcass	Lean meat percentage
T_{TS}	CNVR21	2	1,111	632,707	Meat and Carcass	Ham meat weight

T_{TS}	CNVR21	2	1,111	632,707	Meat and Carcass	Lean meat + bone in ham + back
T_{TS}	CNVR21	2	1,111	632,707	Meat and Carcass	Loin muscle area
T_{TS}	CNVR21	2	1,111	632,707	Meat and Carcass	Average backfat thickness
T_{TS}	CNVR21	2	1,111	632,707	Meat and Carcass	Heart weight
T_{TS}	CNVR21	2	1,111	632,707	Meat and Carcass	Meat color
T_{TS}	CNVR21	2	1,111	632,707	Meat and Carcass	Heart weight
T_{TS}	CNVR21	2	1,111	632,707	Production	Average daily gain
T_{TS}	CNVR21	2	1,111	632,707	Meat and Carcass	Muscle conductivity
T_{TS}	CNVR21	2	1,111	632,707	Meat and Carcass	Head weight
T_{TS}	CNVR21	2	1,111	632,707	Meat and Carcass	Backfat at tenth rib
T_{TS}	CNVR21	2	1,111	632,707	Meat and Carcass	Backfat at last rib
T_{TS}	CNVR21	2	1,111	632,707	Meat and Carcass	Average backfat thickness
T_{TS}	CNVR21	2	1,111	632,707	Meat and Carcass	Loin muscle area
T_{TS}	CNVR21	2	1,111	632,707	Meat and Carcass	Loin weight
T_{TS}	CNVR21	2	1,111	632,707	Meat and Carcass	Backfat weight
T_{TS}	CNVR21	2	1,111	632,707	Meat and Carcass	Backfat at last lumbar

T_{TS}	CNVR21	2	1,111	632,707	Meat and Carcass	Backfat thickness between 3rd and 4th rib
T_{TS}	CNVR21	2	1,111	632,707	Meat and Carcass	Lean meat percentage
T_{TS}	CNVR21	2	1,111	632,707	Meat and Carcass	Average backfat thickness
T_{TS}	CNVR21	2	1,111	632,707	Meat and Carcass	Backfat at last rib
T_{TS}	CNVR21	2	1,111	632,707	Meat and Carcass	Backfat at last lumbar
T_{TS}	CNVR21	2	1,111	632,707	Meat and Carcass	Backfat at tenth rib
T_{TS}	CNVR21	2	1,111	632,707	Meat and Carcass	Average backfat thickness
T_{TS}	CNVR21	2	1,111	632,707	Meat and Carcass	Backfat at tenth rib
T_{TS}	CNVR21	2	1,111	632,707	Meat and Carcass	Backfat at last lumbar
T_{TS}	CNVR21	2	1,111	632,707	Meat and Carcass	Backfat at last rib
T_{TS}	CNVR21	2	1,111	632,707	Meat and Carcass	Loin muscle area
T_{TS}	CNVR21	2	1,111	632,707	Meat and Carcass	muscle protein percentage
T_{TS}	CNVR21	2	1,111	632,707	Meat and Carcass	Backfat at first rib
T_{TS}	CNVR21	2	1,111	632,707	Meat and Carcass	backfat at P2 position
T_{TS}	CNVR21	2	1,111	632,707	Meat and Carcass	Carcass length
T_{TS}	CNVR21	2	1,111	632,707	Meat and Carcass	Lean meat percentage

T_{TS}	CNVR21	2	1,111	632,707	Meat and Carcass	External fat on loin
T_{TS}	CNVR21	2	1,111	632,707	Meat and Carcass	Muscle pH
T_{TS}	CNVR21	2	1,111	632,707	Meat and Carcass	Muscle pH
T_{TS}	CNVR21	2	1,111	632,707	Meat and Carcass	Muscle conductivity
T_{TS}	CNVR21	2	1,111	632,707	Meat and Carcass	Muscle conductivity
T_{TS}	CNVR21	2	1,111	632,707	Production	Average daily gain
T_{TS}	CNVR21	2	1,111	632,707	Meat and Carcass	Muscle pH
T_{TS}	CNVR21	2	1,111	632,707	Meat and Carcass	Carcass length
T_{TS}	CNVR21	2	1,111	632,707	Meat and Carcass	Carcass weight (hot)
T_{TS}	CNVR21	2	1,111	632,707	Meat and Carcass	Muscle pH
T_{TS}	CNVR21	2	1,111	632,707	Meat and Carcass	Muscle conductivity
T_{TS}	CNVR21	2	1,111	632,707	Meat and Carcass	Carcass weight (hot)
T_{TS}	CNVR21	2	1,111	632,707	Meat and Carcass	Neck fat weight
T_{TS}	CNVR21	2	1,111	632,707	Production	Feed conversion ratio
T_{TS}	CNVR21	2	1,111	632,707	Meat and Carcass	Loin weight
T_{TS}	CNVR21	2	1,111	632,707	Meat and Carcass	Carcass weight (hot)

T_{TS}	CNVR21	2	1,111	632,707	Meat and Carcass	Ham weight
T_{TS}	CNVR21	2	1,111	632,707	Meat and Carcass	Shoulder weight
T_{TS}	CNVR21	2	1,111	632,707	Meat and Carcass	Shear firmness
T_{TS}	CNVR21	2	1,111	632,707	Health	Segmented neutrophil number
T_{TS}	CNVR21	2	1,111	632,707	Meat and Carcass	Cutlet weight
T_{TS}	CNVR21	2	1,111	632,707	Meat and Carcass	Loin muscle area
T_{TS}	CNVR21	2	1,111	632,707	Meat and Carcass	Fat to meat ratio
T_{TS}	CNVR21	2	1,111	632,707	Production	Body weight
T_{TS}	CNVR21	2	1,111	632,707	Meat and Carcass	Average backfat thickness
T_{TS}	CNVR21	2	1,111	632,707	Health	O2 partial pressure
T_{TS}	CNVR21	2	1,111	632,707	Health	Oxygen saturation
T_{TS}	CNVR21	2	1,111	632,707	Exterior	Gait score (hind)
T_{TS}	CNVR21	2	1,111	632,707	Health	Hemolytic complement activity (alternative pathway)
T_{TS}	CNVR21	2	1,111	632,707	Health	Hemolytic complement activity (alternative pathway)
T_{TS}	CNVR21	2	1,111	632,707	Health	Hemolytic complement activity (alternative pathway)
T_{TS}	CNVR21	2	1,111	632,707	Health	C3c concentration

T_{TS}	CNVR21	2	1,111	632,707	Health	C3c concentration
T_{TS}	CNVR21	2	1,111	632,707	Health	C3c concentration
T_{TS}	CNVR21	2	1,111	632,707	Health	Creatine kinase level
T_{TS}	CNVR21	2	1,111	632,707	Meat and Carcass	Backfat at last rib
T_{TS}	CNVR21	2	1,111	632,707	Production	Average daily gain
T_{TS}	CNVR21	2	1,111	632,707	Meat and Carcass	Backfat at last rib
T_{TS}	CNVR21	2	1,111	632,707	Meat and Carcass	Average backfat thickness
T_{TS}	CNVR21	2	1,111	632,707	Meat and Carcass	Loin weight
T_{TS}	CNVR21	2	1,111	632,707	Meat and Carcass	Average backfat thickness
T_{TS}	CNVR21	2	1,111	632,707	Health	Interleukin-10 level
T_{TS}	CNVR21	2	1,111	632,707	Health	Toll-like receptor 9 level
T_{TS}	CNVR21	2	1,111	632,707	Production	Bone mineral content
T_{TS}	CNVR21	2	1,111	632,707	Exterior	Osteochondrosis score
T_{TS}	CNVR21	2	1,111	632,707	Meat and Carcass	Average backfat thickness
T_{TS}	CNVR21	2	1,111	632,707	Meat and Carcass	Adipocyte diameter
T_{TS}	CNVR21	2	1,111	632,707	Health	Actinobacillus pleuropneumoniae susceptibility

T_{TS}	CNVR21	2	1,111	632,707	Meat and Carcass	Loin muscle depth
T_{TS}	CNVR21	2	1,111	632,707	Meat and Carcass	Dressing percentage
T_{TS}	CNVR21	2	1,111	632,707	Meat and Carcass	Monounsaturated fatty acid to polyunsaturated fatty acid ratio
T_{TS}	CNVR21	2	1,111	632,707	Meat and Carcass	Linoleic acid content
T_{TS}	CNVR21	2	1,111	632,707	Meat and Carcass	Polyunsaturated fatty acid content
T_{TS}	CNVR21	2	1,111	632,707	Meat and Carcass	Oleic acid content
T_{TS}	CNVR21	2	1,111	632,707	Meat and Carcass	Monounsaturated fatty acid content
T_{TS}	CNVR21	2	1,111	632,707	Meat and Carcass	Polyunsaturated fatty acid to saturated fatty acid ratio
T_{TS}	CNVR21	2	1,111	632,707	Meat and Carcass	Dressing percentage
T_{TS}	CNVR21	2	1,111	632,707	Meat and Carcass	Monounsaturated fatty acid to polyunsaturated fatty acid ratio
T_{TS}	CNVR21	2	1,111	632,707	Meat and Carcass	Linoleic acid content
T_{TS}	CNVR21	2	1,111	632,707	Meat and Carcass	Polyunsaturated fatty acid content
T_{TS}	CNVR21	2	1,111	632,707	Meat and Carcass	Oleic acid content
T_{TS}	CNVR21	2	1,111	632,707	Meat and Carcass	Average backfat thickness
T_{TS}	CNVR21	2	1,111	632,707	Meat and Carcass	Dressing percentage
T_{TS}	CNVR21	2	1,111	632,707	Meat and Carcass	Average backfat thickness

T_{TS}	CNVR21	2	1,111	632,707	Meat and Carcass	Lean meat percentage
T_{TS}	CNVR21	2	1,111	632,707	Meat and Carcass	Monounsaturated fatty acid to polyunsaturated fatty acid ratio
T_{TS}	CNVR21	2	1,111	632,707	Meat and Carcass	Linoleic acid content
T_{TS}	CNVR21	2	1,111	632,707	Meat and Carcass	Polyunsaturated fatty acid content
T_{TS}	CNVR21	2	1,111	632,707	Meat and Carcass	Polyunsaturated fatty acid to saturated fatty acid ratio
T_{TS}	CNVR21	2	1,111	632,707	Meat and Carcass	Oleic acid content
T_{TS}	CNVR21	2	1,111	632,707	Meat and Carcass	Cooking loss
T_{TS}	CNVR21	2	1,111	632,707	Meat and Carcass	Dressing percentage
T_{TS}	CNVR21	2	1,111	632,707	Meat and Carcass	Dressing percentage
T_{TS}	CNVR21	2	1,111	632,707	Meat and Carcass	Average backfat thickness
T_{TS}	CNVR21	2	1,111	632,707	Meat and Carcass	Lean meat percentage
T_{TS}	CNVR21	2	1,111	632,707	Meat and Carcass	Monounsaturated fatty acid to polyunsaturated fatty acid ratio
T_{TS}	CNVR21	2	1,111	632,707	Meat and Carcass	Linoleic acid content
T_{TS}	CNVR21	2	1,111	632,707	Meat and Carcass	Polyunsaturated fatty acid content
T_{TS}	CNVR21	2	1,111	632,707	Meat and Carcass	Oleic acid content
T_{TS}	CNVR21	2	1,111	632,707	Meat and Carcass	Monounsaturated fatty acid content

T_{TS}	CNVR21	2	1,111	632,707	Meat and Carcass	Backfat between 6th and 7th ribs
T_{TS}	CNVR21	2	1,111	632,707	Meat and Carcass	Average backfat thickness
T_{TS}	CNVR21	2	1,111	632,707	Meat and Carcass	Monounsaturated fatty acid to polyunsaturated fatty acid ratio
T_{TS}	CNVR21	2	1,111	632,707	Meat and Carcass	Linoleic acid content
T_{TS}	CNVR21	2	1,111	632,707	Meat and Carcass	Polyunsaturated fatty acid content
T_{TS}	CNVR21	2	1,111	632,707	Meat and Carcass	Oleic acid content
T_{TS}	CNVR21	2	1,111	632,707	Meat and Carcass	Polyunsaturated fatty acid to saturated fatty acid ratio
T_{TS}	CNVR21	2	1,111	632,707	Meat and Carcass	Monounsaturated fatty acid content
T_{TS}	CNVR21	2	1,111	632,707	Meat and Carcass eQTL	Fat androstenone level
T_{TS}	CNVR21	2	1,111	632,707	Meat and Carcass eQTL	Fat androstenone level
T_{TS}	CNVR21	2	1,111	632,707	Meat and Carcass eQTL	Fat androstenone level
T_{TS}	CNVR21	2	1,111	632,707	Meat and Carcass	Dressing percentage
T_{TS}	CNVR21	2	1,111	632,707	Meat and Carcass	Average backfat thickness
T_{TS}	CNVR21	2	1,111	632,707	Meat and Carcass	Lean meat percentage
T_{TS}	CNVR23	2	6,179,112	6,495,647	Meat and Carcass	Average backfat thickness
T_{TS}	CNVR23	2	6,179,112	6,495,647	Meat and Carcass	Loin weight

T_{TS}	CNVR23	2	6,179,112	6,495,647	Meat and Carcass	Loin and ham percentage in carcass
T_{TS}	CNVR23	2	6,179,112	6,495,647	Meat and Carcass	Estimated carcass lean content
T_{TS}	CNVR23	2	6,179,112	6,495,647	Meat and Carcass	Backfat weight
T_{TS}	CNVR23	2	6,179,112	6,495,647	Meat and Carcass	Percentage of backfat and leaf fat in carcass
T_{TS}	CNVR23	2	6,179,112	6,495,647	Meat and Carcass	Backfat thickness between 3rd and 4th rib
T_{TS}	CNVR23	2	6,179,112	6,495,647	Meat and Carcass	Backfat at last rib
T_{TS}	CNVR23	2	6,179,112	6,495,647	Reproduction	Teat number
T_{TS}	CNVR23	2	6,179,112	6,495,647	Meat and Carcass	Average backfat thickness
T_{TS}	CNVR23	2	6,179,112	6,495,647	Meat and Carcass	Ham percentage
T_{TS}	CNVR23	2	6,179,112	6,495,647	Meat and Carcass	Loin percentage
T_{TS}	CNVR23	2	6,179,112	6,495,647	Meat and Carcass	Lean meat percentage
T_{TS}	CNVR23	2	6,179,112	6,495,647	Meat and Carcass	Backfat percentage
T_{TS}	CNVR23	2	6,179,112	6,495,647	Meat and Carcass	Fat-cuts percentage
T_{TS}	CNVR23	2	6,179,112	6,495,647	Meat and Carcass	Lean meat percentage
T_{TS}	CNVR23	2	6,179,112	6,495,647	Meat and Carcass	Ham meat weight
T_{TS}	CNVR23	2	6,179,112	6,495,647	Meat and Carcass	Lean meat + bone in ham + back

T_{TS}	CNVR23	2	6,179,112	6,495,647	Meat and Carcass	Loin muscle area
T_{TS}	CNVR23	2	6,179,112	6,495,647	Meat and Carcass	Average backfat thickness
T_{TS}	CNVR23	2	6,179,112	6,495,647	Meat and Carcass	Heart weight
T_{TS}	CNVR23	2	6,179,112	6,495,647	Meat and Carcass	Meat color
T_{TS}	CNVR23	2	6,179,112	6,495,647	Meat and Carcass	Heart weight
T_{TS}	CNVR23	2	6,179,112	6,495,647	Production	Average daily gain
T_{TS}	CNVR23	2	6,179,112	6,495,647	Meat and Carcass	Muscle conductivity
T_{TS}	CNVR23	2	6,179,112	6,495,647	Meat and Carcass	Head weight
T_{TS}	CNVR23	2	6,179,112	6,495,647	Meat and Carcass	Average backfat thickness
T_{TS}	CNVR23	2	6,179,112	6,495,647	Meat and Carcass	Backfat at last rib
T_{TS}	CNVR23	2	6,179,112	6,495,647	Meat and Carcass	Backfat at last lumbar
T_{TS}	CNVR23	2	6,179,112	6,495,647	Meat and Carcass	Backfat at tenth rib
T_{TS}	CNVR23	2	6,179,112	6,495,647	Meat and Carcass	Average backfat thickness
T_{TS}	CNVR23	2	6,179,112	6,495,647	Meat and Carcass	Backfat at tenth rib
T_{TS}	CNVR23	2	6,179,112	6,495,647	Meat and Carcass	Backfat at last lumbar
T_{TS}	CNVR23	2	6,179,112	6,495,647	Meat and Carcass	Backfat at last rib

T_{TS}	CNVR23	2	6,179,112	6,495,647	Meat and Carcass	Loin muscle area
T_{TS}	CNVR23	2	6,179,112	6,495,647	Meat and Carcass	muscle protein percentage
T_{TS}	CNVR23	2	6,179,112	6,495,647	Meat and Carcass	Backfat at first rib
T_{TS}	CNVR23	2	6,179,112	6,495,647	Meat and Carcass	backfat at P2 position
T_{TS}	CNVR23	2	6,179,112	6,495,647	Meat and Carcass	Carcass length
T_{TS}	CNVR23	2	6,179,112	6,495,647	Meat and Carcass	Lean meat percentage
T_{TS}	CNVR23	2	6,179,112	6,495,647	Meat and Carcass	External fat on loin
T_{TS}	CNVR23	2	6,179,112	6,495,647	Meat and Carcass	Muscle pH
T_{TS}	CNVR23	2	6,179,112	6,495,647	Meat and Carcass	Muscle pH
T_{TS}	CNVR23	2	6,179,112	6,495,647	Meat and Carcass	Muscle conductivity
T_{TS}	CNVR23	2	6,179,112	6,495,647	Meat and Carcass	Muscle conductivity
T_{TS}	CNVR23	2	6,179,112	6,495,647	Production	Average daily gain
T_{TS}	CNVR23	2	6,179,112	6,495,647	Meat and Carcass	Muscle pH
T_{TS}	CNVR23	2	6,179,112	6,495,647	Meat and Carcass	Carcass length
T_{TS}	CNVR23	2	6,179,112	6,495,647	Meat and Carcass	Carcass weight (hot)
T_{TS}	CNVR23	2	6,179,112	6,495,647	Meat and Carcass	Muscle pH

T_{TS}	CNVR23	2	6,179,112	6,495,647	Meat and Carcass	Muscle conductivity
T_{TS}	CNVR23	2	6,179,112	6,495,647	Meat and Carcass	Carcass weight (hot)
T_{TS}	CNVR23	2	6,179,112	6,495,647	Meat and Carcass	Neck fat weight
T_{TS}	CNVR23	2	6,179,112	6,495,647	Production	Feed conversion ratio
T_{TS}	CNVR23	2	6,179,112	6,495,647	Meat and Carcass	Loin weight
T_{TS}	CNVR23	2	6,179,112	6,495,647	Meat and Carcass	Carcass weight (hot)
T_{TS}	CNVR23	2	6,179,112	6,495,647	Meat and Carcass	Ham weight
T_{TS}	CNVR23	2	6,179,112	6,495,647	Meat and Carcass	Shoulder weight
T_{TS}	CNVR23	2	6,179,112	6,495,647	Meat and Carcass	Shear firmness
T_{TS}	CNVR23	2	6,179,112	6,495,647	Health	Segmented neutrophil number
T_{TS}	CNVR23	2	6,179,112	6,495,647	Meat and Carcass	Cutlet weight
T_{TS}	CNVR23	2	6,179,112	6,495,647	Meat and Carcass	Loin muscle area
T_{TS}	CNVR23	2	6,179,112	6,495,647	Meat and Carcass	Fat to meat ratio
T_{TS}	CNVR23	2	6,179,112	6,495,647	Production	Body weight
T_{TS}	CNVR23	2	6,179,112	6,495,647	Meat and Carcass	Average backfat thickness
T_{TS}	CNVR23	2	6,179,112	6,495,647	Health	O2 partial pressure

T_{TS}	CNVR23	2	6,179,112	6,495,647	Health	Oxygen saturation
T_{TS}	CNVR23	2	6,179,112	6,495,647	Exterior	Gait score (hind)
T_{TS}	CNVR23	2	6,179,112	6,495,647	Health	Hemolytic complement activity (alternative pathway)
T_{TS}	CNVR23	2	6,179,112	6,495,647	Health	Hemolytic complement activity (alternative pathway)
T_{TS}	CNVR23	2	6,179,112	6,495,647	Health	Hemolytic complement activity (alternative pathway)
T_{TS}	CNVR23	2	6,179,112	6,495,647	Health	C3c concentration
T_{TS}	CNVR23	2	6,179,112	6,495,647	Health	C3c concentration
T_{TS}	CNVR23	2	6,179,112	6,495,647	Health	C3c concentration
T_{TS}	CNVR23	2	6,179,112	6,495,647	Health	Creatine kinase level
T_{TS}	CNVR23	2	6,179,112	6,495,647	Meat and Carcass	Backfat at last rib
T_{TS}	CNVR23	2	6,179,112	6,495,647	Production	Average daily gain
T_{TS}	CNVR23	2	6,179,112	6,495,647	Meat and Carcass	Backfat at last rib
T_{TS}	CNVR23	2	6,179,112	6,495,647	Meat and Carcass	Average backfat thickness
T_{TS}	CNVR23	2	6,179,112	6,495,647	Health	Interleukin-10 level
T_{TS}	CNVR23	2	6,179,112	6,495,647	Health	Toll-like receptor 9 level
T_{TS}	CNVR23	2	6,179,112	6,495,647	Production	Bone mineral content

T_{TS}	CNVR23	2	6,179,112	6,495,647	Exterior	Osteochondrosis score
T_{TS}	CNVR23	2	6,179,112	6,495,647	Meat and Carcass	Average backfat thickness
T_{TS}	CNVR23	2	6,179,112	6,495,647	Meat and Carcass	Adipocyte diameter
T_{TS}	CNVR23	2	6,179,112	6,495,647	Health	Actinobacillus pleuropneumoniae susceptibility
T_{TS}	CNVR23	2	6,179,112	6,495,647	Meat and Carcass	Backfat between 6th and 7th ribs
T_{TS}	CNVR23	2	6,179,112	6,495,647	Meat and Carcass	Average backfat thickness
T_{TS}	CNVR23	2	6,179,112	6,495,647	Meat and Carcass	Lean meat percentage
T_{TS}	CNVR23	2	6,179,112	6,495,647	Meat and Carcass	Lean meat + bone in ham + back
T_{TS}	CNVR23	2	6,179,112	6,495,647	Meat and Carcass	Lean meat + bone in back
T_{TS}	CNVR23	2	6,179,112	6,495,647	Meat and Carcass	Backfat at last lumbar
T_{TS}	CNVR23	2	6,179,112	6,495,647	Meat and Carcass	Cooking loss
T_{TS}	CNVR23	2	6,179,112	6,495,647	Meat and Carcass	Meat color
T_{TS}	CNVR23	2	6,179,112	6,495,647	Meat and Carcass	Muscle pH
T_{TS}	CNVR23	2	6,179,112	6,495,647	Meat and Carcass	Knuckle ham weight
T_{TS}	CNVR23	2	6,179,112	6,495,647	Meat and Carcass	Fat protein content
T_{TS}	CNVR23	2	6,179,112	6,495,647	Meat and Carcass	NADP-malate dehydrogenase activity

T_{TS}	CNVR23	2	6,179,112	6,495,647	Meat and Carcass	Average backfat thickness
T_{TS}	CNVR23	2	6,179,112	6,495,647	Meat and Carcass	Abdominal fat weight
T_{TS}	CNVR23	2	6,179,112	6,495,647	Meat and Carcass	Backfat at first rib
T_{TS}	CNVR23	2	6,179,112	6,495,647	Meat and Carcass	Backfat at rump
T_{TS}	CNVR23	2	6,179,112	6,495,647	Meat and Carcass	Abdominal fat weight
T_{TS}	CNVR23	2	6,179,112	6,495,647	Meat and Carcass	Backfat at mid-back
T_{TS}	CNVR23	2	6,179,112	6,495,647	Meat and Carcass	Loin weight
T_{TS}	CNVR23	2	6,179,112	6,495,647	Meat and Carcass	Loin and neck meat weight
T_{TS}	CNVR23	2	6,179,112	6,495,647	Meat and Carcass	Palmitic acid content
T_{TS}	CNVR23	2	6,179,112	6,495,647	Meat and Carcass	cis-Vaccenic acid content
T_{TS}	CNVR23	2	6,179,112	6,495,647	Meat and Carcass	Linoleic acid content
T_{TS}	CNVR23	2	6,179,112	6,495,647	Meat and Carcass	Arachidonic acid content
T_{TS}	CNVR23	2	6,179,112	6,495,647	Meat and Carcass	Subcutaneous fat thickness
T_{TS}	CNVR23	2	6,179,112	6,495,647	Meat and Carcass	Myristic acid content
T_{TS}	CNVR23	2	6,179,112	6,495,647	Meat and Carcass	Palmitic acid content
T_{TS}	CNVR23	2	6,179,112	6,495,647	Meat and Carcass	Palmitoleic acid content

T_{TS}	CNVR23	2	6,179,112	6,495,647	Meat and Carcass	Linoleic acid content
T_{TS}	CNVR23	2	6,179,112	6,495,647	Meat and Carcass	Arachidonic acid content
T_{TS}	CNVR23	2	6,179,112	6,495,647	Meat and Carcass	Intramuscular fat content
T_{TS}	CNVR23	2	6,179,112	6,495,647	Meat and Carcass	Myristic acid content
T_{TS}	CNVR23	2	6,179,112	6,495,647	Meat and Carcass	Stearic acid content
T_{TS}	CNVR23	2	6,179,112	6,495,647	Meat and Carcass	Linoleic acid content
T_{TS}	CNVR23	2	6,179,112	6,495,647	Meat and Carcass	Arachidonic acid content
T_{TS}	CNVR23	2	6,179,112	6,495,647	Meat and Carcass	Fatty acid C20:3 to C18:2 ratio
T_{TS}	CNVR23	2	6,179,112	6,495,647	Meat and Carcass	Fatty acid C18:1 to C18:0 ratio
T_{TS}	CNVR23	2	6,179,112	6,495,647	Meat and Carcass	Fatty acid C20:3 to C18:2 ratio
T_{TS}	CNVR23	2	6,179,112	6,495,647	Meat and Carcass	Meat to fat ratio
T_{TS}	CNVR23	2	6,179,112	6,495,647	Meat and Carcass	Obesity index
T_{TS}	CNVR23	2	6,179,112	6,495,647	Meat and Carcass	Palmitic acid content
T_{TS}	CNVR23	2	6,179,112	6,495,647	Meat and Carcass	Oleic acid content
T_{TS}	CNVR23	2	6,179,112	6,495,647	Meat and Carcass	Monounsaturated fatty acid content
T_{TS}	CNVR48	4	1,155,293	1,388,468	Meat and Carcass	Average backfat thickness

T_{TS}	CNVR48	4	1,155,293	1,388,468	Meat and Carcass	Loin muscle area
T_{TS}	CNVR48	4	1,155,293	1,388,468	Meat and Carcass	Carcass weight (hot)
T_{TS}	CNVR48	4	1,155,293	1,388,468	Production	Loin eye area linear
T_{TS}	CNVR48	4	1,155,293	1,388,468	Meat and Carcass	Total lean tissue linear
T_{TS}	CNVR48	4	1,155,293	1,388,468	Meat and Carcass	Water holding capacity
T_{TS}	CNVR48	4	1,155,293	1,388,468	Meat and Carcass	Linoleic acid content
T_{TS}	CNVR48	4	1,155,293	1,388,468	Health	Enterotoxigenic E. coli susceptibility
T_{TS}	CNVR48	4	1,155,293	1,388,468	Meat and Carcass	Shoulder meat weight
T_{TS}	CNVR48	4	1,155,293	1,388,468	Meat and Carcass	Loin muscle area
T_{TS}	CNVR48	4	1,155,293	1,388,468	Meat and Carcass	Loin muscle depth
T_{TS}	CNVR48	4	1,155,293	1,388,468	Meat and Carcass	backfat at P2 position
T_{TS}	CNVR48	4	1,155,293	1,388,468	Meat and Carcass	Ham meat weight
T_{TS}	CNVR48	4	1,155,293	1,388,468	Meat and Carcass	Backfat at last lumbar
T_{TS}	CNVR48	4	1,155,293	1,388,468	Meat and Carcass	Backfat at last rib
T_{TS}	CNVR48	4	1,155,293	1,388,468	Meat and Carcass	Heart weight
T_{TS}	CNVR52	4	126,897,791	127,521,733	Meat and Carcass	Intramuscular fat content

T_{TS}	CNVR52	4	126,897,791	127,521,733	Meat and Carcass	Shear force at first peak
T_{TS}	CNVR52	4	126,897,791	127,521,733	Meat and Carcass	Total shear work
T_{TS}	CNVR52	4	126,897,791	127,521,733	Reproduction	Nonfunctional nipples
T_{TS}	CNVR52	4	126,897,791	127,521,733	Meat and Carcass	Carcass weight (cold)
T_{TS}	CNVR52	4	126,897,791	127,521,733	Health	Calcium level
T_{TS}	CNVR52	4	126,897,791	127,521,733	Meat and Carcass	Carcass weight (cold)
T_{TS}	CNVR52	4	126,897,791	127,521,733	Exterior	Vertebra number
T_{TS}	CNVR52	4	126,897,791	127,521,733	Health	Platelet count
T_{TS}	CNVR52	4	126,897,791	127,521,733	Production	Days to 90 kg
T_{TS}	CNVR52	4	126,897,791	127,521,733	Meat and Carcass	Average backfat thickness
T_{TS}	CNVR52	4	126,897,791	127,521,733	Production	Average daily gain
T_{TS}	CNVR52	4	126,897,791	127,521,733	Meat and Carcass	Average backfat thickness
T_{TS}	CNVR52	4	126,897,791	127,521,733	Production	Average daily gain
T_{TS}	CNVR52	4	126,897,791	127,521,733	Health	PRRS viral load
T_{TS}	CNVR52	4	126,897,791	127,521,733	Health	PRRSV susceptibility
T_{TS}	CNVR52	4	126,897,791	127,521,733	Health	PRRS viral load

T_{TS}	CNVR52	4	126,897,791	127,521,733	Health	PRRSV susceptibility
T_{TS}	CNVR52	4	126,897,791	127,521,733	Production	Average daily gain
T_{TS}	CNVR52	4	126,897,791	127,521,733	Production	Average daily gain
T_{TS}	CNVR52	4	126,897,791	127,521,733	Production	Average daily gain
T_{TS}	CNVR52	4	126,897,791	127,521,733	Production	Average daily gain
T_{TS}	CNVR52	4	126,897,791	127,521,733	Production	Average daily gain
T_{TS}	CNVR52	4	126,897,791	127,521,733	Production	Feed intake
T_{TS}	CNVR52	4	126,897,791	127,521,733	Production	Feed intake
T_{TS}	CNVR52	4	126,897,791	127,521,733	Production	Average daily gain
T_{TS}	CNVR52	4	126,897,791	127,521,733	Production	Average daily gain
T_{TS}	CNVR52	4	126,897,791	127,521,733	Health	PRRS viral load
T_{TS}	CNVR52	4	126,897,791	127,521,733	Health	PRRSV antibody titer
T_{TS}	CNVR52	4	126,897,791	127,521,733	Health	PRRSV antibody titer
T_{TS}	CNVR52	4	126,897,791	127,521,733	Meat and Carcass	Average backfat thickness
T_{TS}	CNVR52	4	126,897,791	127,521,733	Production	Average daily gain
T_{TS}	CNVR52	4	126,897,791	127,521,733	Reproduction	Teat number

T_{TS}	CNVR52	4	126,897,791	127,521,733	Health	PRRS viral load
T_{TS}	CNVR52	4	126,897,791	127,521,733	Health	PRRS viral load
T_{TS}	CNVR65	5	77,179,466	77,352,621	Meat and Carcass	backfat above muscle dorsi
T_{TS}	CNVR65	5	77,179,466	77,352,621	Meat and Carcass	Shoulder subcutaneous fat thickness
T_{TS}	CNVR65	5	77,179,466	77,352,621	Meat and Carcass	backfat above muscle dorsi
T_{TS}	CNVR65	5	77,179,466	77,352,621	Meat and Carcass	Loin muscle area
T_{TS}	CNVR65	5	77,179,466	77,352,621	Meat and Carcass	Meat color
T_{TS}	CNVR65	5	77,179,466	77,352,621	Meat and Carcass	Backfat at mid-back
T_{TS}	CNVR65	5	77,179,466	77,352,621	Meat and Carcass	Backfat at mid-back
T_{TS}	CNVR65	5	77,179,466	77,352,621	Meat and Carcass	Backfat at first rib
T_{TS}	CNVR65	5	77,179,466	77,352,621	Meat and Carcass	Marbling
T_{TS}	CNVR65	5	77,179,466	77,352,621	Meat and Carcass	Meat color
T_{TS}	CNVR65	5	77,179,466	77,352,621	Meat and Carcass	Backfat at rump
T_{TS}	CNVR65	5	77,179,466	77,352,621	Meat and Carcass	Shoulder subcutaneous fat thickness
T_{TS}	CNVR65	5	77,179,466	77,352,621	Meat and Carcass	Meat color
T_{TS}	CNVR65	5	77,179,466	77,352,621	Meat and Carcass	Meat color

T_{TS}	CNVR65	5	77,179,466	77,352,621	Meat and Carcass	Meat color
T_{TS}	CNVR65	5	77,179,466	77,352,621	Meat and Carcass	Backfat at mid-back
T_{TS}	CNVR65	5	77,179,466	77,352,621	Meat and Carcass	Carcass weight (hot)
T_{TS}	CNVR65	5	77,179,466	77,352,621	Meat and Carcass	Muscle pH
T_{TS}	CNVR65	5	77,179,466	77,352,621	Health	Haptoglobin concentration
T_{TS}	CNVR65	5	77,179,466	77,352,621	Health	Cholesterol level
T_{TS}	CNVR65	5	77,179,466	77,352,621	Meat and Carcass	Inside ham weight
T_{TS}	CNVR65	5	77,179,466	77,352,621	Meat and Carcass	Carcass temperature
T_{TS}	CNVR65	5	77,179,466	77,352,621	Meat and Carcass	Empty body protein linear
T_{TS}	CNVR65	5	77,179,466	77,352,621	Meat and Carcass	subjective abnormal odor
T_{TS}	CNVR65	5	77,179,466	77,352,621	Health	Alkaline phosphatase activity
T_{TS}	CNVR65	5	77,179,466	77,352,621	Meat and Carcass	Meat color
T_{TS}	CNVR65	5	77,179,466	77,352,621	Meat and Carcass	Meat color
T_{TS}	CNVR65	5	77,179,466	77,352,621	Meat and Carcass	Meat color
T_{TS}	CNVR65	5	77,179,466	77,352,621	Meat and Carcass	Meat color
T_{TS}	CNVR65	5	77,179,466	77,352,621	Meat and Carcass	Loin muscle area

T_{TS}	CNVR65	5	77,179,466	77,352,621	Meat and Carcass	Loin weight
T_{TS}	CNVR65	5	77,179,466	77,352,621	Meat and Carcass	Ham weight
T_{TS}	CNVR65	5	77,179,466	77,352,621	Meat and Carcass	Carcass temperature
T_{TS}	CNVR65	5	77,179,466	77,352,621	Meat and Carcass	Loin and ham percentage in carcass
T_{TS}	CNVR65	5	77,179,466	77,352,621	Meat and Carcass	Belly weight
T_{TS}	CNVR65	5	77,179,466	77,352,621	Meat and Carcass	Unsaturated fatty acid content
T_{TS}	CNVR65	5	77,179,466	77,352,621	Meat and Carcass	Saturated fatty acid content
T_{TS}	CNVR65	5	77,179,466	77,352,621	Meat and Carcass	Unsaturated fatty acid content
T_{TS}	CNVR65	5	77,179,466	77,352,621	Meat and Carcass	Carcass length
T_{TS}	CNVR65	5	77,179,466	77,352,621	Meat and Carcass	Biceps brachii length
T_{TS}	CNVR65	5	77,179,466	77,352,621	Meat and Carcass	Backfat at tenth rib
T_{TS}	CNVR65	5	77,179,466	77,352,621	Meat and Carcass	Loin muscle area
T_{TS}	CNVR65	5	77,179,466	77,352,621	Health	Interleukin-2 level
T_{TS}	CNVR65	5	77,179,466	77,352,621	Meat and Carcass	Ham weight
T_{TS}	CNVR65	5	77,179,466	77,352,621	Meat and Carcass	Shear force
T_{TS}	CNVR65	5	77,179,466	77,352,621	Meat and Carcass	Backfat at last lumbar

T_{TS}	CNVR65	5	77,179,466	77,352,621	Meat and Carcass	Backfat at last rib
T_{TS}	CNVR65	5	77,179,466	77,352,621	Meat and Carcass	Carcass length
T_{TS}	CNVR65	5	77,179,466	77,352,621	Health	Interferon-gamma level
T_{TS}	CNVR65	5	77,179,466	77,352,621	Production	Average daily gain
T_{TS}	CNVR65	5	77,179,466	77,352,621	Meat and Carcass	Adipocyte diameter
T_{TS}	CNVR65	5	77,179,466	77,352,621	Health	CSFV antibody level
T_{TS}	CNVR105	11	67,375,641	67,671,825	Meat and Carcass	Backfat at mid-back
T_{TS}	CNVR105	11	67,375,641	67,671,825	Meat and Carcass	Loin muscle area
T_{TS}	CNVR105	11	67,375,641	67,671,825	Meat and Carcass	Meat color
T_{TS}	CNVR105	11	67,375,641	67,671,825	Exterior	Time spent drinking
T_{TS}	CNVR105	11	67,375,641	67,671,825	Health	Body temperature
T_{TS}	CNVR105	11	67,375,641	67,671,825	Health	Eosinophil number
T_{TS}	CNVR105	11	67,375,641	67,671,825	Meat and Carcass	Meat color
T_{TS}	CNVR105	11	67,375,641	67,671,825	Meat and Carcass	Drip loss
T_{TS}	CNVR105	11	67,375,641	67,671,825	Meat and Carcass	Percentage type I fibers
T_{TS}	CNVR105	11	67,375,641	67,671,825	Reproduction	Nonfunctional nipples

T_{TS}	CNVR105	11	67,375,641	67,671,825	Meat and Carcass	Lean meat percentage
T_{TS}	CNVR105	11	67,375,641	67,671,825	Meat and Carcass	Average backfat thickness
T_{TS}	CNVR105	11	67,375,641	67,671,825	Production	Feed intake
T_{TS}	CNVR105	11	67,375,641	67,671,825	Meat and Carcass	Backfat at last rib
T_{TS}	CNVR105	11	67,375,641	67,671,825	Meat and Carcass	Muscle pH decline
T_{TS}	CNVR105	11	67,375,641	67,671,825	Meat and Carcass	Muscle fat content
T_{TS}	CNVR105	11	67,375,641	67,671,825	Meat and Carcass	Muscle moisture percentage
T_{TS}	CNVR105	11	67,375,641	67,671,825	Meat and Carcass	Empty body lipid content
T_{TS}	CNVR105	11	67,375,641	67,671,825	Reproduction	Number of stillborn
T_{TS}	CNVR105	11	67,375,641	67,671,825	Meat and Carcass	Empty body lipid content
T_{TS}	CNVR105	11	67,375,641	67,671,825	Reproduction	Nonfunctional nipples
T_{TS}	CNVR105	11	67,375,641	67,671,825	Health	Toll-like receptor 9 level
T_{TS}	CNVR105	11	67,375,641	67,671,825	Meat and Carcass	Number of ribs
T_{TS}	CNVR105	11	67,375,641	67,671,825	Meat and Carcass	Linoleic acid content
T_{TS}	CNVR105	11	67,375,641	67,671,825	Health	CD4-positive leukocyte percentage
T_{TS}	CNVR105	11	67,375,641	67,671,825	Meat and Carcass	Palmitic acid content

T_{TS}	CNVR109	12	60,100	1,998,701	Meat and Carcass	Backfat at tenth rib
T_{TS}	CNVR109	12	60,100	1,998,701	Meat and Carcass	Backfat at mid-back
T_{TS}	CNVR109	12	60,100	1,998,701	Exterior	Ear size
T_{TS}	CNVR109	12	60,100	1,998,701	Meat and Carcass	Backfat at last rib
T_{TS}	CNVR109	12	60,100	1,998,701	Health	Interleukin-10 level
T_{TS}	CNVR109	12	60,100	1,998,701	Health	Toll-like receptor 9 level
T_{TS}	CNVR109	12	60,100	1,998,701	Exterior	Vertebra number
T_{TS}	CNVR109	12	60,100	1,998,701	Exterior	Thoracic vertebra number
T_{TS}	CNVR109	12	60,100	1,998,701	Health	Actinobacillus pleuropneumoniae susceptibility
T_{TS}	CNVR109	12	60,100	1,998,701	Health	Actinobacillus pleuropneumoniae susceptibility
T_{TS}	CNVR109	12	60,100	1,998,701	Meat and Carcass	Myristic acid content
T_{TS}	CNVR109	12	60,100	1,998,701	Meat and Carcass	Myristic acid content
T_{TS}	CNVR109	12	60,100	1,998,701	Meat and Carcass	Myristic acid content
T_{TS}	CNVR109	12	60,100	1,998,701	Meat and Carcass	Myristic acid content
T_{TS}	CNVR109	12	60,100	1,998,701	Meat and Carcass	Myristic acid content
T_{TS}	CNVR109	12	60,100	1,998,701	Production	Feed intake

T_{TS}	CNVR109	12	60,100	1,998,701	Meat and Carcass	Arachidic acid content
T_{TS}	CNVR109	12	60,100	1,998,701	Meat and Carcass	Palmitic acid to myristic acid ratio
T_{TS}	CNVR109	12	60,100	1,998,701	Meat and Carcass	Myristic acid content
T_{TS}	CNVR109	12	60,100	1,998,701	Meat and Carcass	Palmitic acid to myristic acid ratio
T_{TS}	CNVR109	12	60,100	1,998,701	Meat and Carcass	Myristic acid content
T_{TS}	CNVR109	12	60,100	1,998,701	Meat and Carcass	Myristic acid content
T_{TS}	CNVR109	12	60,100	1,998,701	Meat and Carcass	Myristic acid content
T_{TS}	CNVR109	12	60,100	1,998,701	Meat and Carcass	Intramuscular fat content
T_{TS}	CNVR109	12	60,100	1,998,701	Meat and Carcass	Myristic acid content
T_{TS}	CNVR109	12	60,100	1,998,701	Meat and Carcass	Palmitoleic acid content
T_{TS}	CNVR109	12	60,100	1,998,701	Meat and Carcass	Stearic acid content
T_{TS}	CNVR109	12	60,100	1,998,701	Meat and Carcass	cis-Vaccenic acid content
T_{TS}	CNVR109	12	60,100	1,998,701	Meat and Carcass	Arachidic acid content
T_{TS}	CNVR109	12	60,100	1,998,701	Meat and Carcass	Dihomo-gamma-linolenic acid content
T_{TS}	CNVR109	12	60,100	1,998,701	Meat and Carcass	Arachidonic acid content
T_{TS}	CNVR109	12	60,100	1,998,701	Meat and Carcass	Myristic acid content

T_{TS}	CNVR109	12	60,100	1,998,701	Meat and Carcass	Drip loss
T_{TS}	CNVR109	12	60,100	1,998,701	Meat and Carcass	Meat color
T_{TS}	CNVR109	12	60,100	1,998,701	Meat and Carcass	Muscle pH
T_{TS}	CNVR109	12	60,100	1,998,701	Meat and Carcass	Muscle pH
T_{TS}	CNVR109	12	60,100	1,998,701	Meat and Carcass	Dressing percentage
T_{TS}	CNVR109	12	60,100	1,998,701	Meat and Carcass	Average backfat thickness
T_{TS}	CNVR109	12	60,100	1,998,701	Meat and Carcass	Loin weight
T_{TS}	CNVR109	12	60,100	1,998,701	Production	Average daily gain
T_{TS}	CNVR109	12	60,100	1,998,701	Production	Feed conversion ratio
T_{TS}	CNVR109	12	60,100	1,998,701	Production	Feed intake
T_{TS}	CNVR109	12	60,100	1,998,701	Production	Age at slaughter
T_{TS}	CNVR109	12	60,100	1,998,701	Meat and Carcass	Palmitic acid to myristic acid ratio
T_{TS}	CNVR109	12	60,100	1,998,701	Meat and Carcass	Oleic acid to palmitoleic acid ratio
T_{TS}	CNVR109	12	60,100	1,998,701	Meat and Carcass	Muscle pH
T_{TS}	CNVR109	12	60,100	1,998,701	Meat and Carcass	Meat color
T_{TS}	CNVR109	12	60,100	1,998,701	Meat and Carcass	Palmitoleic acid content

T_{TS}	CNVR109	12	60,100	1,998,701	Meat and Carcass	Palmitic acid content
T_{TS}	CNVR109	12	60,100	1,998,701	Meat and Carcass	Palmitic acid content
T_{TS}	CNVR109	12	60,100	1,998,701	Meat and Carcass	Palmitoleic acid content
T_{TS}	CNVR109	12	60,100	1,998,701	Meat and Carcass	Palmitoleic acid to palmitic acid ratio
T_{TS}	CNVR109	12	60,100	1,998,701	Meat and Carcass	Oleic acid to palmitoleic acid ratio
T_{TS}	CNVR109	12	60,100	1,998,701	Meat and Carcass	Palmitic acid content
T_{TS}	CNVR109	12	60,100	1,998,701	Meat and Carcass	Palmitoleic acid content
T_{TS}	CNVR109	12	60,100	1,998,701	Meat and Carcass	Palmitoleic acid to palmitic acid ratio
T_{TS}	CNVR109	12	60,100	1,998,701	Meat and Carcass	Oleic acid to palmitoleic acid ratio
T_{TS}	CNVR109	12	60,100	1,998,701	Meat and Carcass	Oleic acid content
T_{TS}	CNVR109	12	60,100	1,998,701	Meat and Carcass	Oleic acid content
T_{TS}	CNVR109	12	60,100	1,998,701	Meat and Carcass	Myristic acid content
T_{TS}	CNVR109	12	60,100	1,998,701	Meat and Carcass	Myristic acid content
T_{TS}	CNVR109	12	60,100	1,998,701	Meat and Carcass	Palmitic acid to myristic acid ratio
T_{TS}	CNVR109	12	60,100	1,998,701	Meat and Carcass	Oleic acid content
T_{TS}	CNVR109	12	60,100	1,998,701	Meat and Carcass	Monounsaturated fatty acid content

T_{TS}	CNVR109	12	60,100	1,998,701	Meat and Carcass	Monounsaturated fatty acid to saturated fatty acid ratio
T_{TS}	CNVR109	12	60,100	1,998,701	Meat and Carcass	Fatty acid atherogenic index
T_{TS}	CNVR109	12	60,100	1,998,701	Meat and Carcass	Fatty acid atherogenic index
T_{TS}	CNVR109	12	60,100	1,998,701	Meat and Carcass	Double-bond index
T_{TS}	CNVR109	12	60,100	1,998,701	Meat and Carcass	Unsaturated index
T_{TS}	CNVR109	12	60,100	1,998,701	Meat and Carcass	Double-bond index
T_{TS}	CNVR109	12	60,100	1,998,701	Meat and Carcass	Unsaturated index
T_{TS}	CNVR109	12	60,100	1,998,701	Meat and Carcass	Average chain length
T_{TS}	CNVR109	12	60,100	1,998,701	Meat and Carcass	Stearic acid to palmitic acid ratio
T_{TS}	CNVR109	12	60,100	1,998,701	Meat and Carcass	Average chain length
T_{TS}	CNVR109	12	60,100	1,998,701	Meat and Carcass	Stearic acid to palmitic acid ratio
T_{TS}	CNVR109	12	60,100	1,998,701	Meat and Carcass	Eicosadienoic acid content
T_{TS}	CNVR109	12	60,100	1,998,701	Meat and Carcass	Eicosadienoic acid content
T_{TS}	CNVR109	12	60,100	1,998,701	Reproduction	Teat number
T_{TS}	CNVR109	12	60,100	1,998,701	Meat and Carcass	Myristic acid content
T_{TS}	CNVR109	12	60,100	1,998,701	Meat and Carcass	Palmitic acid content

T_{TS}	CNVR109	12	60,100	1,998,701	Meat and Carcass	Palmitoleic acid content
T_{TS}	CNVR109	12	60,100	1,998,701	Meat and Carcass	Oleic acid content
T_{TS}	CNVR109	12	60,100	1,998,701	Meat and Carcass	cis-11-Eicosenoic acid content
T_{TS}	CNVR109	12	60,100	1,998,701	Health	Interferon-gamma to interleukin-10 ratio
T_{TS}	CNVR109	12	60,100	1,998,701	Meat and Carcass	Palmitic acid to myristic acid ratio
T_{TS}	CNVR109	12	60,100	1,998,701	Meat and Carcass	Palmitic acid to myristic acid ratio
T_{TS}	CNVR109	12	60,100	1,998,701	Health	Interferon-gamma to interleukin-10 ratio
T_{TS}	CNVR109	12	60,100	1,998,701	Reproduction	Age at puberty
T_{TS}	CNVR109	12	60,100	1,998,701	Meat and Carcass	Palmitic acid to myristic acid ratio
T_{TS}	CNVR134	14	38,219,290	38,645,949	Meat and Carcass	Meat color
T_{TS}	CNVR134	14	38,219,290	38,645,949	Meat and Carcass	Percentage type I fibers
T_{TS}	CNVR134	14	38,219,290	38,645,949	Meat and Carcass	Percentage type IIb fibers
T_{TS}	CNVR134	14	38,219,290	38,645,949	Meat and Carcass	Percentage type I fibers
T_{TS}	CNVR134	14	38,219,290	38,645,949	Meat and Carcass	Meat color
T_{TS}	CNVR134	14	38,219,290	38,645,949	Production	Feed intake
T_{TS}	CNVR134	14	38,219,290	38,645,949	Meat and Carcass	backfat above muscle dorsi

T_{TS}	CNVR134	14	38,219,290	38,645,949	Health	C3c concentration
T_{TS}	CNVR134	14	38,219,290	38,645,949	Health	Haptoglobin concentration
T_{TS}	CNVR134	14	38,219,290	38,645,949	Meat and Carcass	Stearic acid content
T_{TS}	CNVR134	14	38,219,290	38,645,949	Meat and Carcass	Linoleic acid content
T_{TS}	CNVR134	14	38,219,290	38,645,949	Meat and Carcass	Backfat at last rib
T_{TS}	CNVR134	14	38,219,290	38,645,949	Exterior	Osteochondrosis score
T_{TS}	CNVR134	14	38,219,290	38,645,949	Meat and Carcass	Meat color
T_{TS}	CNVR134	14	38,219,290	38,645,949	Meat and Carcass	Shear force
T_{TS}	CNVR134	14	38,219,290	38,645,949	Meat and Carcass	Shear force at first peak
T_{TS}	CNVR134	14	38,219,290	38,645,949	Meat and Carcass	Shear force at first peak
T_{TS}	CNVR134	14	38,219,290	38,645,949	Meat and Carcass	Shear force at first peak
T_{TS}	CNVR134	14	38,219,290	38,645,949	Meat and Carcass	Loin muscle area
T_{TS}	CNVR134	14	38,219,290	38,645,949	Meat and Carcass	Abdominal fat weight
T_{TS}	CNVR134	14	38,219,290	38,645,949	Meat and Carcass	Leaf fat weight
T_{TS}	CNVR134	14	38,219,290	38,645,949	Meat and Carcass	Intestinal fat weight
T_{TS}	CNVR134	14	38,219,290	38,645,949	Health	Creatinine level

T_{TS}	CNVR134	14	38,219,290	38,645,949	Health	Creatinine level
T_{TS}	CNVR134	14	38,219,290	38,645,949	Health	Potassium level
T_{TS}	CNVR134	14	38,219,290	38,645,949	Health	Calcium level
T_{TS}	CNVR134	14	38,219,290	38,645,949	Meat and Carcass	Adipocyte diameter
T_{TS}	CNVR134	14	38,219,290	38,645,949	Meat and Carcass	Average instron (star probe) force
T_{TS}	CNVR134	14	38,219,290	38,645,949	Meat and Carcass	skatole, sensory panel
T_{TS}	CNVR134	14	38,219,290	38,645,949	Meat and Carcass	subjective boar flavor in lean
T_{TS}	CNVR134	14	38,219,290	38,645,949	Meat and Carcass	subjective boar flavor in fat
T_{TS}	CNVR134	14	38,219,290	38,645,949	Meat and Carcass	subjective abnormal odor
T_{TS}	CNVR134	14	38,219,290	38,645,949	Exterior	Front leg conformation
T_{TS}	CNVR134	14	38,219,290	38,645,949	Meat and Carcass	Meat color
T_{TS}	CNVR134	14	38,219,290	38,645,949	Meat and Carcass	Meat color
T_{TS}	CNVR134	14	38,219,290	38,645,949	Meat and Carcass	Trimmed wholesale product / live weight
T_{TS}	CNVR134	14	38,219,290	38,645,949	Meat and Carcass	Loin muscle area
T_{TS}	CNVR134	14	38,219,290	38,645,949	Meat and Carcass	Diameter of type IIa muscle fibers
T_{TS}	CNVR134	14	38,219,290	38,645,949	Meat and Carcass	Percentage type IIb fibers

T_{TS}	CNVR134	14	38,219,290	38,645,949	Meat and Carcass	Diameter of type IIb muscle fibers
T_{TS}	CNVR134	14	38,219,290	38,645,949	Reproduction	Number of stillborn
T_{TS}	CNVR134	14	38,219,290	38,645,949	Reproduction	Reproductive tract weight
T_{TS}	CNVR134	14	38,219,290	38,645,949	Reproduction	Total number born alive
T_{TS}	CNVR134	14	38,219,290	38,645,949	Reproduction	Total number born alive
T_{TS}	CNVR134	14	38,219,290	38,645,949	Reproduction	Total number born alive
T_{TS}	CNVR134	14	38,219,290	38,645,949	Meat and Carcass	Trimmed wholesale product / carcass weight
T_{TS}	CNVR134	14	38,219,290	38,645,949	Meat and Carcass	Backfat at last lumbar
T_{TS}	CNVR134	14	38,219,290	38,645,949	Meat and Carcass	Average backfat thickness
T_{TS}	CNVR134	14	38,219,290	38,645,949	Exterior	Coping behavior
T_{TS}	CNVR134	14	38,219,290	38,645,949	Health	Melanoma susceptibility
T_{TS}	CNVR138	14	74,176,726	74,990,114	Meat and Carcass	Percentage type I fibers
T_{TS}	CNVR138	14	74,176,726	74,990,114	Meat and Carcass	Percentage type IIb fibers
T_{TS}	CNVR138	14	74,176,726	74,990,114	Meat and Carcass	Percentage type I fibers
T_{TS}	CNVR138	14	74,176,726	74,990,114	Production	Feed intake
T_{TS}	CNVR138	14	74,176,726	74,990,114	Meat and Carcass	backfat above muscle dorsi

T_{TS}	CNVR138	14	74,176,726	74,990,114	Health	C3c concentration
T_{TS}	CNVR138	14	74,176,726	74,990,114	Health	Haptoglobin concentration
T_{TS}	CNVR138	14	74,176,726	74,990,114	Exterior	Osteochondrosis score
T_{TS}	CNVR138	14	74,176,726	74,990,114	Meat and Carcass	Meat color
T_{TS}	CNVR138	14	74,176,726	74,990,114	Meat and Carcass	Shear force
T_{TS}	CNVR138	14	74,176,726	74,990,114	Meat and Carcass	Shear force at first peak
T_{TS}	CNVR138	14	74,176,726	74,990,114	Meat and Carcass	Shear force at first peak
T_{TS}	CNVR138	14	74,176,726	74,990,114	Meat and Carcass	Shear force at first peak
T_{TS}	CNVR138	14	74,176,726	74,990,114	Meat and Carcass	Loin muscle area
T_{TS}	CNVR138	14	74,176,726	74,990,114	Meat and Carcass	Abdominal fat weight
T_{TS}	CNVR138	14	74,176,726	74,990,114	Meat and Carcass	Intestinal fat weight
T_{TS}	CNVR138	14	74,176,726	74,990,114	Meat and Carcass	Average instron (star probe) force
T_{TS}	CNVR138	14	74,176,726	74,990,114	Meat and Carcass	Carcass weight (hot)
T_{TS}	CNVR138	14	74,176,726	74,990,114	Production	Body weight
T_{TS}	CNVR138	14	74,176,726	74,990,114	Meat and Carcass	Ham percentage
T_{TS}	CNVR138	14	74,176,726	74,990,114	Meat and Carcass	Fat-cuts percentage

T_{TS}	CNVR138	14	74,176,726	74,990,114	Meat and Carcass	Dressing percentage
T_{TS}	CNVR138	14	74,176,726	74,990,114	Meat and Carcass	Ham percentage
T_{TS}	CNVR138	14	74,176,726	74,990,114	Meat and Carcass	Carcass length
T_{TS}	CNVR138	14	74,176,726	74,990,114	Meat and Carcass	Loin muscle area
T_{TS}	CNVR138	14	74,176,726	74,990,114	Meat and Carcass	Shoulder meat weight
T_{TS}	CNVR138	14	74,176,726	74,990,114	Meat and Carcass	Carcass weight (cold)
T_{TS}	CNVR138	14	74,176,726	74,990,114	Meat and Carcass	Loin and neck meat weight
T_{TS}	CNVR138	14	74,176,726	74,990,114	Meat and Carcass	Ham weight
T_{TS}	CNVR138	14	74,176,726	74,990,114	Meat and Carcass	Shoulder subcutaneous fat thickness
T_{TS}	CNVR138	14	74,176,726	74,990,114	Meat and Carcass	Average backfat thickness
T_{TS}	CNVR138	14	74,176,726	74,990,114	Meat and Carcass	Backfat at last rib
T_{TS}	CNVR138	14	74,176,726	74,990,114	Production	Feed intake
T_{TS}	CNVR138	14	74,176,726	74,990,114	Meat and Carcass	Head weight
T_{TS}	CNVR138	14	74,176,726	74,990,114	Meat and Carcass	External fat on ham
T_{TS}	CNVR138	14	74,176,726	74,990,114	Meat and Carcass	Heart weight
T_{TS}	CNVR138	14	74,176,726	74,990,114	Meat and Carcass	Backfat at last rib

T_{TS}	CNVR138	14	74,176,726	74,990,114	Meat and Carcass	Ham weight
T_{TS}	CNVR138	14	74,176,726	74,990,114	Meat and Carcass	Carcass length
T_{TS}	CNVR138	14	74,176,726	74,990,114	Meat and Carcass	Meat color
T_{TS}	CNVR138	14	74,176,726	74,990,114	Meat and Carcass	Semimembranosus angle
T_{TS}	CNVR138	14	74,176,726	74,990,114	Meat and Carcass	Meat color
T_{TS}	CNVR138	14	74,176,726	74,990,114	Meat and Carcass	Total shear work
T_{TS}	CNVR138	14	74,176,726	74,990,114	Health	Salmonella count in liver and spleen
T_{TS}	CNVR138	14	74,176,726	74,990,114	Health	Salmonella count in liver
T_{TS}	CNVR138	14	74,176,726	74,990,114	Health	Salmonella count in spleen
T_{TS}	CNVR138	14	74,176,726	74,990,114	Meat and Carcass	Adipocyte diameter
T_{TS}	CNVR138	14	74,176,726	74,990,114	Meat and Carcass	Adipocyte diameter
T_{TS}	CNVR138	14	74,176,726	74,990,114	Meat and Carcass	Adipocyte diameter
T_{TS}	CNVR138	14	74,176,726	74,990,114	Meat and Carcass	Fat protein content
T_{TS}	CNVR138	14	74,176,726	74,990,114	Meat and Carcass	Muscle pH
T_{TS}	CNVR138	14	74,176,726	74,990,114	Meat and Carcass	Meat color
T_{TS}	CNVR138	14	74,176,726	74,990,114	Meat and Carcass	Shoulder weight, Boston

T_{TS}	CNVR138	14	74,176,726	74,990,114	Exterior	Cervical vertebra length
T_{TS}	CNVR138	14	74,176,726	74,990,114	Health	Aspartate aminotransferase activity
T_{TS}	CNVR138	14	74,176,726	74,990,114	Health	Aspartate aminotransferase activity
T_{TS}	CNVR138	14	74,176,726	74,990,114	Health	Aspartate aminotransferase activity
T_{TS}	CNVR138	14	74,176,726	74,990,114	Health	Aspartate aminotransferase activity
T_{TS}	CNVR138	14	74,176,726	74,990,114	Health	Aspartate aminotransferase activity
T_{TS}	CNVR138	14	74,176,726	74,990,114	Health	Aspartate aminotransferase activity
T_{TS}	CNVR138	14	74,176,726	74,990,114	Health	Aspartate aminotransferase activity
T_{TS}	CNVR138	14	74,176,726	74,990,114	Health	Aspartate aminotransferase activity
T_{TS}	CNVR138	14	74,176,726	74,990,114	Health	Aspartate aminotransferase activity
T_{TS}	CNVR138	14	74,176,726	74,990,114	Health	Aspartate aminotransferase activity
T_{TS}	CNVR138	14	74,176,726	74,990,114	Health	Aspartate aminotransferase activity
T_{TS}	CNVR138	14	74,176,726	74,990,114	Health	Aspartate aminotransferase activity
T_{TS}	CNVR138	14	74,176,726	74,990,114	Health	Aspartate aminotransferase activity
T_{TS}	CNVR138	14	74,176,726	74,990,114	Health	Aspartate aminotransferase activity
T_{TS}	CNVR138	14	74,176,726	74,990,114	Health	Mean corpuscular hemoglobin content

T_{TS}	CNVR138	14	74,176,726	74,990,114	Health	Mean corpuscular hemoglobin concentration
T_{TS}	CNVR138	14	74,176,726	74,990,114	Health	Red cell distribution width
T_{TS}	CNVR138	14	74,176,726	74,990,114	Health	Granular leukocyte to lymphocyte ratio
T_{TS}	CNVR138	14	74,176,726	74,990,114	Meat and Carcass	Percentage type I fibers
T_{TS}	CNVR138	14	74,176,726	74,990,114	Meat and Carcass	Shoulder weight
T_{TS}	CNVR138	14	74,176,726	74,990,114	Meat and Carcass	Ham meat weight
T_{TS}	CNVR138	14	74,176,726	74,990,114	Meat and Carcass	Stearic acid content
T_{TS}	CNVR138	14	74,176,726	74,990,114	Health	Basophil number
T_{TS}	CNVR138	14	74,176,726	74,990,114	Health	Basophil number
T_{TS}	CNVR138	14	74,176,726	74,990,114	Health	Basophil number
T_{TS}	CNVR138	14	74,176,726	74,990,114	Health	Basophil number
T_{TS}	CNVR138	14	74,176,726	74,990,114	Health	Basophil number
T_{TS}	CNVR138	14	74,176,726	74,990,114	Health	Basophil number
T_{TS}	CNVR138	14	74,176,726	74,990,114	Health	Periweaning failure to thrive syndrome
T_{TS}	CNVR138	14	74,176,726	74,990,114	Health	Basophil number
T_{TS}	CNVR138	14	74,176,726	74,990,114	Health	Basophil number

T_{TS}	CNVR138	14	74,176,726	74,990,114	Production	Average daily gain
T_{TS}	CNVR138	14	74,176,726	74,990,114	Health	Basophil number
T_{TS}	CNVR138	14	74,176,726	74,990,114	Health	Periweaning failure to thrive syndrome
T_{TS}	CNVR138	14	74,176,726	74,990,114	Health	Basophil number
T_{TS}	CNVR147	14	140,199,680	140,419,493	Meat and Carcass	Meat color
T_{TS}	CNVR147	14	140,199,680	140,419,493	Meat and Carcass	Thawing loss
T_{TS}	CNVR147	14	140,199,680	140,419,493	Meat and Carcass	Meat color
T_{TS}	CNVR147	14	140,199,680	140,419,493	Meat and Carcass	Shear force
T_{TS}	CNVR147	14	140,199,680	140,419,493	Meat and Carcass	Shear force
T_{TS}	CNVR147	14	140,199,680	140,419,493	Meat and Carcass	Estimated carcass lean content
T_{TS}	CNVR147	14	140,199,680	140,419,493	Meat and Carcass	Loin muscle area
T_{TS}	CNVR147	14	140,199,680	140,419,493	Meat and Carcass	Muscle pH
T_{TS}	CNVR147	14	140,199,680	140,419,493	Meat and Carcass	Estimated carcass lean content
T_{TS}	CNVR147	14	140,199,680	140,419,493	Meat and Carcass	Loin muscle depth
T_{TS}	CNVR147	14	140,199,680	140,419,493	Meat and Carcass	Loin muscle area
T_{TS}	CNVR147	14	140,199,680	140,419,493	Meat and Carcass	Loin muscle area

T_{TS}	CNVR147	14	140,199,680	140,419,493	Health	Toll-like receptor 9 level
T_{TS}	CNVR147	14	140,199,680	140,419,493	Meat and Carcass	Loin weight
T_{TS}	CNVR147	14	140,199,680	140,419,493	Meat and Carcass	Belly weight
T_{TS}	CNVR147	14	140,199,680	140,419,493	Meat and Carcass	Belly weight
T_{TS}	CNVR147	14	140,199,680	140,419,493	Meat and Carcass	Number of muscle fibers per unit area
T_{TS}	CNVR147	14	140,199,680	140,419,493	Meat and Carcass	Total muscle fiber number
T_{TS}	CNVR147	14	140,199,680	140,419,493	Meat and Carcass	Diameter of type IIa muscle fibers
T_{TS}	CNVR147	14	140,199,680	140,419,493	Meat and Carcass	Diameter of type IIb muscle fibers
T_{TS}	CNVR167	16	10,588,133	11,083,680	Meat and Carcass	Muscle conductivity
T_{TS}	CNVR167	16	10,588,133	11,083,680	Meat and Carcass	Muscle conductivity
T_{TS}	CNVR167	16	10,588,133	11,083,680	Meat and Carcass	Muscle conductivity
T_{TS}	CNVR167	16	10,588,133	11,083,680	Reproduction	Teat number
T_{TS}	CNVR167	16	10,588,133	11,083,680	Production	Feed conversion ratio
T_{TS}	CNVR167	16	10,588,133	11,083,680	Production	Feed intake
T_{TS}	CNVR167	16	10,588,133	11,083,680	Meat and Carcass	backfat above muscle dorsi
T_{TS}	CNVR167	16	10,588,133	11,083,680	Meat and Carcass	Shoulder subcutaneous fat thickness

T_{TS}	CNVR167	16	10,588,133	11,083,680	Meat and Carcass	Belly meat content
T_{TS}	CNVR167	16	10,588,133	11,083,680	Meat and Carcass	Estimated carcass lean content
T_{TS}	CNVR167	16	10,588,133	11,083,680	Meat and Carcass	Cooking loss
T_{TS}	CNVR167	16	10,588,133	11,083,680	Meat and Carcass	Shear force
T_{TS}	CNVR167	16	10,588,133	11,083,680	Reproduction	Total number born alive
T_{TS}	CNVR167	16	10,588,133	11,083,680	Exterior	Hind leg conformation
T_{TS}	CNVR167	16	10,588,133	11,083,680	Health	C3c concentration
T_{TS}	CNVR167	16	10,588,133	11,083,680	Health	C3c concentration
T_{TS}	CNVR167	16	10,588,133	11,083,680	Health	Change in Mycoplasma hyopneumoniae antibody titer
T_{TS}	CNVR167	16	10,588,133	11,083,680	Meat and Carcass	Carcass weight (hot)
T_{TS}	CNVR167	16	10,588,133	11,083,680	Meat and Carcass	Carcass weight (hot)
T_{TS}	CNVR167	16	10,588,133	11,083,680	Health	Toll-like receptor 9 level
T_{TS}	CNVR167	16	10,588,133	11,083,680	Health	HDL/LDL ratio
T_{TS}	CNVR167	16	10,588,133	11,083,680	Meat and Carcass	Drip loss
T_{TS}	CNVR167	16	10,588,133	11,083,680	Health	Actinobacillus pleuropneumoniae susceptibility
T_{TS}	CNVR167	16	10,588,133	11,083,680	Meat and Carcass	Meat color

T_{TS}	CNVR167	16	10,588,133	11,083,680	Health	Segmented neutrophil number
T_{TS}	CNVR167	16	10,588,133	11,083,680	Health	Interferon-gamma to interleukin-10 ratio
T_{TS}	CNVR167	16	10,588,133	11,083,680	Health	CD4-positive, CD8-positive leukocyte percentage
T_{TS}	CNVR167	16	10,588,133	11,083,680	Exterior	Front feet conformation
T_{TS}	CNVR167	16	10,588,133	11,083,680	Meat and Carcass	Cis-11-Eicosenoic acid to arachidic acid ratio
T_{TS}	CNVR167	16	10,588,133	11,083,680	Health	Mean corpuscular hemoglobin concentration
T_{TS}	CNVR167	16	10,588,133	11,083,680	Meat and Carcass	Bacon depth
T_{TS}	CNVR167	16	10,588,133	11,083,680	Meat and Carcass	Backfat at last lumbar
T_{TS}	CNVR167	16	10,588,133	11,083,680	Meat and Carcass	Meat color
T_{TS}	CNVR167	16	10,588,133	11,083,680	Meat and Carcass	Lung weight
T_{TS}	CNVR167	16	10,588,133	11,083,680	Meat and Carcass	Cooking loss
T_{TS}	CNVR167	16	10,588,133	11,083,680	Meat and Carcass	Heart weight
T_{V16h}	CNVR133	14	16,993,535	17,333,398	Meat and Carcass	Meat color
T_{V16h}	CNVR133	14	16,993,535	17,333,398	Meat and Carcass	Percentage type I fibers
T_{V16h}	CNVR133	14	16,993,535	17,333,398	Meat and Carcass	Percentage type IIb fibers
T_{V16h}	CNVR133	14	16,993,535	17,333,398	Meat and Carcass	Percentage type I fibers

T_{V16h}	CNVR133	14	16,993,535	17,333,398	Meat and Carcass	Marbling
T_{V16h}	CNVR133	14	16,993,535	17,333,398	Meat and Carcass	Meat color
T_{V16h}	CNVR133	14	16,993,535	17,333,398	Meat and Carcass	indole, laboratory
T_{V16h}	CNVR133	14	16,993,535	17,333,398	Meat and Carcass	androstenone, sensory panel
T_{V16h}	CNVR133	14	16,993,535	17,333,398	Production	Feed intake
T_{V16h}	CNVR133	14	16,993,535	17,333,398	Meat and Carcass	backfat above muscle dorsi
T_{V16h}	CNVR133	14	16,993,535	17,333,398	Exterior	Front feet conformation
T_{V16h}	CNVR133	14	16,993,535	17,333,398	Exterior	Hind feet conformation
T_{V16h}	CNVR133	14	16,993,535	17,333,398	Health	C3c concentration
T_{V16h}	CNVR133	14	16,993,535	17,333,398	Health	Haptoglobin concentration
T_{V16h}	CNVR133	14	16,993,535	17,333,398	Meat and Carcass	Stearic acid content
T_{V16h}	CNVR133	14	16,993,535	17,333,398	Meat and Carcass	Linoleic acid content
T_{V16h}	CNVR133	14	16,993,535	17,333,398	Meat and Carcass	Backfat at last rib
T_{V16h}	CNVR133	14	16,993,535	17,333,398	Exterior	Osteochondrosis score
T_{V16h}	CNVR133	14	16,993,535	17,333,398	Health	CD4-negative, CD8-positive leukocyte percentage
T_{V16h}	CNVR133	14	16,993,535	17,333,398	Meat and Carcass	Meat color

T_{V16h}	CNVR133	14	16,993,535	17,333,398	Meat and Carcass	Shear force
T_{V16h}	CNVR133	14	16,993,535	17,333,398	Meat and Carcass	Shear force at first peak
T_{V16h}	CNVR133	14	16,993,535	17,333,398	Meat and Carcass	Shear force at first peak
T_{V16h}	CNVR133	14	16,993,535	17,333,398	Meat and Carcass	Shear force at first peak
T_{V16h}	CNVR133	14	16,993,535	17,333,398	Exterior	rhinitis
T_{V16h}	CNVR133	14	16,993,535	17,333,398	Meat and Carcass	Loin muscle area
T_{V16h}	CNVR133	14	16,993,535	17,333,398	Meat and Carcass	Abdominal fat weight
T_{V16h}	CNVR133	14	16,993,535	17,333,398	Meat and Carcass	Leaf fat weight
T_{V16h}	CNVR133	14	16,993,535	17,333,398	Health	Phagocytic activity
T_{V16h}	CNVR133	14	16,993,535	17,333,398	Exterior	Anal atresia
T_{V16h}	CNVR133	14	16,993,535	17,333,398	Meat and Carcass	Intramuscular fat content
T_{V16h}	CNVR133	14	16,993,535	17,333,398	Meat and Carcass	Intramuscular fat content

753

754 **Table S7.** Enriched QTL for CNVRs associated with physiological and anatomical indicators of heat stress response

Trait	QTL	N QTLs	Total annotated QTLs	P-value	QTL type
T_{ES}	Interleukin-8 level	3	54	0.005113	Health
T_{ES}	Muscle pH	7	54	0.004653	Meat and Carcass
T_{ES}	Shear force	4	54	0.005113	Meat and Carcass
T_{ES}	Splay leg	2	54	0.001732	Exterior
T_{RS}	Abdominal fat weight	2	129	0.04291	Meat and Carcass
T_{RS}	Arachidonic acid content	3	129	0.002237	Meat and Carcass
T_{RS}	Average backfat thickness	10	129	0.001059	Meat and Carcass
T_{RS}	Backfat at last lumbar	3	129	0.013804	Meat and Carcass
T_{RS}	Backfat at last rib	5	129	0.024157	Meat and Carcass
T_{RS}	Backfat percentage	1	129	0.033143	Meat and Carcass
T_{RS}	Bone mineral content	1	129	0.024157	Production
T_{RS}	C3c concentration	3	129	0.003148	Health

T_{RS}	Carcass weight (hot)	3	129	0.024609	Meat and Carcass
T_{RS}	Cutlet weight	1	129	0.024157	Meat and Carcass
T_{RS}	Fatty acid C20:3 to C18:2 ratio	2	129	0.000384	Meat and Carcass
T_{RS}	Heart weight	2	129	0.044607	Meat and Carcass
T_{RS}	Hemolytic complement activity (alternative pathway)	3	129	0.000355	Health
T_{RS}	Lean meat + bone in back	1	129	0.044607	Meat and Carcass
T_{RS}	Lean meat + bone in ham + back	2	129	0.000861	Meat and Carcass
T_{RS}	Linoleic acid content	3	129	0.025304	Meat and Carcass
T_{RS}	Loin weight	3	129	0.026845	Meat and Carcass
T_{RS}	Neck fat weight	1	129	0.024157	Meat and Carcass
T_{RS}	Obesity index	1	129	0	Meat and Carcass
T_{RS}	Oxygen saturation	1	129	0.033143	Health
T_{RS}	Shear firmness	1	129	0.024157	Meat and Carcass
T_{TS}	Adipocyte diameter	6	581	0.007984	Meat and Carcass
T_{TS}	Arachidonic acid content	4	581	0.009643	Meat and Carcass
T_{TS}	Aspartate aminotransferase activity	14	581	5.75E-18	Health

T_{TS}	Average backfat thickness	25	581	0.000379	Meat and Carcass
T_{TS}	backfat above muscle dorsi	4	581	0.007984	Meat and Carcass
T_{TS}	Backfat at last lumbar	8	581	0.000177	Meat and Carcass
T_{TS}	Backfat at last rib	13	581	0.007984	Meat and Carcass
T_{TS}	Backfat at mid-back	6	581	0.000365	Meat and Carcass
T_{TS}	Basophil number	10	581	0.000274	Health
T_{TS}	C3c concentration	6	581	0.000379	Health
T_{TS}	Carcass weight (hot)	8	581	0.001814	Meat and Carcass
T_{TS}	Diameter of type IIa muscle fibers	2	581	0.034131	Meat and Carcass
T_{TS}	Diameter of type IIb muscle fibers	2	581	0.041336	Meat and Carcass
T_{TS}	Estimated carcass lean content	4	581	0.008702	Meat and Carcass
T_{TS}	Fatty acid C20:3 to C18:2 ratio	2	581	0.003661	Meat and Carcass
T_{TS}	Ham meat weight	3	581	0.013231	Meat and Carcass
T_{TS}	Ham percentage	3	581	0.007895	Meat and Carcass
T_{TS}	Heart weight	5	581	0.007895	Meat and Carcass
T_{TS}	Hemolytic complement activity (alternative pathway)	3	581	0.007895	Health

T_{TS}	Interferon-gamma to interleukin-10 ratio	3	581	0.004661	Health
T_{TS}	Lean meat + bone in ham + back	2	581	0.007895	Meat and Carcass
T_{TS}	Linoleic acid content	11	581	1.54E-05	Meat and Carcass
T_{TS}	Loin and ham percentage in carcass	2	581	0.041336	Meat and Carcass
T_{TS}	Loin muscle area	16	581	0.017793	Meat and Carcass
T_{TS}	Loin weight	8	581	0.002929	Meat and Carcass
T_{TS}	Meat color	27	581	0.019621	Meat and Carcass
T_{TS}	Monounsaturated fatty acid to polyunsaturated fatty acid ratio	5	581	0.001246	Meat and Carcass
T_{TS}	Myristic acid content	16	581	1.24E-10	Meat and Carcass
T_{TS}	Obesity index	1	581	0	Meat and Carcass
T_{TS}	Palmitic acid to myristic acid ratio	7	581	3.14E-06	Meat and Carcass
T_{TS}	Percentage type I fibers	4	581	0.003661	Meat and Carcass
T_{TS}	Polyunsaturated fatty acid content	5	581	0.034903	Meat and Carcass
T_{TS}	PRRS viral load	5	581	0.007895	Health
T_{TS}	Shear force at first peak	4	581	0.013231	Meat and Carcass
T_{TS}	subjective abnormal odor	2	581	0.012262	Meat and Carcass

T_{TS}	Toll-like receptor 9 level	5	581	5.88E-05	Health
T_{TS}	Total shear work	2	581	0.017793	Meat and Carcass
T_{V16h}	androstenone, sensory panel	1	32	0.024975	Meat and Carcass
T_{V16h}	CD4-negative, CD8-positive leukocyte percentage	1	32	0.024975	Health
T_{V16h}	Osteochondrosis score	1	32	0.049764	Exterior
T_{V16h}	Percentage type I fibers	2	32	0.001976	Meat and Carcass
T_{V16h}	Phagocytic activity	1	32	0.024975	Health
T_{V16h}	rhinitis	1	32	0.024975	Exterior
T_{V16h}	Shear force at first peak	3	32	9.3E-05	Meat and Carcass

755

Table S8. CNVR overlapping with previous reported in the literature

CNVR identified in this study				CNVR previous reported		
CHR	**Start (bp)**	**End (bp)**	**Type**	**Start (bp)**	**End (bp)**	**Reference**
1	1,296,974	1,637,442	Loss	791,057	1,637,441	Stafuzza et al., 2019
1	1,296,974	1,637,442	Loss	1,637,442	1,843,489	Stafuzza et al., 2019
1	1,296,974	1,637,442	Loss	934,682	1,687,989	Wang et al., 2020
1	1,296,974	1,637,442	Loss	408,640	1,826,726	Qiu et al., 2021
1	2,530,735	2,908,940	Loss	2,667,200	2,812,415	Stafuzza et al., 2019
1	2,530,735	2,908,940	Loss	2,621,338	2,908,940	Wang et al., 2020
1	2,530,735	2,908,940	Loss	2,443,530	2,535,265	Qiu et al., 2021
1	4,621,444	4,690,022	Loss	4,630,315	4,690,022	Stafuzza et al., 2019
1	4,621,444	4,690,022	Loss	4,621,444	4,644,117	Wang et al., 2020
1	16,313,130	16,384,057	Loss	16,313,130	16,423,967	Stafuzza et al., 2019
1	16,313,130	16,384,057	Loss	16,313,130	16,423,967	Wang et al., 2020
1	20,559,479	21,017,894	Loss	20,559,479	20,646,252	Stafuzza et al., 2019
1	20,559,479	21,017,894	Loss	20,559,479	20,605,283	Wang et al., 2020
1	20,559,479	21,017,894	Loss	20,937,207	21,244,650	Qiu et al., 2021
1	26,407,492	26,757,112	Loss	26,383,627	26,856,773	Stafuzza et al., 2019
1	53,876,081	54,033,593	Loss	53,913,932	54,144,185	Stafuzza et al., 2019
1	77,402,476	77,616,272	Loss	77,121,687	78,587,646	Stafuzza et al., 2019
1	77,402,476	77,616,272	Loss	77,402,476	77,616,272	Wang et al., 2020
1	77,402,476	77,616,272	Loss	77,557,668	77,673,521	Qiu et al., 2021
1	77,973,487	78,233,457	Loss	77,121,687	78,587,646	Stafuzza et al., 2019
1	77,973,487	78,233,457	Loss	77,973,487	78,061,517	Wang et al., 2020
1	236,249,595	236,578,086	Loss	236,322,472	236,472,874	Qiu et al., 2021
1	296,787,813	296,854,248	Gain	296,787,813	296,820,153	Stafuzza et al., 2019
1	296,787,813	296,854,248	Gain	296,854,248	296,990,508	Wang et al., 2020
1	307,493,558	307,591,248	Loss	307,419,517	307,718,072	Stafuzza et al., 2019
1	307,493,558	307,591,248	Loss	307,375,644	307,718,072	Wang et al., 2020
2	1,111	632,707	Loss	0	16,416	Stafuzza et al., 2019
2	1,111	632,707	Loss	16,417	632,707	Stafuzza et al., 2019
2	1,111	632,707	Loss	1,111	632,707	Wang et al., 2020
2	1,111	632,707	Loss	27,459	2,407,984	Qiu et al., 2021
2	1,728,741	1,792,444	Loss	27,459	2,407,984	Qiu et al., 2021
2	6,179,112	6,495,647	Loss	2,599,113	7,209,835	Stafuzza et al., 2019
2	6,179,112	6,495,647	Loss	6,433,744	7,143,618	Qiu et al., 2021

2	12,967,586	13,092,623	Gain	12,776,098	13,042,380	Qiu et al., 2021
2	24,340,490	24,950,665	Loss	23,588,944	25,881,871	Stafuzza et al., 2019
2	38,779,149	39,302,035	Loss	38,779,149	39,302,035	Stafuzza et al., 2019
2	102,222,805	102,440,993	Gain	101,918,372	103,098,050	Stafuzza et al., 2019
2	102,222,805	102,440,993	Gain	102,231,770	102,528,479	Qiu et al., 2021
2	106,076,632	106,307,761	Loss	105,908,671	106,135,493	Qiu et al., 2021
2	110,341,590	110,423,447	Loss	110,005,387	110,423,447	Stafuzza et al., 2019
2	110,341,590	110,423,447	Loss	109,934,488	110,341,590	Wang et al., 2020
2	130,241,255	130,487,175	Loss	130,371,168	130,487,175	Stafuzza et al., 2019
2	137,484,909	137,871,651	Loss	137,484,909	137,652,218	Stafuzza et al., 2019
2	137,484,909	137,871,651	Loss	137,539,178	137,652,218	Wang et al., 2020
2	139,079,932	139,475,283	Loss	138,737,642	139,418,070	Stafuzza et al., 2019
2	157,653,015	158,139,060	Loss	156,951,510	158,488,428	Stafuzza et al., 2019
2	157,653,015	158,139,060	Loss	157,653,015	158,725,835	Wang et al., 2020
2	158,549,163	158,748,978	Loss	157,653,015	158,725,835	Wang et al., 2020
3	60,993	905,589	Loss	56,943	240,240	Stafuzza et al., 2019
3	60,993	905,589	Loss	240,241	364,888	Stafuzza et al., 2019
3	60,993	905,589	Loss	364,889	667,215	Stafuzza et al., 2019
3	60,993	905,589	Loss	667,216	1,045,800	Stafuzza et al., 2019
3	60,993	905,589	Loss	56,943	1,093,425	Wang et al., 2020
3	60,993	905,589	Loss	162,027	2,071,648	Qiu et al., 2021
3	1,157,712	1,540,289	Loss	1,045,801	1,243,957	Stafuzza et al., 2019
3	1,157,712	1,540,289	Loss	1,243,958	1,368,601	Stafuzza et al., 2019
3	1,157,712	1,540,289	Loss	1,368,602	1,695,804	Stafuzza et al., 2019
3	1,157,712	1,540,289	Loss	1,368,601	1,389,228	Wang et al., 2020
3	1,157,712	1,540,289	Loss	1,456,146	1,803,026	Wang et al., 2020
3	1,157,712	1,540,289	Loss	162,027	2,071,648	Qiu et al., 2021
3	1,775,581	1,803,026	Loss	1,695,805	1,797,693	Stafuzza et al., 2019
3	1,775,581	1,803,026	Loss	1,797,694	3,709,764	Stafuzza et al., 2019
3	1,775,581	1,803,026	Loss	1,456,146	1,803,026	Wang et al., 2020
3	1,775,581	1,803,026	Loss	162,027	2,071,648	Qiu et al., 2021
3	11,450,046	11,519,897	Loss	11,428,687	11,519,897	Stafuzza et al., 2019
3	11,450,046	11,519,897	Loss	11,450,046	11,519,897	Wang et al., 2020
3	17,333,664	17,509,970	Loss	16,839,756	17,428,593	Stafuzza et al., 2019
3	69,789,999	70,298,496	Loss	68,404,896	70,024,504	Stafuzza et al., 2019
3	69,789,999	70,298,496	Loss	69,556,858	69,916,171	Qiu et al., 2021

3	69,789,999	70,298,496	Loss	70,206,783	70,405,384	Qiu et al., 2021
3	102,698,568	102,763,903	Loss	102,720,554	103,294,448	Qiu et al., 2021
3	113,053,130	113,163,300	Loss	113,098,233	113,206,566	Qiu et al., 2021
4	1,155,293	1,388,468	Loss	1,037,908	3,046,732	Stafuzza et al., 2019
4	1,155,293	1,388,468	Loss	1,166,037	1,322,698	Wang et al., 2020
4	1,155,293	1,388,468	Loss	884,022	2,188,011	Qiu et al., 2021
4	17,865,227	18,008,464	Loss	17,865,227	18,008,464	Stafuzza et al., 2019
4	19,578,395	19,626,320	Loss	19,375,745	19,802,086	Qiu et al., 2021
4	27,913,643	28,349,829	Loss	27,832,880	29,731,872	Stafuzza et al., 2019
4	73,783,788	74,095,578	Loss	73,747,755	74,095,578	Stafuzza et al., 2019
4	73,783,788	74,095,578	Loss	72,992,609	74,231,975	Qiu et al., 2021
4	80,721,007	80,767,798	Loss	80,754,393	81,229,506	Qiu et al., 2021
4	126,897,791	127,521,733	Loss	126,897,791	128,153,004	Stafuzza et al., 2019
4	126,897,791	127,521,733	Loss	127,128,614	127,162,411	Qiu et al., 2021
4	127,645,367	127,879,136	Loss	126,897,791	128,153,004	Stafuzza et al., 2019
4	127,645,367	127,879,136	Loss	127,744,808	127,765,026	Wang et al., 2020
4	131,676,536	132,009,191	Loss	131,423,303	131,918,945	Stafuzza et al., 2019
4	131,676,536	132,009,191	Loss	131,539,062	131,691,287	Wang et al., 2020
5	2,847	285,237	Loss	2,847	1,787,761	Stafuzza et al., 2019
5	2,847	285,237	Loss	2,847	4,879	Wang et al., 2020
5	2,847	285,237	Loss	267,257	337,175	Wang et al., 2020
5	2,847	285,237	Loss	222,125	1,460,083	Qiu et al., 2021
5	548,113	1,210,042	Loss	2,847	1,787,761	Stafuzza et al., 2019
5	548,113	1,210,042	Loss	548,113	775,856	Wang et al., 2020
5	548,113	1,210,042	Loss	222,125	1,460,083	Qiu et al., 2021
5	2,006,549	2,052,182	Loss	1,853,897	3,057,476	Stafuzza et al., 2019
5	2,006,549	2,052,182	Loss	1,897,047	2,033,140	Wang et al., 2020
5	2,144,424	2,559,524	Loss	1,853,897	3,057,476	Stafuzza et al., 2019
5	2,144,424	2,559,524	Loss	2,520,748	2,546,827	Wang et al., 2020
5	2,144,424	2,559,524	Loss	2,249,879	2,281,918	Qiu et al., 2021
5	2,144,424	2,559,524	Loss	2,494,251	2,811,761	Qiu et al., 2021
5	2,935,602	3,182,357	Loss	1,853,897	3,057,476	Stafuzza et al., 2019
5	2,935,602	3,182,357	Loss	3,057,477	3,095,194	Stafuzza et al., 2019
5	2,935,602	3,182,357	Loss	3,095,195	3,136,770	Stafuzza et al., 2019
5	2,935,602	3,182,357	Loss	2,975,876	3,198,349	Wang et al., 2020
5	29,640,202	29,787,794	Gain	29,640,202	29,952,075	Stafuzza et al., 2019

5	63,917,069	64,229,196	Loss	63,787,481	64,458,916	Qiu et al., 2021
5	64,347,352	64,392,680	Loss	63,787,481	64,458,916	Qiu et al., 2021
5	77,179,466	77,352,621	Loss	77,085,316	77,253,445	Qiu et al., 2021
5	99,716,210	99,952,686	Loss	99,696,730	99,972,762	Stafuzza et al., 2019
5	99,716,210	99,952,686	Loss	99,674,382	99,882,649	Qiu et al., 2021
5	110,482,927	111,027,924	Loss	110,220,891	111,027,924	Stafuzza et al., 2019
5	110,482,927	111,027,924	Loss	110,482,927	111,027,924	Wang et al., 2020
6	1,033,257	1,281,226	Loss	504,971	1,122,428	Stafuzza et al., 2019
6	1,033,257	1,281,226	Loss	1,122,428	1,281,225	Stafuzza et al., 2019
6	1,033,257	1,281,226	Loss	1,281,226	1,593,899	Stafuzza et al., 2019
6	1,033,257	1,281,226	Loss	215,317	1,588,597	Wang et al., 2020
6	1,033,257	1,281,226	Loss	51,842	1,462,744	Qiu et al., 2021
6	2,952,600	3,336,730	Loss	2,899,444	2,952,600	Stafuzza et al., 2019
6	2,952,600	3,336,730	Loss	2,952,601	4,085,043	Stafuzza et al., 2019
6	2,952,600	3,336,730	Loss	2,487,882	2,952,600	Wang et al., 2020
6	2,952,600	3,336,730	Loss	3,152,461	3,577,211	Wang et al., 2020
6	2,952,600	3,336,730	Loss	2,262,060	3,625,829	Qiu et al., 2021
6	132,124,953	132,543,418	Mixed	132,116,850	133,090,986	Stafuzza et al., 2019
6	132,124,953	132,543,418	Mixed	132,322,578	132,814,494	Wang et al., 2020
6	132,647,018	132,704,049	Loss	132,116,850	133,090,986	Stafuzza et al., 2019
6	132,647,018	132,704,049	Loss	132,322,578	132,814,494	Wang et al., 2020
7	30,314,760	30,550,361	Loss	30,277,462	30,340,595	Stafuzza et al., 2019
7	31,976,416	32,267,617	Loss	31,800,221	32,499,186	Stafuzza et al., 2019
7	37,900,142	37,967,748	Loss	37,857,382	38,057,569	Qiu et al., 2021
7	50,084,357	50,518,151	Loss	50,231,835	50,286,342	Wang et al., 2020
7	50,084,357	50,518,151	Loss	50,429,945	51,376,033	Qiu et al., 2021
7	58,397,650	58,558,358	Loss	58,529,872	58,558,358	Wang et al., 2020
7	112,964,257	113,292,023	Loss	113,081,934	113,391,764	Stafuzza et al., 2019
7	112,964,257	113,292,023	Loss	112,784,720	113,122,517	Qiu et al., 2021
8	23,033,602	23,328,747	Loss	23,033,602	24,033,377	Stafuzza et al., 2019
8	23,033,602	23,328,747	Loss	23,147,683	23,234,622	Wang et al., 2020
8	23,033,602	23,328,747	Loss	22,905,249	23,111,564	Qiu et al., 2021
8	108,840,104	108,903,615	Loss	108,799,389	108,903,615	Stafuzza et al., 2019
8	114,376,195	114,407,527	Loss	114,376,195	114,407,527	Stafuzza et al., 2019
8	114,376,195	114,407,527	Loss	114,376,195	114,407,527	Wang et al., 2020
8	122,249,328	122,288,920	Gain	122,249,328	122,365,670	Wang et al., 2020

8	122,249,328	122,288,920	Gain	122,083,319	122,505,268	Qiu et al., 2021
8	123,960,362	124,128,258	Loss	123,895,414	123,996,880	Stafuzza et al., 2019
8	123,960,362	124,128,258	Loss	123,895,414	123,996,880	Wang et al., 2020
8	131,207,688	131,694,842	Loss	131,207,688	131,694,842	Stafuzza et al., 2019
8	131,207,688	131,694,842	Loss	130,821,518	131,495,872	Qiu et al., 2021
8	137,114,772	137,134,554	Loss	135,332,909	137,509,645	Stafuzza et al., 2019
9	130,785,204	130,830,299	Gain	130,802,093	131,113,367	Qiu et al., 2021
9	148,629,187	148,681,260	Loss	148,280,848	148,877,122	Stafuzza et al., 2019
10	5,204,072	5,514,795	Loss	5,282,479	5,608,014	Stafuzza et al., 2019
10	5,204,072	5,514,795	Loss	5,459,685	5,591,980	Wang et al., 2020
10	39,272,858	39,507,554	Loss	39,272,858	39,507,554	Stafuzza et al., 2019
10	47,123,541	47,259,902	Loss	47,188,024	47,475,119	Wang et al., 2020
11	11,663,909	11,724,233	Loss	11,663,909	11,891,740	Stafuzza et al., 2019
11	32,127,787	32,515,591	Loss	31,956,957	32,154,968	Stafuzza et al., 2019
11	40,013,884	40,160,781	Loss	39,919,176	42,118,356	Stafuzza et al., 2019
11	40,013,884	40,160,781	Loss	39,893,652	40,308,946	Qiu et al., 2021
11	47,243,159	47,452,970	Loss	47,282,526	47,452,970	Stafuzza et al., 2019
11	59,735,869	61,470,768	Mixed	58,988,824	62,480,762	Stafuzza et al., 2019
11	59,735,869	61,470,768	Mixed	59,153,609	60,030,798	Qiu et al., 2021
11	59,735,869	61,470,768	Mixed	61,386,952	61,678,667	Qiu et al., 2021
11	64,479,055	65,142,186	Loss	64,674,579	65,203,181	Stafuzza et al., 2019
11	64,479,055	65,142,186	Loss	64,478,176	64,942,423	Qiu et al., 2021
11	67,375,641	67,671,825	Loss	67,375,641	67,422,576	Stafuzza et al., 2019
11	67,375,641	67,671,825	Loss	67,422,577	67,548,214	Stafuzza et al., 2019
11	67,375,641	67,671,825	Loss	67,278,759	67,422,576	Wang et al., 2020
11	86,175,659	86,395,677	Loss	85,498,496	86,896,318	Stafuzza et al., 2019
11	86,175,659	86,395,677	Loss	86,022,171	86,552,276	Wang et al., 2020
11	86,708,117	86,796,356	Loss	85,498,496	86,896,318	Stafuzza et al., 2019
12	60,100	1,998,701	Mixed	0	320,417	Stafuzza et al., 2019
12	60,100	1,998,701	Mixed	320,418	437,614	Stafuzza et al., 2019
12	60,100	1,998,701	Mixed	437,615	490,193	Stafuzza et al., 2019
12	60,100	1,998,701	Mixed	490,194	634,357	Stafuzza et al., 2019
12	60,100	1,998,701	Mixed	634,358	884,329	Stafuzza et al., 2019
12	60,100	1,998,701	Mixed	884,330	985,539	Stafuzza et al., 2019
12	60,100	1,998,701	Mixed	985,540	2,445,965	Stafuzza et al., 2019
12	60,100	1,998,701	Mixed	1,279	1,759,150	Wang et al., 2020

12	60,100	1,998,701	Mixed	146,373	2,371,834	Qiu et al., 2021
12	6,034,340	6,161,500	Loss	6,028,598	6,484,229	Stafuzza et al., 2019
12	6,034,340	6,161,500	Loss	6,028,598	6,161,500	Wang et al., 2020
12	7,385,966	7,581,758	Gain	7,385,966	7,800,339	Stafuzza et al., 2019
12	7,385,966	7,581,758	Gain	7,565,937	7,668,938	Qiu et al., 2021
12	23,645,644	23,760,296	Loss	23,645,644	23,760,296	Wang et al., 2020
12	23,645,644	23,760,296	Loss	23,605,417	24,199,377	Qiu et al., 2021
12	46,257,013	46,339,202	Loss	46,290,007	46,339,202	Wang et al., 2020
13	12,386,754	12,485,442	Loss	12,442,742	12,598,280	Qiu et al., 2021
13	81,326,561	81,437,311	Loss	81,236,265	81,437,311	Stafuzza et al., 2019
13	102,306,232	102,458,997	Loss	102,377,734	102,458,997	Stafuzza et al., 2019
13	102,306,232	102,458,997	Loss	102,377,734	102,458,997	Wang et al., 2020
13	194,292,500	194,386,412	Loss	194,099,336	194,470,218	Stafuzza et al., 2019
13	194,665,680	196,342,442	Loss	195,800,128	197,449,273	Stafuzza et al., 2019
13	194,665,680	196,342,442	Loss	194,854,804	195,215,153	Qiu et al., 2021
13	196,810,429	197,241,857	Loss	195,800,128	197,449,273	Stafuzza et al., 2019
13	196,810,429	197,241,857	Loss	197,092,574	197,462,836	Qiu et al., 2021
13	200,335,858	200,366,615	Loss	200,335,858	201,166,260	Stafuzza et al., 2019
13	200,765,190	201,339,708	Loss	200,335,858	201,166,260	Stafuzza et al., 2019
13	200,765,190	201,339,708	Loss	200,767,905	200,928,287	Qiu et al., 2021
13	204,430,769	204,569,521	Loss	204,187,794	204,458,963	Qiu et al., 2021
13	204,734,507	204,819,522	Loss	204,798,820	204,845,516	Qiu et al., 2021
13	206,943,236	207,322,709	Loss	206,903,047	207,119,934	Stafuzza et al., 2019
13	206,943,236	207,322,709	Loss	206,903,047	207,062,660	Wang et al., 2020
13	206,943,236	207,322,709	Loss	206,578,011	208,240,759	Qiu et al., 2021
13	216,912,741	217,056,683	Loss	216,907,306	217,122,230	Stafuzza et al., 2019
13	216,912,741	217,056,683	Loss	216,907,306	217,689,499	Wang et al., 2020
13	218,141,951	218,612,146	Loss	218,111,694	218,612,146	Stafuzza et al., 2019
13	218,141,951	218,612,146	Loss	217,778,010	218,612,146	Wang et al., 2020
14	52,573,859	52,621,172	Loss	52,573,859	53,488,013	Stafuzza et al., 2019
14	73,479,608	73,695,090	Loss	73,670,990	73,788,843	Wang et al., 2020
14	74,176,726	74,990,114	Loss	74,915,088	75,672,762	Stafuzza et al., 2019
14	102,480,650	102,988,071	Loss	102,629,597	102,728,645	Stafuzza et al., 2019
14	102,480,650	102,988,071	Loss	102,629,356	102,703,160	Qiu et al., 2021
14	104,441,890	105,084,009	Mixed	103,891,750	104,759,248	Stafuzza et al., 2019
14	132,285,105	132,353,947	Loss	132,324,567	132,650,143	Qiu et al., 2021

14	136,444,819	137,178,653	Loss	136,557,301	137,063,119	Stafuzza et al., 2019
14	136,444,819	137,178,653	Loss	136,655,094	136,799,764	Qiu et al., 2021
14	136,444,819	137,178,653	Loss	137,077,958	137,148,948	Qiu et al., 2021
14	139,546,885	139,906,120	Loss	139,484,309	141,719,266	Qiu et al., 2021
14	140,199,680	140,419,493	Loss	139,484,309	141,719,266	Qiu et al., 2021
14	141,068,807	141,208,015	Loss	139,484,309	141,719,266	Qiu et al., 2021
14	151,966,127	153,374,972	Loss	152,135,829	152,836,608	Stafuzza et al., 2019
14	151,966,127	153,374,972	Loss	152,836,609	152,918,637	Stafuzza et al., 2019
14	151,966,127	153,374,972	Loss	152,918,638	153,836,231	Stafuzza et al., 2019
14	151,966,127	153,374,972	Loss	152,072,031	153,836,231	Wang et al., 2020
15	9,519,813	10,711,345	Loss	9,886,601	10,424,015	Stafuzza et al., 2019
15	9,519,813	10,711,345	Loss	10,104,238	10,362,171	Wang et al., 2020
15	9,519,813	10,711,345	Loss	8,291,413	9,850,344	Qiu et al., 2021
15	12,597,728	12,844,713	Loss	12,320,526	12,844,713	Stafuzza et al., 2019
15	17,097,658	17,123,356	Loss	16,828,036	17,304,533	Stafuzza et al., 2019
15	30,831,468	31,122,672	Loss	30,852,279	31,429,514	Qiu et al., 2021
15	33,345,253	33,617,369	Loss	33,268,982	33,365,983	Stafuzza et al., 2019
15	33,345,253	33,617,369	Loss	33,365,984	33,617,369	Stafuzza et al., 2019
15	48,845,490	49,845,075	Loss	48,790,892	49,439,076	Stafuzza et al., 2019
15	69,448,740	69,693,811	Loss	69,276,645	70,035,825	Stafuzza et al., 2019
15	69,448,740	69,693,811	Loss	69,276,645	69,693,811	Wang et al., 2020
15	125,908,102	126,154,684	Loss	117,834,922	127,553,332	Stafuzza et al., 2019
15	126,439,963	127,295,381	Loss	117,834,922	127,553,332	Stafuzza et al., 2019
15	126,439,963	127,295,381	Loss	127,116,371	127,140,502	Qiu et al., 2021
15	127,544,621	127,786,638	Loss	117,834,922	127,553,332	Stafuzza et al., 2019
15	134,842,540	134,994,861	Loss	134,531,547	134,919,214	Stafuzza et al., 2019
15	134,842,540	134,994,861	Loss	134,742,181	134,919,214	Wang et al., 2020
15	137,449,752	137,725,895	Loss	137,417,592	140,139,156	Qiu et al., 2021
15	138,365,140	138,453,739	Gain	137,417,592	140,139,156	Qiu et al., 2021
15	154,198,036	154,217,738	Loss	151,295,030	154,922,053	Stafuzza et al., 2019
15	154,198,036	154,217,738	Loss	154,198,036	154,963,296	Wang et al., 2020
15	154,516,149	154,590,998	Loss	151,295,030	154,922,053	Stafuzza et al., 2019
15	154,516,149	154,590,998	Loss	154,198,036	154,963,296	Wang et al., 2020
16	2,294,773	2,931,783	Loss	2,278,462	3,066,542	Stafuzza et al., 2019
16	2,294,773	2,931,783	Loss	2,366,658	2,421,778	Wang et al., 2020
16	2,294,773	2,931,783	Loss	2,568,549	3,066,542	Wang et al., 2020

16	2,294,773	2,931,783	Loss	2,389,967	3,024,209	Qiu et al., 2021
16	10,588,133	11,083,680	Loss	10,595,674	10,894,800	Qiu et al., 2021
16	11,287,880	11,615,935	Loss	11,509,437	11,667,410	Stafuzza et al., 2019
16	14,404,612	14,706,916	Loss	14,337,125	14,605,020	Qiu et al., 2021
16	30,289,787	30,566,627	Loss	30,289,787	30,566,627	Stafuzza et al., 2019
16	85,407,012	86,024,383	Loss	84,005,681	85,843,097	Stafuzza et al., 2019
16	85,407,012	86,024,383	Loss	85,843,098	85,889,875	Stafuzza et al., 2019
16	85,407,012	86,024,383	Loss	85,889,876	86,024,383	Stafuzza et al., 2019
16	85,407,012	86,024,383	Loss	85,677,427	86,024,383	Wang et al., 2020
17	2,202,762	2,730,970	Loss	2,038,218	2,679,834	Stafuzza et al., 2019
17	2,202,762	2,730,970	Loss	2,300,590	2,434,592	Wang et al., 2020
17	2,202,762	2,730,970	Loss	2,446,954	2,580,356	Qiu et al., 2021
17	2,202,762	2,730,970	Loss	2,619,190	2,774,389	Qiu et al., 2021
17	3,434,809	3,642,846	Loss	3,459,318	3,642,846	Stafuzza et al., 2019
17	3,434,809	3,642,846	Loss	3,335,446	3,557,919	Qiu et al., 2021
18	6,247,938	6,366,290	Loss	6,303,226	6,366,290	Stafuzza et al., 2019
18	6,247,938	6,366,290	Loss	6,331,960	6,525,480	Wang et al., 2020
18	32,234,894	32,451,272	Loss	32,189,513	32,295,375	Stafuzza et al., 2019
18	38,984,087	39,185,391	Loss	38,488,658	39,185,391	Stafuzza et al., 2019

757

758

CHAPTER 5: General conclusions

This study has contributed to understanding the genetic architecture underlying HS response indicators and related traits in pigs. The new insights on the genetic background of HS response traits provides valuable knowledge for designing breeding goals aiming to enhance resilience in pigs.

As discussed on Chapter 2, including non-additive genetic effects do not improve the accuracy of genomic breeding values for performance traits in purebred pigs. However, it did lead to a significant re-ranking of selection candidates depending on the model fitted, especially models including epistasis effects. Furthermore, most of the HS response indicators in crossbred pigs presented low non-additive genetic variance estimates, except for the panting score and hair density traits.

As presented on Chapter 3, the candidate genes for the HS response indicators and with potential pleiotropic effects identified are involved in heat shock protein activities, immune response, and cellular oxidative stress, indicating the importance of these biological processes in HS response. Additionally, physiological and anatomical indicators of HS response exhibited some variants with pleiotropic effects, indicating that some genomic regions influence multiple physiological and anatomical indicators of HS response. Many candidate genes with potential pleiotropic effects are associated with catalytic activities to reduce cell damage from oxidative stress and cellular mechanisms related to immune response were identified, providing valuable insights for breeding programs aimed at improving HS resilience in pigs. The findings have significant implications for advancing breeding programs aimed at improving heat tolerance in pigs.

In Chapter 4, various CNVs and CNVRs were detected in the population. The most prevalent CNVRs were found to overlap with genes associated with responses to cellular oxidative stress and immune reactions. These findings suggest that these CNVRs

may affect the regulation of biological processes related to adaptation and resilience to HS. Additionally, 15 CNVRs were significantly associated with skin and vaginal temperatures, which are physiological indicators of HS response in lactating sows. These CNVRs overlapped several genes and QTL involved in immune and stress responses, which are important biological processes in the HS response.